Travel Time Estimation using Bluetooth Technology with a Focus on Reliability and Accuracy

Araghi, Bahar Namaki

Publication date:
2013

Document Version
Accepted author manuscript, peer reviewed version

Travel Time Estimation Using Bluetooth Technology with a Focus on Reliability and Accuracy

Bahar Namaki Araghi

Supervisor: Associate Prof. Harry Lahrmann	Co-Supervisor: Dr. Rajesh Krishnan
Traffic Research Group Department of Civil Engineering Aalborg University	Centre for Transport Studies Department of Civil & Environmental Engineering Imperial College London

Paper 1: Namaki Araghi, B., Tørholm, L.C., Krishnan, R., Olesen, J.H. & Lahrmann, H. "Reliability of Bluetooth Technology for Travel Time Estimation". Journal of Intelligent Transportation Systems: Technology, Planning, and Operations, Accepted author version posted online: 28 October 2013.

Paper 2: Namaki Araghi, B., Tørholm, L.C., Krishnan, R., Olesen, J.H. & Lahrmann, H. "Use of Low-Level Sensor Data to Improve the Accuracy of Bluetooth-Based Travel Time Estimation". Journal of the Transportation Research Board. Volume 2338, No. 1, pp.29-34, 2013.

Paper 3: Namaki Araghi, B., Skoven Pedersen, K., Tørholm, L.C., Krishnan, R. & Lahrmann, H. "Accuracy of Travel Time Estimation using Bluetooth Technology: Case Study Limfjord Tunnel Aalborg". 2012. International Journal of Intelligent Transportation Systems Research, 1-26.

Paper 4: Namaki Araghi, B., Tørholm, L.C., Krishnan, R. & Lahrmann, H. "Application of Bluetooth Technology for Mode-Specific Travel Time Estimation on Arterial Roads: Potentials and Challenges". Presented in Trafikdage Conference at Aalborg University, 27-28 August, Aalborg, Denmark. 2012.

Paper 5: Namaki Araghi, B. Krishnan, R. & Lahrmann, H. "Mode-Specific Travel Time Estimation Using Bluetooth Technology". Journal of Intelligent Transportation Systems: Technology, Planning, and Operations. Accepted author version posted online: 26 May 2015.

Paper 6: Namaki Araghi, B., Wang, Y., Malinovskiy Y., Corey, J. & Lahrmann, H. "Comparing multiple travel time data collection technologies: a state route 522 case study". Accepted for the 22nd ITS World Congress 2015, Bordeaux, France.

This thesis has been submitted for assessment in partial fulfillment of the PhD degree. The thesis is based on the submitted or published scientific papers which are listed above. Parts of the papers are used directly or indirectly in the extended summary of the thesis. As part of the assessment, co-author statements have been made available to the assessment committee and are also available at the Faculty. The thesis is not in its present form acceptable for open publication but only in limited and closed circulation as copyright may not be ensured.

Travel Time Estimation Using Bluetooth Technology with a Focus on Reliability and Accuracy

Bahar Namaki Araghi

Supervisor:
Associate Prof. Harry Lahrmann

Traffic Research Group
Department of Civil Engineering
Aalborg University

Co-Supervisor:
Dr. Rajesh Krishnan

Centre for Transport Studies
Department of Civil & Environmental Engineering
Imperial College London

Department of Development and Planning

2014

ISBN 978-87-91404-69-6

ABSTRACT

The use of Bluetooth technology for travel time estimation has been emerging over the past few years. An increasing number of Bluetooth-enabled devices among road users, the anonymity of Bluetooth devices, ease of deployment and maintenance of Bluetooth sensors, along with an acceptable accuracy demonstrates the potential of this technology for wider deployment. However, the technology is also known to have some issues such as the reliability of Bluetooth detections, location ambiguity associated with the detection events, low sampling rate and its negative impact on reliability, and the difficulty of distinguishing between multiple travel modes (e.g. motor vehicles, bicycles and pedestrians). These issues could adversely affect the accuracy and reliability of the estimated travel time.

The main objective of the thesis is to understand the accuracy and reliability of travel times estimated using Bluetooth data, and to develop methods to make Bluetooth based travel time estimates more accurate and reliable. In this context, this PhD thesis first explores the factors that have an impact on the reliability and accuracy: the percentage of Bluetooth devices captured by a pair of Bluetooth sensors and the relative location of the detection events with respect to the sensors. The Bluetooth device discovery procedure, in conjunction with the shape and the size of the detection zone determine the capture rate of Bluetooth devices as well as the number and relative location of detection records for a given device. While a larger detection zone yields a higher capture rate resulting in more reliable travel time estimates, it also results in location ambiguity causing inaccuracy in travel time estimates. This highlighted the importance of the trade-off between accuracy and reliability. Based on the understanding gained by this exercise, methods to improve the travel time estimation were developed.

The next stage of the research focused on the choice of aggregation method and the required sample size for travel time profile estimation using Bluetooth technology. It was shown that both the choice of the aggregation method and the sample size influence the accuracy of the travel time profile. Three conventional aggregation methods including arithmetic mean, geometric mean and harmonic mean were used to construct the travel time profile. The accuracy of these methods was tested against the ground truth. Comparing the three aggregation methods show that employing the harmonic mean and geometric mean could significantly reduce the impact of outliers, especially in intervals with a low sample size. Moreover, the range of optimum sample size for aggregation was determined using sensitivity analysis. It was found that a sample size of 5-15 travel time records per 15 minutes improves the accuracy.

The next part of the research focused on travel time estimation methods with a view to improve the accuracy. Each Bluetooth device may trigger multiple detection events at a sensor and there are a number of alternative ways to estimate the travel time using these detection events. Eight travel time estimation methods were presented and tested for two different sensor designs; sensors with a single antenna or multiple antennae. Moreover, it was assumed that the Radio Signal Strength Indication (RSSI) could be used as a parameter for determining the most reliable detection event with the minimum location ambiguity. In the case of sensors with single antenna, travel time estimated based on detection event with the highest RSSI provided more accurate travel time estimate. This indicated the validity of the assumption. For sensors with multiple antennae design, the time of a device passing by the sensor was estimated based on a combination of multiple antennae events with the highest RSSI. Comparison of these methods proved that that new method which combines detection events recorded by various antennae could yield more accurate results.

A new method to improve the accuracy of Bluetooth-based travel time estimation in a heterogeneous traffic environment (i.e. arterial roads with mixed traffic) was also developed as a part of this research. The new method classifies the devices carried by various modes (i.e. motor vehicles, bicycles and pedestrians) and estimates mode-specific travel times. Accuracy of this method was tested against the ground truth, Automated Number Plate Recognition (ANPR), and a commercially deployed Bluetooth-based travel time estimation method. The results show that the proposed method provides a more accurate travel time estimate than the commercially deployed Bluetooth-based method, with a level of accuracy comparable to that of ANPR. This proved the potential of Bluetooth technology for accurate travel time estimation on arterial roads with multiple travel modes.

Lastly, a comprehensive side-by-side evaluation of two types of Bluetooth sensors versus ANPR, magnetometers and floating car data was carried out at two test locations in the United States of America. ANPR was used as the ground truth in this comparison exercise. The comparative study shows that although Bluetooth had a significantly lower sampling rate than ANPR and magnetometers, it was capable of providing accurate travel time estimation.

ABSTRAKT

Anvendelse af Bluetooth til måling af rejsetider har været stigende igennem de senere år. Baggrunden herfor har været, at et stigende antal trafikanter har eller flere åbne Bluetooth-radioer, at det er nemt at etablere og vedligeholde Bluetooth sensorer, der kan aflæse Bluetooth-radioerne, at en Bluetooth-radio er anonym og at teknologien har demonstreret en acceptabel nøjagtighed. Dette er baggrunden for at der er et stort potentiale for en udbredelse af teknologien. På den anden side er det også kendt, at teknologien har nogle problemer, som fx med hvilken sikkerhed en åben radio kan detekteres, og præcist hvor den befinder sig i forhold til sensoren, når den detekteres. Der er også problemet med, at kun en del af trafikanterne har en åben Bluetooth radio samtidig med at det kan være vanskeligt at skelne mellem forskellige typer trafikanter (biler, cykler og fodgængere). Disse problemer kan påvirke nøjagtigheden og påvideligheden af den målte rejsetid.

Målet med denne Phd.-afhandling har været både at forstå nøjagtighed og pålidelighed, når Bluetooth data bruges til estimering af rejsetider, men også at udvikle metoder til at gøre Bluetooth baserede rejsetider mere præcise og pålidelige. I denne sammenhæng vil afhandlingen først undersøge de faktorer, der har indflydelse på pålidelighed og præcision: Den procentdel af Bluetooth-radioer som registreres af to Bluetooth-sensorer og den relative placering af Bluetooth-radioerne, når de registreres af sensorerne.

Den måde som Bluetooth-radioen registreres på, sammenholdt med formen og størrelsen af detekteringszonen, bestemmer registreringsgraden af Bluetooth-radioer sammen med antal og relative placering af registreringer for en given enhed. Mens en større detekteringszone giver en højere registreringsgrad, betyder det også større unøjagtighed om, hvor præcist Bluetooth-radioen er på registreringstidspunktet – og dermed større unøjagtighed i rejsetidsestimatet. Dette sætter fokus på betydningen af et trade-off mellem præcision og pålidelighed. Baseret på en forståelse heraf er der i afhandlingen udviklet metoder til forbedring af rejsetidsestimering.

Den næste fase af afhandlingen er fokuseret på valget af aggregeringsmetoder og den nødvendige stikprøvestørrelse for rejsetidestimering. Det vises, at både valget af aggregeringsmetoden og stikprøvestørrelsen påvirker nøjagtigheden af rejsetiden. Tre normalt anvendte metoder til beregning af middelværdien på rejsetiden er brugt: den aritmetiske, den geometriske og den harmoniske. Nøjagtigheden af disse metoder blev testet mod "Ground Truth". Sammenligning af de tre opregningsmetoder viser, at den harmoniske middelværdi og den geometriske middelværdi reducerede virkningen af outliers, især hvis stikprøve var lille. Desuden blev den optimale stikprøvestørrelse bestemt ved hjælp af en følsomhedsanalyse. Det blev konstateret, at en stikprøve på 5-15 rejsetidsobservationer pr. kvarter giver en acceptabel nøjagtighed.

Den næste del af afhandlingen fokuserer på metoder til estimering af rejsetider med henblik på at forbedre nøjagtigheden. Hver Bluetooth-radio kan udløse flere registreringer ved passage af en sensor, og der er en række forskellige måder at estimere rejsetiden ved hjælp af disse registreringer. Afhandlingen afprøver otte metoder til estimering af rejsetid og tester to forskellige sensortyper, en sensor med en enkelt antenne og en med flere antenner. Desuden er det undersøgt, om maxstyrken af radiosignalet (RSSI) kan bruges som en parameter for den bedste registrering af sensorens placering. Med en enkelt antenne gav registreringen med den højeste RSSI det mest præcise skøn på rejsetiden. For sensorer med flere antenner, blev tidspunktet for en enheds passage af sensoren estimeret ved en kombination af, hvornår registreringerne på de forskellige antenner gav den højeste RSSI. Sammenligning af de afprøvede metoder viste, at metoden, der kombinerer registreringer fra forskellige antenner kunne give mere præcise resultater.

I afhandlinger er der også udviklet en ny metode til at forbedre nøjagtigheden af rejsetider baseret på Bluetooth i et heterogent trafikmiljø (dvs. veje med blandet trafik). Den udviklede metode kan klassificere Bluetooth-radioerne i forhold til, om de er tilknyttet en bil eller en cykel og give et skøn over rejsetiden for de forskellige transportmidler. Nøjagtighed af den udviklede metode blev testet mod "Ground Truth", automatisk nummerpladeaflæsning (ANPR), og et kommercielt Bluetooth-baserede produkt til rejsetidsmåling. Resultaterne viser, at den foreslåede metode giver en lidt mere nøjagtig rejsetidsestimat end det kommercielle produkt, og at nøjagtigheden kan sammenlignes med ANPR. Dette viser potentialet i Bluetooth-teknologien til også at give en nøjagtig estimering af rejsetiden på veje med blandet trafik.

Endelig blev der gennemført en omfattende sammenligning af udstyr til rejsetidsmåling på to lokaliteter i USA. Sammenligningen omfattede to typer Bluetooth-sensorer versus ANPR, magnetometre og Floating Car Data. ANPR blev brugt som "Ground Truth" i denne test. Testen viste, at selv om Bluetooth havde en signifikant lavere samplingfrekvens end ANPR og magnetometre, var teknologien stadig i stand til at give en præcis estimering af rejsetiden.

DECLARATION OF ORIGINALITY

At various stages during this PhD, I have been involved in collaborative efforts with both academic and industrial colleagues. In certain cases, the output of this collaboration is included in this thesis to better explain and support the research presented. In particular, my research has built upon collaborative work with my supervisors and other colleagues, working on several collaborative research papers that were presented at various conferences and submitted for journal publication. These are listed in the reference section and are all my own work.

I hereby declare that besides the collaboration referred to above I have personally carried out the work described in this dissertation.

…………………

Bahar Namaki Araghi

COPYRIGHT DECLARATION

ACKNOWLEDGEMENTS

First and foremost I would like to thank my supervisors Professor Harry Lahrmann and Dr Rajesh Krishnan for offering me the opportunity to study in Intelligent Transport Systems (ITS). Without their inspirational guidance, excellent supervision and financial support, this thesis would not have been accomplished.

I am very grateful to Danish Road Directorate, who provided me with the financial support over the course of my PhD. I would like to thank Blip Systems Company and specially Lars Tørholm Christensen, Claus Elsborg, Søren Ulrik, Preben Fugl Andersen, and Peter Knudsen for providing me with BlipTrack sensors and travel time data for different case studies.

I must also thank Jonas Hammershøj Olesen from COWI for providing me with the data for Århus used within this thesis.

I would like to thank Prof. Yinhai Wang, Yegor Malinovskiy, and Jonathan Corey from University of Washington in Seattle, United States for hosting me during my study abroad and great collaboration on the project for error modelling and evaluation of various travel timed data collection technologies. I would like also to thank Ted Bailey from Washington State Department of Transportation (WSDOT) for their support and great collaboration during the data collection in Seattle and evaluation study of various technologies.

I would like to appreciate the great support from the ITS Department of Danish Road Directorate, specially Lene Mårtensson, Raza Muhammed, Kasper Grøndahl Rosenstand, and Olof Åke Egemalm. I would like also thank Ulrich Clausen from Aalborg Municipality for their support over the course of my PhD study.

I would also like to express my gratitude to my colleagues and officemates during the past three years.

Special thanks go to my friends especially thank to Meghdad who always encouraged me to keep on with my work. Without his love, patience and sacrifices this thesis would never have been finished.

Last but not least, I dedicate this work to my parents and other family members in Iran for their continuous support and encouragement.

GLOSSARY

ALPR	Automated License Plate Reader
ANPR	Automated Number Plate Reader
APVD	Aggregated Probe Vehicle Data
ATIS	Advanced Travelers Information Systems
ATMS	Advanced Traffic Management Systems
AVI	Automatic Vehicle Identification
AVL	Automatic Vehicle Location
CCD	Charge-Coupled Devices
DAC	Device Access Code
CFD	Cumulative Frequency Distributions
DRG	Dynamic Route Guidance
EDI	Eberle Design Inc
FHS	Frequency Hopping Synchronisation
FHSS	Frequency-Hopping Spread Spectrum
FHWA	Federal Highway Administration
ITS	Intelligent Transportation Systems
GPS	Global Positioning System
LAN	Local Area Network
LCD	Liquid-Crystal Display
LED	Light-Emitting-Diode
MAC	Media Access Control
MAD	Mean Absolute Deviation
MAPE	Mean Absolute Percent Error
MPE	Mean Percent Error
PC	Personal Computer
PDA	Personal Digital Assistant
RMSE	Root Mean Squared Error
RSSI	Radio Signal Strength Indication
SDPE	Standard Deviation Of Percentage Error
SR	State Route
TCI	TrafficCast International
UTM	Universal Transverse Mercator coordinate system
VDPU	Video Detection Processor Unit
VIL	Virtual Induction Loop
VIP	Video Image Processor
VRIS	Vehicle Re-Identification System

CONTENTS

LIST OF FIGURES

LIST OF TABALES

CHAPTER 1

INTRODUCTION OF BLUETOOTH TECHNOLOGY

1. Problem Statement

Advanced Traveller Information Systems (ATIS) and Advanced Traffic Management Systems (ATMS) have become increasingly common in the last decade. In this context, the need for accurate and reliable travel time information for these systems has become important. Access to short-term travel time information can significantly influence the decision making on both the supply side (i.e. efficient management of the network capacity) and the demand side (i.e. mode choice, route choice and departure time choice of travellers) of transportation system.

A number of different technologies have been used to measure or estimate travel time, such as Inductive Loop Detectors (ILD), Automated Number Plate Recognition (ANPR) systems, Global Positioning System (GPS) etc. Each technology has its strengths and weaknesses and no technology has been accepted as an ideal solution for travel time estimation. Moreover, spatial coverage of currently deployed travel time monitoring systems are limited due to high implementation and operating costs of the above technologies and limited budgets available with government agencies. Hence, there is need for a cost effective, accurate and reliable technology to provide travel time information.

Since 2005, Bluetooth technology has been evaluated as a means for travel time estimation. Bluetooth is a short-range data transmission protocol amongst electronic devices. The Bluetooth protocol uses an electronic identifier, or a tag, in each device called the Media Access Control address, or the MAC address for short. The MAC address serves as an electronic nickname so that electronic devices can keep track of who is who during data communications. Vehicles with detectable Bluetooth-enabled devices can be observed by Bluetooth sensors installed by the road-side. Bluetooth sensors record the MAC address and the detection time, that can later be used for travel time estimation using the principle of re-identification.

Bluetooth technology has a number of advantages. In this context, increasing number of Bluetooth-enabled devices among road users, anonymity of MAC addresses, flexibility of deployment and maintenance of Bluetooth sensors can be considered. Moreover, the acceptable accuracy of travel time estimation using Bluetooth technology (Haghani et al., 2010; Puckett and Vickich, 2010; Barcelo et al., 2010) have resulted in an emerging interest for further evaluation of this technology as a cost-effective method for travel time estimation.

Since no current data sources link MAC addresses with personal information, Bluetooth sensors tracking Bluetooth-enabled devices (i.e.) is more acceptable to the public compared to the GPS or ANPR which are directly linked with the personal information of the users. Furthermore, an increasing numbers of Bluetooth-enabled devices not only do not impose any additional cost to the Intelligent Transportation Systems (ITS) infrastructure but also provide better opportunities for estimating travel time based on MAC address tracking. Larger numbers of Bluetooth-enabled devices increases the sampling size of the Bluetooth-based dataset, hence improving the accuracy and the reliability of Bluetooth-based travel time estimations. Moreover, Bluetooth technology is not sensitive to the weather conditions (i.e. fog, darkness etc.). These characteristics make Bluetooth an interesting technology to be used for travel time measurements in road network.

As for any other technologies, Bluetooth technology has a number of disadvantages. Although Bluetooth has been demonstrated as a promising technology, there remains problems such as over-counting of a single vehicle carrying more than one Bluetooth-enabled device (e.g. buses), low sampling rate and the difficulty of distinguishing between multiple travel modes (e.g. motor vehicles, bicycles and pedestrians). This PhD thesis aims to address some of these challenges facing the application of Bluetooth technology for travel time estimation.

1.1 Background of the Applications of Bluetooth Technology in Travel Time Estimation

To date, Bluetooth technology has been used for a wide range of applications. In the initial stages, implementation of Bluetooth protocol in ITS started with focus on communication between systems (Bhagwat 2001, Bechler et al. 2001, and Aloi et al. 2003).

Bluetooth device tracking began in Europe, in Bath (UK), London (UK) and Apeldoorn (The Netherlands) for pedestrian detection and tracking applications (O'Neill et al. 2006). The initial efforts were focused upon determining the correlation between Bluetooth and pedestrian activity as well as determining the travel speed. Although Bluetooth was not as widely prevalent as today, the results of the study demonstrated a strong correlation between detections and total volume, indicating that Bluetooth devices were sufficiently well distributed within population (O'Neill et al. 2006).

The use of Bluetooth MAC address data for traffic monitoring began with a study in 2008 Ahmed et al. 2008). In this study, the Bluetooth MAC address associated with a probe vehicle was tracked by a Bluetooth and WiFi-based mesh network. The Bluetooth MAC address matching algorithms for travel time data collection and measurements were developed and tested jointly by the Indiana Department of Transportation and Purdue University in a research project (Wasson et al. 2008). The results indicated that travel time trends were easy to discern by visual inspection and demonstrated the feasibility of using Bluetooth MAC address matching for travel time estimation. However, data from arterial highways showed a significantly larger variance compared to data from freeways, which has been attributed to the impact of traffic signals and the variability that is introduced when motorists divert from the network. Wasson et al. (2010) tried to evaluate travel mobility metrics for a rural interstate highway work zone along I-65 in north-western Indiana, USA. This study involved automated collection and processing of Bluetooth probe data from multiple field collection sites, communication of travel delays to the motoring public, assessment of driver diversion rates, and development of proposed metrics to evaluate work zone mobility performance. Consequently, it has been concluded that leveraging the pervasive presence of consumer Bluetooth devices provides an opportunity to obtain travel time measurement samples during construction work. Due to the desire for expansion of coverage of traffic monitoring from the freeways to urban arterials in Houston region, Puckett and Vickich (2009) investigated the feasibility of utilising Bluetooth technology on arterial streets to collect travel time data. The demonstration of this technique as a viable method for estimating travel times in a corridor was successfully proven on the basis of a single study conducted in Houston.

At the 88th Annual Meeting of Transportation Research Board in 2009, Tarnoff et al. (2009) presented the results of evaluation of a Bluetooth MAC address detector developed by the University of Maryland. The results indicate that Bluetooth-based method is one of the most cost-effective approaches for travel time data collection. A series of studies have been conducted by the Department of Civil & Environmental Engineering of the University of Maryland under the supervision of Prof. Haghani to evaluate the application and accuracy of the data obtained using Bluetooth technology. Haghani et al. (2010) introduced Bluetooth sensors as a new and effective means of freeway ground truth travel time data collection. In this research, sampling rates, sampling errors, privacy concerns, data collection and filtering of the data obtained by Bluetooth devices have been investigated. Floating car data (FCD) were used as the "ground-truth" to evaluate the accuracy of the highway travel time information generated by the Bluetooth based estimation method. Results showed that travel times estimated using Bluetooth are not significantly different from the actual travel times. In this research, authors have also developed a four-step offline filtering algorithm to eliminate outliers from Bluetooth data. The performance of the filtering system was compared to alternative algorithms and it was shown to be a robust and effective method for processing travel times collected by Bluetooth sensors.

Malinovskiy et al. (2010) discussed of Bluetooth sensors and the application of multiple devices in tandem to improve the results of data collection using Bluetooth technology. This research compared Bluetooth MAC address-based travel-time sensors developed by the authors with standard ANPR cameras commonly used for travel time data collection. The test results indicate that although Bluetooth sensors tended to be biased towards slower vehicles, the travel time measurements obtained were representative of the ground truth travel time data measured by the ANPRs. This clearly emphasised the potential application of this approach for travel time data collection.

More recently, the application of Bluetooth technology in evaluating arterial traffic characteristics (i.e. segment travel time, and average running speed) before and after changes to signal timing were investigated (Quayle et al. 2010). A comparison between recorded Bluetooth MAC IDs and traditional GPS floating car data demonstrated that larger dataset from the Bluetooth measurements more effectively captured performance characteristics of the arterial. The authors concluded that real-time MAC reader information provides substantial opportunity to add new control and performance monitoring capability to other ITS components, such as ramp metering, transit signal priority systems and adaptive signal control.

The Pennsylvania Department of Transportation (PennDOT) (2010) conducted and participated in an independent study to evaluate the appropriateness of Bluetooth technology for travel time measurement. Travel time results, match-rate, and cost of implementing Bluetooth technology were compared with those of EZPass, a tag-based electronic tolling system. It was concluded that the travel times measured using Bluetooth technology were comparable to those obtained by EZPass tag readers. Analysis of the match rate indicated that the minimum number of data points required to accurately estimate traffic conditions were collected by both systems. The cost of Bluetooth technology including pole, excluding power, communication, data formatting and system integration estimated around one third of the tag readers. Additionally, installation and maintenance of the Bluetooth devices appear to be rather uncomplicated and the range of the readers gives the ability to easily cover one direction of a multi-lane highway using a single reader.

Tsubota et al. (2011) analysed the travel time on a signalised arterial route in Brisbane using Bluetooth data and examined the potential use of “Duration” data. Bluetooth data could not only provide a direct measurement of travel time between pairs of sensors, but also could provide “duration” data. Duration data represents the time spent by Bluetooth devices within the detection range of Bluetooth sensors. If the sensors are located at signalised intersections, this duration can be correlated with intersection delays, and hence represents valuable information for traffic monitoring. This research confirmed Bluetooth based travel time estimates were representative of the traffic situation such as morning and evening peak during weekdays and bi-modal travel-time (i.e. vehicles and bicycles) in a particular link.

Saunier and Morency (2011) aimed to develop travel time reliability indicators through comparing the outputs of different data collection methods (i.e. FCD, GPS, ANPR and Bluetooth) used for monitoring highways. In this study, the accuracy and reliability of Bluetooth data were compared with GPS traces. Results indicated that both technologies agree during non-congested conditions but the methods did not produce consistent outputs during the congested peak period.

Lahrmann et al. (2010) investigated the application of Bluetooth sensors for measuring speed and travel time. A comparative study was conducted on the data obtained by Bluetooth technology and the data from floating car using GPS. Results have been compared with respect to the travel time, coverage and penetration rate. It has been proved that Bluetooth

technology can be considered as an alternative technology for travel time measurements. The result also conforms the outputs of the research by PennDOT (2010).
Previous studies all indicate the capability of Bluetooth technology for travel time measurement. These studies are superficial and issues such as multiple detection event[1]s, location ambiguity, shape and size of detection zone, speed of passing vehicle and mode of travel and their impacts on accuracy and reliability of travel time estimation have never been examined. These factors are explained in the following section.

1.2 A Brief Primer on Bluetooth Technology

Bluetooth is a short-range data transmission protocol amongst electronic devices. The Bluetooth protocol uses a unique electronic identifier, or a tag, in each device, called a Machine Access Control address or Media Access Control Address (MAC). The MAC address serves as an electronic nickname so that electronic devices can keep track of who is who during data communications (Haghani et al. 2010).
The main units in Bluetooth technology are the Bluetooth sensor (known also as reader) and the Bluetooth-enabled device. The Bluetooth readers record anonymous "MAC" addresses from Bluetooth-enabled devices as they travel down the roadway. The Bluetooth-enabled devices are mainly electronic devices with the Bluetooth set to the active mode and with discoverable communication capability. These devices (e.g., navigators, mobile phones, headsets etc.) broadcast their unique 48-bit MAC addresses to communicate with other devices within range. Vehicles carrying discoverable Bluetooth-enabled devices are detected by Bluetooth sensors installed at multiple locations along the road network. The MAC address and its detection time are recorded by the sensors, which then can be used for travel time estimation, this is called a detection event (Hamedi et al. 2010), see Figure 1-1.

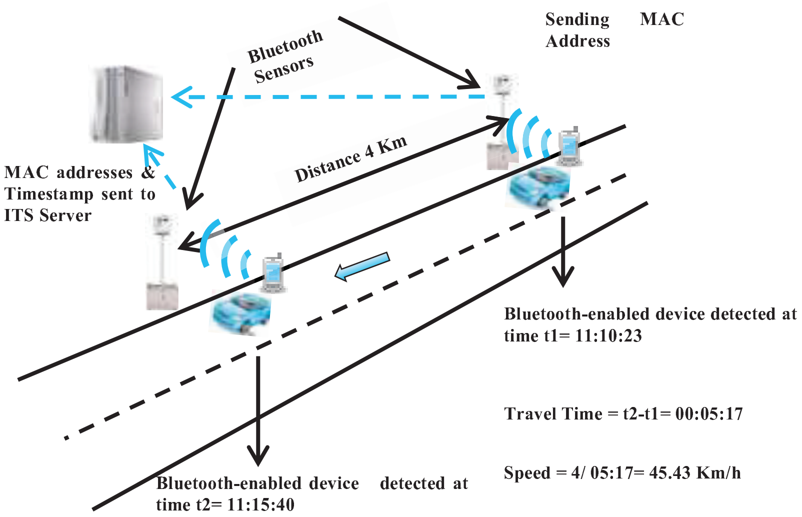

Figure 1-1. Application of Bluetooth technology for travel time estimation

The Bluetooth sensors manufactured by various vendors differ in terms of design; however, the main components of the sensors are common. They include a procession unit, a communication unit, GPS antenna, internal clock, power supply, cover and mounting brackets

[1] When a vehicle carrying a detectable Bluetooth-enabled device travels past a Bluetooth sensor, the sensor records the MAC address of the device and its detection time; this is called a detection event.

and Bluetooth radio antenna. Details of these components are provided in Appendix I. Figure 1-2 shows the main components of Bluetooth sensors from Blip systems.

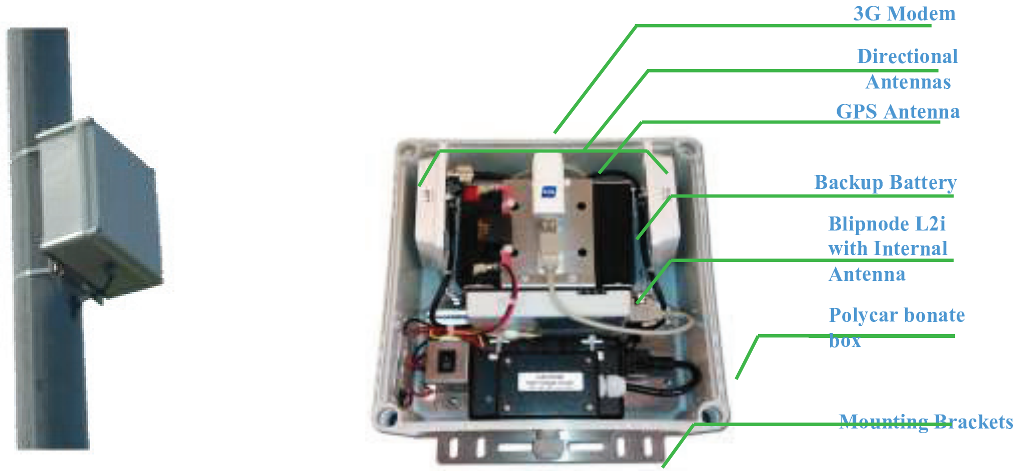

Figure 1-2. BlipTrack sensor design and components (Source: BlipSystems 2010).

1.2.1 Size and Shape of the Bluetooth Sensors Detection Zone

Bluetooth sensors can detect vehicles inside an area within their antenna's range, referred to as the detection zone. The shape and size of the Bluetooth sensor detection zone depends on the type (e.g. directional and Omnidirectional) antenna, power and configuration. A Bluetooth sensor may use a single or multiple antennae. Depending on the choice of antennae and their configuration, size and shape of Bluetooth detection zone differ typically between 70-300 metres along the road. The shape of detection zone typically depends on the antenna configuration. The foot print of the detection zone for Bluetooth sensors with single antenna and multiple antennae are schematically shown in Figure 1-3 and Figure 1-4.

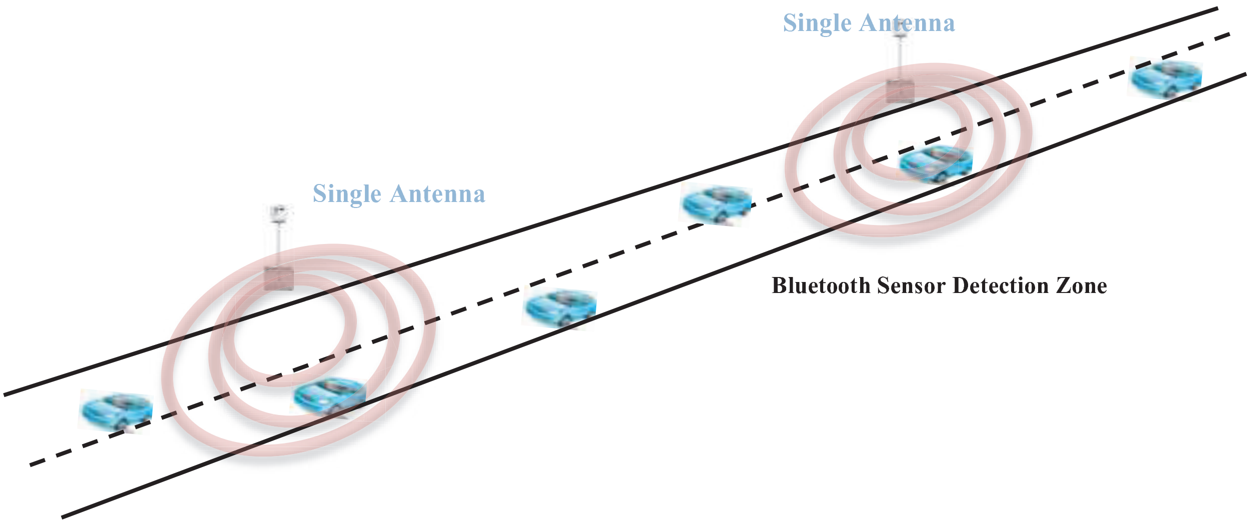

Figure 1-3. Detection zone footprint for single antenna configuration

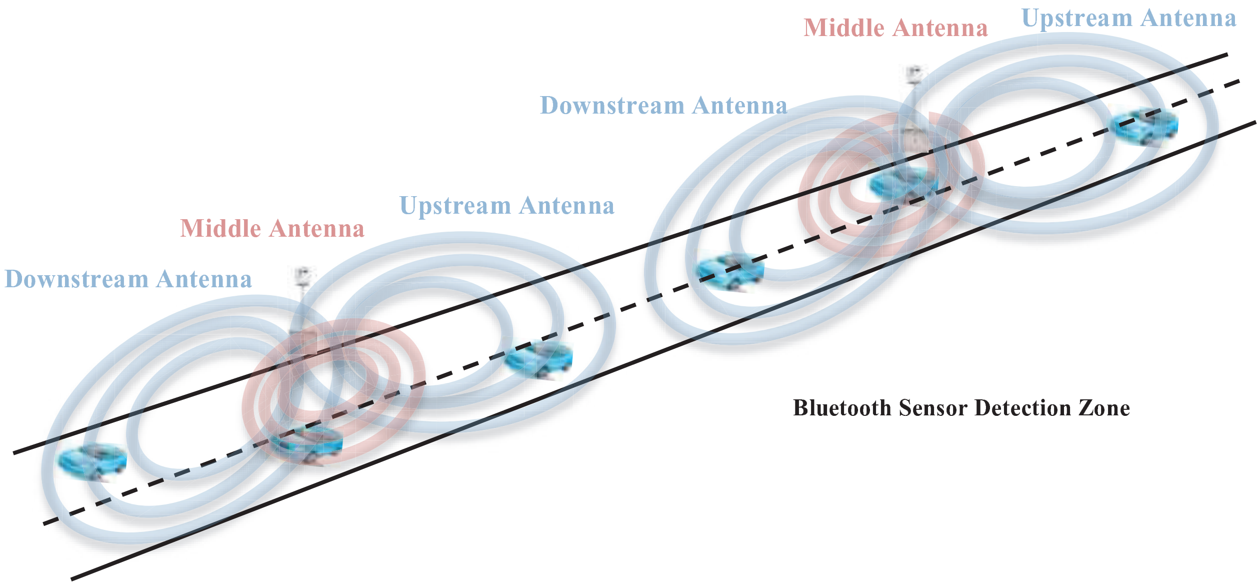

Figure 1-4. Detection zone footprint for multiple antenna configurations

1.2.2 Bluetooth Frequency Hopping Spread Spectrum

Bluetooth has been designed to operate in a noisy radio frequency environment. It operates in the 2.4 GHz frequency band, which is a globally unlicensed frequency spectrum and is shared with other devices. Thus, for channel access control Bluetooth uses Frequency-Hopping Spread Spectrum (FHSS) (Franssens, 2010) and divides the band into 79 channels (each 1 MHz wide) and changes channels up to 1600 times per second to avoid interference with coexisting devices (see Figure 1-5)(Han et al. 2012).

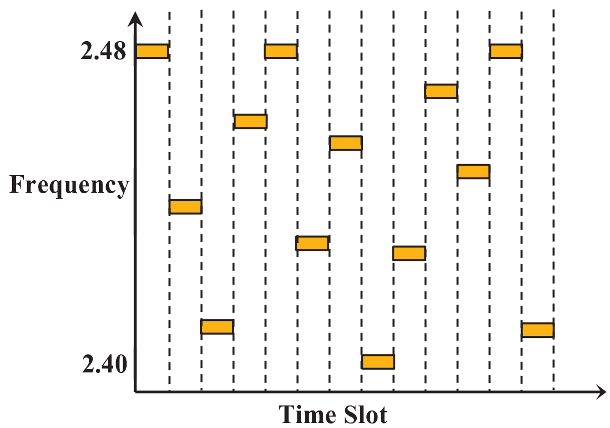

Figure 1-5. A time slot of Bluetooth protocol frequency hopping

1.2.3 Bluetooth Discovery Procedure

In Bluetooth communication, a piconet is a basic networking unit consisting of one master and a number of slave devices (Chakraborty et al. 2010). The device that initiates the process of forming a piconet is designed as the master. The process of initiating a piconet (i.e. discovery procedure) consists of two sequential steps: inquiry and paging. The inquiry process is designed to scan for other discoverable devices within range, and exchange the necessary information to set-up an actual connection (Figure 1-6 node A and B). In the inquiry phase, the master invites other devices to form a piconet. In the inquiry phase in order to find the discoverable devices, the master solicits responses by transmitting a standard

packet, called ID (identifier) packet, on different hop channels (i.e. different frequencies), and listens for response packets, called FHS (frequency hopping synchronisation) packets, from potential slave devices (Chakraborty et al. 2010). The sender of FHS packet puts its own 48-bits unique MAC address and the internal clock-offset, so that the master recognizes which device is willing to join the master to form a piconet (Franssens, 2010; Chakraborty et al. 2010).
After this discovery is completed, a paging procedure is started to actually set up a connection (Figure 1-6, node C until G). The master device pages the slave device, which in return sends a reply containing its Device Access Code (DAC) on the appropriate frequency selected by the page response hopping sequence. The slave will then switch to the master's channel parameters, by which a link is established and data can be exchanged. The master coordinates the transmissions of itself and its slaves by alternating in 625μs timeslots between master and slaves using time-division multiplexing. The discovery procedure and FHSS for multiple slaves are shown in Figure 2-4. For more information regarding the Bluetooth discovery procedure, refer to Franssens (2010).

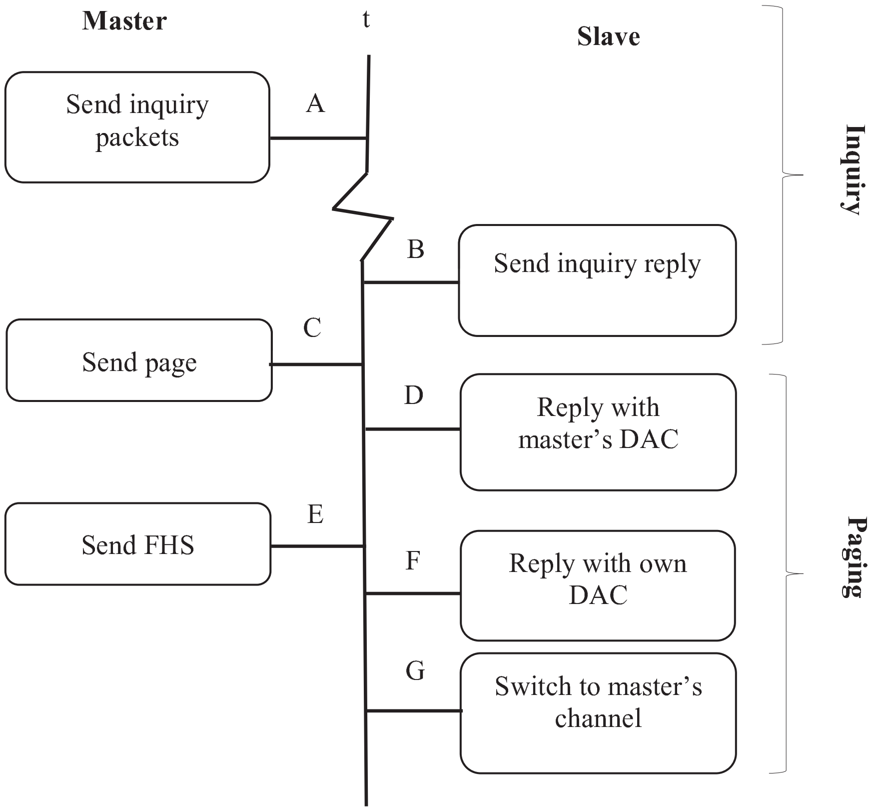

Figure 1-6. Inquiry and paging procedure (Franssens, 2010)

In order to be able to track a passing Bluetooth-enabled device, it is only necessary to conduct the inquiry phase to detect the device. The paging phase and connection establishment is not needed. This is due to the fact that the required information for establishing a detection event (i.e., the MAC address and clock-offset) is recorded in the inquiry phase. According to existing literature, the inquiry detection time of a single device may take up to 10.24 seconds, but the vast majority of devices are discovered within 5 seconds (Franssens, 2010; Chakraborty et al. 2010; Jiang et al. 2004). Nevertheless, the inquiry detection time of a device could in practice take shorter or longer. The inquiry detection time is complex to calculate mainly due to the following issues:

- Differences in the handsets' Bluetooth implementation, Bluetooth 1.0 vs. Bluetooth 1.2, or Bluetooth 2, and whether interlaced[2] inquiry scan is enabled or disabled[3].
- The fact that in travel time data collection, the Bluetooth-enabled device is moving along the road and is in the coverage of overlapping antennae. Overlapping coverage areas will increase detection time which could result in minor interferences in detection procedures.
- The noisy environment and the number of Bluetooth-enabled devices competing for connection with the sensor could also affect the required time for inquiry. Discovery procedure for multiple Bluetooth-enabled devices is shown in Figure 1-7.

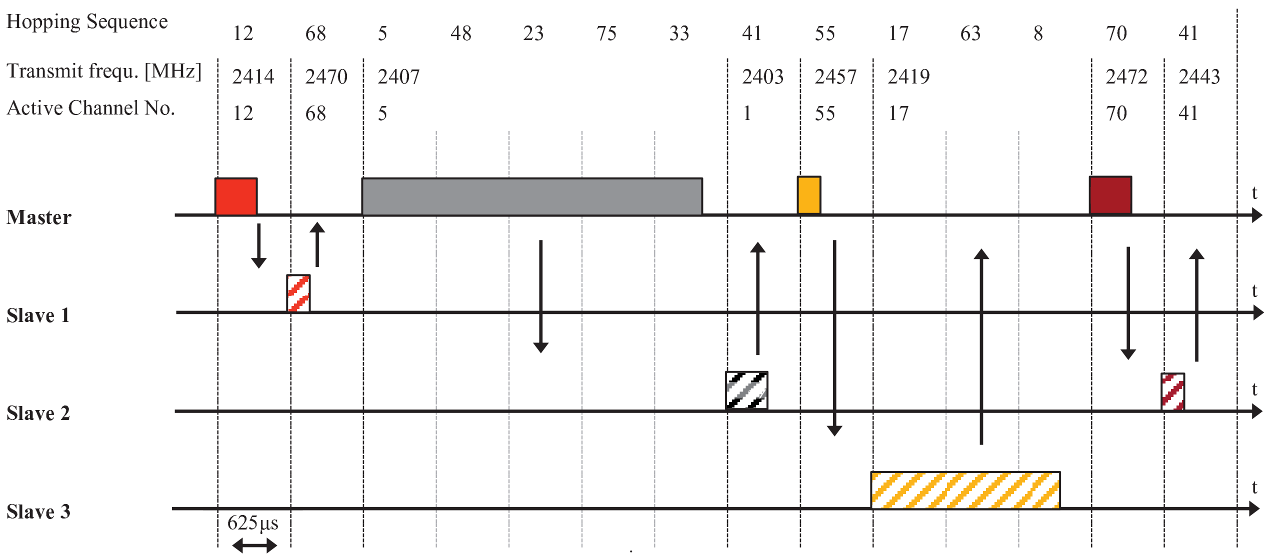

Figure 1-7. Communication between master and slave units (Source: Johnson Consulting, 2004)

1.2.4 The Bluetooth-Enabled Devices

The Bluetooth-enabled devices are mainly electronic devices with the Bluetooth active and visible communication capability. These could be mobile phones, navigators, headsets, radios with Bluetooth communication capability. It is possible to detect the type of device from the MAC address. The 11-bits of the 48-bit MAC address contain the information of the type of device and the vendor company referred to as Class of Device (CoD). The CoD represents the major and minor classes which are intended to define a general family of devices with which any particular implementation wishes to be associated. Figure 1-8 shows the CoD field for the first Bluetooth format type. List of major service classes are also listed in Table 1-1. Thus, it is possible to identify the CoD (e.g. mobile phone versus headset) using the MAC addresses. The CoD information can be utilised for distinguishing the type of road users and also removing outliers in the dataset. This factor will be further explores in this thesis.

---

[2] . Interlaced inquiry scan speeds up the discovery process by 2x to a maximum of 2.5 seconds and can be as fast as 25 milliseconds (Graber et. al 2004).

[3] . In the original scheme, because the master repeats a specific packet train many times, a slave node could miss the whole packet train if it listens to a channel that belongs to the other packet train (e.g., inquiry A train/scan B train, or inquiry B train/scan A train). To prevent such situations, the interlaced scan allows a slave node to scan two trains (i.e., A and B) in a row. Thus, the probability of missing an inquiry packet becomes negligible (cited by Lee et al. 2010).

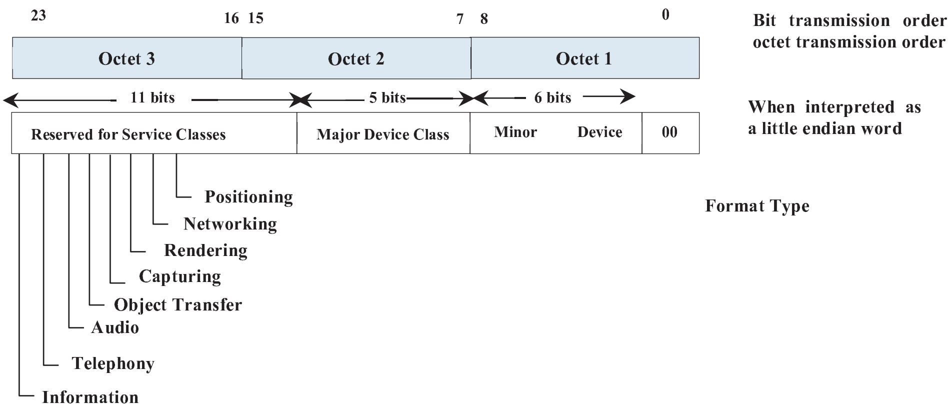

Figure 1-8. The class of device/service field (first format type) (Source: Bluetooth Org. 2009)

Table 1-1. Major service classes

Bit #	Major Service Class
13	Limited Discoverable Mode [Ref #1]
14	(reserved)
15	(reserved)
16	Positioning (Location identification)
17	Networking (LAN, Ad hoc, ...)
18	Rendering (Printing, Speaker, ...)
19	Capturing (Scanner, Microphone, ...)
20	Object Transfer (v-Inbox, v-Folder, ...)
21	Audio (Speaker, Microphone, Headset service, ...)
22	Telephony (Cordless telephony, Modem, Headset service, ...)
23	Information (WEB-server, WAP-server, ...)

1.2.5 Information Collected by Bluetooth Sensors

A Bluetooth sensor records the following information for each detected device. In this study, this information is referred to as low-level sensor data. These parameters are explained bellow:

- The MAC Address
- Time-stamp: The Bluetooth sensors are recording the MAC addresses and time-stamped them. Depending on the shape and size of the sensor's detection zone, it is possible to have multiple detections recorded for a unique MAC address. In such cases, the Bluetooth sensor records all the detected time-stamps.
- Radio (Received) Signal Strength Indication (RSSI): The RSSI is an indication of the power level being received by the antenna. The magnitude of the RSSI is highly dependent on the distance of the device from the sensor location.
- The CoD
- Sensor-ID: The sensor-ID shows the ID of the sensor that detects the MAC address. This information also can be used to identify the travel direction of the passing vehicle.

1.3 Challenges Facing Application of Bluetooth Technology for Travel Time Estimation

1.3.1 Detection Reliability

In this study, “Detection Reliability” of Bluetooth is defined as the percentage of device-trips that are captured by Bluetooth sensors during the experiment. The percentage of MAC addresses captured by Bluetooth sensors could significantly influence the accuracy of travel time estimates. There are several factors that can create variation in the sampling rates, refer to 1.2.2 and 1.2.3. A low sampling rate could lead to travel time estimation inaccuracy.

1.3.2 Location Ambiguity

A detection event could be triggered anywhere within the detection zone. In this study, “Location Ambiguity” is defined as the spatial error associated with detection events. Bluetooth sensors have large detection zones compared to other VRIS technologies such as ANPR cameras. A larger detection zone increases the probability of detecting a Bluetooth-enabled device in a fast-moving vehicle; however, it increases the probability of multiple detection events triggered by a single device. This could lead to location ambiguity and reduced accuracy of travel time estimation.

1.3.3 Aggregation Method and Sample Size

Travel time data are usually reported in an aggregated form. In this context, the method used for aggregation of non-homogeneous data could play a significant role in reducing the accuracy of the outputs. It is worth mentioning that this problem is not limited to Bluetooth technology and is a common issue in various travel time data collection methods. However, with Bluetooth technology it is not possible to directly distinguish between the roads users based on the MAC addresses, hence this issue become more important. Arithmetic mean (i.e. average) is one of the most common aggregation methods used for Bluetooth data analysis. Nevertheless, using the average value as the basis of analysis can be misleading as the average itself can be affected by outliers. This highlights the importance of using more robust estimators as well as using appropriate outlier removal algorithms.

Optimum sample size is another embedded problem along with the choice of aggregation method. Likewise, such problem is not limited to the Bluetooth technology and is a common problem in majority of technologies used for travel time data collection. However, due to the lower sample size of Bluetooth technology, this problem becomes more important. Therefore, understanding the relationship between sample size and accuracy of travel time estimation using Bluetooth technology is of interest.

1.3.4 Methods of Travel Time Estimation

Accuracy of travel time estimations by Bluetooth Technology depends upon how location ambiguity is handled by estimation method. Figure 1-9 illustrates an example of a situation in which the MAC address of the Bluetooth device in the car is detected thrice, slightly before, middle, and after the exact location of Bluetooth sensors. As can be seen in Figure 1-9, there are 9 different possible ways to calculate the travel time of this vehicle using the recorded detection event data. This raises the question of which one of these estimations is the most accurate one. Therefore, this study aims to reduce the impact of location ambiguity on accuracy of travel time estimation by means of developing new methods.

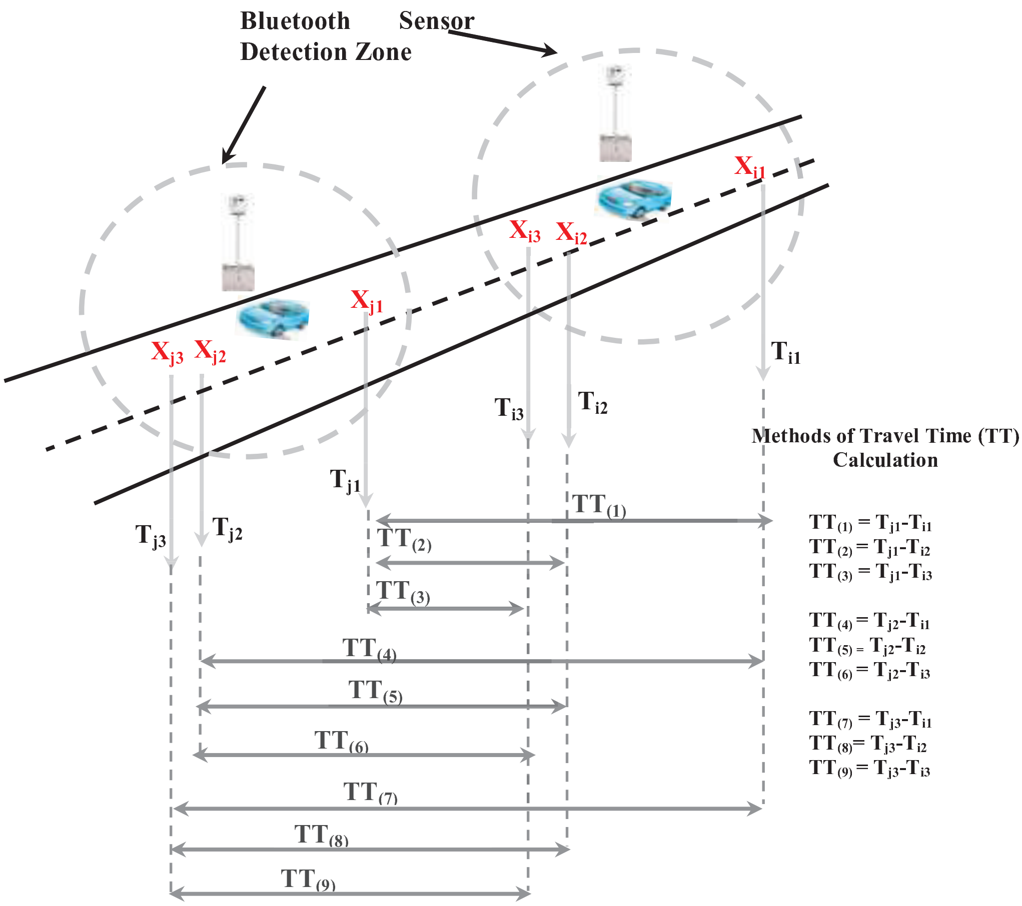

Figure 1-9. Methods of travel time calculation in the case of a multiple detection event

1.3.5 Mode Classification

Majority of studies on application of Bluetooth technology for travel time measurement were conducted in motorways, where the problem of distinguishing between mixed traffic (i.e. cyclists and cars) is less significant due to homogeneous nature of traffic stream.

In arterial roads, traffic is no longer homogeneous. Increased heterogeneity of road users in urban areas, including the presence of cyclists, could reduce the accuracy of travel time measured by Bluetooth technology. Improving the accuracy of travel time estimation on arterial roads depends on how modes could be distinguished. Therefore, mode identification is important and this research plans to use the information of CoD to develop new method to address this issue.

1.4 Objectives of the Study

The objectives of this PhD research can be summarised as follows:

1. Evaluate the reliability of Bluetooth technology and estimate the location ambiguity associated with Bluetooth detections,
2. Identify the influence of aggregation method and sample size on accuracy of estimated travel time,
3. Develop methods for travel time estimation to minimise the impact of location ambiguity, without compromising on reliability,
4. Develop new methods for mode-specific travel time estimation, utilising CoD information,

5. Compare the accuracy of travel time estimated by Bluetooth technology versus other sensor technologies, to provide a holistic overview of the accuracy and reliability of Bluetooth Technology compared to other technologies in the market.

1.5 Organisation of the Thesis

This PhD thesis is organised as follows:

Chapter 1 presents the background of this research and describes its scope and objectives.

Chapter 2 focuses on evaluation of Bluetooth detection reliability and location ambiguity.

Chapter 3 explores the effects of sample sizes and aggregation method in travel time estimation.

Chapter 4 developed new travel time estimation method based on the results obtained in Chapter 2 and evaluates the accuracy of these methods.

Chapter 5 developed a new method for mode-specific travel time estimation using Bluetooth technology to improve the accuracy of travel time estimation on arterial roads with mixed traffic.

Chapter 7 summarises the findings of this research and suggests avenues for further research.

CHAPTER 2

RELIABILITY AND LOCATION AMBIGUITY OF BLUETOOTH TECHNOLOGY

2. Introduction

When a vehicle carrying a detectable Bluetooth-enabled device travels past a Bluetooth sensor, the sensor records the MAC address of the device and its detection time; this is called a detection event.

The number of detection events registered for a passing Bluetooth-enabled device can be variable. This is a complex phenomenon and depends on a number of factors, which could be categorised into two major groups. First, factors related to the Bluetooth sensor detection zone, including size, shape and time span that the device is within the detection zone, refer to Section 1.2.1. Second, factors related to the Bluetooth device discovery procedure, refer to Sections 1.2.2 and 1.2.3. This includes parameters such as strength and speed of a transmitting device, the Bluetooth sensor's ping cycle (0.1 seconds), the proximity of the roadside Bluetooth sensor (Quayle et al. 2010), clock drift, and noise in background (e.g. number of Bluetooth-enabled devices communicating with the sensor over a short period of time).

The reliability and accuracy of travel time estimates not only depend on the percentage of MAC addresses captured by pair of Bluetooth sensors (i.e., penetration rate), but also the relative positions at which the detection events have been recorded. A larger detection zone increases the probability of detecting a Bluetooth-enabled device in a fast moving vehicle, and correspondingly increases the penetration rate. Apparently, the higher the penetration rate, the higher the reliability of travel time estimates. While a larger detection zone increases the penetration rate, it also contributes to larger location ambiguity. The larger the location ambiguity, the lower the accuracy of estimated travel time. Therefore, a trade-off needs to be made between the penetration rate and the size of the detection zone. These factors are explored further in following sections.

2.1 Earlier Studies about Multiple Detection Events

The location error associated with the discovery procedure of Bluetooth-enabled devices and its corresponding impact on travel time estimation were also discussed by Malinovskiy et al. (2010). It was stated that the frequency hopping protocol allows a random error of up to 10.24 seconds in device discovery time, which may result in variable location errors depending on the vehicle's speed. Finally, it was concluded that these errors can impact the travel time data accuracy significantly if the link is short, since the location errors are relatively high for the link distance.

The noise and spatial errors associated with a larger detection zone were also discussed by Malinovskiy et al. (2010). The authors mentioned that larger detection zones are subject to more noise and bigger spatial errors, as a vehicle may be detected anywhere within the zone. Meanwhile, a larger detection zone also corresponds to a bigger sample size. In this study, the impact of the range of the antennae on sample rate and spatial error were evaluated. It was found that larger detection zones capture more vehicles, including faster ones. Furthermore, it was concluded that since the spatial error obtained is random, the spatiotemporal error incurred due to a larger detection area is mitigated when an average of a sufficient sub-sample is taken. Furthermore, it was concluded that since the spatial error obtained is random, the spatiotemporal error incurred due to a larger detection area is mitigated when an average of a sufficient sub-sample is taken.

2.2 Multiple Detection Event and Bluetooth Discovery Procedure

As discussed in section 1.2.3, the Bluetooth discovery procedure consists of three main stages; inquiry phase, paging, and connection establishment. However, in the application of Bluetooth for tracking, the inquiry phase is essential; however, the paging phase and connection establishment phase are not needed. This is due to the fact that the information required for establishing a detection event (i.e., the MAC address and clock-offset) is recorded in the inquiry phase. According to existing literature, the inquiry detection time of a single device may take up to 10.24 seconds, but the vast majority of devices are detected within 5 seconds (Franssens, 2010; Chakraborty et al. 2010; Jiang et al. 2004). Nevertheless, the inquiry detection time of a device may in practice take shorter or longer. The inquiry detection time is complex to calculate mainly due to the following reasons.

- Differences in the handsets' Bluetooth implementation, Bluetooth 1.0 vs. Bluetooth 1.2, or Bluetooth 2, and whether interlaced[1] inquiry scan is enabled or disabled (cited by Lee et al. 2010).
- The fact that in travel time data collection, the Bluetooth-enabled device is moving along the road and is in the coverage of overlapping antennae. Overlapping coverage areas will increase detection time.
- The noisy environment and the number of Bluetooth-enabled devices competing for connection with the sensor could also affect the required time for inquiry. Discovery procedure for multiple Bluetooth-enabled devices is shown in **Error! Reference source not found.**.

Depending on the speed of the passing Bluetooth device and the time span the device is within the range of the sensor, it may be detected many times as it passes by a single station or none at all. The number of missing devices could influence the estimated counts obtained by Bluetooth technology.

2.2.1 Multiple Detection Events and Bluetooth Sensor's Ping Cycle

Ping stands for Packet Inter-Network Groper. Ping is usually a quick test to ensure that your connection is valid. Bluetooth sensors have a very short ping cycle; typically 0.1 seconds (Quayle et al., 2010). Depending on the strength and speed of the passing Bluetooth-enabled device, it may be detected many times as it passes by a single Bluetooth station or none at all. This mainly relates to the strength of the transmitting device, the location of the device relative to the Bluetooth sensor, and also the time span that the device is within range of the reader (Quayle et al., 2010 and Blogg et al., 2010).

2.2.2 Multiple Detection Event and Size of Detection Zone

Detection zone refers to the area monitored by the sensor on the road; the sensor detects passing vehicles travelling through the detection zone. Bluetooth sensors can detect vehicles inside an area within their antenna's range. The shape and size of a Bluetooth sensor detection zone depends on the type (i.e., directional and omnidirectional), power and configuration of the antenna.. Having a range of detection reaching 100-300m enables the Bluetooth sensor to track unique MAC address of a Bluetooth-enabled device as it passes the detection zone.
Although a larger detection zone increases the probability of detecting a Bluetooth-enabled device in a fast moving vehicle, it increases the probability of multiple detection events triggered by a single device. Since the locations of detection events recorded for a passing Bluetooth-enabled device is not recorded, the ambiguity of location of the detected vehicle can lead to decreased accuracy of travel time estimation using Bluetooth data. The larger the distance of recorded detection event from the actual sensor location, the larger the effect of location ambiguity. Therefore, the accuracy of travel time estimates not only depend on the

[1] . Interlaced inquiry scan speeds up the discovery process by 2x to a maximum of 2.5 seconds and can be as fast as 25 milliseconds (Graber et. al 2004).

percentage of MAC addresses captured by each Bluetooth sensors (i.e., reliability), but also the relative positions at which the detection events have been recorded.

2.2.3 Multiple Detection Event and Detection Interference

Bluetooth-enabled devices with a class 1 radio can be detected at distances up to 100 metres away. However, physical barriers could significantly reduce the capture rate of Bluetooth-enabled devices. Physical barriers for example a metal car door, and to a lesser degree, plastic-caps for weather protection of the antennas can influence the transmitted signal and hence reduce the capture rate. In order to reduce the interference, the antennae should ideally be placed at the vehicle's window height.

In this study an experimental evaluation is conducted to assess the detection reliability of Bluetooth-enabled devices passing by a sensor as well as to investigate how detection events are distributed based on their distances from the sensor location (i.e. location ambiguity).
The main objectives of this experimental evaluation are first to explore the impacts of all influencing parameters on multiple detection events; second to examine the location ambiguity associated with size of detection zone; third to evaluate the accuracy of various travel time estimation method. In order to evaluate the impacts of all influencing parameters on multiple detection events, a new concept called "Detection Reliability" has been introduced. The detection reliability itself is a term requiring a definition of which criteria are actually considered. In this study, the detection reliability of Bluetooth is defined as the percentage of device-trips that are captured by Bluetooth sensors during the experiment.

2.3 The Experimental Set-up and Evaluation

Experiment set-up and data collection were conducted by COWI consulting, Denmark. Details of the experiment set-up and the methods are explained in the following sections:

2.3.1 Location of the Experiment

The sensors were installed at the intersection of Grenåvej-Ellebjergvej on the roadside noise barriers Figure 2-1 and at the intersection of the Grenåvej-Skolevangs Alle on a gantry pole in the median of Grenåvej Figure 2-2 in Aarhus, Denmark. The distance between the two Bluetooth sensors was 610 metres. An aerial photograph of the corridor is shown in Figure 2-3.

2.3.2 Data Collection

The experiment consisted of a single vehicle equipped with 18 Bluetooth-enabled devices and a GPS logger. The vehicle plied between two Bluetooth sensors 74 times. The vehicle was continuously driven back and forth between the sensors. In order to ensure that the individual trips could be distinguished from one another, the trips started approximately 825 metres west of Grenåvej-Skolevangs Alle and ended 1 km east of Grenåvej-Ellebjergvej. There was also a short pause of 4 minutes between each run, i.e., between the end of a trip and the start of the next trip. This was mainly done to ensure that the experimental vehicle was out of range between each trip.

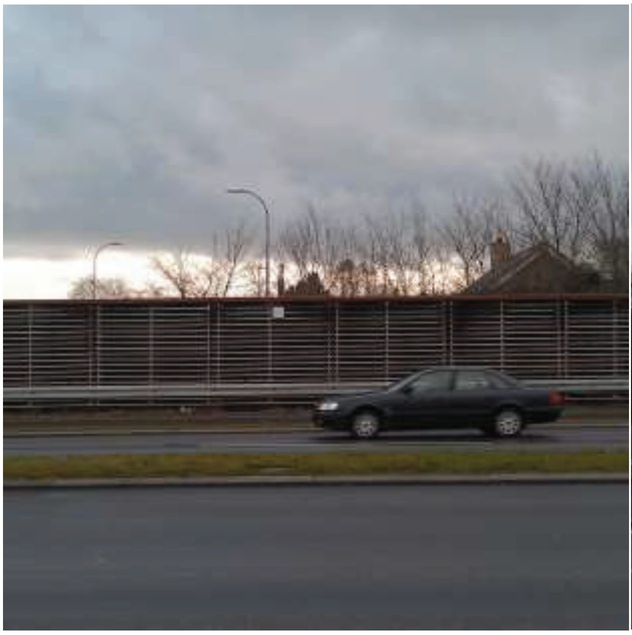

Figure 2-1. The Bluetooth sensor installed on the noise barrier at Grenåvej-Ellebjergvej

Figure 2-2. The Bluetooth sensor installed on the portal at Grenåvej-Skolevangs Alle

Figure 2-3. Locations of Bluetooth sensors on Ellebjergvej-Skolevangs Alle, Århus, Denmark (Source: Google Map)

2.3.3 Bluetooth-Enabled Devices

The experimental vehicle carried 18 different Bluetooth-enabled devices, consisting of thirteen conventional mobile phones, four smart phones and one tablet. The devices are listed in Table 2-1. The Bluetooth-enabled devices were set on the visible mode so that they could be detected by the roadside sensors.

Table 2-1. List of Bluetooth devices used in the experiment

Types of Device	Device Name	Bluetooth Protocol Version
Conventional Mobile Phones	Nokia_c1_01	2.1
	Nokia_c1_02	2.1
	Nokia_c1_03	2.1
	Nokia_c1_04	2.1
	Nokia_c1_05	2.1
	Nokia_c1_06	2.1
	Nokia_c1_07	2.1
	Nokia_c1_08	2.1
	Nokia_c1_09	2.1
	Nokia_c1_10	2.1
	Nokia_2960	2.0
	SE_W580i	2.0
	SE_W880i	2.0
Smart Phones	HTC_s710	2.0
	HTC_s730	2.0
	HTC_740	2.0
	HTC_HD2	2.1
Tablet	Moto-Zoom	2.1

2.3.4 Bluetooth Sensors

The Bluetooth sensors used in this study were obtained from Blip Systems. The sensor model is the BlipTrack, consisting of two directional antennae and one omnidirectional antenna, with a USB modem for 3G connectivity and an electricity connection. The typical detection zone of a BlipTrack sensor is shown in Figure 6. The size of the detection zone varies from 70-200m on either side of the sensor along the road. The sensors relay each detection event to a central server using their 3G connection. The clocks of the Bluetooth sensors were synchronised before the experiment.

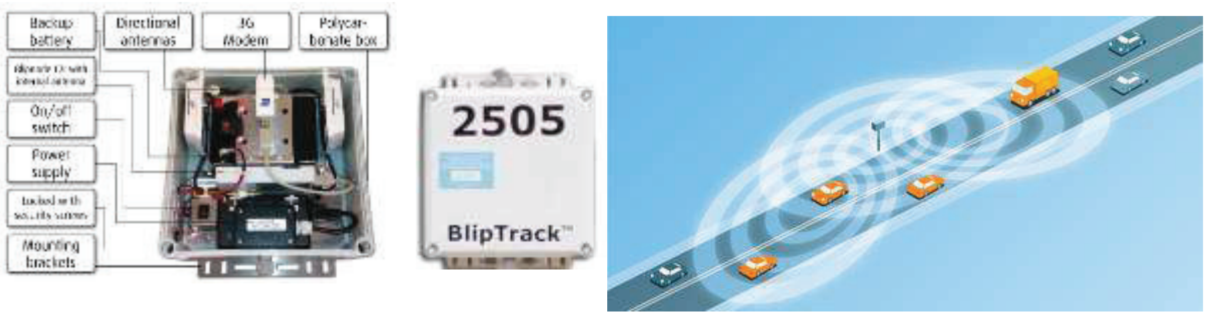

Figure 2-4. BlipTrack™ sensors and their detection zone (Source: Blip Systems)

2.3.5 GPS Data

In this study, GPS data was collected to conduct two sets of analysis:

First, GPS data were used to investigate how Bluetooth detection events are distributed around the sensor, depending on the size of the detection zone. In this case, GPS traces were used to geo-reference the Bluetooth detection events (i.e., determine the actual location of the detection event). The GPS device logged its position every second. The timestamps from the GPS device and Bluetooth sensors were matched with +/- 0.5 second accuracy, which at 70 km/h corresponds to approximately +/- 10-metre location ambiguity along the road. This level of accuracy was deemed sufficient in this context using engineering judgement.

2.3.6 Evaluation

First, reliability of Bluetooth detection was evaluated based on the number of missing devices per each trip. Second, in order to evaluate the impact of size of detection zone on location ambiguity, it was investigated how detection events were scattered around the sensor location. The matched GPS coordinate was used to calculate the distance, D_{de}, along the road between the Bluetooth sensor and the vehicle location during the detection event. In order to calculate the D_{de}, a hypothetical line is constructed perpendicular to the road at each sensor location, shown in Figure 8. The GPS coordinates (WGS84)[2] are converted to UTM coordinates so that the distances can be determined using simple geometric calculations. The distance between a detection event location (X_i,Y_i) and the hypothetical line $(A.X_i + B.Y_i + C = 0)$ is given by:

$$RD_{de} = \frac{|A.X_i + B.Y_i + C|}{\sqrt{A^2 + B^2}}$$ **Equation 2-1**

Where:
A: The coefficient of X
B: The coefficient of Y
C: The constant
(X_i,Y_i): The coordinates of the point

The coordinates and the formula for the hypothetical lines are given in Table 2-2.

Table 2-2. Points coordinates and the hypothetical line coefficients

Point	Coordinates		Coefficients		Formula
	X	Y	Slope	Constant	Hypothetical line
Skolevangs Alle	575799.374 575838.782	6228640.211 6228590.754	-1.2549	6951258.672	$Y_1 = -1.2549X_1 + 6951258.672$
Ellebjergvej	576407.015 576382.648	6228780.658 6228852.947	-2.9667	7938779.621	$Y_2 = -2.9667X_2 + 7938779.621$

Second, GPS data were used to evaluate the impact of location ambiguity on the accuracy of Bluetooth travel time estimates. In this case, GPS data were used to calculate the actual travel time, referred to as the ground truth. The ground truth data is used as the basis for evaluating the accuracy of Bluetooth travel time estimates. Discussions concerning travel time estimation methods by Bluetooth technology will be presented in Chapter 4.

---

[2] . WGS84: World Geodetic Systems 1984

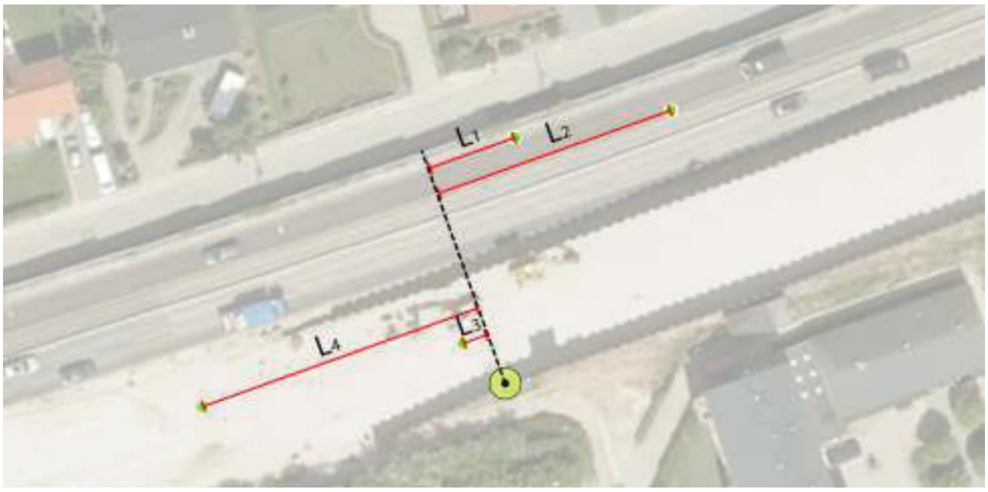

- - - - Hypothetical line ——— Perpendicular Distance

Figure 2-5. Hypothetical line and perpendicular line

2.4 Results

Results of the experimental evaluation are presented in following sections.

2.4.1 Detection Reliability Analysis

Raw detection metrics for each device trip combination is shown in Table 2-4 and Table 2-5 for the two sensor locations, where missed detections are shown as gaps in the tables. Using the data illustrated in the two tables, the percentage of successful detections per trip and for each device type is calculated; these percentages are also given in Table 2-4 and Table 2-5.

The analysis shows that, on average, Bluetooth-enabled devices are detected more than 80% of the time. However, there may be situations when this percentage is lower. It should be kept in mind that the low number of detection events recorded for some of the trips may not be directly related to the reliability of the Bluetooth-enabled devices. There might be other factors such as localisation factors (e.g., proximity to the roadside sensor, sensor's location and mount design, driving speeds, etc.); communication problems etc., which are likely to influence the detection rate. The differences between detection rates at the two sensors were examined further. Comparison shows that the roadside installation at Ellebjergvej (i.e. Eastern sensor) had a higher detection rate compared to the sensor installed on the median at Skolevangs Alle (i.e. Western sensor). The number of detection events recorded by each antenna at each location is given in Table 2-3.

Table 2-3. Number of detection events recorded by each antenna at each location

Location	Antenna	Number of Detection based on Trips Direction	
		Skolevangs Alle- Ellebjergvej	**Ellebjergvej- Skolevangs Alle**
Skolevangs Alle (Figure 2-2)	**West**	614	753
	East	632	1350
	Middle	19	191
	Total	**1265**	**2294**
Ellebjergvej (Figure 2-1)	**West**	991	736
	East	2408	1026
	Middle	297	63
	Total	**3696**	**1825**

Figure 2-6 clearly shows that the detection rate is lower when the vehicle is travelling in one direction compared to the other for each sensor location. This is due to the distance of the

sensor from the roadside, impact of inference caused by the pole as well as the antenna configuration. For the roadside installation (Figure 2-1), the detection rate is lower when the vehicle is travelling on the far side of the road. Similarly, for the median installation (Figure 2-2), the antennae face one direction of traffic (East-West) and the detection rate is lower when the vehicle is travelling on the other side (West-East) of the road. This is more apparent in the case of the central antenna because of occlusion due to the pole on which the Bluetooth sensor is mounted, see Figure 2-6.
The other factor that could explain the difference is road geometry, as the western sensor was installed at a curved section of the road. This can affect the detection range and hence reduce the rate of detection events. These findings outline the importance of the impact of antenna configuration, the location of the installed sensor and the mount design. These factors affect Bluetooth-enabled device detection rate and hence travel time reliability, especially for roads with high short-term travel time variability. These engineering aspects should be given due consideration in order to achieve reliable travel time estimates using Bluetooth sensors.

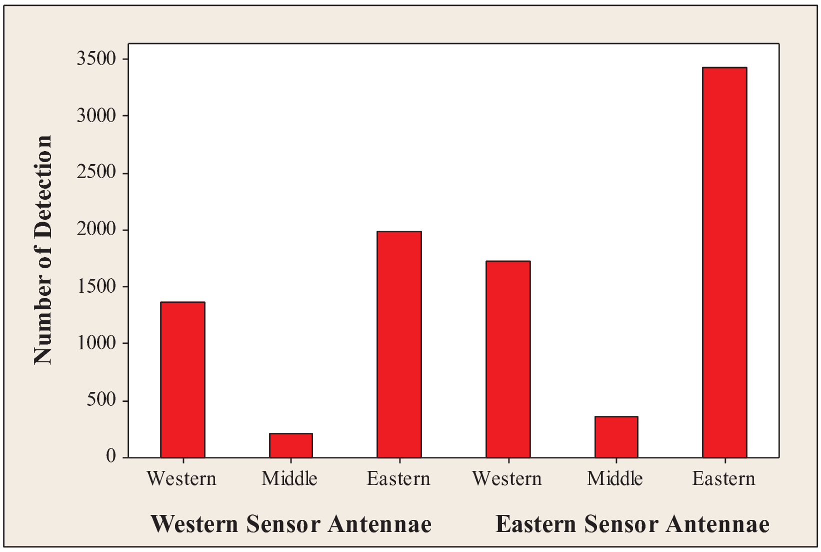

Figure 2-6. Number of detections for each antenna

Table 2-4. Reliability analysis of Bluetooth-enabled devices - Skolevangs Alle

Trip ID	Nr.detected Devices	Detection Rate	Nr.undetected Devices
1	18	100%	0
2	15	83%	3
3	18	100%	0
4	18	100%	0
5	16	89%	2
6	16	89%	2
7	15	83%	3
8	16	89%	2
9	18	100%	0
10	18	100%	0
11	18	100%	0
12	18	100%	0
13	13	72%	5
14	13	72%	5
15	13	72%	5
16	15	83%	3
17	18	100%	0
18	13	72%	5
19	18	100%	0
20	2	11%	16
21	16	89%	2
22	13	72%	5
23	18	100%	0
24	18	100%	0
25	7	39%	11
26	9	50%	9
27	18	100%	0
28	12	67%	6
29	18	100%	0
30	14	78%	4
31	18	100%	0
32	18	100%	0
33	16	89%	2
34	15	83%	3
35	18	100%	0
36	16	89%	2
37	17	94%	1
38	15	83%	3
39	15	83%	3
40	9	50%	9
41	12	67%	6
42	15	83%	3
43	14	78%	4
44	12	67%	6
45	15	83%	3
46	11	61%	7
47	18	100%	0
48	12	67%	6
49	15	83%	3
50	14	78%	4
51	13	72%	5
52	7	39%	11
53	17	94%	1
54	12	67%	6
55	17	94%	1
56	12	67%	6
57	18	100%	0
58	18	100%	0
59	16	89%	2
60	14	78%	4
61	15	83%	3
62	16	89%	2
63	12	67%	6
64	12	67%	6
65	17	94%	1
66	17	94%	1
67	15	83%	3
68	11	61%	7
69	16	89%	2
70	9	50%	9
71	16	89%	2
72	15	83%	3
73	11	61%	7
74	12	67%	6
Average	15	81%	3

Device	Nr. of missing detections per device	Percentage of missing	Average nr. Detection
Nokia_c1_01	6	8%	7
Nokia_c1_02	22	30%	4
Nokia_c1_03	11	15%	5
Nokia_c1_04	14	19%	5
Nokia_c1_05	20	27%	7
Nokia_c1_06	13	18%	7
Nokia_c1_07	10	14%	7
Nokia_c1_08	9	12%	5
Nokia_c1_09	19	26%	5
Nokia_c1_10	15	20%	6
Nokia_2960	8	11%	7
SE_W580i	11	15%	5
SE_W880i	6	8%	7
HTC_s710	23	31%	3
HTC_s730	20	27%	3
HTC_740	16	22%	5
HTC_HD2	18	24%	4
Moto-Zoom	12	16%	5

Table 2-5. Reliability analysis of Bluetooth-enabled devices - Ellebjergvej

Nr.undetected Devices	Detection Rate	Nr.detected Devices	Moto-Zoom	HTC_HD2	HTC_740	HTC_s730	HTC_s710	SE_W880i	SE_W580i	Nokia_2960	Nokia_c1_10	Nokia_c1_09	Nokia_c1_08	Nokia_c1_07	Nokia_c1_06	Nokia_c1_05	Nokia_c1_04	Nokia_c1_03	Nokia_c1_02	Nokia_c1_01	Trip ID
0	100%	18																			1
2	89%	16																			2
0	100%	18																			3
1	94%	17																			4
1	94%	17																			5
1	94%	17																			6
1	94%	17																			7
0	100%	18																			8
0	100%	18																			9
0	100%	18																			10
0	100%	18																			11
0	100%	18																			12
2	89%	16																			13
3	83%	15																			14
6	67%	12																			15
0	100%	18																			16
1	94%	17																			17
1	94%	17																			18
2	89%	16																			19
0	100%	18																			20
2	89%	16																			21
0	100%	18																			22
0	100%	18																			23
0	100%	18																			24
0	100%	18																			25
10	44%	8																			26
2	89%	16																			27
1	94%	17																			28
9	50%	9																			29
2	89%	16																			30
1	94%	17																			31
0	100%	18																			32
4	78%	14																			33
1	94%	17																			34
1	94%	17																			35
4	78%	14																			36
1	94%	17																			37
3	83%	15																			38
7	61%	11																			39
2	89%	16																			40
3	83%	15																			41
5	72%	13																			42
6	67%	12																			43
1	94%	17																			44
11	39%	7																			45
3	83%	15																			46
3	83%	15																			47
3	83%	15																			48
4	78%	14																			49
2	89%	16																			50
3	83%	15																			51
1	94%	17																			52
4	78%	14																			53
0	100%	18																			54
4	78%	14																			55
0	100%	18																			56
5	72%	13																			57
3	83%	15																			58
0	100%	18																			59
2	89%	16																			60
3	83%	15																			61
1	94%	17																			62
0	100%	18																			63
5	72%	13																			64
1	94%	17																			65
1	94%	17																			66
5	72%	13																			67
4	78%	14																			68
4	78%	14																			69
0	100%	18																			70
7	61%	11																			71
0	100%	18																			72
5	72%	13																			73
2	89%	16																			74
Average			9	13	7	17	17	5	11	8	10	10	6	5	3	4	14	13	18	3	Nr.of missing detections per device
2	87%	16	18%	18%	9%	23%	23%	7%	15%	11%	14%	14%	8%	7%	4%	5%	19%	18%	24%	4%	Percentage of missing
			9	13	7	17	17	5	11	8	10	10	6	5	3	4	14	13	18	3	Average nr. Detection

2.4.2 Location Ambiguity

The accuracy of travel time measured by Bluetooth sensors is influenced by the location ambiguity of detection events. The closer the detection event to the sensor location, the more accurate the estimate of the time that the device passes by the sensor, and correspondingly, the travel time estimate (see Figure 2-7). Hence, in order to understand the extent of location ambiguity, geo-referenced detection events were plotted on a map for visual inspection (see Figure 2-7). It is clear that the sensors have a large detection area. This is consistent with information from the product literature that the sensors have a detection range of 70-200m on either side of the sensor.

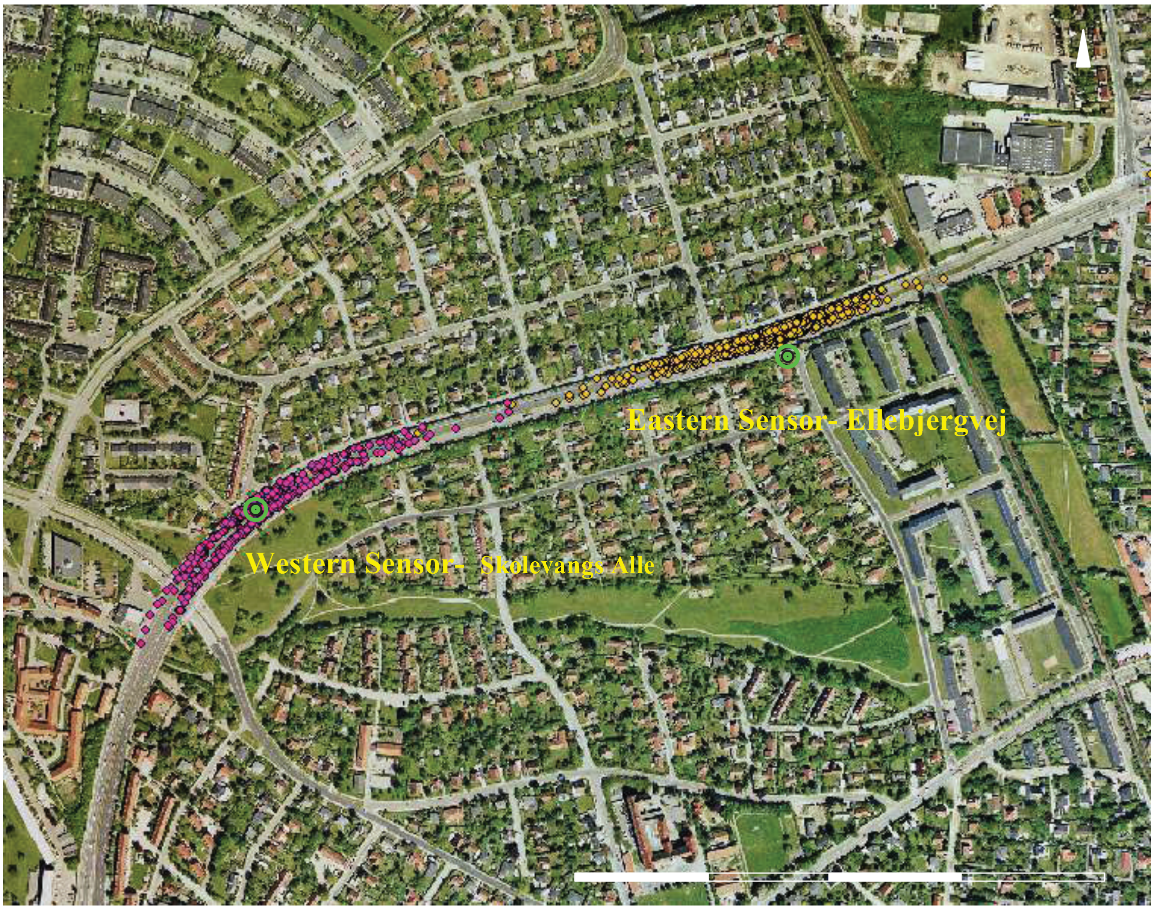

Figure 2-7. Geo-referenced detection events for both sensor locations (Source: Google Map)

The distribution of detection event location is further examined by means of boxplot charts, shown in Figure 2-8 and Figure 2-9. Each boxplot represent the lowest value, the highest value, the median or middle value, the first quartile value (i.e. the lowest 25-percent of the data), and the third quartile value (i.e. the highest 25-percent) of the data. Though most of the detection events are within the range specified in the product literature, the detection range can be as high as half a kilometre, as illustrated by detection events recorded by the antennae at the Ellebjergvej Eastern sensor. The width of the boxplots for middle antennae show that the collected data by this antennae were in the range of 100 metres before and after the sensor location while majority of

the detections were in a distance less than 50 metres. Larger spread in the of boxplots for the side antennae show a wider detection range and also the dot points spread out show that some of the detections were detected in a larger distance of up to 500 metres from the sensor. Hence there is a larger location ambiguity for the detections recorded by these antennae.
Results of the detection range analysis for three antennae are summarised in Table 2-6. For both sensors, it is clear that the middle antenna has a shorter detection range compared to the side antennae and correspondingly its detection rate is significantly lower than the side antennae. On one hand, the detection events recorded by the middle antenna are triggered in closer distances to the sensor (i.e., lesser location ambiguity); thus, it could provide a more accurate estimate of the time the device passes by the sensor.

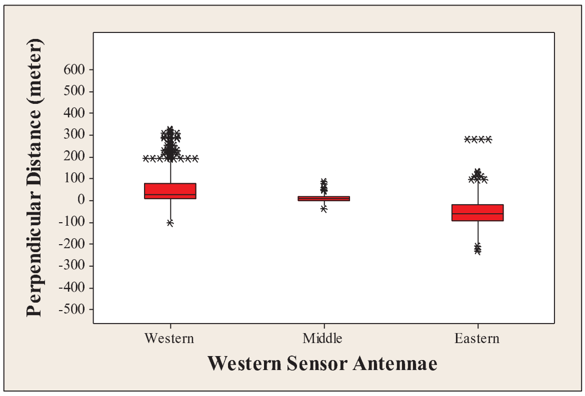

Figure 2-8. The detection range of three antennae at Skolevangs Alle-western sensor

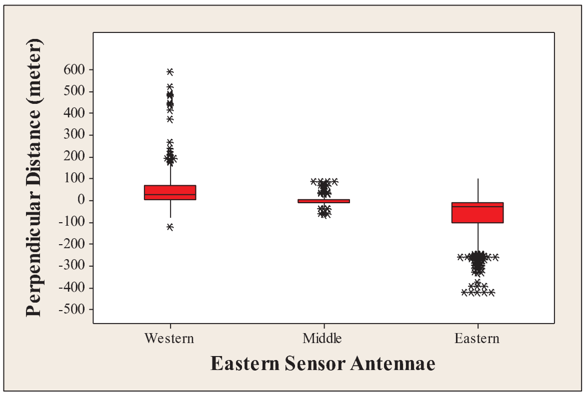

Figure 2-9. The detection range of three antennae at Ellebjergvej- eastern sensor

Table 2-6. Detection range of different antennae

Parameter		**Antenna Detection Range**					
		Skolevangs Alle			**Ellebjergvej**		
		Western	Middle	Eastern	Western	Middle	Eastern
Mean		54.24	14.51	64.00	45.85	14.58	65.75
Std. Error		1.61	0.91	1.03	1.25	0.79	1.21
95%Confidence Interval for Mean	**Lower Bound**	51.09	12.73	61.97	43.40	13.03	63.38
	Upper Bound	57.39	16.30	66.03	48.30	16.13	68.12
5% Trimmed Mean		47.14	13.14	61.42	40.25	12.38	58.60
Median		32.16	11.29	60.73	31.69	10.18	32.80
Variance		3527.24	172.42	2117.58	2700.28	223.34	5026.51
Std. Deviation		59.39	13.13	46.02	51.96	14.94	70.90
Minimum		0.21	0.69	0.43	0.74	0.73	0.73
Maximum		328.35	87.17	280.06	590.08	86.47	420.60
Range		328.14	86.48	279.63	589.34	85.74	419.88
Interquartile Range		65.78	11.96	69.50	59.30	8.35	94.11
Skewness		1.83	2.10	0.66	3.82	2.68	1.40
Kurtosis		3.62	6.74	0.47	26.91	8.13	1.78
Detection Rate		39%	6%	55%	31%	7%	62%

Distributions of detection range for various antennae are shown for western and eastern sensors in Figure 2-8and Figure 2-9. These illustrate how the detection ranges for different antennae vary around the sensor. Note that distance values (i.e., positive/negative) in these figures represent the direction from which the device was detected by each antenna (e.g., -50 means that the sensor detected the device 50 metres upstream of the actual sensor centre line). These results are obtained using raw detection events, which means all multiple detection events recorded for a unique MAC address in a single trip are used. For this reason, it should be kept in mind that the results obtained in this study are not directly related to the accuracy of travel time estimates by the BlipTrack hardware. Patterns shown in Figure 2-10 and Figure 2-11clearly indicate that the middle antenna has a shorter detection range and smaller standard deviation of detected events distances compared to the other antennae

The eastern and western antennae cover a larger detection zone, which concurrently increases the probability of detecting a larger number of passing Bluetooth-enabled devices at farther distances or vehicles with higher speed (i.e., increases detection rate), see also Figure 2-7. In order to further investigate how the detection events are scattered around the sensor, cumulative distributions of the distances are analysed. This helps to clarify what percentage of the detections fall within specific ranges such as 25, 50 and 100 metres. Cumulative distributions of detection range for three antennae are shown in Figure 2-12 and Figure 2-13for Western and Eastern sensors respectively[3].

Numerical results of the cumulative distribution of detection rates at 25, 50 and 100 metres, by various antennae are summarised in Table 2-7. As can be seen, more than 95% of the detections made by middle antennae are located within a distance of less than 50 metres from the centre of the sensors. This illustrates the accuracy and quality of the detections made by middle antennae. Detection events recorded by the side antennae are also closely distributed around the sensor. As shown, around 60% of the detections are made within 50 metres of the centre of the sensors. Moreover, 80% of the detections are within a 100-metre distance. These indicate that although the detection ranges for Bluetooth sensors' antennae are wide, they are capable of capturing most of the devices within an acceptable range of 50-100 metres (i.e., a low level of location ambiguity).

Table 2-7. Cumulative detection rate of the antennae at various distances

Distance (metre)	Detection Rate vs. Distance							
	Skolevangs Alle				Ellebjergvej			
	Western	Middle	Eastern	Total	Western	Middle	Eastern	Total
25	42%	82%	26%	35%	46%	85%	45%	48%
50	64%	99%	42%	54%	65%	95%	57%	62%
100	82%	100%	80%	82%	89%	100%	73%	80%

[3] . These figures also show that detection events obtained by middle antennae are scattered close to the centre of the sensor and most detections fall within a range of 50 metres. For this reason, it should be kept in mind that the results yielded by this methodology are not directly related to the accuracy of travel time estimates by the BlipTrack hardware. This is due to the fact that in practice, the system uses specific algorithms to select the most accurate detection event for an individual device recorded by each antenna. Then it interpolates the most accurate pass by time from this information.

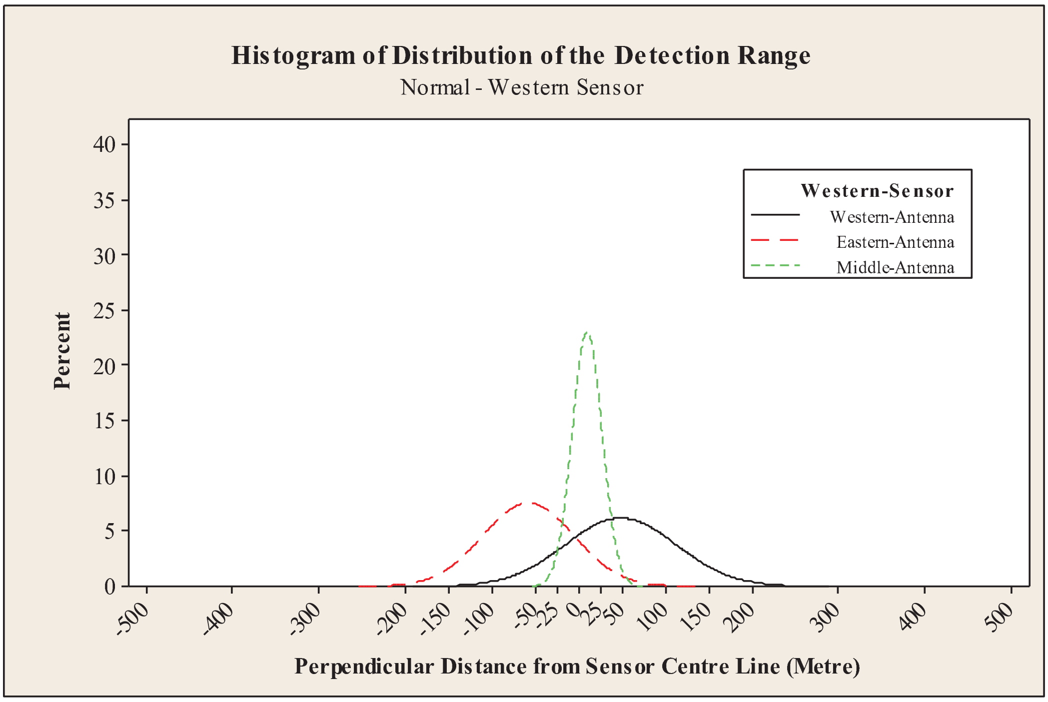

Figure 2-10. Histogram of distribution of detection range for three antennae of the sensor at Skolevangs Alle

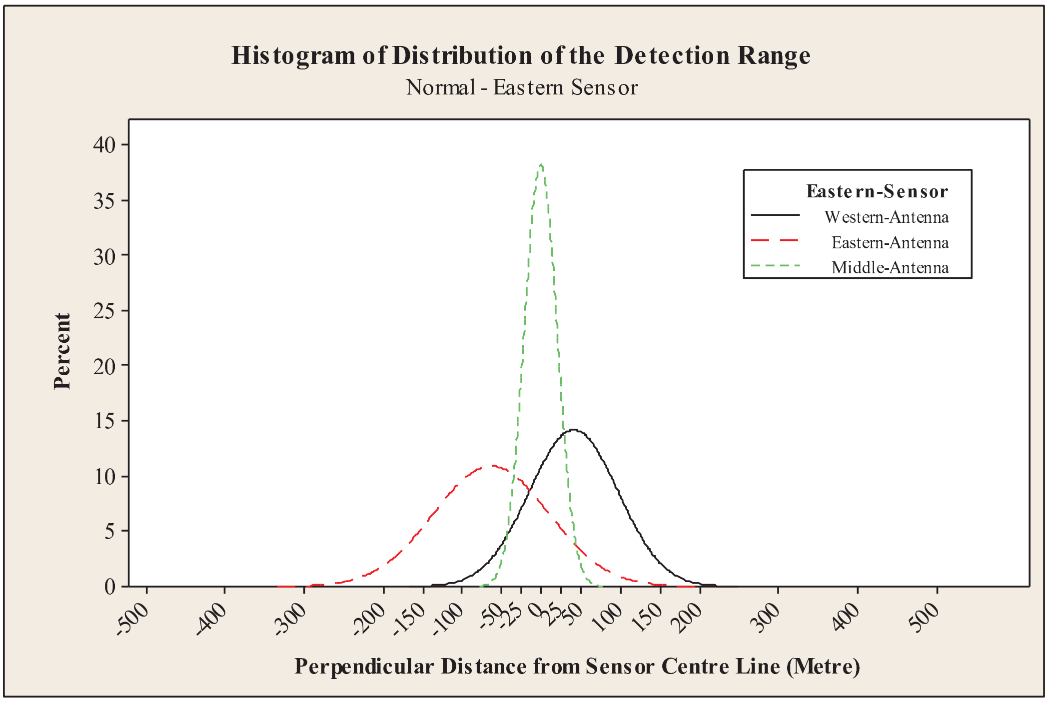

Figure 2-11. Histogram of distribution of detection range for three antennae of the sensor at Ellebjergvej

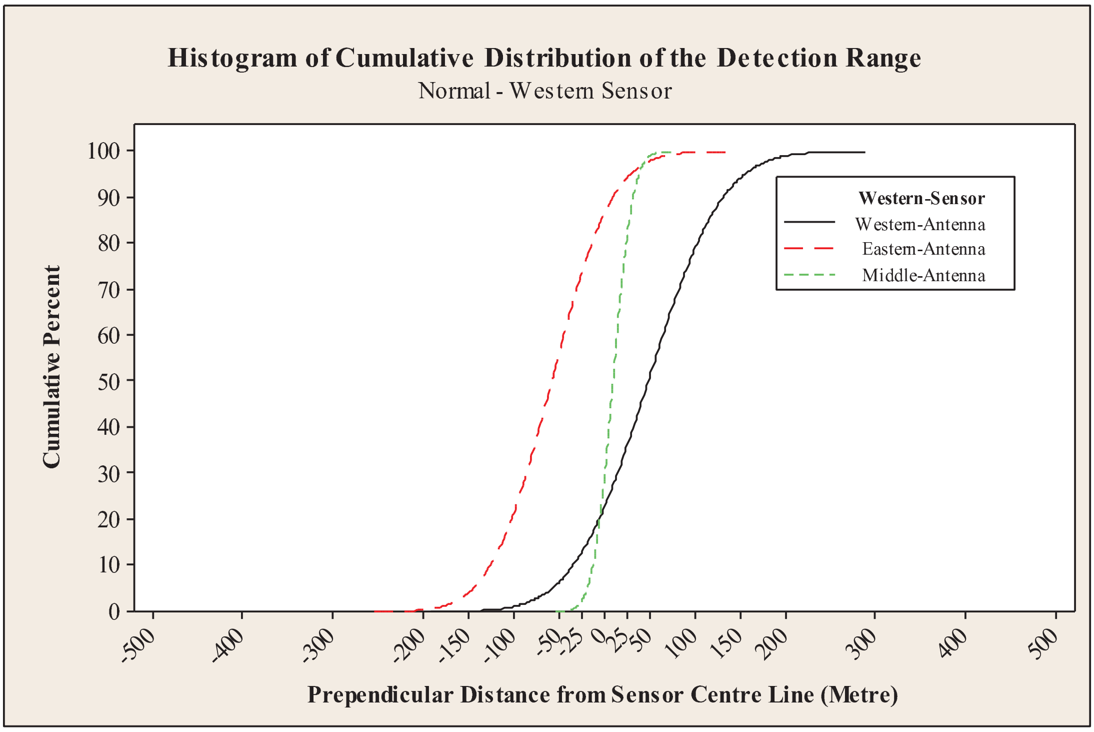

Figure 2-12. Cumulative distribution of detection range for three antennae, Western sensor

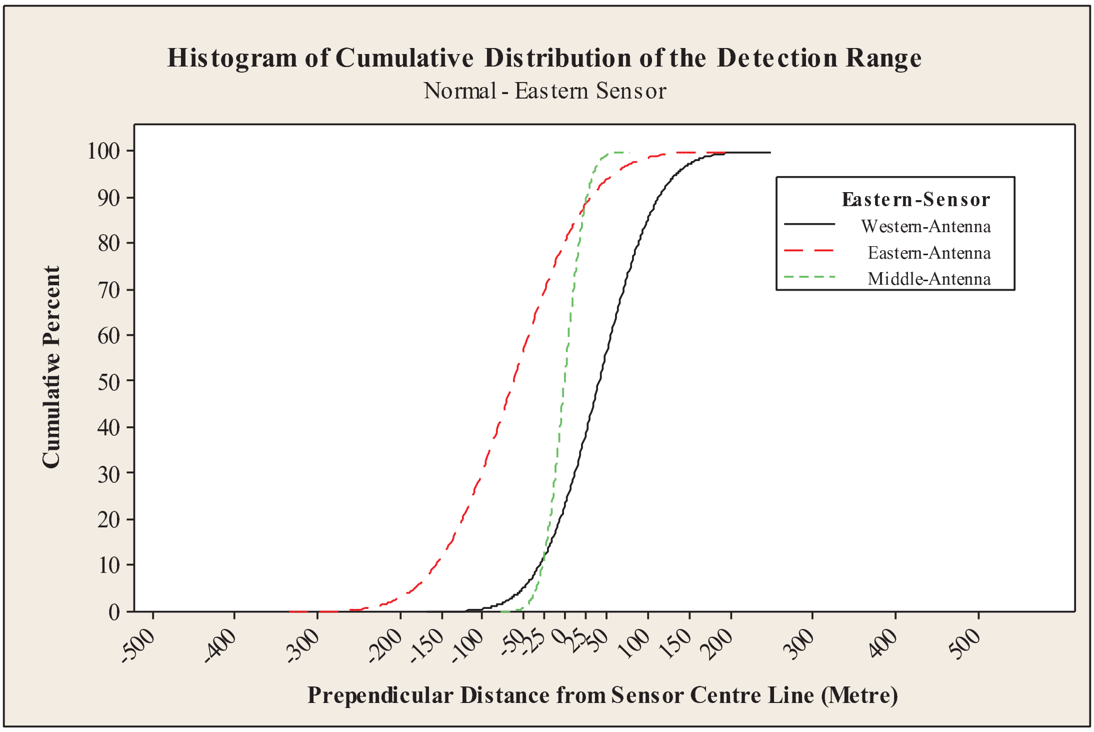

Figure 2-13. Cumulative distribution of detection range for three antennae, Eastern sensor

2.5 Conclusion

This chapter discussed different aspects of the reliability of Bluetooth detections and location ambiguity. The influence of Bluetooth sensors' detection zone size and discovery procedure on the number of detection events triggered for a single passing Bluetooth-enabled device (i.e. multiple detection events) were discussed. It was shown that while a larger detection zone increases the probability of detecting a vehicle travelling at high speed; it also contributes to a larger location ambiguity of multiple Bluetooth detections.

Based on the results of the controlled experiment, the detection reliability (i.e. capture rate) of Bluetooth was found 84%. However, the detection rate could be lower on some occasions. The difference in detection rates between the Eastern sensor and Western sensor illustrates the importance of the impact of the location of the installed sensor and the mount design. These factors could affect Bluetooth-enabled device detection rate. These engineering aspects should be given due consideration in order to achieve reliable results using Bluetooth sensors.

The relation between size of the detection zone and extend of the location ambiguity were evaluated by means of Geo-coded Bluetooth detections. The results showed that although the detection range of BlipTrack sensors is 70-200 metres on each side of the sensor, more than 80% of the detections are within the range of 100 meters from the sensor centre line.

According to the reasults of this chapter, there should be a trade-off between the size of detection zone and the optimum capture rate. The larger detection zone reduces the number of non-detected Bluetooth devices (i.e. missed detections) passing the sensors and correspondingly increases the capture rate. However, the larger detection zone could lead to a larger location ambiguity of the detected devices which could negatively influence the accuracy of estimated travel time.

As mentioned in Chapter 1, the low sampling rate of Bluetooth technology could ifluence the accuracy of travel time estimation. Lower sample size would increase the risk of outliers on the accuracy of aggregated travel time. In the following chapter, the effects of sample size and aggregation methods on travel time estimation will be discussed.

CHAPTER 3

THE EFFECT OF SAMPLE SIZES AND AGGREGATION METHOD ON TRAVEL TIME ESTIMATION

3. Aggregation Method and Associated Impact on Detection Reliability and Accuracy

Travel time data are usually reported in an aggregated form (e.g. average or reported travel time during a 5 minute period). The method used for aggregation of individual travel time observations could play a significant role in the accuracy of the estimated travel time. This issue is not limited to Bluetooth technology and is a common issue in travel time estimation using the principle of vehicle re-identification (e.g. ANPR).

Arithmetic mean (i.e. average) is one of the most common aggregation methods used for Bluetooth data analysis. The aggregated value is used either directly to create profiles of travel time or to be used as the basis for outlier detection algorithms (Quayle et. al. (2010); Haghani et. al. (2010); Malinovsky et. al. (2010); Barcelo et. al. (2010)). Weakness in the existing literature is that outlier treatment methods are mainly determined based upon the average value (Quayle et. al. (2010) and Malinovsky et. al (2010)). Nevertheless, using the average value as the basis of analysis can be misleading as the average itself can be affected by outliers. These outliers could be low-speed vehicles (i.e. heavy-trucks, bicycles) or high-speed vehicles (i.e. ambulances or police cars) in case of highways. As a result, the simple average is highly prone to the outliers. This issue is more pertinent to Bluetooth compared to ANPR since it is not possible to identify the type of a vehicle based on the MAC address. This highlights the importance of using more robust estimators as well as using appropriate outlier removal algorithms.

Determining minimum required sample size to obtain accurate and reliable travel time estimation is another issue in this context. The outlier bias becomes more important since Bluetooth has smaller sample size, especially when compared to technologies such as ANPR. Therefore, it is important to understand the relationship between sample size and accuracy of Bluetooth-based travel time estimation.

3.1 Aggregation Methods for Travel Time Profile Construction

A wide range of simple to complex aggregation methods can be considered for profile construction. In this study, three conventional aggregation methods: Arithmetic mean, Geometric mean, and Harmonic mean are investigated.

Arithmetic mean is the simplest method for aggregating the data over a time interval. However, existence of outliers in that interval could significantly influence the accuracy of the estimated travel time. Hence, it is imortant to understand how arithmetic mean differs from other aggregation method and also evaluate how it is influenced by the existence of outliers in the dataset. In this Chapter, arithmetic mean is indicated by the prefix (Ari).

Since the estimated travel time on each interval may not be independent from other, it is tried to examine whether implementing the geometric mean could reduce the impact of the outliers on Bluetooth-based estimated travel time. In this Chapter, geometric mean is indicated by the prefix (Geo).

Unlike the arithmetic mean, the harmonic mean gives less significance to high-value outliers– providing a truer picture of the central tendencies in data. Since, the harmonic mean tends strongly toward the least elements of the list, it may (compared to the arithmetic mean) mitigate the influence of large outliers and increase the weight of small values. In this Chapter, geometric mean is indicated by the prefix (Har). Formulae and details of these methods are given in Appendix II.

In this study, in order to figure out which method could provide more accurate and robust travel time estimates, the profiles constructed by each method is compared with FCD (i.e. ground truth). Since the two sources of FCD were aggregated for 15 and 30 minutes intervals, it is necessary to use the same time intervals for Bluetooth data. In order to estimate the 15 and 30 minutes travel time four simple estimation methods are used. These methods include minimum, maximum, average and median which are as follows:

1. Min-BT: Travel time estimate is the minimum travel time of all Bluetooth-based travel time observations during a given time period. The minimum travel time is unaffected by slower vehicles with non-typical driver behaviour and represents the fastest vehicle in normal traffic conditions. Min-BT is a good indicator for congestion detection applications.

$$\textit{Min-BT}= Minimum(TT_1, TT_2, TT_3, \dots, TT_n)_{15minutes} \qquad \textbf{Equation 3-1}$$

2. Max-BT: Travel time estimate is the maximum travel time of all Bluetooth technology based travel time observations during a given time period.

$$\textit{Max-BT}= Maximum(TT_1, TT_2, TT_3, \dots, TT_n)_{15minutes} \qquad \textbf{Equation 3-2}$$

3. Avg-BT: Travel time estimate is the average travel time of all Bluetooth-based travel time observations during a given time period. This method is used by most Bluetooth technology based travel time estimation studies. The average travel time is calculated based on all the records in a 15-minute time interval.

$$\textit{Avg-BT}= Average(TT_1, TT_2, TT_3, \dots, TT_n)_{15minutes} \qquad \textbf{Equation 3-3}$$

4. Med-BT: Travel time estimate is the median travel time of all Bluetooth-based travel time observations during a given time period. The median is less prone to outliers caused by slow or fast vehicles compared to the other estimators. Hence, it has the potential to be used as an alternative for the simple average travel time.

$$\textit{Med-BT}= Median(TT_1, TT_2, TT_3, \dots, TT_n)_{15minutes} \qquad \textbf{Equation 3-4}$$

Where:
TT_i: Travel Time for i^{th} recorded vehicle calculated based on the median of multiple travel time detections $TT_i = Median(tt_{i1}, tt_{i2}, tt_{i3}, \dots, tt_{im})_{i^{th}-Vehicle}$
m: The different values of travel time recorded for i^{th} vehicle according to the multiple detection
n: The total number of recorded vehicles in each 15-minute time interval

3.2 Sample Size for Travel Time Estimation

In order to evaluate the impact of sample size on the accuracy and reliability of the estimators, two main approaches are adopted as follows:

- Approach 1 (App.1): All time intervals are included in profile construction
- Approach 2 (App.2): Only time intervals with sample size more than 30 are included in profile construction

The results of the two approaches are compared. An estimator is considered to be robust when its accuracy is high and also less influenced by the sample size changes. The methods of accuracy evaluation are explained in section 3.3. For further exploring the impacts of sample size on the accuracy of travel time, a sensitivity analysis is conducted on a range of sample sizes from 0 to 30. For testing the accuracy and robustness of different estimators, both qualitative (i.e. visual) and quantitative (i.e. accuracy measures) statistical methods are used which are explained in the next section.

3.3 Experiment Set-up and Evaluation

In order to evaluate the impacts of aggregation methods as well as estimating the optimum sample size for aggregation two experiments were conducted. Both experiments were on a same site but over two different time periods. First experiment was conducted over the period of 2 years (i.e. mid 2006-mid 2008) and the second experiment was over the period of 1 month (4th January 2010 - 4th February 2010). Details of the two experiment are presented in following sections. In both experiments, Floating Car Data (FCD) collected to be used as a ground-truth in order to evaluate the accuracy of the estimates obtained by various agregation method using Bluetooth data.

3.3.1 Location of the Experiment

A section 5 km in length on the E45 motorway between Forbindelsesvejen and Humlebakken including Limfjord tunnel was selected as the study route, see Figure 3-1. The Average Daily Traffic (ADT) for North-South and South-North directions were 45400 and 51100 respectively. Considering the maximum speed of 130km/h and minimum speed of 80 km/h in the E45 motorway the expected range of travel time would be about 138.5 second to 225 seconds. As shown, the study route has four main entrances and exits points.

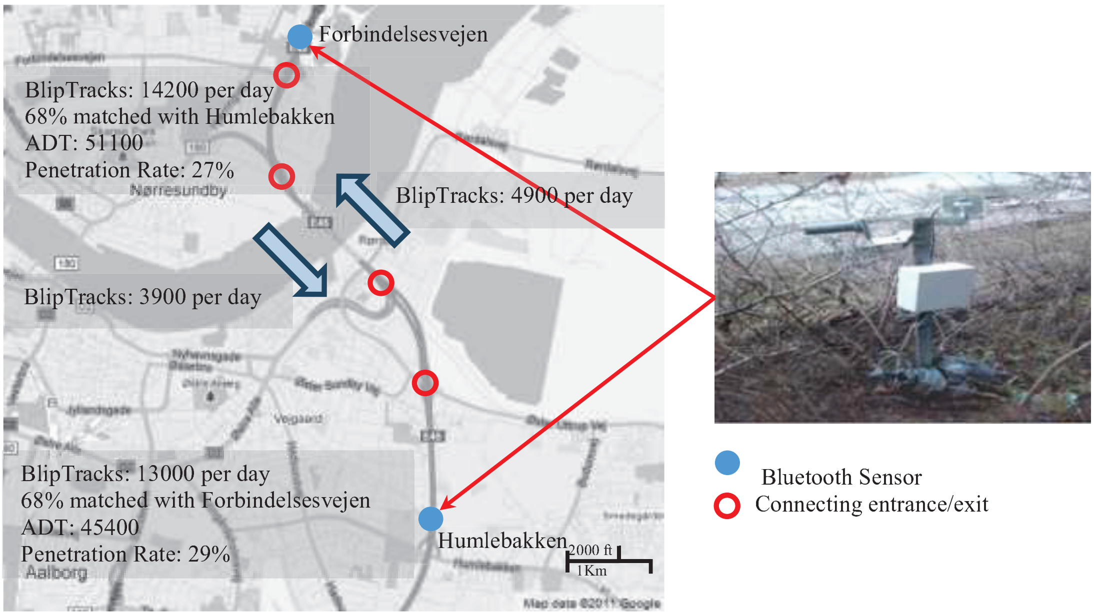

Figure 3-1. Study area and location of Bluetooth sensors (Google Map)

3.3.2 Ground Truth

Two sets of FCD are used as the ground truth, namely GPS-V1 and GPS-V2.

3.3.2.1 GPS-V1

The first set of FCD was collected as a part of a evaluation research project on Intelligent Speed Adaptation (Lahrmann et al. 2010). The FCD was collected using GPS traces received from 152

motor vehicles over a period of 2 years (i.e. mid 2006-mid 2008). The averages of GPS traces were aggregated for 15-minute intervals during the day to create a GPS travel time profile.
Figure 3-2 and Figure 3-3 show the time plots of the FCD. It can be seen that there is a morning peak for North-South direction and an afternoon-peak for the South-North direction. It is assumed that there are no major changes in traffic patterns over the period of the study and the travel time profiles created using Bluetooth and FCD data are comparable.

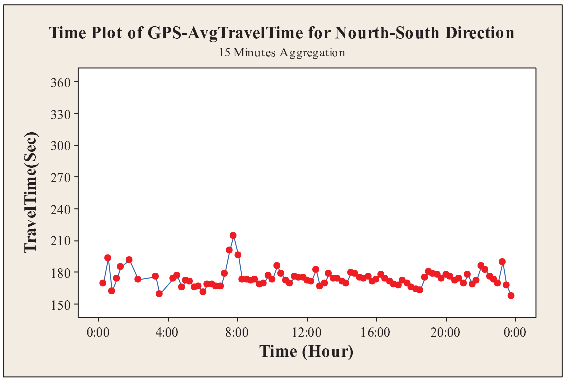

Figure 3-2. Time plot of GPS-V1 Avg-travel time for North-South direction

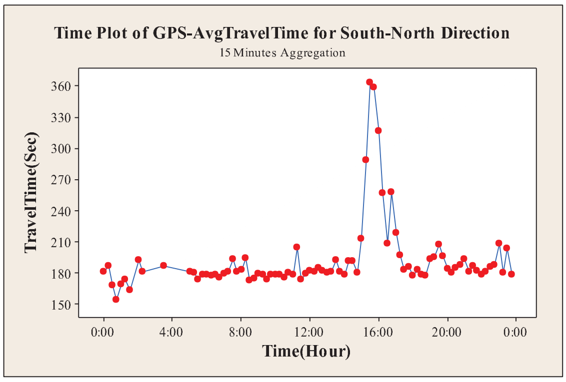

Figure 3-3. Time plot of GPS-V1 Avg-travel time for South-North direction

3.3.2.2 GPS-V2

The second set of FCD was obtained from the Danish Road Directorate (DRD). The DRD uses GPS data from a number of different types of vehicles. A total of 800 vehicles are currently delivering data, for further information refer to Holm et al. (2009) and Holm et al. (2011). The dataset obtained from DRD is based on the GPS traces recorded over the period of 4th January 2010 through 4th February 2010. The averages of GPS traces were aggregated for 30-minute intervals during the day to create the GPS travel time profile. Figure 3-4 and Figure 3-5 show the time plots of the FCD.

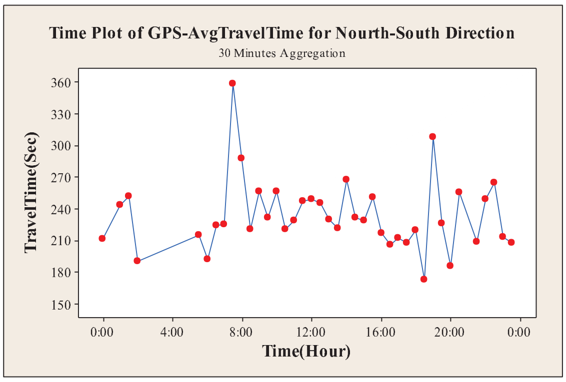

Figure 3-4.Time plot of GPS-V2 Avg-travel time for North-South direction

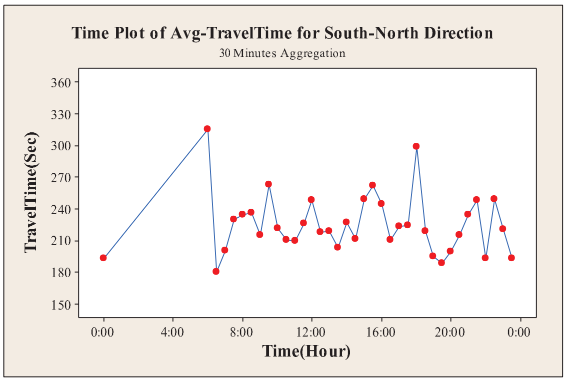

Figure 3-5. Time plot of GPS-V2 Avg-travel time for South-North direction

3.3.2.3 Bluetooth Data

BlipTrack sensors from Blip Systems were used in this study to collect Bluetooth data. Due to the specific configuration of BlipTrack's antennae, these sensors are able to provide time-stamped and directional information for passing Bluetooth devices through a back-end server. Bluetooth travel

time data were collected through two Bluetooth sensors installed alongside the roadway at the bases of the guard rail posts.
The position of the Bluetooth sensors is shown in Figure 3-1. Bluetooth data were collected during a one-month period between 4th January 2010 and 4th February 2010. In order to avoid the problem of multiple detections by Bluetooth sensors, for travel time estimation, the median of the recorded timestamps for a single MAC address was used at each Bluetooth sensor as time pass-by.
It is assumed that there are no major changes in traffic patterns over the period of mid 2006-mid 2008 and the travel time profiles created using Bluetooth and FCD data are comparable.

3.3.3 Accuracy Evaluation

The accuracy analyses are conducted in two phases. In Phase (1) the Bluetooth dataset for the whole month period, including the data recorded during weekends, is used for the initial analysis. In Phase (2), data from weekends are removed from the analysis before calculating the average daily profile of travel time data.

3.3.3.1 Qualitative Analysis Using Probability Plots and Time Plots.

In order to compare the distribution of BT versus GPS datasets, in Phase (1) probability plots are used. A P-P plot shows a variable's (i.e. travel time) cumulative probability against the cumulative probability of the test or reference distribution. The straighter the line formed by the P-P plot, the more the variable's distribution conforms to the test distribution [8].
The normal probability plot is formed by:

- Vertical axis: represents the observed values
- Horizontal axis: represents the expected outcomes

Being normally distributed provides a wide range of opportunities for using parametric statistical tests to analyse the data. Moreover, based on knowledge of normal distribution (μ,σ) it is possible to model travel time variation and to predict short-term travel time for the intervals with low sample size and missing values. Hence, in this study, BT, GPS-V1, and GPS-V2 travel time data are tested against normal distribution.
These P-P plots provide a visual comparison of how the both sources of the data are spread out in comparison to the normal distribution hypothetic line. At the same time, the P-P plots show how the BT and GPS-V1, and GPS-V2 are matched. The match or coverage rate between BT, GPS-V1, and GPS-V2 is considered as the proportion of the data that overlap each other. The candidate BT estimator is the one that has a better match with GPS-V1 and GPS-V2 compared to the others.
In addition, time plots are used for visual comparison. Time plots are used to compare the Bluetooth-based travel time profile with the travel time profile of GPS-V1 and GPS-V2. This method could represent the variation of Bluetooth-based travel time profiles in comparison to the ground truth over the course of a day.

3.3.3.2 Quantitative Analysis of Accuracy

In order to have a numerical evaluation of the accuracy of Bluetooth travel time estimation, three accuracy measures are used. These metrics include Mean Percentage Error (MPE), Mean Absolute Percentage Error (MAPE) and Root Mean Squared Error (RMSE). These measures represent the variation of estimations (i.e. Bluetooth) from the ground truth (i.e. FCD).

$$MPE = 100.\frac{1}{N}\sum_{i=1}^{N}\frac{(\widehat{T} - T_i)}{T_i}$$ **Equation 3-5**

$$\mathrm{MAPE} = 100.\frac{1}{\mathrm{N}}\sum_{\mathrm{i}=1}^{\mathrm{N}}\frac{|\widehat{\mathrm{T}} - \mathrm{T_i}|}{\mathrm{T_i}}$$ **Equation 3-6**

$$\mathrm{RMSE} = \sqrt{\frac{1}{\mathrm{N}}\sum_{\mathrm{i}=1}^{\mathrm{N}}(\widehat{\mathrm{T}} - \mathrm{T_i})^2}$$ **Equation 3-7**

Where:
$\boldsymbol{N}$: The total number of observed time periods
$\boldsymbol{T_i}$: Travel time during the i^{th} time period generated using GPS dataset
$\widehat{\boldsymbol{T}}_i$: Estimated mean travel time during the i^{th} record using Bluetooth technology

In order to determine the impact of sample size, App.1 and App.2 were implemented. In the first approach (App.1), profile values from all the 15-minute intervals were included in the evaluation of accuracy metrics. In the second approach (App.2), data from all intervals with fewer than 30 records in the Bluetooth dataset were excluded before the BT travel time profile was created. Intervals with no observations recorded for GPS-V1 and GPS-V2 are also excluded from analysis. In order keep the profiles compatible, the corresponding intervals from Bluetooth dataset are also excluded from analysis, respectively.

3.4 Results

Results of the analysis for Phase (1) and Phase (2) are summarised in the following section. Phase (1) used the unfiltered Bluetooth dataset to examine the impact of outliers and determine the most robust estimation methods. In Phase (1) the Bluetooth data were aggregated using arithmetic mean over 15-minute and 30-minute time intervals. Two sets of analyses were conducted in Phase (1): qualitative analysis using PP-Plots and quantitative accuracy analysis using accuracy metrics.
In Phase (2), after filtering the Bluetooth dataset, the arithmetic mean, geometric mean and harmonic mean were used to aggregate the data over 15-minute and 30-minute time intervals. In Phase (2) also, two sets of analysis were conducted in order to define the most accurate method. First, the Bluetooth-based travel time profiles were compared with GPS-V1 and GPS-V2. Second, the accuracy metrics for these methods were calculated.

3.4.1 Results of Analysis in Phase (1):

Phase (1) concerns initial analysis of the whole month period including data recorded in weekends. In this phase, Bluetooth-based travel time is only estimated using arithmetic mean.
The main objective of this phase was to evaluate the impact of sample size more than 30. Results of the average and standard deviation of various estimators are summarised in Table 3-1. Results show that by removing the intervals that have a sample size of fewer than 30, a number selected using engineering judgement to illustrate the hypothesis, the standard deviation of the Bluetooth-based estimations was reduced significantly. The same pattern was observed for GPS-V2. However, removing the intervals with low sample size from GPS-V1 resulted in increasing the standard deviation. In App.2, the difference between the mean values of Min-BT, Med-BT and

Avg-BT with GPS-V1 and GPS-V2 reduced, while the difference between mean values for Max-BT with GPS-V1 and GPS-V2 increased.

Table 3-1. Mean and Std. deviation of Bluetooth estimations for App.1 and App.2

Direction	Travel Time Estimator	Mean (sec)		Std. Deviation (sec)	
		App.1	App.2	App.1	App.2
South-North	AriMin-BT	194.97	182.44	321.21	132.31
	AriMax-BT	7867.77	10102.48	5234.13	4184.4
	AriAvg-BT	927.41	986.76	802.24	612.12
	AriMed-BT	290.51	248.18	576.07	262.12
	Avg-GPS-V1	192.29	202.53	35.26	47.01
	Avg-GPS-V2	215.96	224.96	30.18	28.74
North- South	AriMin-BT	190.30	168.44	191.47	27.746
	AriMax-BT	2005.7	2622.56	1241.95	936.03
	AriAvg-BT	379.94	349.72	270.69	102.32
	AriMed-BT	257.57	218.35	250.99	47.83
	Avg-GPS-V1	174.39	175.30	8.63	9.688
	Avg-GPS-V2	223.05	233.90	39.31	33.73

3.4.1.1 Results for Qualitative Analysis Using Probability Plots

In phase (1), the qualitative (P-P plots) and quantitative (accuracy measures) analysis are performed for both directions for App.1 and App.2 and also for both GPS-V1 and GPS-V2 respectively. In first step, normal probability plots are fitted to the data (Figure 3-6 and Figure 3-7). In general, results of the P-P plots (for both directions and App.1 and App.2) reflect that at 95% confidence level (CI) neither Bluetooth nor GPS-V1 and GPS-v2 follow the normal distribution. In other words, travel time obtained by Bluetooth and FCD are not normally distributed.

The visual comparison between GPS-V1 and GPS-V2 and Bluetooth also show that the Min-BT and Med-BT have a better match with GPS-V1 and GPS-V2 compare to Max-BT and Avg-BT. Results of the P-P plots for App.2 show a slightly better match between data compared to App.1. However, this needs to be evaluated quantitatively. A similar pattern was observed for the North-South direction is shown, which is not presented in this study. PP-Plots of Bluetooth vs. GPS-V1 and GPS-V2 for South-North direction are presented in Figure 3-6and Figure 3-7.

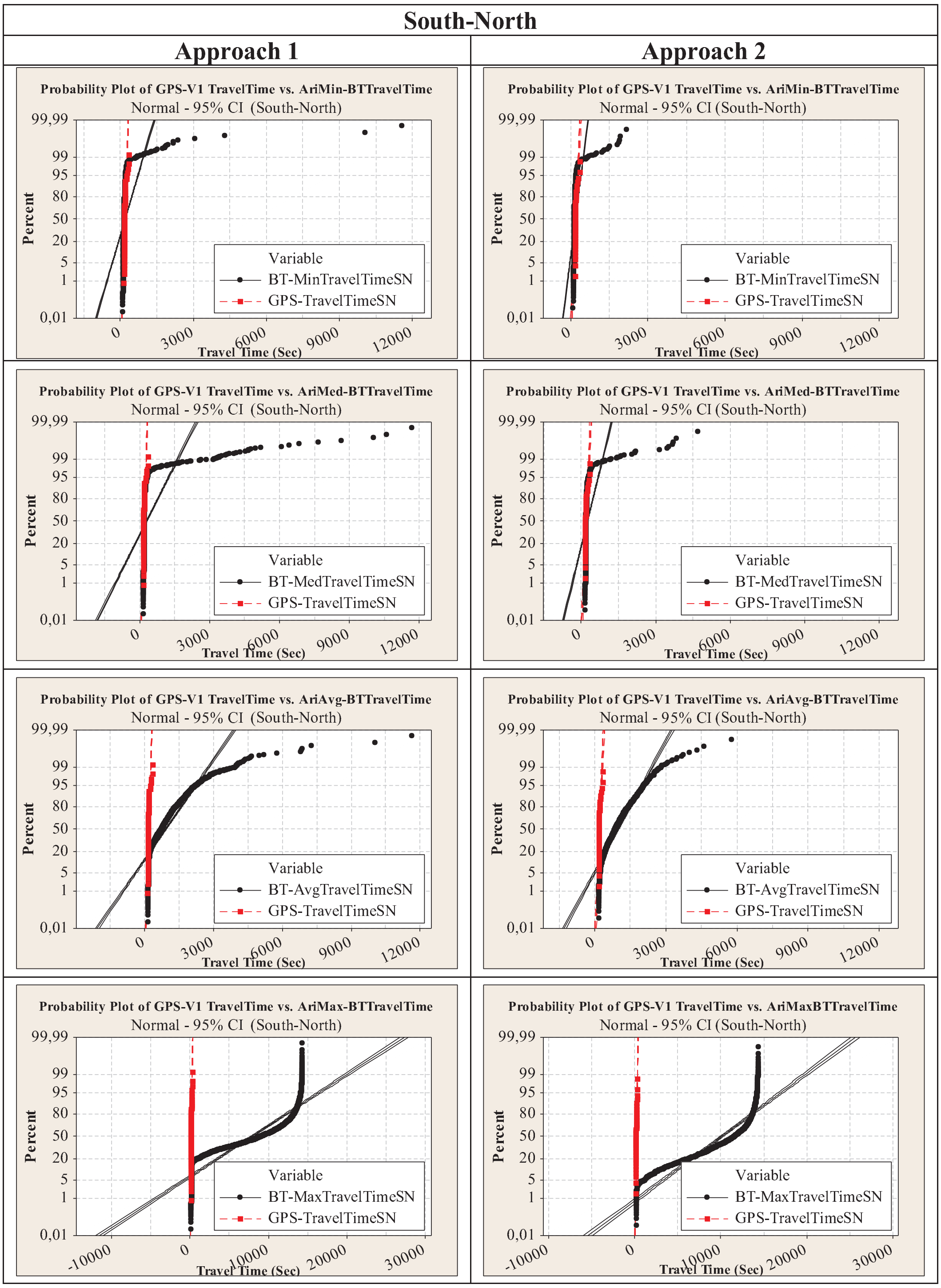

Figure 3-6. Probability plots of GPS-V1 travel time vs. Bluetooth (South-North)

South-North

Approach 1	Approach 2

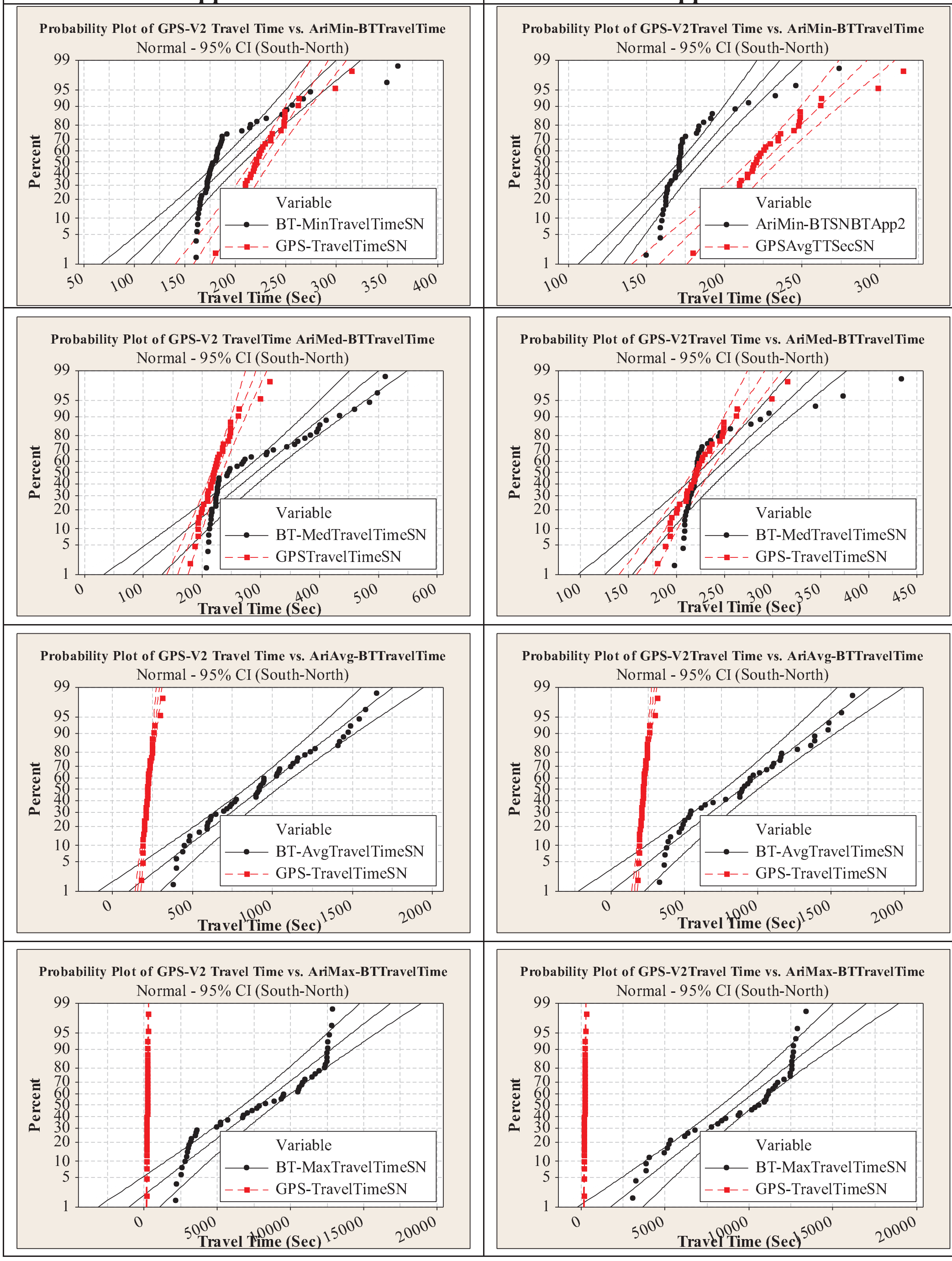

Figure 3-7. Probability plots of GPS-V2 travel time vs. Bluetooth (South-North)

3.4.1.2 Results for Quantitative Analysis Using Accuracy Measures

In the second step, the accuracy of Bluetooth estimations are evaluated using MPE, MAPE and RMSE metrics seperately for two cases where GPS-V1 and GPS-V2 used as ground truth (see Table 3-2 and Table 3-3). These accuracy metrics also confirm that the Min-BT gives the most accurate estimates of the travel time followed by Med-BT for both directions. This clearly is consistent with the outputs of P-P plots (Figure 3-6 and Figure 3-7). These results presented in the tables highlight the accuracy of Bluetooth-based travel time estimation and also show that Min-BT and Med-BT have the potential to be used as an alternative method for Avg-BT.

In general, App.2 shows better accuracy compared to App.1. This underscores the importance of sample size in travel time estimation. It is clear from the positive values of MPE that Bluetooth tends to over-estimate the travel time for both directions.

The close match between travel time profiles generated using Bluetooth and GPS-V1 and GPS-V2 data confirms our assumption concerning the validity of using Bluetooth data for travel time estimation. Results also show that the variance of Bluetooth based travel time estimates are significantly higher than that of GPS-V1 and GPS-V2 (Table 3-1). This also can be attributed to the larger detection zone, the low penetration rate of Bluetooth and route choice ambiguity of vehicles sensed by Bluetooth sensors. These results are in line with the results of a previous study in the United States (Malinovsky et. al. 2010).

Table 3-2. Accuracy measures of Bluetooth estimations for 15 minutes aggregation, GPS-V1 used as the ground truth

Direction	Travel Time Estimator	MPE (%)		MAPE (%)		RMSE (sec)	
		App.1	App.2	App.1	App.2	App.1	App.2
South-North	AriMin-BT	**3.04**	**-6.89**	**15.58**	**11.15**	**64.88**	**33.00**
	AriMax-BT	4286.00	4813.12	4286.00	4813.12	9013.29	9903.91
	AriAvg-BT	401.74	371.29	401.74	371.29	844.21	808.84
	AriMed-BT	**50.75**	**24.12**	**51.29**	**24.72**	**151.39**	**62.35**
North- South	AriMin-BT	**7.32**	**-3.66**	**11.27**	**5.50**	**41.63**	**11.48**
	AriMax-BT	1089.52	1325.81	1089.52	1325.81	2026.46	2373.46
	AriAvg-BT	113.19	95.44	113.19	95.44	213.21	174.53
	AriMed-BT	**43.05**	**25.73**	**43.05**	**25.73**	**98.61**	**49.99**

Table 3-3. Accuracy measures of Bluetooth estimations for 30 minutes aggregation, GPS-V2 used as the ground truth

Direction	Travel Time Estimator	MPE (%)		MAPE (%)		RMSE (sec)	
		App.1	App.2	App.1	App.2	App.1	App.2
South-North	AriMin-BT	**-14.03**	**-19.36**	**19.82**	**20.50**	**57.71**	**58.03**
	AriMax-BT	4104.95	4278.21	4104.95	4278.21	9614.12	9954.21
	AriAvg-BT	350.56	320.22	350.56	320.22	854.97	798.65
	AriMed-BT	**23.83**	**7.67**	**29.32**	**15.49**	**96.87**	**55.71**
North- South	AriMin-BT	**-19.88**	**-27.93**	**23.96**	**27.93**	**67.11**	**73.29**
	AriMax-BT	826.40	964.33	826.40	964.33	2027.15	2299.70
	AriAvg-BT	59.56	45.66	59.63	46.66	152.21	115.78
	AriMed-BT	**6.02**	**-6.82**	**17.09**	**10.09**	**69.27**	**33.66**

3.4.2 Results of Analysis in Phase (2):

3.4.2.1 Results for Qualitative Analysis Using Time Plots

In Phase (2) analysis are conducted for weekdays and weekends records are excluded from analysis. For the South-North direction, the Bluetooth-based travel time profile is compared with the corresponding GPS dataset (see Figure 3-8 through Figure 3-11). Results of the North-South direction are presented in Appendix II.. Comparisons of all the estimation methods are shown in graphs (a). In order to have a detailed view of how Min-BT and Med-BT are scattered around the ground truth, the time plot for these estimators are also separately presented in graphs (b) in a more zoomed view. The results clearly confirm the observations in Phase (1). Min-BT and Med-BT still have the best concurrence with GPS-V1 and GPS-V2 compared to Avg-BT and Max-BT. The time plots clearly show how Avg-BT is influenced by extreme values in the interval and could be significantly biased. Moreover, implementations of the harmonic mean and geometric mean tend to reduce the impact of outliers in the dataset and provide a better similarity between Bluetooth estimates and GPS-V1 and GPS-V2 profiles.

a: Comparison of Min-BT, Max-BT, Avg-BT and Med-BT for three aggregation technique

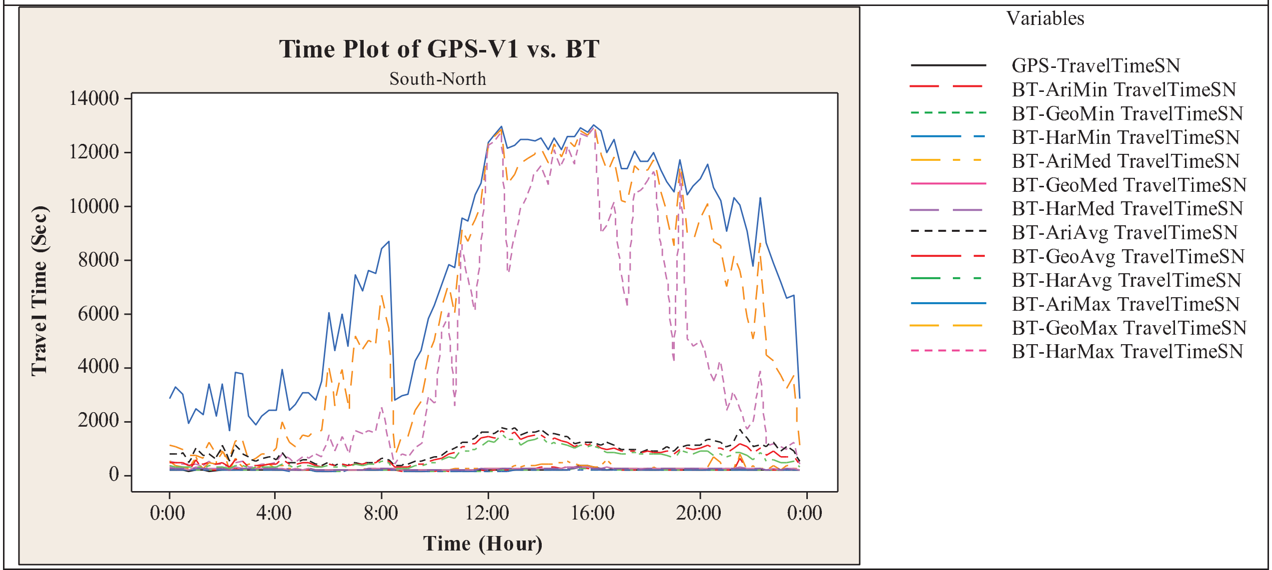

b: Comparison of Min-BT, and Med-BT for three aggregation technique

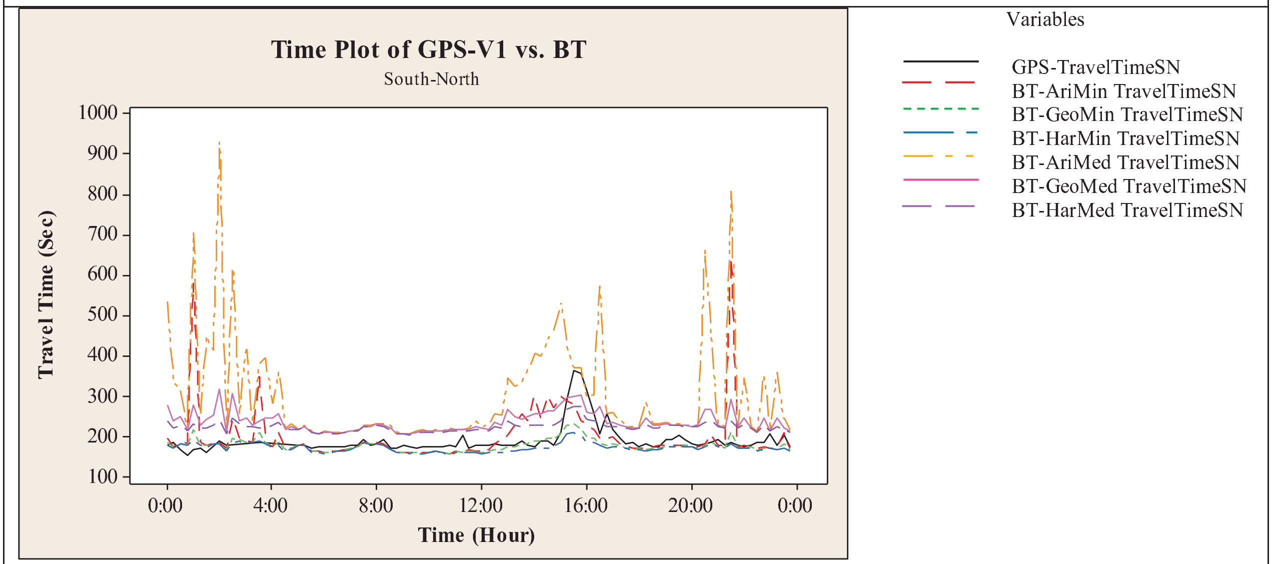

Figure 3-8. Time plot of GPS-V1 vs. BT travel time estimates for App.1 for South-North direction

a: Comparison of Min-BT, Max-BT, Avg-BT and Med-BT for three aggregation technique

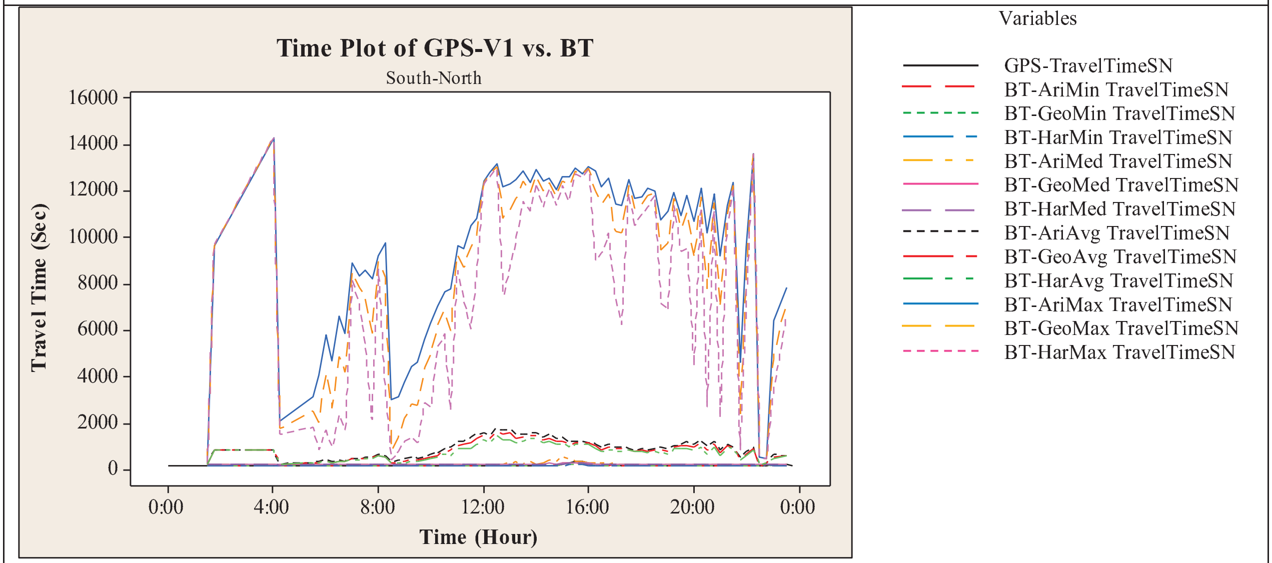

b: Comparison of Min-BT, and Med-BT for three aggregation technique

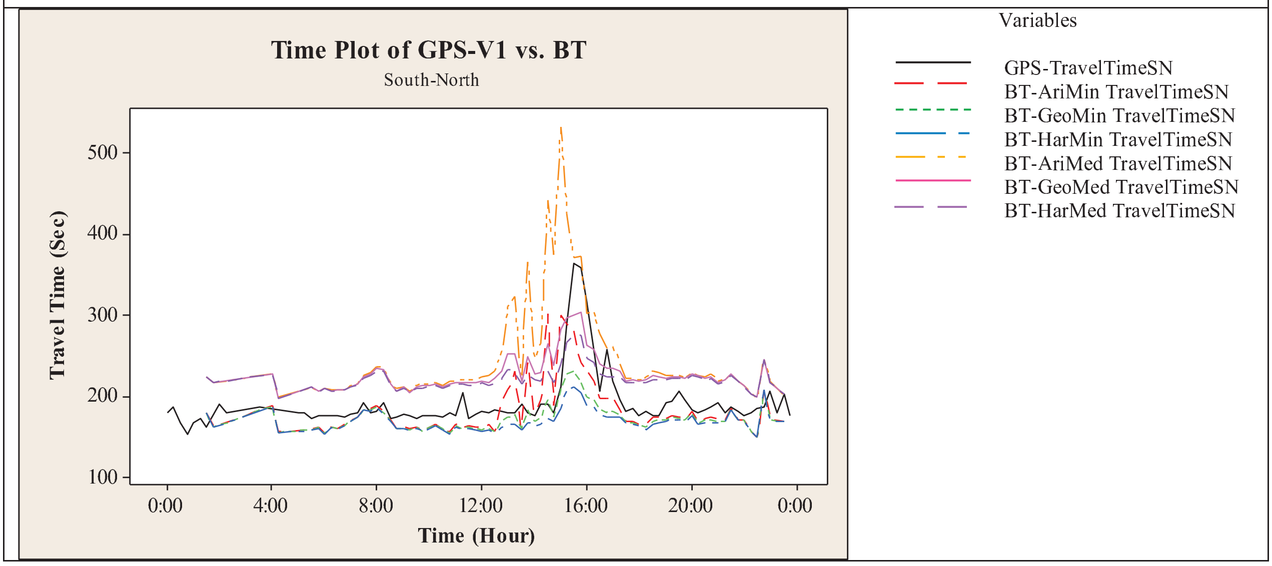

Figure 3-9. Time plot of GPS-V1 vs. BT travel time estimates for App.2 for South-North direction

a: Comparison of Min-BT, Max-BT, Avg-BT and Med-BT for three aggregation technique

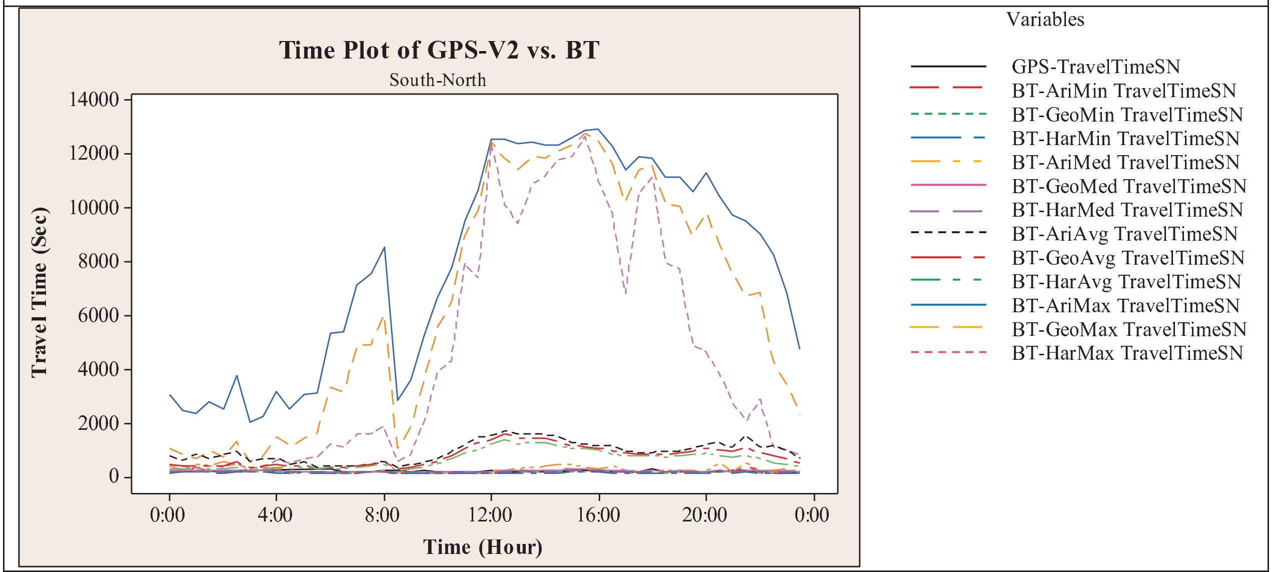

b: Comparison of Min-BT, and Med-BT for three aggregation technique

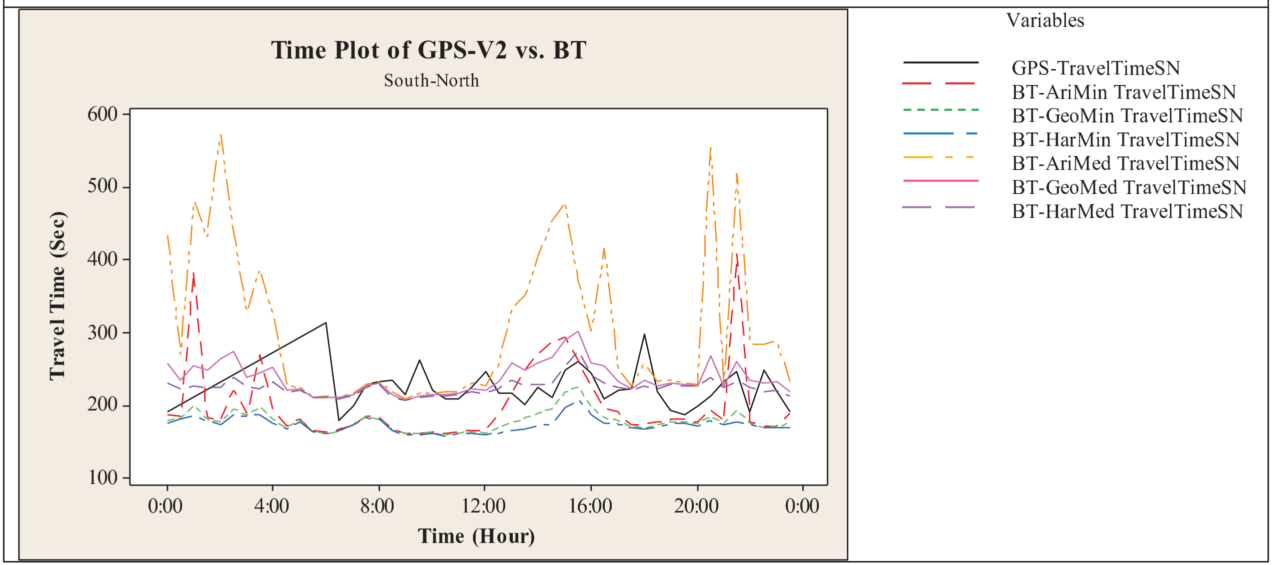

Figure 3-10. Time plot of GPS-V2 vs. BT travel time estimates for App.1 for South-North direction

a: Comparison of Min-BT, Max-BT, Avg-BT and Med-BT for three aggregation technique

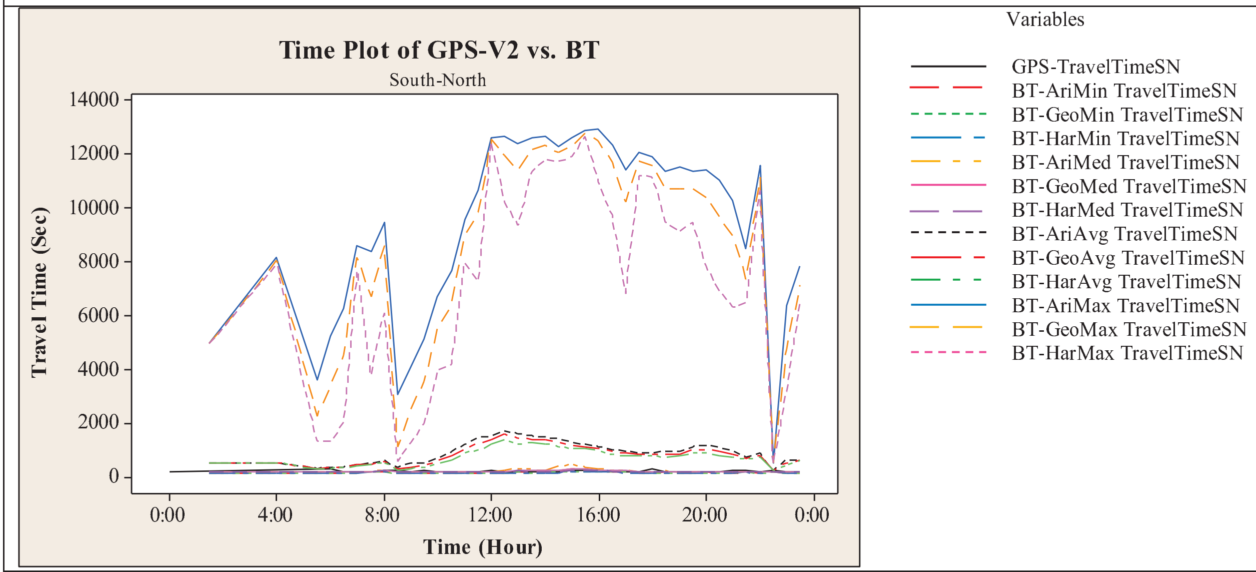

b: Comparison of Min-BT, and Med-BT for three aggregation technique

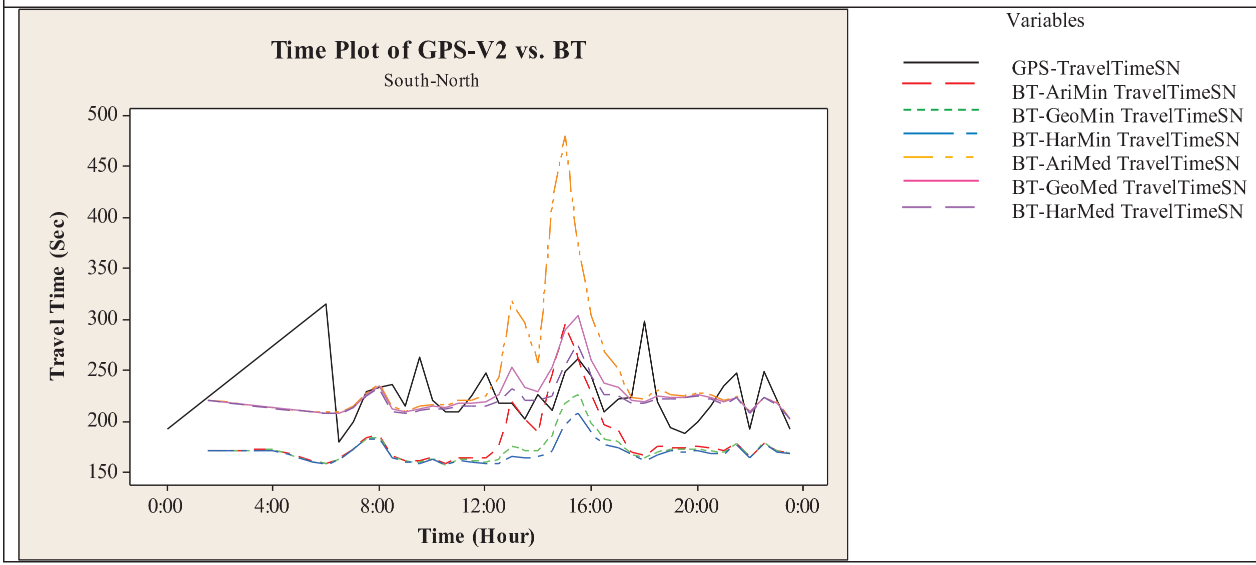

Figure 3-11. Time plot of GPS-V2 vs. BT travel time estimates for App.2 for South-North direction

3.4.2.2 Results for Quantitative Analysis Using Accuracy Measures

In order to determine the most accurate estimation and aggregation methods, quantitative accuracy metrics are calculated in the following section. Results of the accuracy analysis for Phase (2) are summarised in Table 3-4 and Table 3-5. The Min-BT and Med-BT still are the most accurate estimation methods followed by Avg-BT and Max-BT. In analysis based on GPS-V1, implementation of App.2 on average improves the accuracy of Min-BT and Med-BT estimates significantly in some cases more than 50% improvement is observed. However, in case of GPS-V2 the improvements are less obvious.

Analysis for GPS-V1 show that for AriMin-BT, GeoMin-BT and HarMin-BT in App.1 and App.2, MPE are less than 10%, MAPE less than 10% and RMSE about 30 seconds for South-

North direction. Similarly, for the North-South direction AriMin-BT, GeoMin-BT and HarMin-BT in App.1 and App.2 yield MPE less than 10%, MAPE less than 10% and RMSE about 40 seconds in App.1 and 12 seconds in App2. Similar patterns are also observed for the AriMed-BT, Geo-MedBT and HarMed-BT. Analyses for GPS-V2 show that the AriMed-BT, GeoMed-BT and HarMed-BT are more accurate than the AriMin-BT, GeoMin-BT and HarMin-BT. The accuracy in this case is also very high with about less than 10% for MPE and MAPE and also RMSE about 30 seconds. In this case, for North-South direction implementation of App.2 lead to slightly higher error. These results indicate the high accuracy of travel time estimates obtained by BT and also highlights the importance of choice estimation method and aggregating the data.

Table 3-4. Accuracy measures of Bluetooth estimations, GPS-V1 as ground truth

		Travel Time	MPE (%)		MAPE (%)		RMSE (sec)	
	Direction	**Estimator**	**App.1**	**App.2**	**App.1**	**App.2**	**App.1**	**App.2**
GPS-Source1 - 15 Minutes Aggregation	South-North	AriMin-BT	6.64	-4.91	17.05	10.88	76.86	32.82
		AriMax-BT	4283.48	4777.18	4283.48	4777.18	9046.51	9913.39
		AriAvg-BT	418.17	386.66	418.17	386.66	888.21	851.68
		AriMed-BT	58.27	27.79	58.41	27.93	174.54	74.44
		GeoMin-BT	**-5.78**	**-9.58**	**8.75**	**10.39**	**31.34**	**34.45**
		GeoMax-BT	3487.83	4310.05	3487.83	4310.05	8009.25	9253.14
		GeoAvg-BT	330.02	338.47	330.02	338.47	731.85	751.96
		GeoMed-BT	24.89	18.33	26.27	19.94	53.95	40.75
		HarMin-BT	-8.51	-11.36	9.77	12.03	35.00	38.92
		HarMax-BT	2456.51	3577.48	2456.51	3577.48	6571.62	8217.73
		HarAvg-BT	263.81	290.30	263.81	290.30	605.96	648.40
		HarMed-BT	18.82	15.60	21.07	18.23	42.16	37.94
	North-South	AriMin-BT	8.42	-3.31	12.26	5.80	45.21	12.49
		AriMax-BT	1108.26	1330.35	1108.26	1330.35	2060.03	2401.97
		AriAvg-BT	116.71	96.94	116.71	96.94	219.41	178.23
		AriMed-BT	45.42	26.37	45.42	26.37	103.55	51.34
		GeoMin-BT	1.43	-4.06	6.27	6.15	15.40	12.80
		GeoMax-BT	898.91	1214.48	898.91	1214.48	1769.33	2228.11
		GeoAvg-BT	97.20	90.98	97.20	90.98	177.59	167.02
		GeoMed-BT	32.46	24.58	32.46	24.58	62.22	45.98
		HarMin-BT	**-0.59**	**-4.67**	**5.38**	**6.40**	**12.07**	**13.05**
		HarMax-BT	652.64	1047.29	652.64	1047.29	1385.43	1978.49
		HarAvg-BT	84.73	85.57	84.73	85.57	154.01	156.97
		HarMed-BT	27.78	23.37	27.78	23.37	50.42	42.99

Table 3-5. Accuracy measures of Bluetooth estimations, GPS-V2 as ground truth

		Travel Time	MPE (%)		MAPE (%)		RMSE (sec)	
	Direction	Estimator	App.1	App.2	App.1	App.2	App.1	App.2
GPS-Source2 - 30 Minutes Aggregation	South-North	AriMin-BT	-10.82	-17.46	19.74	19.49	60.55	56.70
		AriMax-BT	4124.73	4280.10	4124.73	4280.10	9657.98	9976.25
		AriAvg-BT	369.45	333.21	369.45	333.37	905.70	836.34
		AriMed-BT	30.92	10.97	35.53	18.04	119.42	66.62
		GeoMin-BT	-19.81	-21.95	19.81	21.95	55.98	59.64
		GeoMax-BT	3470.95	3886.79	3470.95	3886.79	8582.19	9270.54
		GeoAvg-BT	302.49	290.45	302.49	290.61	758.59	735.50
		GeoMed-BT	6.63	2.11	12.66	9.81	36.22	31.66
		HarMin-BT	-22.23	-23.60	22.23	23.60	59.93	62.43
		HarMax-BT	2482.87	3247.50	2482.87	3247.50	6999.73	8079.48
		HarAvg-BT	243.66	247.85	243.66	248.01	627.25	630.37
		HarMed-BT	1.69	-0.54	8.96	7.86	29.23	28.62
	North-South	AriMin-BT	-19.03	-27.49	19.74	27.49	60.55	71.87
		AriMax-BT	842.48	978.85	4124.73	978.85	9657.98	2340.73
		AriAvg-BT	62.55	47.63	369.45	47.74	905.70	119.52
		AriMed-BT	7.88	-6.27	35.53	9.49	119.42	31.27
		GeoMin-BT	-23.24	-27.98	19.81	27.98	55.98	73.10
		GeoMax-BT	684.81	888.20	3470.95	888.20	8582.19	2159.67
		GeoAvg-BT	49.15	43.25	302.49	43.36	758.59	108.86
		GeoMed-BT	-0.32	-7.19	12.66	10.21	36.22	32.90
		HarMin-BT	-24.56	-28.45	22.23	28.45	59.93	74.29
		HarMax-BT	494.64	758.65	2482.87	758.65	6999.73	1889.49
		HarAvg-BT	40.18	39.31	243.66	39.42	627.25	99.29
		HarMed-BT	-3.46	-7.85	8.96	10.69	29.23	34.11

The accuracy of Min-BT and Med-BT also show that these values can be used as better alternatives for the Avg-BT both for estimating travel time and outlier removal algorithms. The high accuracy of Min-BT and Med-BT indicate that these estimators can be used for detecting the abnormal traffic situations such as congestion. In many cases instead of using complicated outlier removal algorithms, the Min-BT and Med-BT can be well representative of the traffic situation. Med-BT tends to be less sensitive to the sample size changes compared to Min-BT. Hence, it is suggested to implement Med-BT as it is shown to be more robust when sample sizes are lower.

The significant difference between the Max-BT and Avg-BT compared to other estimators can be explained based on the number of access points (i.e. entrance and exit) which connects the study route with the neighbourhood area. In long corridors with a number of connections, drivers have the possibility to divert from the corridor and return to it in the distance between the two Bluetooth sensors. Therefore, the Max-BT represents the impact of diverted vehicles, as well as slow vehicles. Similarly, the Avg-BT which is calculated based on all the records including Max-BT, and this estimate directly gets affected by outliers. One of the limitations of this study is that the truth dataset (FCD obtained using GPS) was calculated based on average travel times whereas median might have been a more robust representation of truth. Moreover, it would be more informative if there was a direct comparison between different BT estimation (Min-BT, Med-BT and Max-BT) with similar estimates of FCD, instead of using average FCD as the basis for evaluating various estimators.

3.4.2.3 Sample Size Sensitivity Analysis

Results of the accuracy metrics for App.1 and App.2 show that the accuracies of the estimated travel times are influenced by the sample sizes. In order to further investigate this relationship, a sensitivity analysis for Min-BT and Med-BT for a range of sample sizes from 1 to 30 are conducted. The accuracy metrics for each sample size are calculated. Accordingly, the sample size which yields the highest accuracy is selected as the optimum. Results for the sensitivity analysis for South-North direction are shown in Figure 3-12, and Figure 3-13. Results of the North-South direction are presented in Appendix II. In general, it can be seen that by increasing the size of the sample the accuracy tends to increase however this trend levelled out after the sample size reached a specific size. Therefore, it is important to find the optimum number of sample size.

As shown in Figure 3-12 and Figure 3-13, the optimum number of sample varies for each case. However, it could be seen that the sample sizes between the ranges of 5 to 15 could lead to more accurate and reliable results for arterial roads in Denmark. Increasing this range for filtering the data does not necessary increase the accuracy. The optimum sample size is a function of short-term travel time variability.

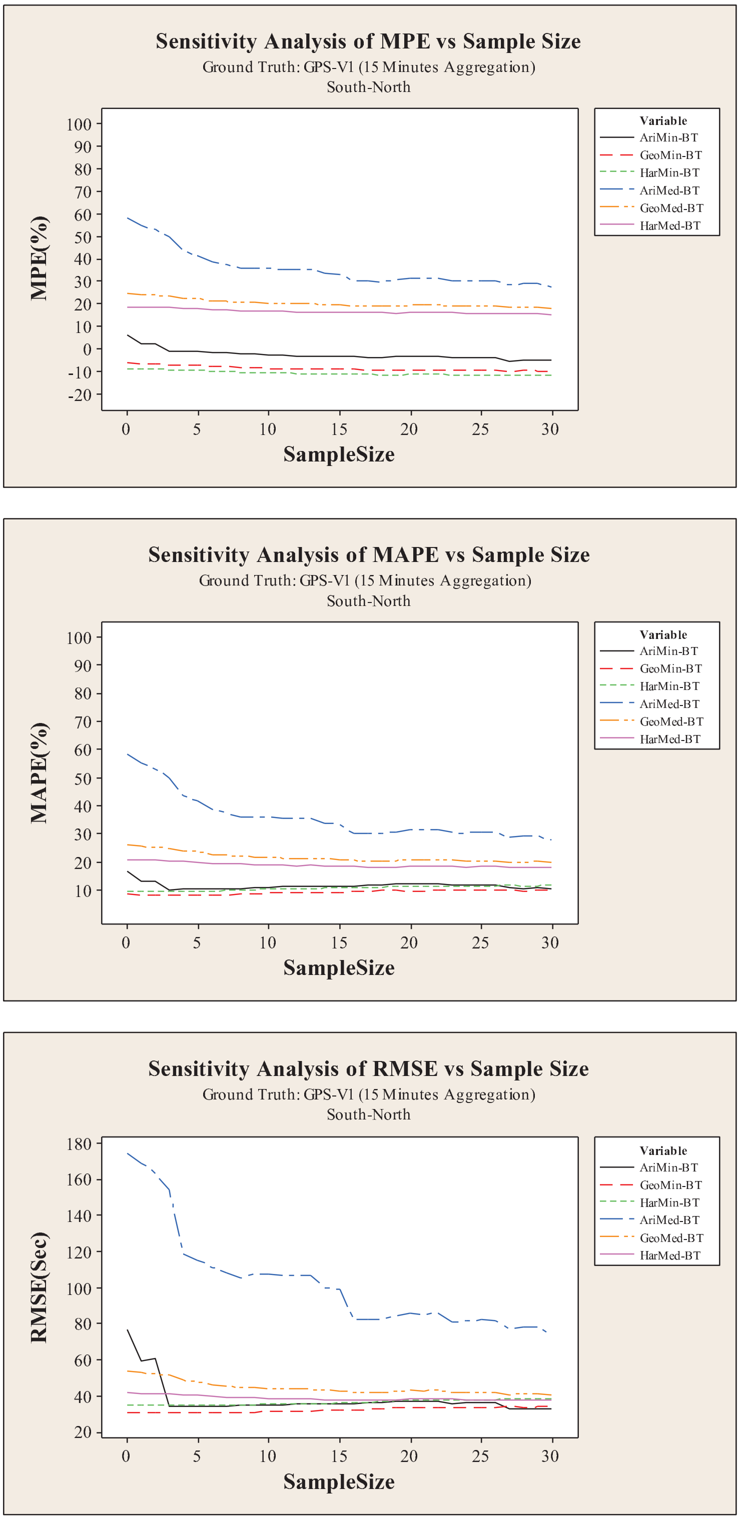

Figure 3-12. Sensitivity analysis of MPE, MAPE, and RMSE vs. sample size for GPS-V1 for South-North direction

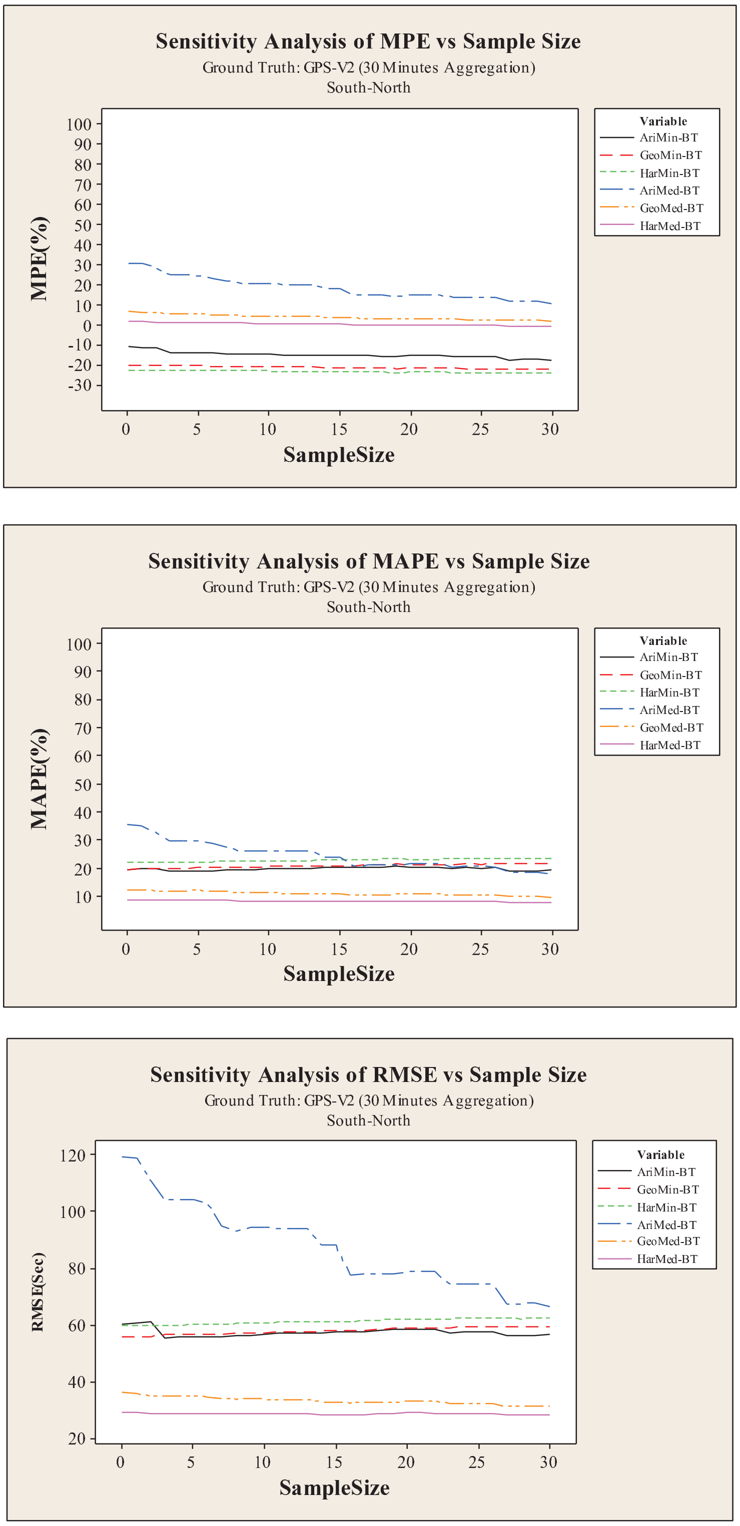

Figure 3-13. Sensitivity analysis of MPE, MAPE, and RMSE vs. sample size for GPS-V2 for South-North direction

Comparing the results for the App.1 and App.2 confirm the importance of sample size. It is clear that by removing the intervals having less than 30 detections, a number determined using engineering judgement, the variation in Bluetooth data is reduced (Table 3-1). However, it doesn't necessary increase the accuracy of the estimations. In this regard, results of the sensitivity analyses show that although the optimum number of the minimum sample size varies a lot for each case, but it seems that the range of sample of 5-15 values could provide accurate travel time estimation.

3.5 Conclusion

The issue of low sample size and choice of aggregation method for profile construction have been discussed. In this Chapter, three aggregation techniques including arithmetic mean, geometric mean and harmonic mean were used to construct the travel time profiles using the Bluetooth dataset. Two sources of FCD were used as the ground truth in order to quantify and evaluate the accuracy of travel time profiles estimated using Bluetooth data. Comparing the three aggregation methods show that using the harmonic mean and geometric mean could significantly reduce the impact of outliers, especially in intervals with low sample and high risk of outliers for profile construction.

Four different estimators, namely Min-BT, Max-BT, Med-BT and Avg-BT, were used to estimate travel times using Bluetooth technology, during each time interval which was used as input to the profile estimator. Results show that Min-BT and Med-BT are more robust in the presence of outliers in the dataset and can provide more accurate travel time estimates compared to Max-BT and Avg-BT.

In order to quantify the impact of sample size on accuracy of travel time estimates, a series of sensitivity analyses were conducted. It was found that the range of sample of 5-15 values could be used as the optimum range of sample size for improving the accuracy of the estimated travel time.

In addition to the sample size and aggregation method, the choice of estimation method could influence the accuracy of Bluetooth-based travel time. In this Chapter, median of the multiple detections recorded for a single Bluetooth device was used for travel time estimation. In the following Chapter, a wide range of other alternative methods are evaluated to minimise the impact of location ambiguity on the estimated travel time.

CHAPTER 4

TRAVEL TIME ESTIMATION USING BLUETOOTH TECHNOLOGY

4. Introduction

The use of Bluetooth Technology as a cost-effective method of travel time estimation has been evolving rapidly in the recent past. As discussed in Section 1.3.4, one of the main problems in application of Bluetooth technology for travel time estimation is its large detection zone, which could reduce the accuracy of estimation. Therefore, one of the main challenges in the application of Bluetooth technology is to identify or develop methods for dealing with this location ambiguity.

The issue of multiple Bluetooth detection events and its impact on travel time estimation has been considered by various researchers in the past (Quayle et al. 2010 and Malinovskiy et al. 2010). However, the treatment of this issue has remained simplistic so far. Most previous studies simply used the first detection event namely *Enter-Enter* as the best estimate (Malinovskiy et al. 2010; Haghani et al. 2010; Brennan et al. 2010; Saunier et al. 2010; and Tsubota et al. 2010) without a systematic analysis of how to optimally make use of multiple detection events. However, as shown in Figure 4-1 and Figure 4-2, Travel time obtained by *Enter-Enter* (i.e. $TT_{(Enter\text{-}Enter)}$) is not necessarily the best estimation and it is possible that $TT_{(Median\text{-}Median)}$, which is based upon the median, is more accurate.

In Malinovskiy et al. (2010), the authors also discussed the application of *First-First*[1] *(i.e. Enter-Enter)*, *Last-Last*[2] (i.e. *Leave-Leave*) and *Median* matching as other alternative methods for travel time estimation. In their study, *last-last* was used in order to reduce the effect of intersection delay. The authors concluded that although this approach demonstrated better results than *First-First* or *Median* matching, it was still insufficient to completely circumvent the problem, as the last timestamp may still occur within the intersection area due to noise and signal blockage issues.

These findings highlight the importance of developing methods of estimating travel time using multiple Bluetooth detection events. In order to explore this issue, an experimental evaluation was conducted to collect real-world Bluetooth data as well as the corresponding travel time data using GPS. A number of different travel time estimation methods were defined and tested. The details of the evaluation are presented in the next section.

4.1 Alternative Methods of Travel Time Estimation Using Multiple Bluetooth Detections

Two main sensor designs are shown in Figure 4-1 and Figure 4-2 in order to explain the issues associated with multiple detection events and travel time estimation. Figure 4-1 depicts a more general case in which detection zone is either shaped by a single antenna or the combined coverage of all antennae is considered as a single zone. Figure 4-2 illustrates the case where the detection zone is shaped by a combination of multiple antennae.

In the scenario illustrated in Figure 4-1, a Bluetooth device is detected three times by each sensor while in Figure 4-2 the MAC address of the Bluetooth-enabled device is detected six times by different antennae. Therefore, depending on which detection events are used, there are different methods to calculate the travel time.

[1] . This method uses the last detection event and is called *First-First or Enter-Enter.*

[2] . This method uses the last detection event and is called *Last-Last or Leave-Leave.*

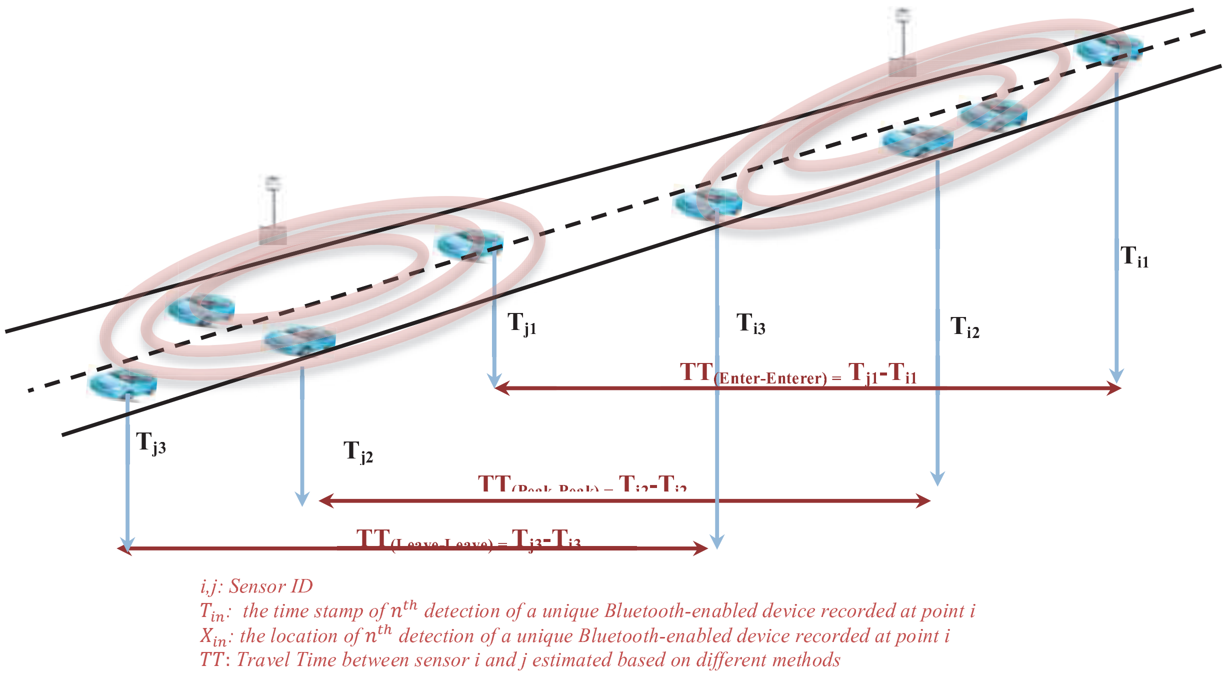

Figure 4-1. Travel time estimation using multiple detection events in case of single antenna and aggregated antennae

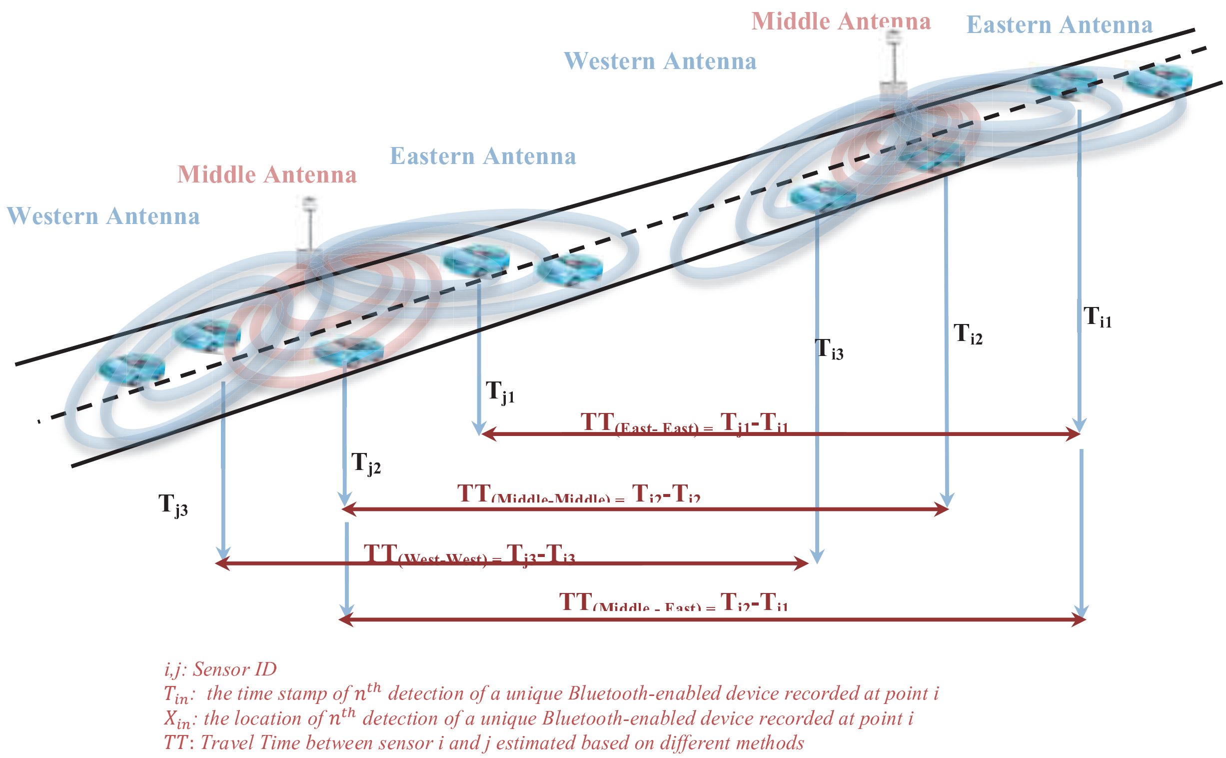

Figure 4-2. Travel time estimation using multiple detection events in case of multiple antennae

4.1.1 Detection Zone Shaped By Single Antenna

In this case, detection events used for the travel time estimation are independent of which antenna is detecting the record. This case is important as most Bluetooth manufacturers use only one omnidirectional antenna. Three travel time estimation methods are considered as follow:

4.1.1.1 Enter-Enter

The first detection event at upstream and downstream sensors is used for travel time estimation.

$$TT_{ji_{(Enter-Enter)}} = T_{j_{(Enter)}} - T_{i_{(Enter)}} \qquad \textbf{Equation 4-1}$$

Where:

$TT_{ji_{(Enter-Enter)}}$: Travel time between point *j* and *i* based on the first detection event at point *j* and *i*

$T_{j_{(Enter)}}$: Timestamp of the first detection at downstream point *j*

$T_{i_{(Enter)}}$: Timestamp of the first detection at upstream point *i*

4.1.1.2 Leave-Leave

The last detection event at upstream and downstream sensors is used for travel time estimation.

$$TT_{ji_{(Leave-Leave)}} = T_{j_{(Leave)}} - T_{i_{(Leave)}} \qquad \textbf{Equation 4-2}$$

Where:

$TT_{ji_{(Leave-Leave)}}$: Travel time between point *j* and *i* based on the last detection event at point *j* and *i*

$T_{j_{(Leave)}}$: Timestamp of the last detection at downstream point *j*

$T_{i_{(Leave)}}$: Timestamp of the last detection at upstream point *i*

4.1.1.3 Peak-Peak

The detection event with the maximum RSSI at upstream and downstream sensors is used for travel time estimation. The magnitude of RSSI is highly dependent on the distance of the Bluetooth-enabled device from the sensor location. In other words, if a detection event is recorded with a high RSSI value, it is more likely that it is at a location closer to the sensor. The relationship between the distance and perceived signal strength was explored in previous studies (Franssens, 2010). As a proof of concept, this relationship was tested by the author, in a field experiment conducted in Århus; see Figure 4-3. In this method the underlying hypothesis is that the detection event with maximum RSSI will result in highest accuracy for travel time estimation.

$$TT_{ji_{(Peak-peak)}} = T_{j_{(Peak)}} - T_{i_{(Peak)}} \qquad \textbf{Equation 4-3}$$

Where:

$TT_{ji_{(Peak-Peak)}}$: Travel time between point *j* and *i* based on the detections with maximum RSSI at point *j* and *i*

$T_{j_{(Peak)}}$: Timestamp of the detection event with the maximum RSSI at downstream point *j*

$T_{i_{(Peak)}}$: Timestamp of the event with the maximum RSSI at upstream point *i*

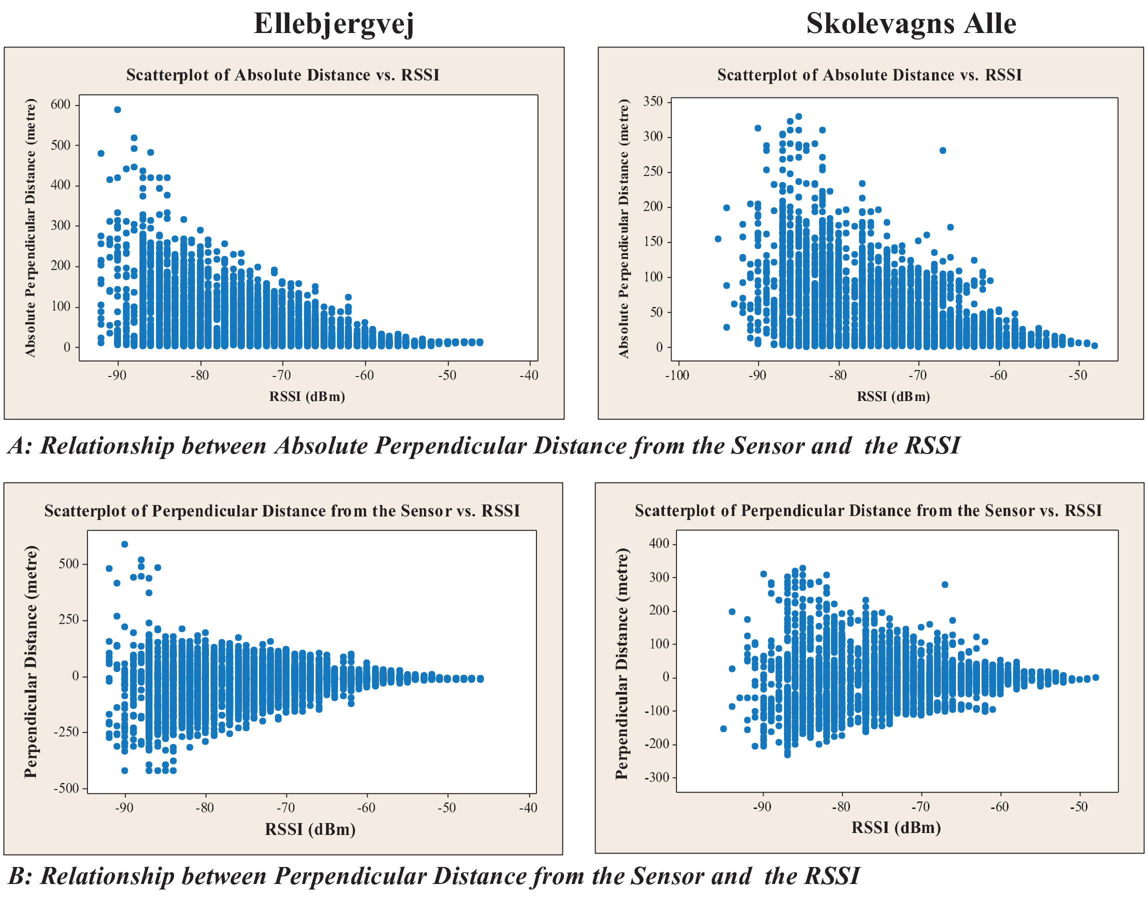

C: SD Plot Relationship between Perpendicular Distance from the Sensor and the RSSI for Various Trips

dBm: dB per milliwatt

Figure 4-3. Relation between distance and RSSI; case study Århus

4.1.2 Detection Zone Shaped By Multiple Antennae

In this case, the Bluetooth sensor consists of multiple antennae and detection recorded by each antenna is seperately provided. Different rules can be used to determine the detection event to be used for travel time estimation. In this study, five different methods for estimating the travel time are proposed.

4.1.2.1 Middle-Middle:

Detection events with maximum RSSI obtained by the middle antennae at upstream and downstream sensors are used for travel time estimation.

$$TT_{ji_{(Middle-Middle)}} = T_{j_{(Middle)}} - T_{i_{(Middle)}}$$ **Equation 4-4**

Where:

$TT_{ji_{(Middle_p-Middle_p)}}$: Travel time between point j and i based on detection with maximum RSSI at middle antennae at point j and i

$T_{j_{(Middle)}}$: Timestamp of the detection event recorded by middle antenna with the maximum RSSI at downstream point j

$T_{i_{(Middle)}}$: Timestamp of the detection event recorded by middle antenna with the maximum RSSI at upstream point i

4.1.2.2 East-East:

Detection events with maximum RSSI obtained by East-facing antennae are used for travel time estimation.

$$TT_{ji_{(East-East)}} = T_{j_{(East)}} - T_{i_{(East)}}$$ **Equation 4-5**

Where:

$TT_{ji_{(East-East)}}$: Travel time between point j and i based on detection event with maximum RSSI at the East-facing antennae at point j and i

$T_{j_{(East)}}$: Timestamp of the detection event recorded by East-facing antenna with the maximum RSSI at downstream point j

$T_{i_{(East)}}$: Timestamp of the event recorded by East-facing antenna with the maximum RSSI at upstream point i

4.1.2.3 West-West:

Detection events with maximum RSSI obtained by West-facing antennae are used for travel time estimation.

$$TT_{ji_{(West-West)}} = T_{j_{(West)}} - T_{i_{(West)}}$$ **Equation 4-6**

Where:

$TT_{ji_{(West-West)}}$: Travel time between point j and i based on detection event with maximum RSSI at the West-facing antennae at point j and i

$T_{j_{(West)}}$: Timestamp of the detection event recorded by West-facing antennae with the maximum RSSI at downstream point *j*

$T_{i_{(West)}}$: Timestamp of the detection event recorded by West-facing antennae with the maximum RSSI at upstream point *i*

4.1.2.4 East-West Mixed Method:

The average of the timestamps recorded by East-facing and West-facing antennae is used for travel time estimation.

$$TT_{ji_{(EastWest-EastWest)}} = T_{j_{(EastWest)}} - T_{i_{(EastWest)}} \quad \textbf{Equation 4-7}$$

Where:

$TT_{ji_{(EastWest-EastWest)}}$: Travel time between point j and i based on detection event with maximum RSSI at the East-facing and West-facing antennae at point j and i

$T_{j_{(EastWest)}}$: Timestamp of the detection event recorded by the East-facing and West-facing antennae with the maximum RSSI at downstream point *j*

$T_{i_{(EastWest)}}$: Timestamp of the event recorded by the East-facing and West-facing antennae with the maximum RSSI at upstream point *i*

4.1.2.5 Combined Method

A combination of data from multiple Bluetooth detection events is used as a new method. This method is developed based on the characteristics and design factors of BlipTrack; however, the method is generic and can be applied to other sensor with different design and antennae configurations. As shown in section 1.2, BlipTrack sensors have three antennae. In Chapter 2, it was found that detection events recorded by the middle antenna (i.e. short-range antenna) are at a closer distance to the sensors locations, hence these detection events have the lowest location ambiguity. However, the number of detection events captured by the middle antenna is significantly lower compared to the other two antennae. Thus, a trade-off is needed between location ambiguity and sampling rate. Therefore, a *Combined* method was developed to address this issue. This method seeks to minimise the influence of location ambiguity by using the combination of detections and improve the accuracy of estimated travel time. In this method, the time when a vehicle passes the sensor is estimated by the following algorithm:

- If a vehicle is detected by the short-range antenna once, the sensor "pass by" time is the time stamp for that detection.
- If a vehicle is detected by the short-range antenna more than once, the sensor "pass by" time is the time stamp with the highest RSSI.
- If a vehicle is detected by both directional antennae, the sensor "pass by" time is calculated by on an interpolation between the readings from each directional antenna with highest RSSI.
- If a vehicle is only detected by one of the directional antennae, the sensor "pass by" time is calculated by a synthesis of the antenna readings. In this case, the detection event with the highest RSSI recorded by the directional antenna is used, and adjusted relative to the array of detection event RSSIs recorded by the sensor.

Pseudo code for calculation of combined-method is shown below. Moreover various stages of the method are shown in Figure 4-4.

#U: refer to upstream, #D: refer to downstream

#First step calculating the time pass by using Middle antenna detections

if $(D\_DetectionEvent_{MiddleAntenna} > 0 \ \& \ U\_DetectionEvent_{MiddleAntenna} > 0)$

{

$TravelTime_{Combined} = D\_DetectionEvetn_{MiddleAntenna} - U\_DetectionEvetn_{MiddleAntenna}$

}

else

#Second step calculating the time pass by using Combination of both west and east antennae detections

{

if $(D\_DetectionEvent_{EastAntenna} > 0 \ \& \ D\_DetectionEvent_{WestAntenna} > 0 \quad \&$
$U\_DetectionEvetn_{EastAntenna} > 0 \ \& \ U\_DetectionEvent_{WestAntenna} > 0)$

{

$$U\_InterpolatedTimePassby = \frac{(U\_DetectionEvent_{EastAntenna} + U\_DetectionEvent_{WestAntenna})}{2}$$

$$D\_InterpolatedTimePassby = \frac{(D\_DetectionEvent_{EastAntenna} + D\_DetectionEvent_{WestAntenna})}{2}$$

$TravelTime_{Combined} = D\_InterpolatedTimePassby - U\_InterpolatedTimePassby$

}

#Third step calculating the time pass by using interpolated values of west or east antennae detections based on RSSI

if $((D\_DetectionEvent_{EastAntenna} > 0 \ \& \ D\_DetectionEvent_{WestAntenna} = 0) \quad \&$
$U\_DetectionEvent_{EastAntenna} > 0 \ \& \ U\_DetectionEvent_{WestAntenna} = 0)$

{

$$U_{InterpolatedTimePassby} = (U_{DetectionEvetn_{EastAntenna}} + (\frac{U\_MaxRSSI_{EastAntenna} * U\_MaxRSSI_{MiddleAntenna}}{U\_MaxRSSI_{MiddleAntenna}}))$$

$$D_{InterpolatedTimePassby} = (D_{DetectionEvetn_{EastAntenna}} + (\frac{D\_MaxRSSI_{EastAntenna} * D\_MaxRSSI_{MiddleAntenna}}{D\_MaxRSSI_{MiddleAntenna}}))$$

$TravelTime_{Combined} = D\_InterpolatedTimePassby - U\_InterpolatedTimePassby$

}

if $((D\_DetectionEvent_{EastAntenna} > 0 \ \& \ D\_DetectionEvent_{WestAntenna} = 0) \quad \&$
$U\_DetectionEvent_{EastAntenna} = 0 \ \& \ U\_DetectionEvent_{WestAntenna} > 0)$

{

$$U_{InterpolatedTimePassby} = (U_{DetectionEvetn_{EastAntenna}} + (\frac{U\_MaxRSSI_{EastAntenna} * U\_MaxRSSI_{MiddleAntenna}}{U\_MaxRSSI_{MiddleAntenna}}))$$

$$D_{InterpolatedTimePassby} = (D_{DetectionEvetn_{WestAntenna}} + (\frac{D\_MaxRSSI_{WestAntenna} * D\_MaxRSSI_{MiddleAntenna}}{D\_MaxRSSI_{MiddleAntenna}}))$$

$TravelTime_{Combined} = D\_InterpolatedTimePassby - U\_InterpolatedTimePassby$

}

if $((D\_DetectionEvent_{EastAntenna} = 0 \ \& \ D\_DetectionEvent_{WestAntenna} > 0) \quad \&$
$U\_DetectionEvent_{EastAntenna} > 0 \ \& \ U\_DetectionEvent_{WestAntenna} = 0)$

{

$$U_{InterpolatedTimePassby} = (U_{DetectionEvetn_{WestAntenna}} + (\frac{U\_MaxRSSI_{WestAntenna} * U\_MaxRSSI_{MiddleAntenna}}{U\_MaxRSSI_{MiddleAntenna}}))$$

$$D_{InterpolatedTimePassby} = (D_{DetectionEvetn_{EastAntenna}} + (\frac{D\_MaxRSSI_{EastAntenna} * D\_MaxRSSI_{MiddleAntenna}}{D\_MaxRSSI_{MiddleAntenna}}))$$

$TravelTime_{Combined} = D\_InterpolatedTimePassby - U\_InterpolatedTimePassby$

}

if $((D\_DetectionEvent_{EastAntenna} = 0 \ \& \ D\_DetectionEvent_{WestAntenna} > 0) \quad \&$
$U\_DetectionEvent_{EastAntenna} = 0 \ \& \ U\_DetectionEvent_{WestAntenna} > 0)$

{

$$U_{InterpolatedTimePassby} = (U_{DetectionEvetn_{WestAntenna}} + (\frac{U\_MaxRSSI_{WestAntenna} * U\_MaxRSSI_{MiddleAntenna}}{U\_MaxRSSI_{MiddleAntenna}}))$$

$$D_{InterpolatedTimePassby} = (D_{DetectionEvetn_{WestAntenna}} + (\frac{D\_MaxRSSI_{WestAntenna} * D\_MaxRSSI_{MiddleAntenna}}{D\_MaxRSSI_{MiddleAntenna}}))$$

$TravelTime_{Combined} = D\_InterpolatedTimePassby - U\_InterpolatedTimePassby$

}

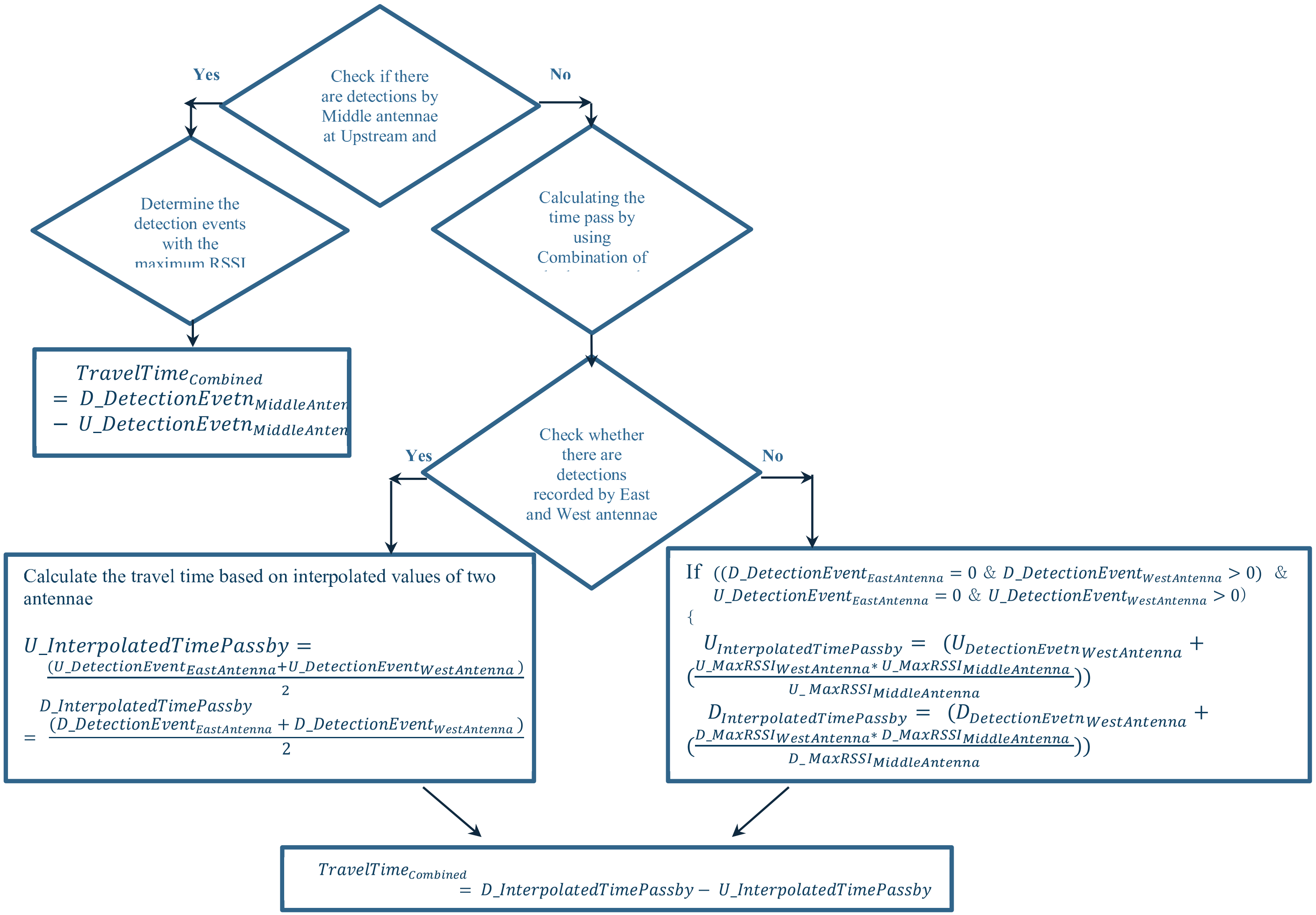

Figure 4-4. Flow chart of the Combined method

4.2 Results

Accuracy of all the eight methods are calculated based on the data collected in the Århus experiment, described in section 2.6.

4.2.1 Qualitative Analysis of Travel Time Estimation Methods

Figure 4-5 and Figure 4-6 compare the distributions of the travel time obtained by various methods versus ground truth (GPS) for the single antenna sensor design. These histograms are presented for the both West-East and East-West directions. Three methods namely *Enter-Enter*, *Leave-Leave* and *Peak-Peak* methods are used. It is clear from the results that the travel time obtained by the *Peak-Peak* method more closely resembles the GPS derived travel time distribution compared to *Enter-Enter* and *Leave-Leave* methods. However, results of *Peak-Peak* method are slightly offset in Figure 4-6. This could actually reflect the interference caused by the pole and curve.

Figure 4-7 and Figure 4-8 compare the distribution of the travel time obtained by various methods versus GPS data for the multiple antennae sensor designs. These histograms are presented for the both West-East and East-West directions. Results of the multiple antennae design in Figure 4-7 clearly show that the the *Middle-Middle* method yield the closest distribution to the GPS data. This is mainly due to the smaller size of detection zone and correspondingly lower location ambiguity. However, distribution of the result by *Middle-Middle* antennae is slightly biased for the West-East direction, as shown in Figure 4-8. This could also reflect the interference caused by the pole and curve in this location. In both figures, the combinations of *East-West* method are also closely distributed around the GPS data. These results confirm the assumptions used for the development of the combined method. Correspondingly, *Combined* method also provides a distribution close to the ground truth.

Figure 4-9 and Figure 4-10 represent the joint comparisons of the both designs for the both West-East and East-West directions. Results of the single antenna design versus multiple antennae design in Figure 4-9 and Figure 4-10 reflect that *Combined* and *Peak-Peak* methods produce travel time distributions that are closer to GPS data. This implies that the *Combined* and *Peak-Peak* methods are more accurate alternatives to the conventional *Enter-Enter* and *Leave-Leave* methods.

4.2.2 Quantitative Analysis of Travel Time Estimation Methods

The accuracy metric, RMSE, for all above mentioned methods are summarised in Table 4-1; the metrics are given for each direction of traffic separately as well as the combined accuracy metric for both directions. The numeric values of the RMSE conform to the qualitative patterns in Figure 4-9 and Figure 4-10.

It is clear that travel time estimated using detection events recorded by the middle antennae yields the most accurate results. This is in line with expectations, since the middle antenna has the smallest detection zone and thus the least location ambiguity. However, the detection rate of middle antennae is well below 10% (refer to Chapter 2). Sampling rate also become important when short-term travel time variability is high. Therefore, it is important to have an alternative estimation method where there is no record from the middle antennae. While there is no marked difference in accuracy between the *East-East* and *EastWest-EastWest* methods, the RMSE value is the lowest for the *Combined* method. RMSE figures show that *Combined* method has the highest accuracy (i.e. lowest RMSE value), followed by *Middle-Middle* method. These indicate

that the commonly used naïve method such as *Enter-Enter and Leave-Leave* have poor accuracy compared to proposed methods.
The higher accuracy of *Peak-Peak* method in comparison to *Enter-Enter* and *Leave-Leave* methods also supports the hypothesis that a higher RSSI leads to lower location ambiguity of the detection event. Thus, the value of the RSSI could be used as an indicator for selecting the closest detection event to the sensor location and minimising the effect of location ambiguity.

Table 4-1. Evaluating the accuracy of travel time obtained by various methods

Method	**RMSE (sec)**		
	Both Direction	**West-East**	**East-West**
Middle-Middle	**4.62**	**7.80**	**3**
East-East	6.35	4.25	7.44
West-West	20.24	27.07	7.55
EastWest-EastWest	6.27	4.19	6.85
Combined	**4.69**	**4.48**	**4.88**
Enter-Enter	7.93	8.38	7.49
Leave-Leave	12.52	7.23	15.94
Peak-Peak	**6.60**	**5.67**	**7.35**

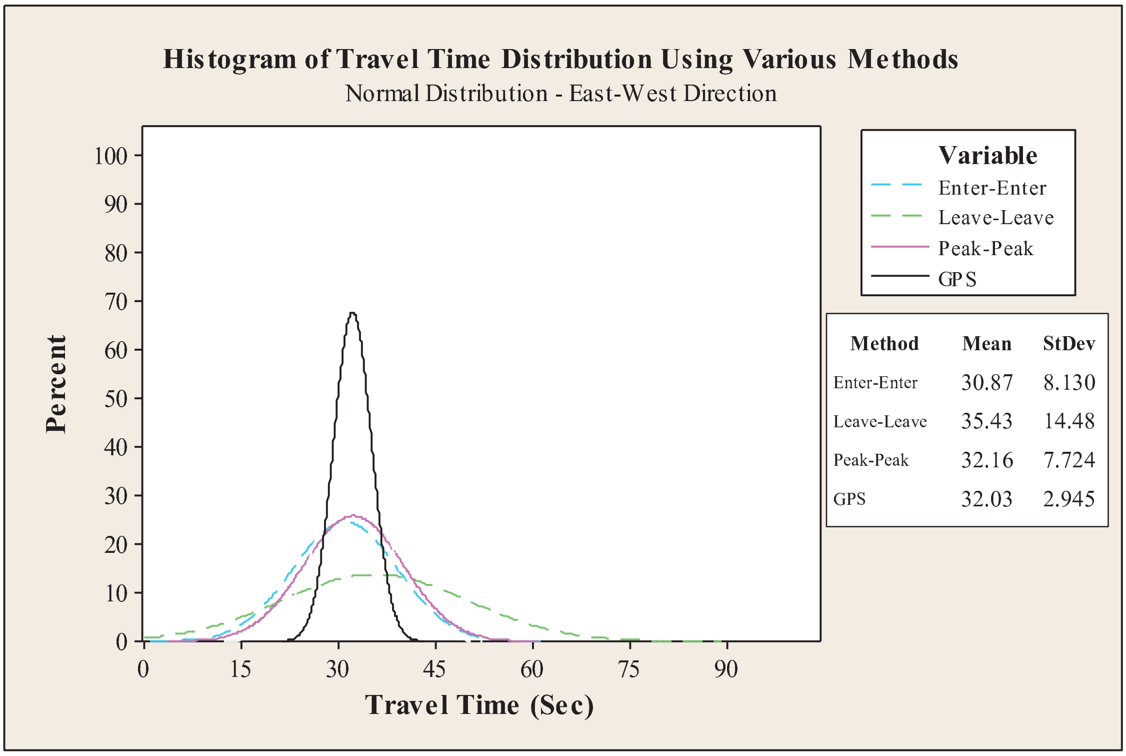

Figure 4-5. Histogram of travel time estimates using various methods for East-West direction (single antenna/aggregated antennae design)

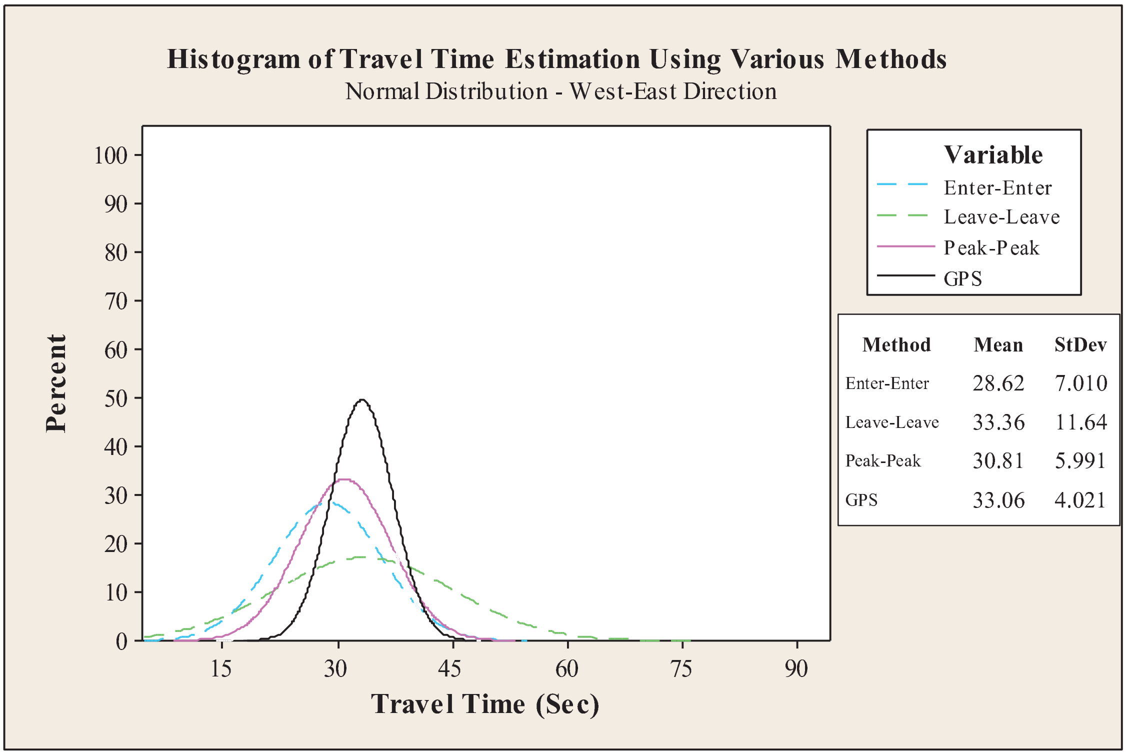

Figure 4-6. Histogram of travel time estimates using various methods for West-East direction (single antenna/aggregated antennae design)

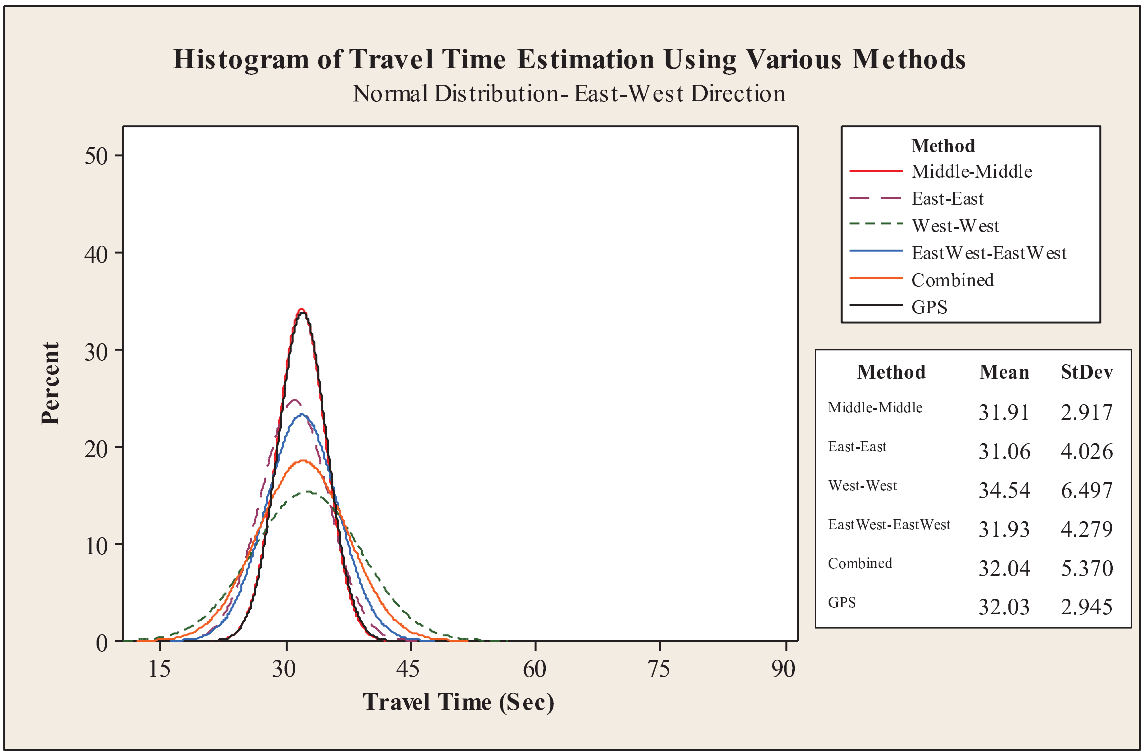

Figure 4-7. Histogram of travel time estimates using various methods for East-West direction (multiple antennae design)

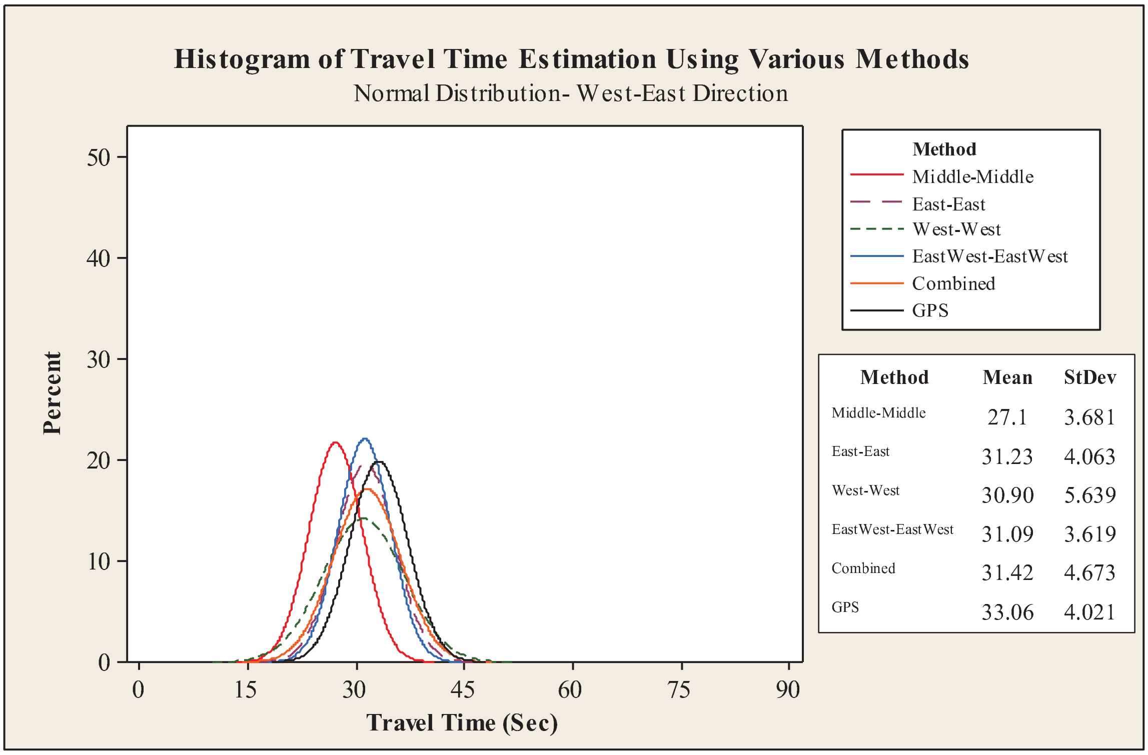

Figure 4-8. Histogram of travel time estimates using various methods for West-East direction (Multiple antennae design).

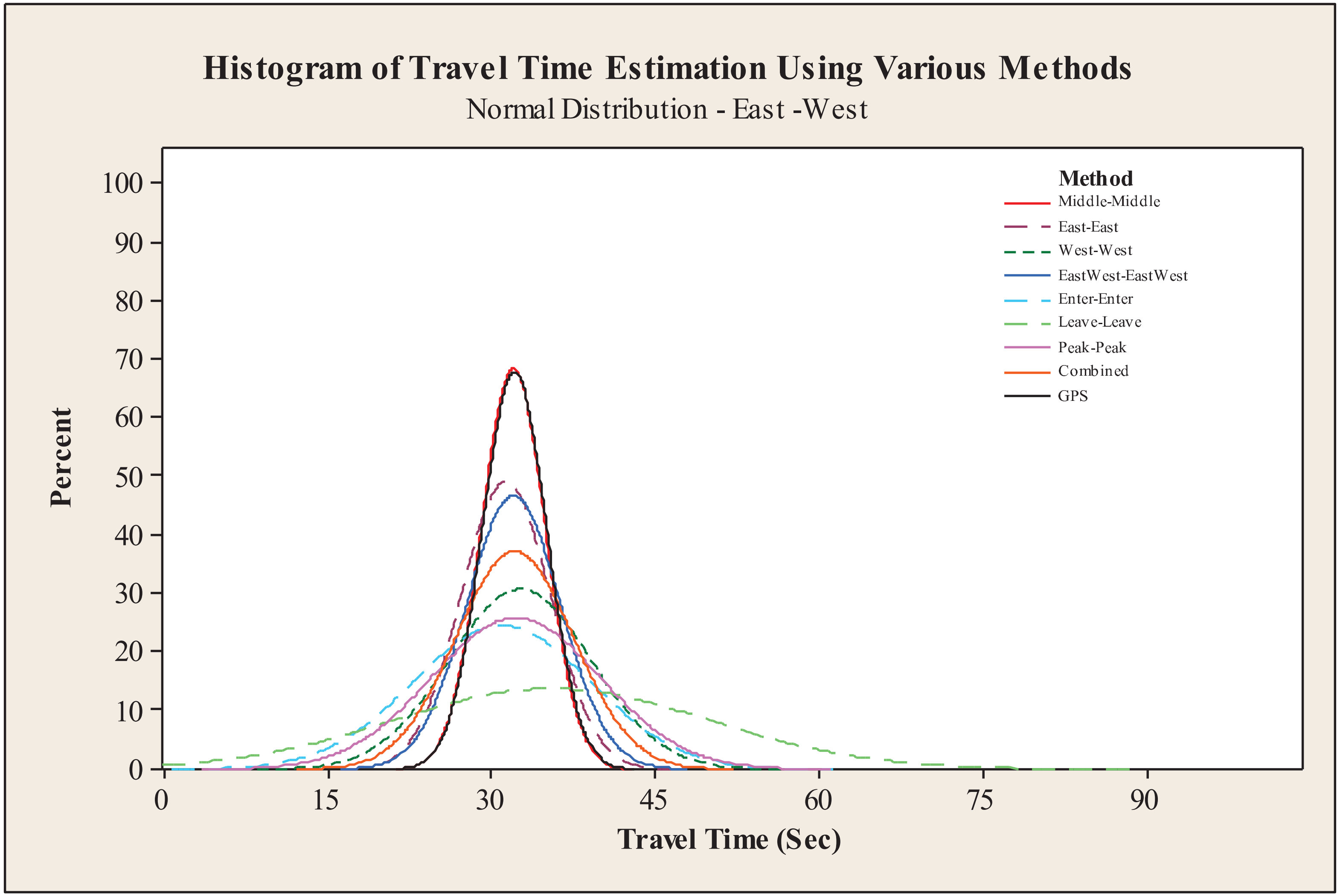

Figure 4-9. Joint comparison between various methods for East-West direction

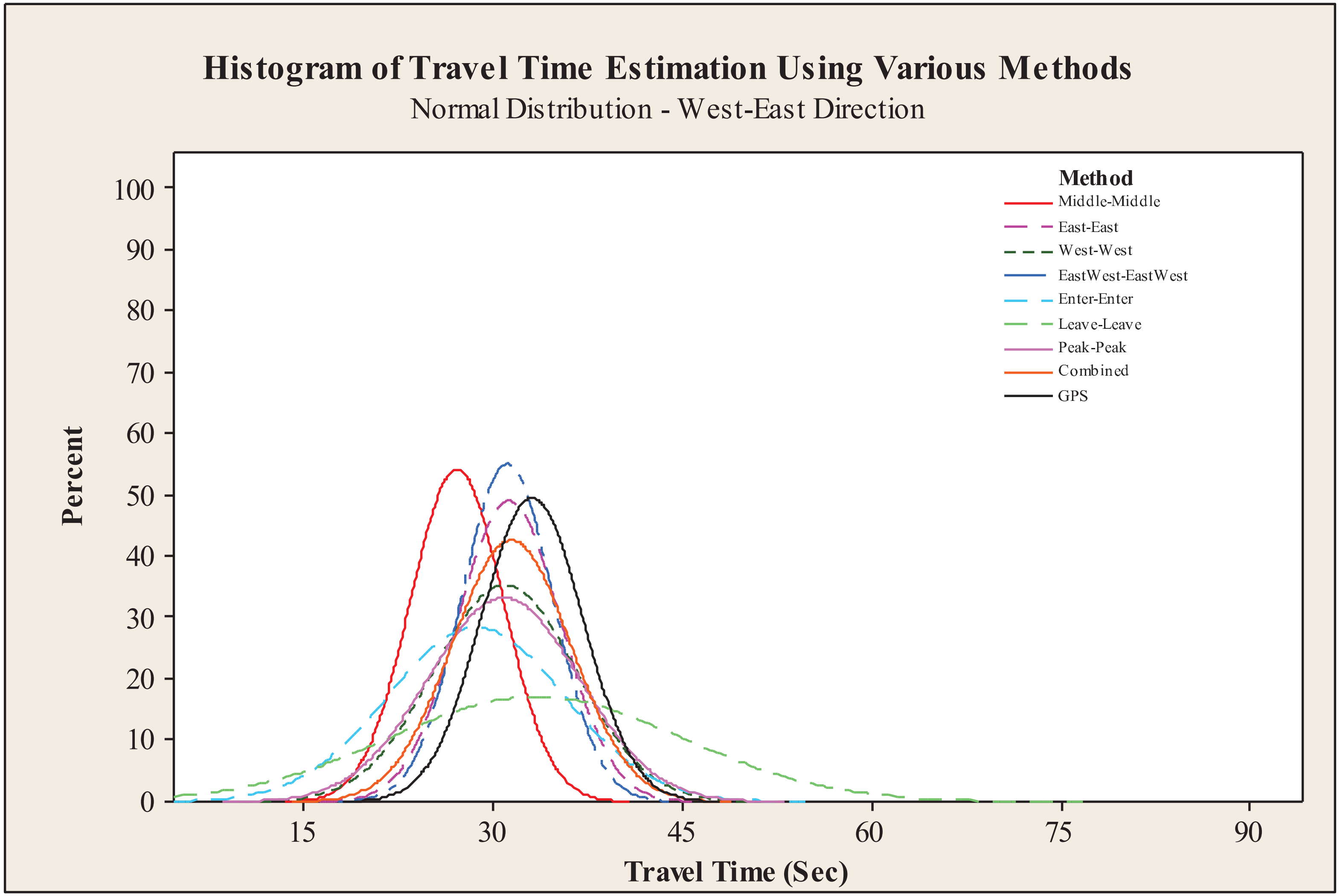

Figure 4-10. Joint comparison between various methods for East-West direction

4.3 Conclusion

Bluetooth devices may trigger multiple detection events at a sensor and there are a number of alternative ways to estimate travel time using Bluetooth detection events. In this study, eight travel time estimation methods were outlined and tested for two different sensor designs; sensors with single antenna or multiple antennae. Comparing the accuracy of all the methods shows that *Middle-Middle* followed by the *Combined* method has the highest accuracy (i.e. lowest RMSE value) followed by *Peak-Peak* method.

For single antenna design, the higher accuracy of the *Peak-Peak* method in comparison to *Enter-Enter* and *Leave-Leave* methods implies that higher RSSI leads to lower location ambiguity for the detection event. Thus, the value of the RSSI could be used as an indicator for selecting the closest detection event to the sensor location and minimising the effect of location ambiguity. It is concluded that *Peak-Peak* method is simple and more accurate than the *Enter-Enter* and *Leave-Leave* methods, which makes it a suitable alternative to these methods.

For multiple antenna design, a sensor with three antennae consisting of one short range antenna and two long-range antennae were discussed. The short-range antenna has the smallest detection zone and hence the least location ambiguity. However, the smaller the size of the detection zone, the lower the penetration rate, which can reduce the accuracy of estimates. Therefore, there has to be a trade-off between acceptable level of location ambiguity and penetration rate for designing the configuration and coverage of the antennae. Hence, *Combined* method is developed to investigate how combination of detection events obtained by various antennae can be used to improve the accuracy of travel time estimates. For multiple antennae design, the *Middle-Middle* and the *Combined* method yield the most accurate result. The accuracy of *Combined* method proposed in this study revealed the fact that new methods that combine detection events recorded by various antennae could yield better results.

This Chapter explored various methods of using multiple Bluetooth detections to develop more accurate travel time estimate for an individual device. Next Chapter will investigate the issue of travel time estimation using Bluetooth technology in mixed traffic condition. In order to distinguish between motor vehicles, bicycles and pedestrians in arterial roads, a new method will be developed. The method aims to classify the Bluetooth detections based on information of CoD, travel time, etc. as well as provide a mode-specific travel time estimate.

CHAPTER 5

MODE-SPECIFIC TRAVEL TIME ESTIMATION USING BLUETOOTH TECHNOLOGY

5. Introduction

Research to date has primarily focused on the application of Bluetooth technology for travel time estimation on motorways, where there is typically no need to distinguish between multiple travel modes. However, arterial roads and other city streets experience a mix of transport modes (i.e. motor vehicles, bicycles and pedestrians). Therefore, applying Bluetooth technology to estimate mode-specific travel time under heterogeneous traffic conditions remains a challenge. Heterogeneous traffic can affect both accuracy and reliability of travel time estimated using Bluetooth technology. This problem is particularly relevant in cities with a high volume of bicycle traffic. This chapter aims to examine the feasibility of estimating mode-specific travel time using MAC address tracking data under mixed traffic conditions.

5.1 Mode-Specific Travel Time Estimation Using Bluetooth Technology

Speed of vehicle groups on motorways is almost homogeneous and mainly dominated by motor vehicles. Hence, the problem of distinguishing between pedestrians, bicycles and motor vehicles has been largely ignored in the highways context.

The problem of mode-specific travel time estimation is mostly relevant to arterial roads experiencing mixed traffic. Estimating travel time using Bluetooth technology in arterial roads without classifying the modes of detected devices could give a biased result. For example, in an uncongested traffic condition, the average travel time from Bluetooth detections could overestimate the actual travel time of the motor vehicles and consequently underestimate the bicycles travel time. Therefore, it is necessary to develop methods to distinguish between different modes i.e. classification and allocation of the travel time observations depending on the types of road users and their characteristics.

In this chapter, a new method is presented to classify Bluetooth detection events into two groups, bicycles and motor vehicles. In this method, main underlying parameters are information recorded for the detected device (i.e. CoD and RSSI), speed or travel time of the detected device, and the location of the Bluetooth sensors over the network. Due to differences in functionality of Bluetooth-enabled devices (i.e. navigator, phones, computers etc.), it is assumed that some classes of the devices are exclusively used by specific modes. For example, navigators for route finding are mainly used in motor vehicles and accordingly, it is not expected that pedestrians and bicycles carry such devices. As mentioned in Section 1.3, the CoD represents the type of device. Hence, the information about the CoD can be used to identify the mode which carries the device.

The RSSI could also be used as supplementary information for distinguishing between motor vehicles and bicycles. As explained in Section 1.3, the magnitude of RSSI is highly dependent to the distance of the passing device from the sensor location. Moreover, it is also known that physical barriers such as body of the car, glass etc., would indeed reduce the level of received RSSI. Hence, the level of received RSSI could be another indication of the mode type, where a lower RSSI could be attributed to the Bluetooth-enabled devices in motor vehicles.

Another indicative parameter is the speed or travel time of the detected device. Obviously, the travel time of motor vehicles in uncongested urban arterials is significantly shorter than bicycles (i.e. motor vehicles are usually faster than bicycles). However, during congested traffic condition this condition may no longer be valid; as the bicycles are not hindered by congestion and they may have shorter travel time than motor vehicles. Hence, the mode identification is more challenging during congested peak hours.

Information about the location of the Bluetooth sensors over the road network could also be used to determine the mode. For example, sensors installed on motorways detect only motor vehicles while a sensor placed on arterial roads may detect motor vehicles, bicycles as well as pedestrians. It is fairly straight forward to filter out pedestrians due to their low walking speed, and pedestrian identification is considered outside the scope of this chapter.

In this chapter the methodology and algorithm developed by the author for the mode classification of Bluetooth detections are presented.

5.2 Methods of Mode Classification

In order to classify the Bluetooth detections different approaches can be used. The simplest method is the static cut-off classification method. This method determines an upper and a lower limit for an acceptable data band. These limits are usually defined based on a set number of standard deviation from the mean or median. If the travel time value for any detection is more than the set number of standard deviations above the mean, the method would consider that detection as an outlier (i.e. in this case a bicycle). Moreover, if the detection is below the lower limit value, it would be allocated to the fastest mode group. The disadvantage of using this method is that intra-day travel time variability is disregarded. Generally, in order to overcome the problem of intra-day travel time variability in outlier filtering, automated outlier screening algorithms is proposed (Quayle et al., 2010).

In order to overcome the problems with static cut-off, clustering techniques and automated screen approach are evaluated in this chapter as alternative methods to distinguish between motor vehicles and bicycles. Candidate method will be the method that could provide more accurate travel time estimates.

5.2.1 Clustering Method

Clustering techniques have been widely used in data mining and classification applications in transport studies. The objective of clustering is to classify the data into a number of clusters so that the data within a cluster is similar or related to one another and different or unrelated to the data belonging to other clusters. Different frames are considered to classify clustering mechanisms. One of the widely accepted frames is to classify clustering techniques into hierarchical, partial and hybrid clustering (Tayall and Raghuwanshi, 2010). The distinction between them is whether the set of cluster is nested or un-nested. The nested set permits clusters to have overlap or sub-clusters that are organised as a tree, whereas un-nested set consists of non-overlapping clusters such that each data is in exactly one cluster. Unlike traditional methods, hybrid clustering assigns any member of dataset a probability of belonging to each cluster. Then clusters will be shaped by assigning the members to the cluster with the highest probability (Anderson and Weiner, 2004).

In a previous study conducted by the author, the application of the three clustering methods namely hierarchical, k-mean and two-step for classification of Bluetooth datasets were evaluated for mode classification and the estimation of mode-specific travel time during uncongested traffic situations (Namaki Araghi et. al, 2010). Although results showed that all the methods were efficient, the two-step clustering method which belongs to hybrid clustering technique is used in this chapter. The reason is that there are a number of features employed by the two-step clustering algorithm which differentiate it from traditional clustering algorithms. Such features are ability to handle very large datasets, ability to handle both continuous and categorical variables and ability to determine the optimum number of clusters automatically (Zhang, et al., 1996; Chiu et al., 2001; Theodoridis and Koutroumbas, 1999). The name two-step clustering is already an indication that the algorithm is based on a two-stage approach: firstly, the algorithm undertakes a procedure to form pre-clusters. The main objective of the first stage is to reduce the size of the distance matrix that contains distances between all possible pairs of the cases in the dataset. The pre-cluster step uses a sequential clustering approach (Theodoridis and Koutroumbas, 1999). It scans the records one by one and decides if the current record should merge with the previously formed clusters or start a new cluster based on the distance criterion. When pre-clustering is complete, all cases in the same pre-cluster are treated as a single entity. Secondly, the algorithm conducts a modified Hierarchical agglomerative clustering procedure by combining the objects sequentially to form homogenous clusters. This is done by building a so-called cluster feature tree whose "leaves" represent distinct objects in the dataset (Mooi and Sarstedt, 2011).

Advantage of the two-step clustering compared to static cut-off method is that, this method could implement both travel time as a numerical variable and CoD as the categorical variable at the same time. This provides a better opportunity for classifying the mode of the devices detected by Bluetooth sensors.

5.2.2 Automated Screening Classification Method

As an alternative, an automated screening approach is used to develop a new mode-classification algorithm for distinguishing between detection events obtained from Bluetooth devices carried by motor vehicles and bicycles, and improve the accuracy of travel time estimation. The proposed method takes into account the intra-day variability of travel time. The main objective of this method is to improve the accuracy of motor vehicle travel time estimation in arterial roads by filtering out the Bluetooth detections triggered from other road users (i.e. bicycles and pedestrians). The method is based on three main parameters:

- Differences in the functionality and detection procedure of various Bluetooth-enabled devices
- Information about the location of the Bluetooth sensors over the road network
- Traffic condition

5.2.2.1 Differences in Functionality and Detection Procedure of Various Bluetooth-Enabled Devices

As mentioned earlier, due to differences in functionality of Bluetooth-enabled devices, it is expected that some groups of Bluetooth-enabled devices to be used only by specific modes. The MAC address includes information of the type of device called CoD, refer to section 1.3. Therefore, CoD information is involved in the method.

In addition to the difference in the functionality, the differences in detection procedure of devices could also be used as an indicative parameter for classification. Difference in detection procedure is mainly related to the number of detections recorded for a unique MAC address and also the level of received RSSI.

Generally, bicycles are slower than the cars in an uncongested traffic situation; hence the time span that the device is within the sensor's detection zone is longer. Therefore, it is probable that devices carried by bicycles will have more detection events than devices carried in cars. Moreover, it is also expected that the RSSI recorded for a bicycle would be higher than the one recorded for a motor vehicle under identical conditions as a result of the effect of the metal body of the vehicle.

5.2.2.2 Information about the Location of the Bluetooth Sensors over the Road Network

Layout and placement of the Bluetooth sensors on the road network provide a basis for filtering and classifying various types of the users. In this context, three different types of sensor placement scenarios are considered as follows:

- ***Sensor Located on Highway or Freeway***
  Motorways or freeways could be considered as a homogeneous traffic environment where only motor vehicles are present. Therefore, devices detected at these locations could most probably be carried on a motor vehicle. Therefore, Bluetooth devices identified by the sensors installed on motorways could be categorised as motor vehicles.

- ***Sensor Located on Bicycles Path***
  Bluetooth devices identified by sensors installed on isolated and exclusive bicycle paths can be categorised as bicycles. . The accuracy of bicycle categorisation increases where the bicycle paths are spatially separated from motorist traffic, as opposed to bicycle paths parallel to roads, where the detection zones of Bluetooth sensors (approximately 300m) do not cover the motorised road. Figure 5-1 shows an isolated exclusive bicycle lane.

Figure 5-1. Isolated cyclist exclusive lane
(Source: Cambridge Cycling Campaign, 2008)

- ***Sensor Located on Arterial Roads***
  Sensors placed in a heterogeneous traffic environment capture Bluetooth devices present in different traffic modes (i.e. motorised and non-motorised traffic). Therefore, it is difficult to identify the devices carried by bicycles based on devices identified by sensors installed on arterial roads. .

In the algorithm presented in this chapter, sensors located on highways and bicycles paths are used as filtering gates or check points for classifying the mode. This means that by checking the sequence of the detection recorded for a unique MAC address at different sensors it is possible to define the mode of the detected device with some degree of certainty. Note that, this inference could only be used during a specific moving time window because of inter-modal journeys; except for Audio/Video devices, the users of mobile phones could switch between different modes. For checking the sequences of the detections, the time window plays a critical role. The length of the time interval itself needs to be optimised; in this chapter, a fixed interval of 30 minutes is used.

Arterial sensors could not act as check points similar to the sensors located on highways or bike paths. However, it is possible to incorporate the information from these sensors into classification method by including the factor of speed and limiting the time window. In most cases, the speed of a cyclist would not exceed 16 km/h. Therefore, the frequency of detections for cyclist is supposed to be lower than motor vehicles i.e. higher travel time of bicycles. Considering this point, the time required for a detected device to ply between two sensor locations (i.e. travel time) could be as another indicative parameter. Figure 5-2 displays how the layout of the sensors on a road network could provide further information about types of the road users being tracked by Bluetooth sensors.

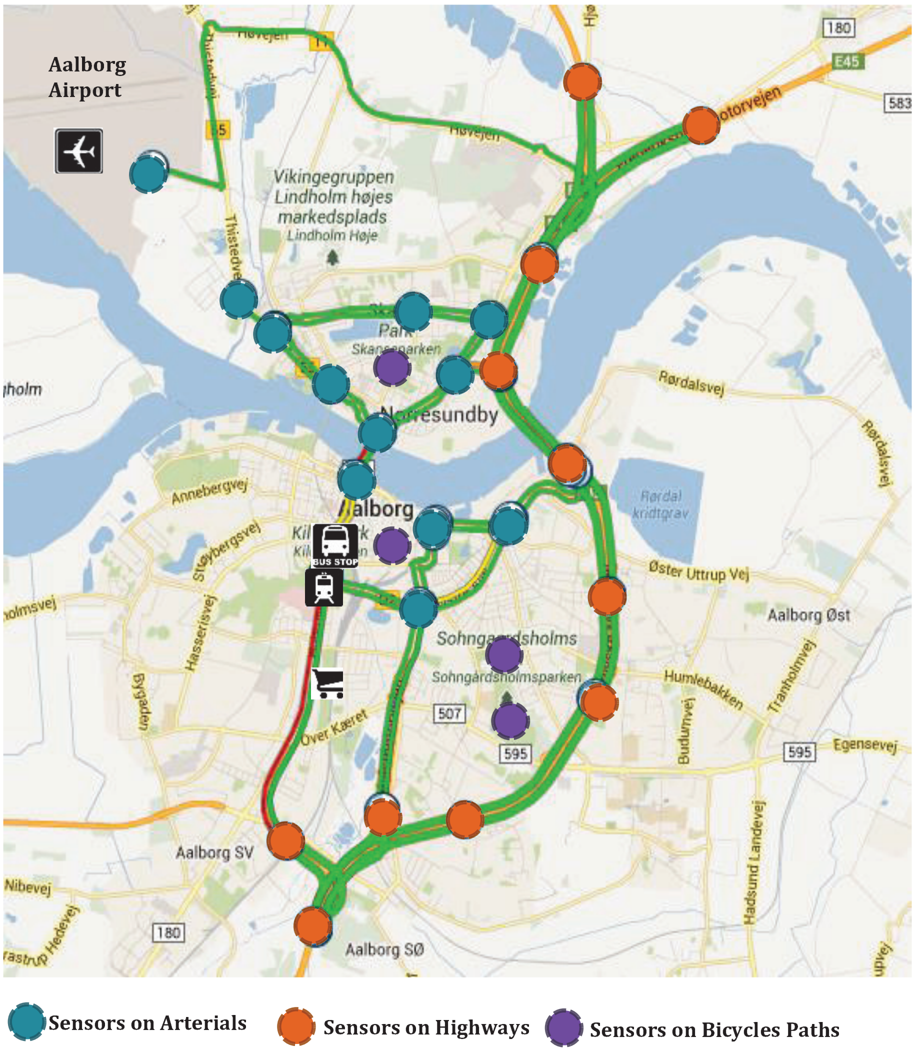

Figure 5-2. Layout of Bluetooth sensors on a road network and their role as a checkpoints for mode classification (Map source: Google Maps)

5.2.2.3 Traffic Condition

Traffic condition during peak and off-peak hours could also provide basis for distinguishing between types of road users. Differences in travel time and speed of various modes during uncongested and congested traffic conditions are usually significant. For example, motor vehicles are significantly faster than the bicycles in uncongested traffic. However, bicycles may travel faster than motor vehicles under congested conditions, especially when bicycles have exclusive lanes (see Figure 5-3).

In order to explain this situation, Figure 5-4 shows travel time data collected for motor vehicles and bicycles by video recording on Limfjordsbroen in Aalborg. During off-peaks intervals of

15:00-15:05 and 15:22-15:30 the band of the motor vehicles' travel time is easily distinguishable from bicycles' travel time. However, over the peak period of 15:05-15:22 the motor vehicles' travel time increases due to the congestion and overlaps with bicycles' travel time band. This emphasises the importance of a dynamic screening method with the capability of modifying the filtering criteria for different traffic conditions, as opposed to a static cut-off method.

Figure 5-3. Cyclist on exclusive lane take over the cars on stopped on congested traffic (Source: Vancouver Sun, 2012)

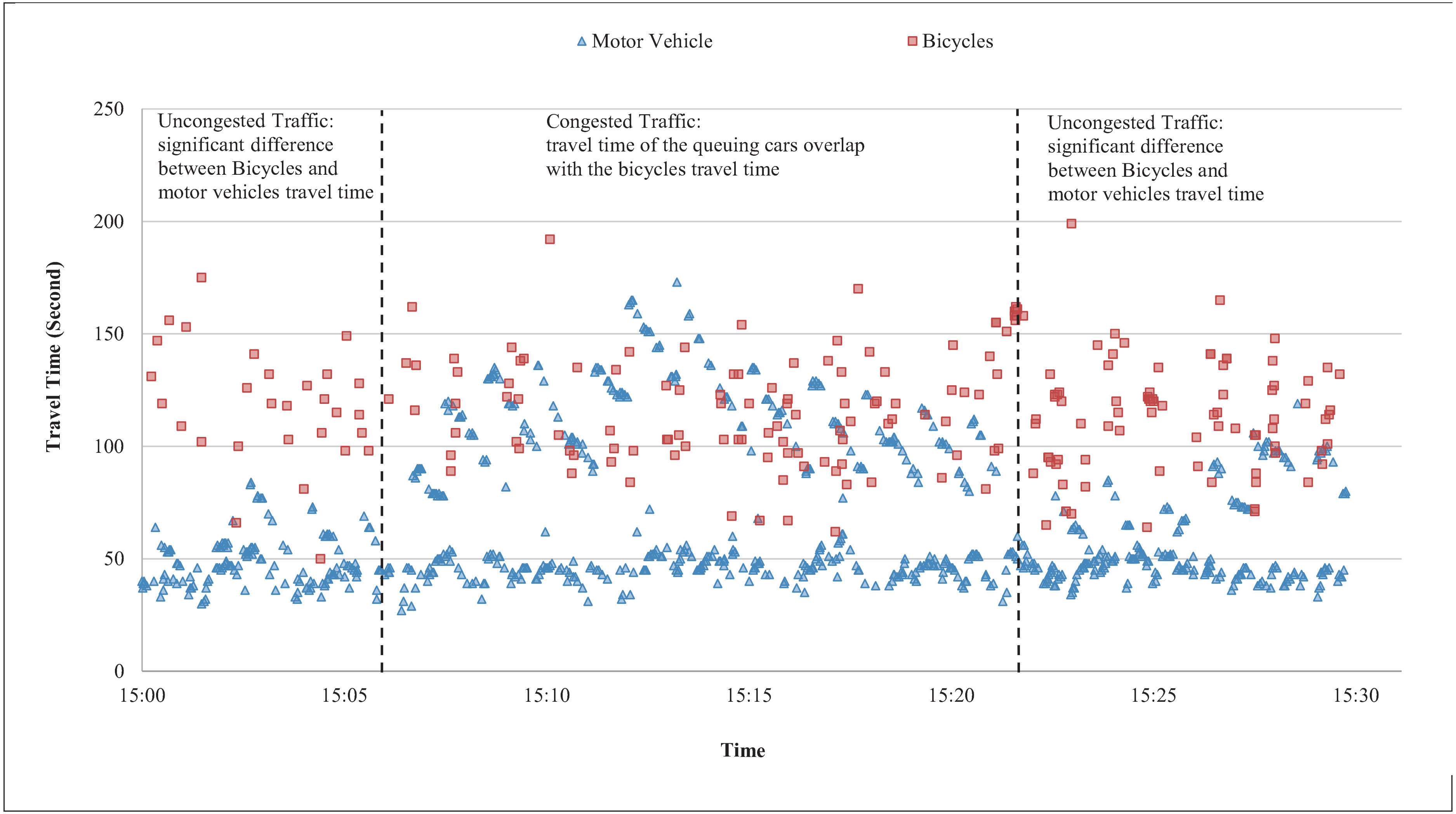

Figure 5-4. Time plot of the motor vehicles and bicycles travel time over peak and off-peak on Limfjordsbroen, Aalborg, Denmark.

5.2.2.4 Methodology and Algorithm

The automated screening mode-classification method is a probabilistic method. This means that, the output of the algorithm represents the most probable mode carrying the device. The term mode of the detected device is used interchangeably as the mode of travel (i.e. vehicle or bicycle) that the device was carried with.

The flowchart shown in Figure 5-5 outlines the various stages of proposed mode classification algorithm. As can be seen in Figure 5-5 different layers of filtration are proposed. While all the layers are explained in this section, the method could be implemented using any combination of layers. The algorithm is explained below.

a) Travel Time Filtration

The method starts with creating an array of last predetermined x number of detected travel time obtained by MAC address matching. Each entry will be tested to check whether it is within the pre-specified range of accepted travel time:

$$Median\_TravelTime_{TT_x} - n \times Standard\ Deviation \leq Travel\ Time_i \leq Median\_TravelTime_{TT_x} + n \times Standard\ Deviation \qquad \textbf{Equation 5-1}$$

Where:

x: The predetermined size of array

n: The factor of Standard Deviation

TT_x: The array of x detected travel times

$Travel\ Time_i$: Travel time of i^{th} detection

$Median\_TravelTime_{TT_x}$: Median of the array of x detected travel times

Note: In the mode specific algorithm the value of x is set to 5, the reason for that is based on the optimum aggregation sample size discussed in Chapter 3. The value of n will be determined based on sensitivity analysis.

b) CoD Filtration

After comparing the travel time of the new entry with the array of previous record, two possibilities could be considered:

- If the travel time is within the accepted boundary (Equation 5-1), this record will be flagged as non-outlier. In the second step, the CoD of the device is checked. If the CoD belongs to the major class of Audio/Video, this record will be kept in the category of motor vehicles. If the CoD belongs to other categories than the Audio/video, it will be kept as highly potential motor vehicle.

- If the travel time is out of the accepted boundary (Equation 5-1), this record will be suspended. The second step checks the CoD. If the CoD belongs to the major class of Audio/Video, this record will be flagged as highly potential slow vehicle. If the CoD belongs to other categories than the Audio/Video, it will be kept as highly potential bicycle. The number of detection events recorded for the device could also be optionally checked. In this case, if the number of detections is more than the other records in array x, then it will be flagged as bicycle. For further evaluation, the RSSI will also be checked; if the RSSI is higher than the RSSI recorded for other Audio/Video devices then the detection will be categorised as bicycle with higher level of confidence.

c) Benchmark Filtration

In both cases, in order to check for inter modal changes an extra step is introduced. This stage checks the sequence of the detection events recorded for that specific device over the whole network of Bluetooth sensors during a predetermined time window. The main idea is to use the information of the location of the Bluetooth sensors (i.e. benchmark points) to check for the mode type. If in the pre-specified time window Y (i.e. value of the Y could be modified to 30 or 60 minutes before the device is detected) there are observations of that specific MAC address on benchmark sensors (i.e. highways or exclusive bicycle paths) then this MAC address will be flagged for further analysis. Different possibilities could be considered as follows:

- If the record is already assigned to the category of motor vehicles, it will be checked whether there is a previous record on highway sensors. In case there is a record in the past Y minutes then it will be assigned to the category of the motor vehicles with a high level of confidence.
- If the record is assigned to the category of a bicycle, it will be checked whether there is a previous record on exclusive bicycle paths or on highway benchmarks. In case there is a record in the past Y minutes on a bicycle path and no detection events on highway benchmark sensors then it will be assigned to the category of the bicycles with a high level of confidence. However, if there is a detection event recorded on highways, then it will be assigned to the category of bicycle with a potential of mode-change during the journey.

By increasing the time window and upper limit of the accepted travel time, the method could potentially be used to identify pedestrians also. However, pedestrian identification is considered outside the scope of this research.

A computer program is written in Perl programming language by the author to implement the proposed method. This program also evaluates the accuracy and efficiency of the developed method against other data sources. In this study, due to the time limitation, logic inlayer *c* is not implemented in the Perl program. Experiment set-up and data collection are explained in the following section.

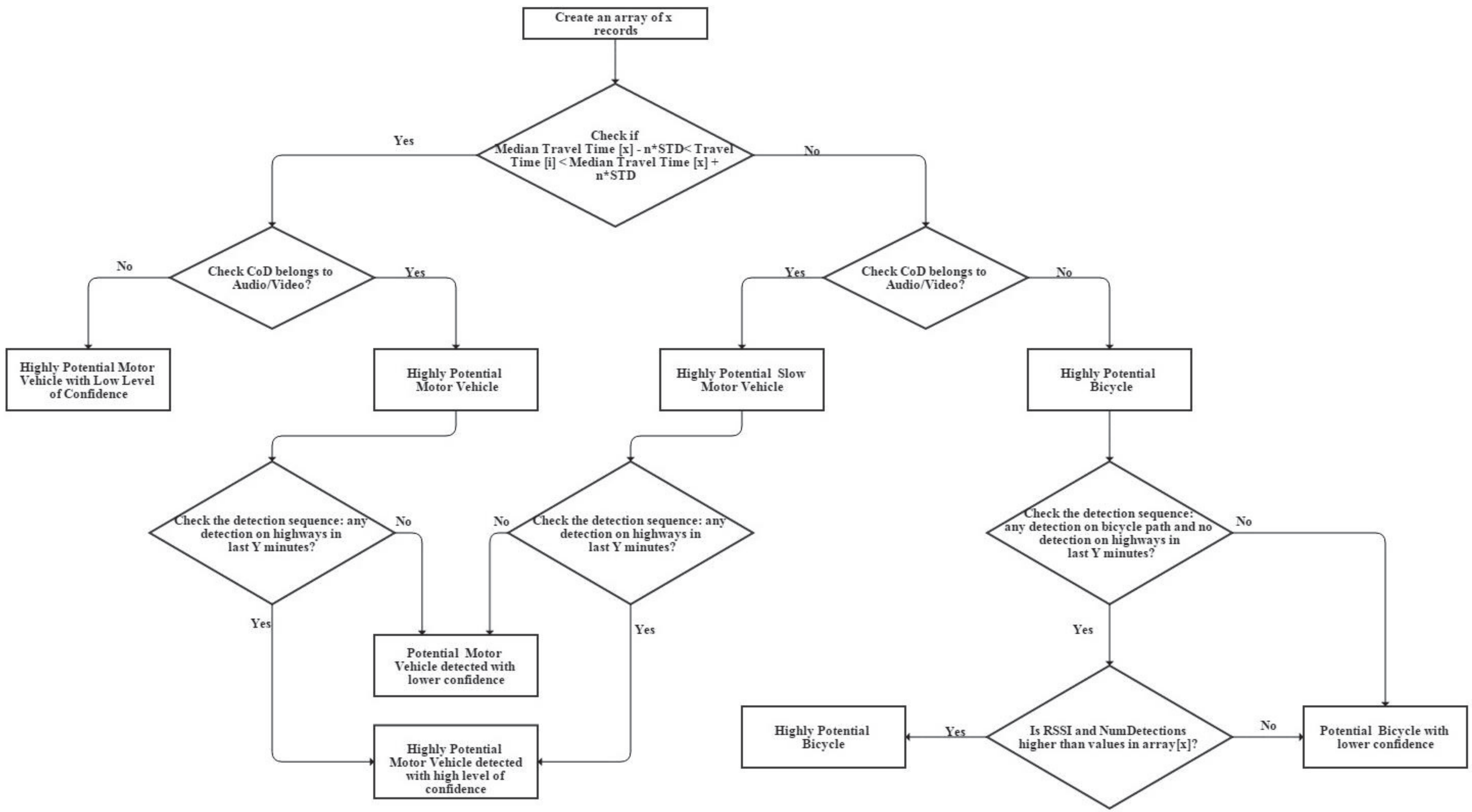

Figure 5-5. Mode classification algorithm

5.3 Experiment Set-up

In order to evaluate the accuracy of the mode-specific travel time estimation algorithm, an experiment was designed. In this experiment travel time data from ANPR, Bluetooth and video cameras were estimated on the same stretch of an arterial road namely Limfjordsbroen in Aalborg, Denmark. On this segment, Bluetooth sensors and ANPR systems were installed on the same pole as shown in Figure 5-7 and Figure **5-8**. The video recordings were used to extract the ground truth travel time and used as the basis of validation. The reason for including three sources of data was to further explore the accuracy of travel time estimated by different data sources. ITSTechnik Company provided the ANPR data used in this study. In case of ANPR, this system only monitors the motor vehicle traffic. Therefore, the existence of bicycle on same road segment would not influence the accuracy of the ANPR estimated motor vehicles travel time. Bluetooth sensors used in this study were from Blip Systems (refer to Section 1.3). When it comes to Bluetooth-based travel time data, two methods were used. The first was based on Blip Systems outputs of real travel time and the second source was based on outputs of the proposed algorithm using raw Bluetooth detection records.

5.3.1 Location of the Experiment

The road stretch is about 600 metres long and is equipped with both ANPR systems and Bluetooth sensors installed on same poles. An aerial photograph of the corridor is shown in Figure 5-6. The choice of the bridge location was based on minimising the impact of noise caused by pedestrians on the analysis and reducing the impact of geometric design on the cyclists' speed. In this context, a number of criteria are considered as follows:

1. A link with mixed traffic and appropriate number of both motor vehicles and bicycles, in order to obtain a proper sample size.
2. A link with limited number of pedestrians, to minimise the disturbance from pedestrians carrying Bluetooth-enabled devices.
3. A link with normal topography which is not so steep to avoid significant influence on the bicycle speed compared to motor vehicles during off-peak.
4. A link with no or minimum number of access roads to residential or industrial places, so as to minimise the diversion of the travellers.

The data were collected for southbound traffic on 19th November 2013. About 5 hours of traffic. from 13:15 to 18:00 were recorded by video cameras and transcribed to ascertain the ground truth. The ground truth data set consisted of 5690 motor vehicles and 1113 bicycles.

Figure 5-6. Location of Bluetooth and ANPR sensors on Limfjordsbroen bridge, Aalborg (Source: Google Maps)

The location of the ANPR and Bluetooth sensors are shown in the Figure 5-7and Figure **5-8**.

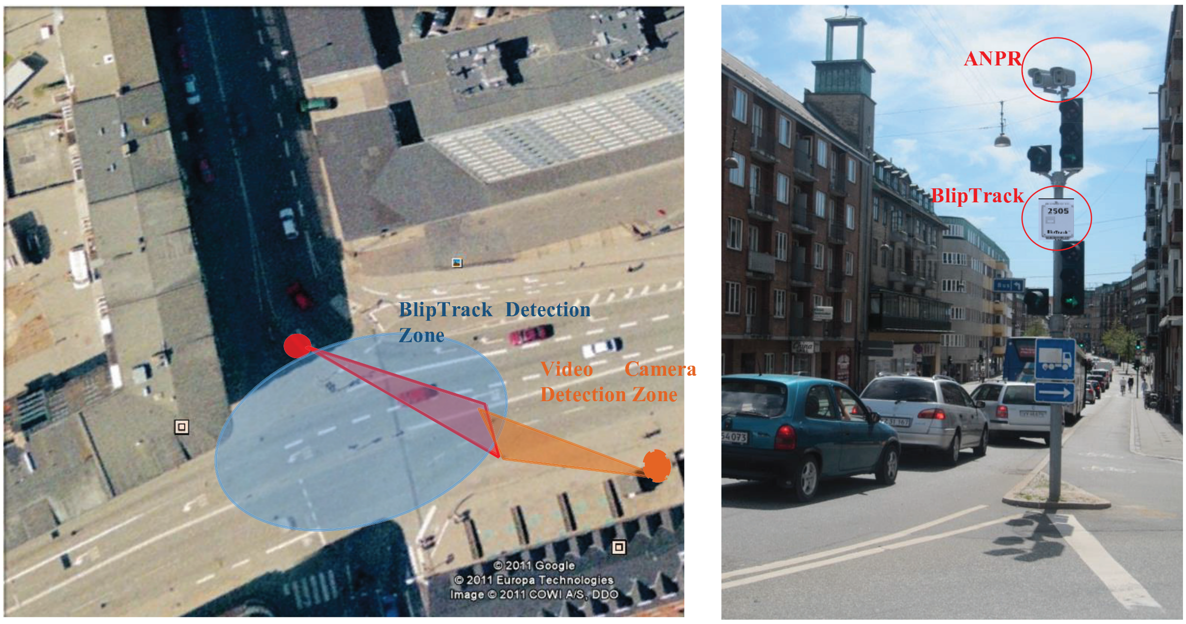

Figure 5-7. Location of ANPR and BlipTrack sensors on point A

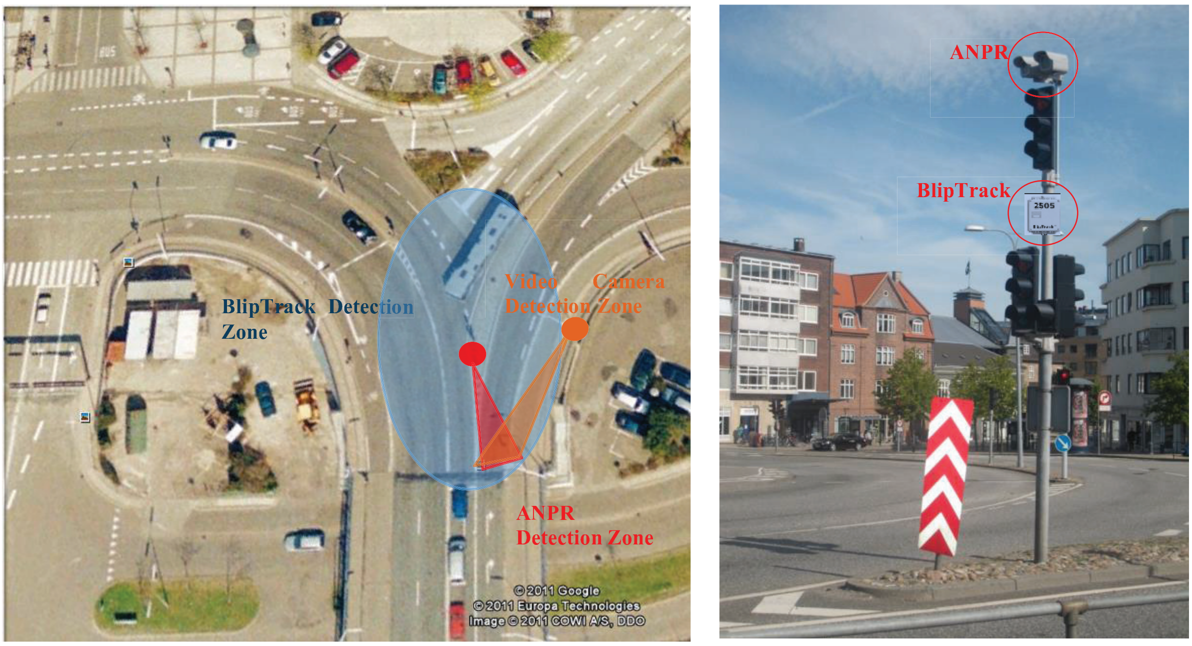

Figure 5-8. Location of ANPR and BlipTrack sensors on point B

5.3.2 Accuracy Evaluation

Mode-specific travel time estimates obtained from the proposed method, ANPR and the BlipTrack sensor were compared against the ground truth. The ground truth was determined by manually transcribing the travel time of vehicles from a video recording of the traffic. In addition, mode-specific travel time for motor vehicles estimated based on Bluetooth data using a clustering method (i.e. two-step clustering method) was also evaluated against the ground truth. In order to conduct the accuracy evaluation, first the distributions of the travel time data are compared with the ground truth by means of time plots. Second, three accuracy measures including MPE, MAPE, and RMSE were used to provide a numerical evaluation of the error associated with each of the method (for details of the accuracy measures refer to Section 3.3.3). In order to use a consistent data format, the comparisons are made based on 5 minutes median aggregated travel time and capture rates. The median aggregation is used based on the results of aggregation method comparison mentioned in Section 3.4.1. Note that, in the automated screening algorithm as well as cluster analysis, the travel time values larger than 216 seconds are not included in the analysis. This is due to the assumption that the bicyclist speed could not be less than 10 km/h. This limit also helps to filter out longer travel times associated with pedestrians.

5.4 Results

Results of the analyses are presented in the following sections.

5.4.1 Sensitivity Analysis

As mentioned, for determining the acceptable travel time boundaries in Equation 5-1, the value of n needs to be specified. The higher value of n gives a larger range for travel time variations and vice versa the lower value of n stringent the limits. In order to determine the optimum value of n a sensitivity analysis for values of 0.5, 1, 1.5, and 2 were conducted. In each case, accuracy of the algorithm travel time estimate is compared with ground truth using MAPE. The optimum value is the one which lead to higher accuracy. Results of the sensitivity analysis are shown in Figure 5-9. As can be seen, $n = 1$ produces the most accurate results. For the rest of analysis, the value of n is set to 1.

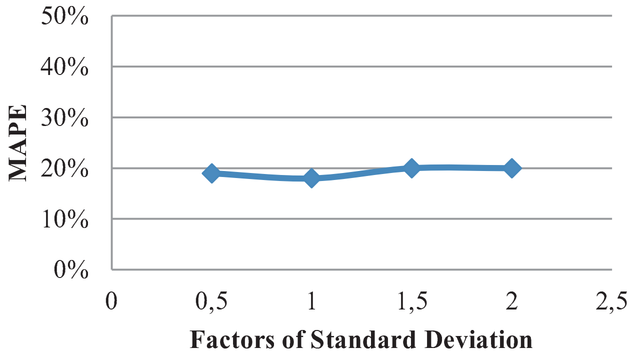

Method	MPE (%)	MAPE (%)	RMSE (Second)
Non-Filtered	6	21	18
Filtered 0.5 STD	4	19	16
Filtered 1STD	**3**	**18**	**16**
Filtered 1.5 STD	5	20	18
Filtered 2 STD	5	20	17

Figure 5-9. Sensitivity analysis of Std deviation factors

5.4.2 Descriptive Statistics

The time plot for various data sources are presented in Figure 5-10. This figure shows how the various data sources overlap with the ground truth. It is clear that there is a good overlap between the results of the algorithm, cluster analysis, and also BlipTrack travel time data. ANPR data are more scattered than other datasets. Additionally, overlap between bicycles and motor vehicles data can be partially observed during the period of 15:00 to 15:30.

Descriptive statistics are summarised in Table **5-1**. The average travel time for ANPR, BlipTrack, cluster analysis and mode-specific method are close to the ground truth. Penetration rates are calculated based on the number of travel time records obtained by each method. The penetration rate for clustering method and algorithm are reported both for filtered values as well as the records being reported as outliers or bicycles. As shown, ANPR has the highest penetration rate with 74%, followed by mode-specific method, cluster analysis and BlipTrack. Moreover, the penetration rate for filtered datasets using mode-specific algorithm and cluster analysis are 2.25 times more than the BlipTrack. Apparently, having more strict filtering method in BlipTrack algorithm leads to lowest standard deviation. Table **5-1** also shows the number of outliers being filtered from automated-screening and cluster analysis algorithms. It should be noted that a significantly lower number of outliers in case of cluster analysis and mode-specific algorithm is due to the filtration of travel times higher than 216 seconds. This resulted in a smaller sample of bicycles or outliers.

Table 5-1. Descriptive statistics for various methods

Methods	N	Sample Rate	Min	Max	Median	Mean		STD
		Percent	Second	Second	Second	Second	Std. Error	Second
Motor Vehicles Ground Truth	5690	-	22	140	58	59.94	0.219	16.498
Bikes Ground Truth	1137	-	71	236	136	139.06	0.710	23.943
ANPR	4213	74	10	554	52	70.24	0.999	64.89
BlipTrack	283	4	42	142	57	60.80	0.895	15.057
Filtered Cluster Analysis	520	9	29	169	56	62.32	0.923	21.037
Outliers Cluster Analysis	45	-	43	216	122	115.5	7.202	48.312
Filtered Mode Specific	493	9	14	216	56	65.69	1.245	27.643
Outliers Mode Specific	19	-	35	169	83	83.74	7.765	33.846

5.4.3 Accuracy Analysis

In order to use a consistent data format, the comparisons are made based on 5 minutes median aggregated travel time. The 5 minutes median aggregated results are presented in Figure 5-11. Results of the accuracy measures are summarised in Table 5-2. The maximum accepted level of error is deemed as 25%; for further information on this threshold, refer to Section 6.1. All the methods have a MAPE below 25%; therefore, results of all the methods can be considered acceptable. However, the proposed mode-specific travel time methods along with ANPR have the most accurate results with a MAPE of 18% and 17% respectively. This indicates the capability of the proposed mode-specific travel time method in reducing the impact of noise associated with bicycles or other outliers. This also implies that by using information recorded by Bluetooth sensors such as CoD and RSSI, it is indeed possible to distinguish between various modes in mixed traffic environment and improve travel time accuracy.

Table 5-2. Accuracy measures of the travel time estimation methods for 5-minutes median aggregated datasets

Method	MPE (%)	MAPE (%)	RMSE (Seconds)
ANPR	-5	17	15
BlipTrack	7	23	18
Cluster Analysis	5	20	18
Non-Filtered 1STD*	6	21	18
Filtered 1STD**	**3**	**18**	**16**

*. Results of the algorithm before filtering the detected bicycle
**. Results of the algorithm after filtering the detected bicycle

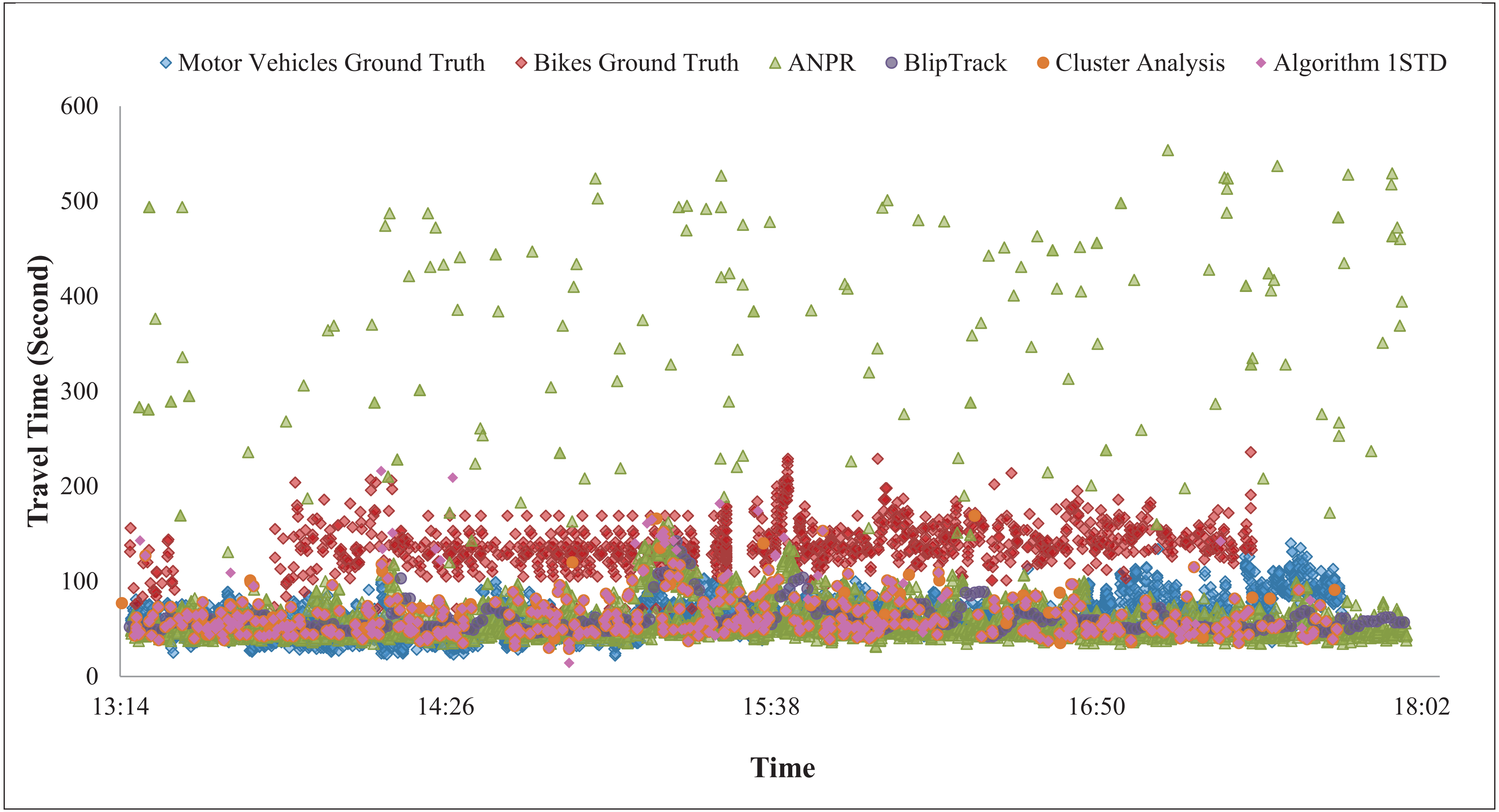

Figure 5-10. Travel time plots for various methods

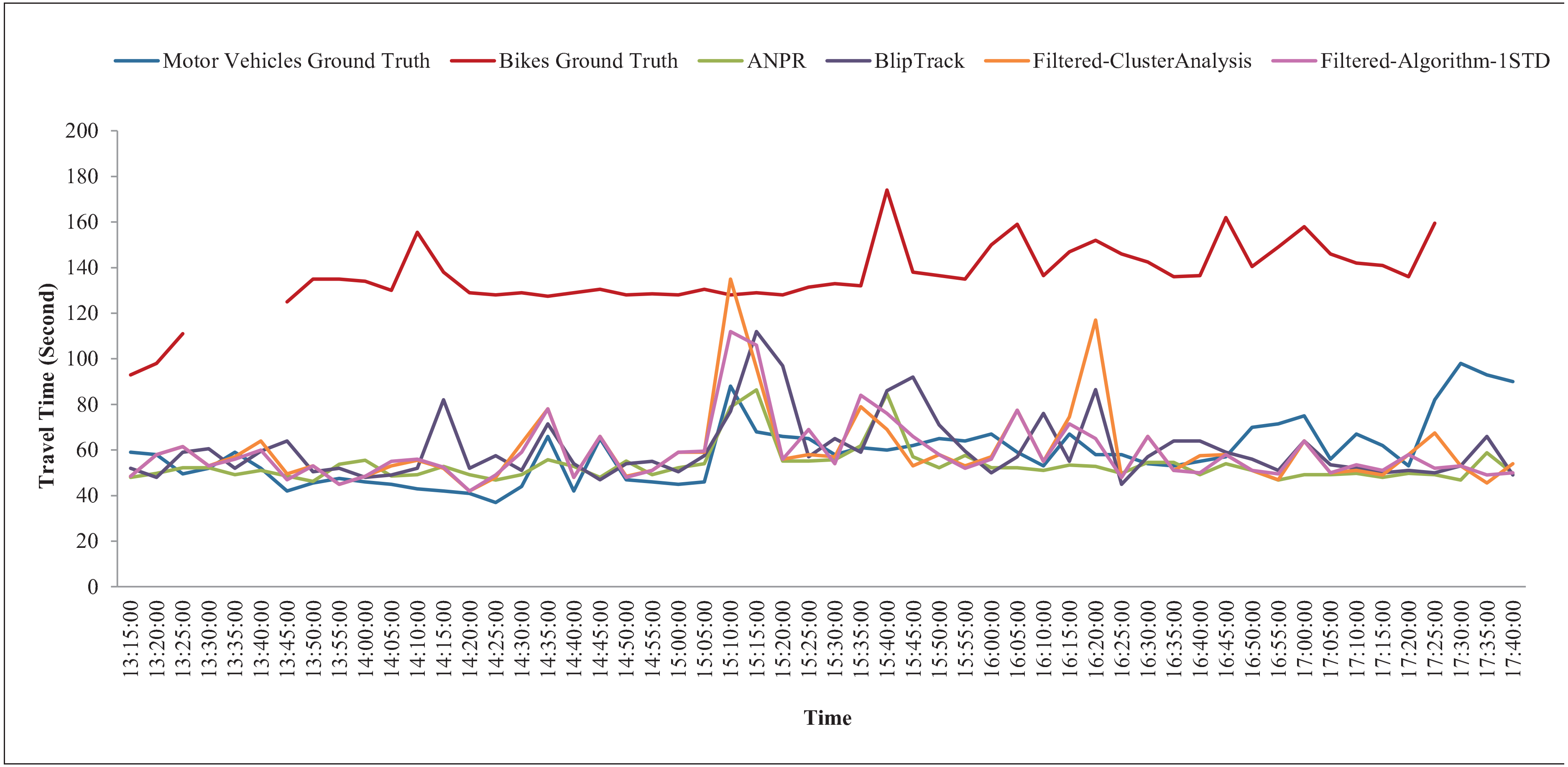

Figure 5-11. Travel time plots for 5-minutes median aggregated datasets

5.5 Conclusion

Compared to traditional systems such as ANPR that only monitor motor vehicle traffic, Bluetooth sensors detect devices in motor vehicles, bicycles and those carried by pedestrians. There is no direct way to categorise the detection events recorded by Bluetooth sensors into different modes. Therefore, travel time estimation using Bluetooth sensors on urban arterial roads with multiple travel modes can be inaccurate. A new method to distinguish travel modes and estimate mode-specific travel time was presented in this paper. The method is based on three main parameters: differences in the functionality between various Bluetooth-enabled devices as determined using the CoD of the device, information about the location of the Bluetooth sensors over the road network and the detection sequence of a given Bluetooth device by multiple sensors and traffic conditions. The proposed method aims to distinguish between the Bluetooth detections recorded by devices carried by motorised and non-motorised modes and provide mode-specific travel time estimates.

Accuracy of the mode-specific travel time estimation method was evaluated against ground truth data obtained from video recordings, and also against ANPR, BlipTrack and a naïve clustering method using Bluetooth detection data. The estimated travel time using ANPR, BlipTrack, cluster analysis and mode-specific method were all close to the ground truth. Results of accuracy analysis showed that the proposed method provides travel time estimates with almost the same level of accuracy as ANPR; with a MAPE of 18% against 17% from ANPR, and better accuracy compared to commercially available Bluetooth based travel time estimation methods. This indeed proves the capability of Bluetooth technology to be used as an alternative method for arterial travel time estimation under mixed traffic conditions. The results highlights the accuracy improvement resulting from the use of CoD and RSSI information along with the commonly used MAC address data, which is a novel contribution in this chapter. Ability of the proposed method distinguishing between Bluetooth detections obtained by various modes gives rise to the possibility of providing bicycle travel time estimates using Bluetooth at a significantly lower cost compared to current alternatives and demonstrates an advantage over ANPR that can monitor only motor vehicles.

In the next Chapter, Bluetooth technology will be compared with a number of traffic data collection technologies in terms of travel time accuracy and sampling rate. This will provide a more detailed understanding of the accuracy of Bluetooth technology versus other conventional technologies.

CHAPTER 6

EVALUATION OF BLUETOOTH TECHNOLOGY COMPARED TO OTHER SENSOR TECHNOLOGIES

6. Introduction

The accuracy and reliability of Bluetooth technology were evaluated in previous studies (Haghani et al., 2010; Puckett and Vickich, 2010; Barcelo et al., 2010). A report by Saunier and Morency (2011), evaluates Bluetooth, GPS, video counters and floating cars along a common stretch of highway in the greater Montreal Area. The study found strong correlations between the datasets and provided basic information regarding the limitations of each approach. A recent study conducted by the University of Washington STAR Lab (Wang et. al, 2011) compared travel time data quality between number plate readers and the STAR Lab Bluetooth sensors on the SR-522 corridor, Seattle. Other data were not included in the comparison. Overall, Bluetooth showed a travel time difference of roughly 10% when compared to ANPR sensors. Another study carried out by the Texas Transportation Institute (Middleton, et al., 2012) compared data from a number of providers that employ GPS, cell phone tracking and fixed sensor technologies, while examining relative (per mile) costs. Basic accuracies for Bluetooth, loops, video, radar and magnetometers are also provided. The report recommended testing these technologies on a common corridor to have a better overview of their travel time accuracy. As mentioned, the previous evaluations are usually limited either in terms of duration of data collection or number of technologies used for comparison. Therefore, conducting a comprehensive comparative study of Bluetooth technology with other existing technologies will provide more insight into the advantages and disadvantages of this method.

6.1 Importance of Accuracy of Travel Time Estimation

There are very few studies available that evaluate the effectiveness of various travel time data collection technologies side-by-side, thus it is often unclear which approach should be used for a given application. Therefore, a comprehensive overview of existing technologies as well as a side-by-side evaluation will provide more insight into selecting the appropriate technology for a given application. This evaluation is intended to provide decision support for transportation agencies selecting travel time systems based on the accuracy and reliability of each system.

The choice of a system and its corresponding accuracy could play a significant role in the benefits of the information provided for the users (i.e. utility) according to a FHWA report by Toppen and Wunderlich (2003). The relationship between accuracy of the information obtained by ATIS and the benefits for the users was determined for a case study in Los Angeles (see Figure 6-1). The researchers found that when accuracy drops below a critical point, users are better off not using the data provided by the ATIS and relying instead on experience with historical traffic patterns. In Figure 6-1, there are four utility curves representing the utility realised during morning peak trips, evening peak trips, off peak and all trips. For evening peak trips, represented by the green line on top, the per trip utility realised on 25 minute trip for perfect and near perfect data was two dollars. The point at which the ATIS data became worthless to users was at approximately 21% accuracy, where using the ATIS data produce negative utility values. Beyond a certain point, below 5% error for example, it makes little sense to invest in improving accuracy as users realise little to no increased benefit. In this case, funds for ATIS improvements would be better spent in areas besides improving accuracy, such as expanding coverage to other roadways (Toppen and Wunderlich, 2003). Therefore, a trade-off needs to be made based on the required accuracy and the costs of implementing ATIS technologies. Figure 6-1 shows that as travel time error approaches 20% users realise no value from ATIS data. Innamaa (2009) stated that the net benefit from an advanced traveller information service was positive in earlier studies only if the error in service reporting was below the range of 10–25%, but the cost-efficiency of the service was likely to suffer if error levels below 5% were being pursued. In this study, based on earlier studies by Innamma (2009), Toppen and Wunderlich, (2003), and Jung et al. (2003) the ATIS error band is defined as 10-25%.

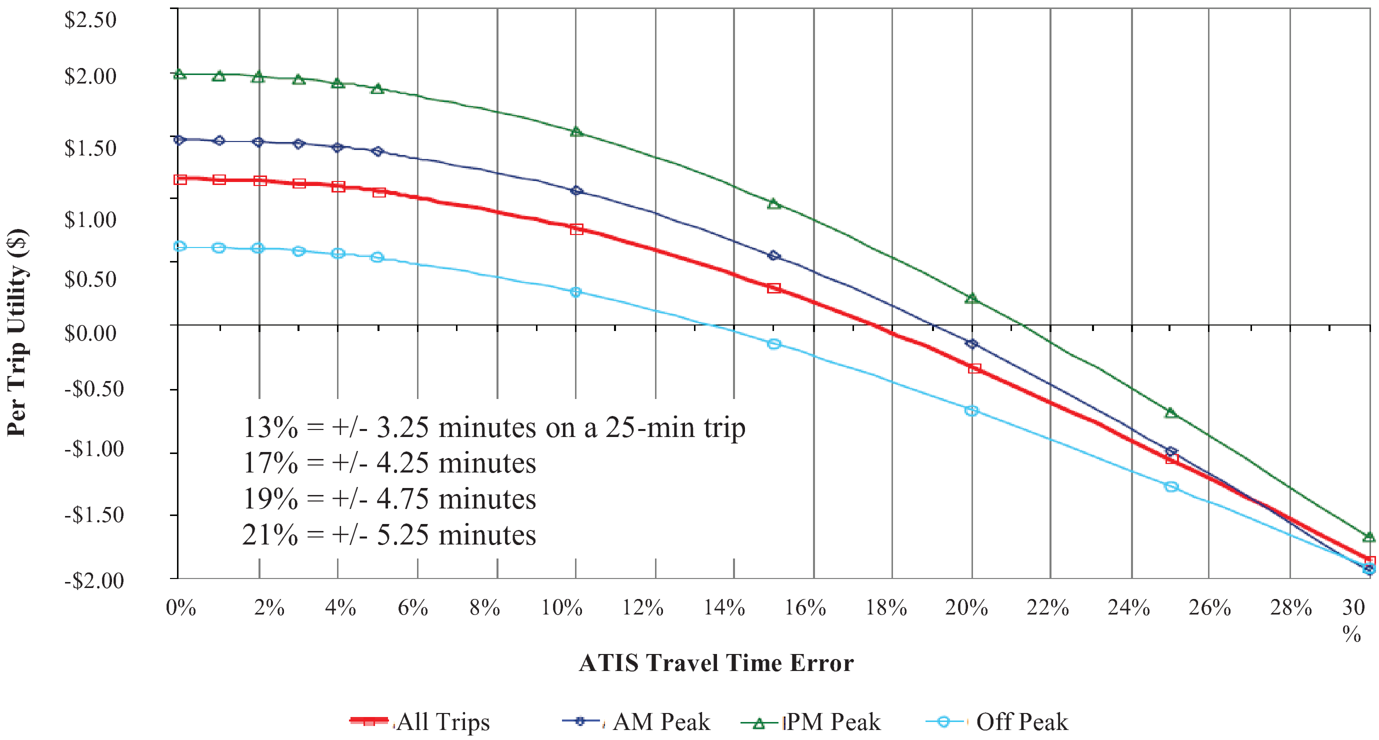

Figure 6-1. Benefit-accuracy relationship for case study in Los Angeles (Source: Toppen and Wunderlich, 2003)

Since each technology captures data at different resolutions and accuracy, it is important to know what resolution/match rate/density of data points are necessary to predict reliable travel times at a stated level of confidence. Hence, conducting a side-by-side comparative study of the various technologies on a common corridor is intended to provide ITS planners the data required to make cost effective decisions regarding deployment of surveillance technologies to support ATIS solutions.

In this Chapter, side-by-side comparisons of the various available travel time data collection technologies is carried out using data from two corridors. The first evaluation corridor is State Route 522, (SR 522), which is an urban commuting corridor to and from Seattle, Washington, United States (See Figure 6-1Figure 6-2). The second evaluation corridor is a rural section of Interstate 90 (I-90) east of Seattle, Washington, United States (See Figure 6-3). The main objectives of this comparative study of Bluetooth technology with other existing technologies can be summarised as follows:

- Compare Bluetooth technology with a number of travel time, volume and speed data collection technologies side-by-side;
- Determine the relative accuracy and performance (Error Matrix) of Bluetooth technology compared to the other technologies;

- Determine the relative reliability of Bluetooth technology compared to the other technologies.

6.2 Different Methods for Travel Time Data Collection

Several data collection techniques can be used to measure or collect travel time. Many of the technologies being evaluated in this study use different methodologies to generate travel time information. These various techniques can be classified into a few generalised methodologies, such as those using: probe vehicles, vehicle re-identification, and volume and speed estimation methods (also referred to as flow estimation techniques). Note that the flow estimation technique is presented for completeness. These techniques are designed to collect travel times and average speeds on designated roadway segments or links. A general overview of the various techniques is provided in the following sections.

6.2.1 Probe Vehicles Method

The probe vehicle method utilises instrumented vehicles in the traffic stream to collect travel times (Travel Time Data Collection Handbook, 1998). An ITS probe vehicle can be a private, public transit, or a commercial vehicle. Generally, methods of travel time estimation via probe vehicles a rely on GPS systems to gather data regarding position and speed. These GPS systems may be integrated into the vehicle, such as for fleet vehicle operations or portable systems such as smart phones. Other systems in use include transponder and radio-based systems. The goal of the probe vehicle based methodologies is to estimate travel times for all vehicles in the traffic stream based upon high quality travel time data from a subset of vehicles in traffic.

6.2.1.1 ITS Probe Vehicle Data Collection Systems

Probe vehicles may be equipped with several different types of electronic transponders or receivers, from passive transponders to live GPS transmissions.

a. Signpost-Based Automatic Vehicle Location (AVL) - This technique has mostly been used by transit agencies. With an AVL system, probe vehicles communicate at intervals with a transmitter and receiver infrastructure. Note that these systems may be active, with vehicles frequency broadcasting data, or passive, where transponders only broadcast when queried by the receivers infrastructure. Depending on the frequency and quality of data transmitted, AVL systems may operate like probe vehicles, or more as a vehicle re-identification system, discussed later.

b. Automatic Vehicle Identification (AVI) or Radio Navigation- Radio navigation systems use triangulation techniques to locate radio transponders on vehicles, and are used in route guidance and communication systems. Data are collected by communication between probe vehicles and a radio tower infrastructure (Mathew, 2013). Typically, this type of system is used for fleet dispatch, such as for transit, commercial or government vehicle dispatch.

c. Global Positioning System (GPS) - GPS based systems are increasingly found at the personal level with dedicated GPS navigation systems and smart phones being the most common implementations. Some of these systems broadcast data back to service providers for use in providing real-time traffic data.

6.2.1.2 General Advantages and Disadvantages of Probe Vehicles

The advantages and disadvantages of this method can be summarised as follows(Travel Time Data Collection Handbook, 1998):

Advantages
- Low cost per unit of data
- Continuous data collection
- Automated data collection
- Data are in electronic format
- No disruption of traffic

Disadvantages
- High implementation cost (depending on system used)
- Fixed infrastructure constraints - Coverage area, including locations of antenna
- Requires skilled software

6.2.2 Vehicle Re-Identification Method
Re-identification relies on recording unique characteristics (i.e. a signature) of the target vehicle to be used to identify the target vehicle at subsequent sensor locations. Vehicle re-identification is the process of collecting vehicle identification data (i.e. signature) and the timestamp of vehicles passing a road side reader device and matching against data from another reader passed by the target vehicle to determine the travel time between reader locations.

6.2.2.1 Vehicle Re-Identification Data Collection Systems
Probe vehicles may be equipped with several different types of electronic transponders or receivers.

a. Vehicle Signature Matching
Estimates travel time by matching (or correlating) unique vehicle signatures between sequential observation points. These methods can utilise a number of point detectors. Travel time is then the differences in the times that each (matched) vehicle arrives at the upstream and downstream sensor stations. One characteristic of signature matching systems is a time delay built into data collection related to the time it takes for vehicles to travel from one detector to the next.
Examples of signature matching technologies include licence plate readers, inductive loop detector signature re-identification, magnetometer signature re-identification and Bluetooth/WiFi MAC address re-identification. The unique signature differentiating vehicles in each case is different, but the methodology is the same. As previously discussed, transponder based systems with low frequency data collection may operate more like signature based re-identification systems than probe vehicle based systems.

b. Platoon Matching
Platoon matching is a special case of vehicle re-identification that relies on the fact that vehicles tend to travel in platoons. This method estimates average travel time by matching unique features of vehicle platoons such as the position and/or distribution of vehicle gaps or unique vehicles. Platoon matching assumes that vehicles in a platoon will travel at approximately the same speed and retain approximately the same order between sensor locations. Because of these assumptions, platoon matching generally requires closely spaced detection points to prevent platoons from changing too drastically for the algorithms to re-identify between sensors.

6.2.2.2 General Advantages and Disadvantages of Vehicle Re-Identification

The advantages and disadvantages of this method can be summarised as (Travel Time Data Collection Handbook, 1998):

Advantages

- Travel times from a large sample of motorists
- Simple technique
- Automated data collection
- Data are in electronic format
- Provides a continuum of travel times during the data collection period
- No disruption of traffic

Disadvantages

- Travel time data limited to locations where readers can be positioned;
- Limited geographic coverage
- Requires skilled software
- Inherent personal privacy risk except for ILD nad magnetometers

6.2.3 Point Base Volume and Speed Estimation Method

Volume and speed estimation technologies rely on the classical steady-state traffic flow relationship between the traffic stream flow rate (q), the traffic stream density (k), and the traffic stream space-mean-speed ($\bar{u}_s$) derived by Lighthill and Witham (1955) as follows:

$$q = k.\bar{u}_s \qquad \textbf{Equation 6-1}$$

Traffic stream speeds are typically measured in the field using a variety of spot speed measurement technologies. These approaches try to extrapolate local point data into corridor level information. The average traffic stream speed can be computed in two different ways: a time-mean speed and a space-mean speed. The difference in speed computations is attributed to inherent difference in definitions of time-mean speed and a space-mean speed. The space-mean speed reflects the average speed over a spatial section of roadway, while the time-mean speed reflects the average speed of the traffic stream passing a specific stationary point (Rakha and Zhang, 2005).

6.2.3.1 Point Base Volume and Speed Estimation Data Collection Systems

The most common point based spot speed measurement technologies can be mentioned as inductive loop detectors and virtual loop detectors.

a. Inductive Loop Detectors (ILD)

The most common of these spot speed measurement technologies is an inductive loop detector set to report presence or occupancy (the percentage of time an ILD detects the presence of a vehicle) (Rakha and Zhang, 2005). ILD's measure the traffic flow, traffic speed, and the percentage of time that the detector is occupied. The traditional practice for estimating speeds from single loop detectors is based on the assumption of a constant average effective vehicle length.

b. Video Detection

Video detection systems works based on the principle of virtual loop detectors (VIL). A VIL is a virtual detector created by processing the input of another sensor type into that of a standard induction loop. VILs are designed to play the same role as a legacy ILD to interface with existing equipment. In this way, a VIL service gathers real time information of the vehicles traversing this virtual detector (Gramaglia et. al, 2013). In general, VILs try to mimic the data obtained by inductive loops and collect data about vehicle flow, presence, count, and occupancy. Because of this close emulation VILs share many of the same strengths and weaknesses of traditional ILDs.

6.2.3.2 Magnetic Signature Matching
This method relies on matching vehicle signatures from wireless sensors. The sensors provide a noisy magnetic signature of a vehicle and the precise time when it crosses the sensors. A match (re-identification) of signatures at two locations gives the corresponding travel time of the vehicle.

6.2.3.3 General Advantages and Disadvantages
Advantages
- Travel times from a large sample of motorists
- Simple technique
- Provides a continuum of travel times during the data collection period
- Performs well in both high and low volume traffic and in different weather conditions (Sreedevi, 2005).

Disadvantages
- Expensive deployment and maintenance costs (Particularly for invasive ILDs)
- Trouble measuring low-speed vehicles (Some VILs may be better or worse)
- Only provide point values to estimate link travel times
- Limited spatial coverage
- Issues with reliability and sensitivity, primarily from improper connections and installation
- Inability to directly measure speed. If speed is required, then a two-loop speed trap is employed or an algorithm involving loop length, average vehicle length, time over the detector, and number of vehicles counted is used with a single loop detector (Sreedevi, 2005)(Some VILs may be able to measure speed directly).

6.3 Experiment Design and Data Collection
In order to evaluate the accuracy of Bluetooth technology versus other sensors, two case studies were conducted in a joint collaboration with Washington State Department of Transport (WSDOT) and University of Washington, Seattle, United States.
Two test sites are used for this study; State Route 522 (SR 522) northwest of Seattle and I-90 across Snoqualmie Pass east of Seattle. Both corridors are located in Washington State. The main reason to use these test sites was that the WSDOT has already instrumented sections of SR 522 and I-90 with substantial sensing capabilities. Moreover, running tests on both sites with different functional classifications, the SR 522 test corridor is an urban arterial and the I-90 corridor is a rural freeway, allows the systems to be examined under different conditions. The different link lengths also provide an opportunity to evaluate the errors related to short corridors versus long corridors. Each site is detailed in the following sections.

6.3.1 SR 522 Freeway Test in Seattle, Washington

A section of SR 522 between NE 153^{rd} Street and 83^{rd} Place NE in Seattle, Washington was selected as one of the test sites to conduct the side-by-side comparison, see Figure 6-2. This site consists of 3 links between the following four intersections:

- Point 1: SR 522 and NE 153^{rd} Street
- Point 2: SR 522 and State Route 104 (SR 104)
- Point 3: SR 522 and 68^{th} Avenue NE
- Point 4: SR 522 and 83^{rd} Place NE

Four intersections break the SR 522 corridor into 3 segments. The westbound segments are SR 522 and 83^{rd} Place NE to SR 522 and 68^{th} Avenue NE, SR 522 and 68^{th} Avenue NE to SR 522 and SR 104 Junction and SR 522 and SR 104 Junction to SR 522 and NE 153^{rd} Street. For brevity's sake these names will be shortened in the text to 83^{rd} Pl. NE to 68^{th} Ave. NE, 68^{th} Ave. NE to SR 104, and SR 104 to NE 153^{rd} St. Where space is constrained the following abbreviations will be used (with Excel chart abbreviations in parentheses): 83^{rd} → 68^{th} (83rd > 68th), 68^{th} → SR 104 (68th > SR 104) and SR 104 → 153^{rd} (SR 104 > 153rd). Likewise, the eastbound segments are SR 522 and NE 153^{rd} Street to SR 522 and SR 104 Junction, SR 522 and SR 104 Junction to SR 522 and 68^{th} Avenue NE, and SR 522 and 68^{th} Avenue NE to SR 522 and 83^{rd} Place NE. The eastbound segment short names are NE 153^{rd} St. to SR 104, SR 104 to 68^{th} Ave. NE, and 68^{th} Ave. NE to 83^{rd} Pl. NE. Finally, the eastbound abbreviations (and Excel abbreviations) are: 153^{rd} → SR 104 (SR 104 > 153rd), SR 104 → 68^{th} (SR 104 > 68th), and 68^{th} → 83^{rd} (68th > 83rd).

WSDOT has instrumented the SR 522 corridor with substantial sensing capabilities. Currently, the SR 522 corridor is equipped with Pips Technology licence plate readers, EDI and Reno inductive loops, TrafficCast BlueTOAD Bluetooth sensors, Blip Systems combination Bluetooth and WiFi sensors, Traficon video detection units, Sensys Networks magnetometers and a 3^{rd} party data feed from INRIX. In the case of loop detectors (ILD or VIL), one system is implemented at each intersection, providing count data. Figure 6-2 shows the location of the sensors along the SR-522 corridor. Arrows with different colour represent sensor availability on each segment for eastbound and westbound, respectively.

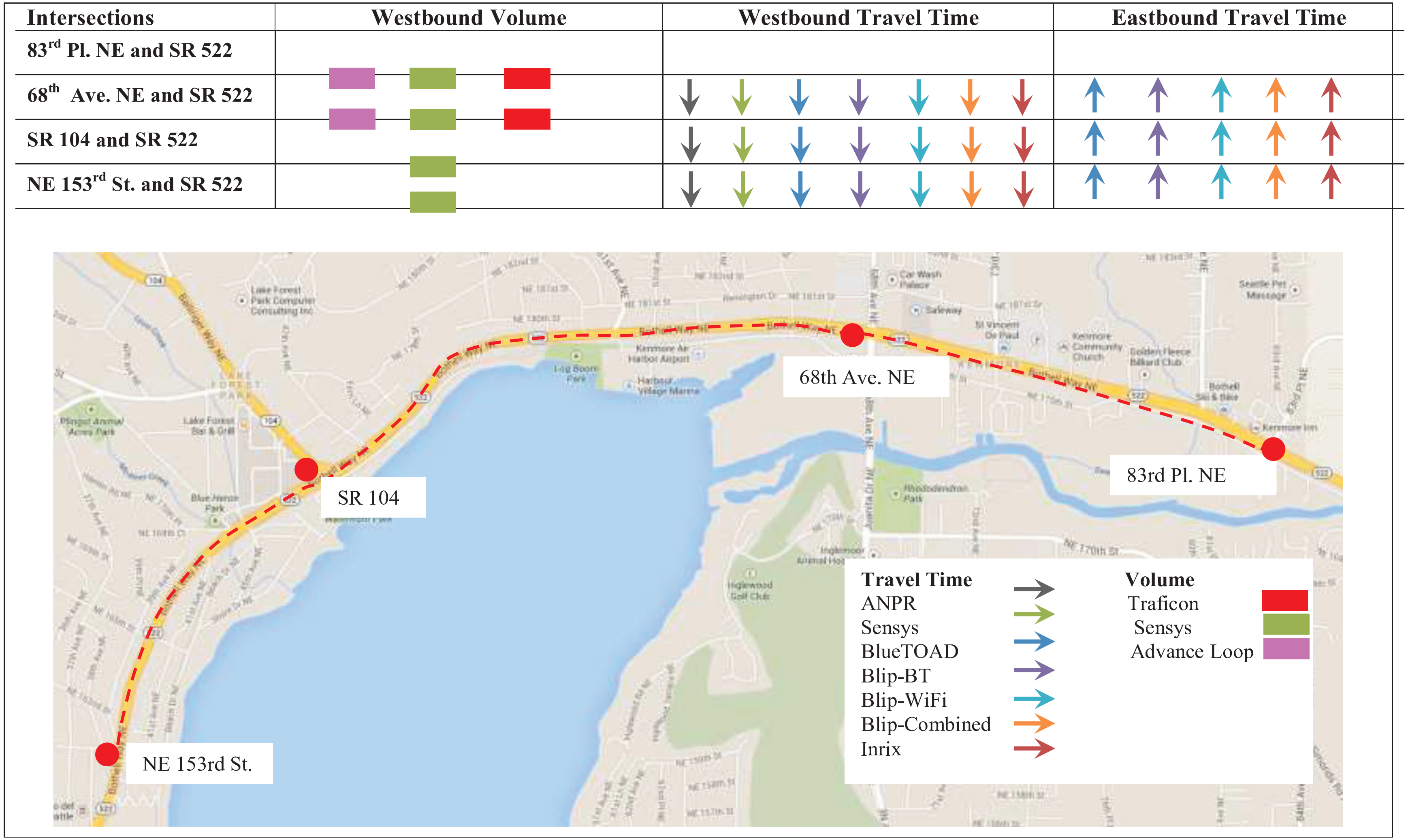

Figure 6-2. Sensor locations and segments along the SR 522 corridor (Source: Google Map)

6.3.2 I-90 Freeway Test at Snoqualmie Pass, Washington

A section of I-90 between North Bend, Washington and Ellensburg, Washington was selected as the other test site in order to conduct the side-by-side comparison for longer rural corridors. Given the longer links inherent to this test corridor and that there are no traffic signals between data collection sites, the research team expect there to be fewer confounding factors in the data at this site. Conversely, there are fewer sensor types installed along I-90, so there is less opportunity for comparing results between sensor types. This site consisted of 3 links between following mileposts:

- Point 1: I-90 at milepost 32
- Point 2: I-90 at milepost 52
- Point 3: I-90 at milepost 70
- Point 4: I-90 at milepost 109

The segment names for I-90 are much simpler with segments being named in the form of milepost X to milepost Y and the abbreviation MP being used for milepost. The westbound routes then become milepost 109 to milepost 70, milepost 70 to milepost 52, and milepost 52 to milepost 32. Eastbound segments are milepost 32 to milepost 52, milepost 52 to milepost 70 and milepost 70 to milepost 109. These names are shortened to the abbreviations MP 109 → MP 70 (MP 109 > MP 70), MP 70 → MP 52 (MP 70 > MP 52), and MP 52 → MP 32 (MP 52 > MP 32) for westbound and similarly for eastbound. Figure 6-3 below shows the location of the sensors along the I-90 Snoqualmie Pass Corridor. Arrows with different colour represent sensor availability on each segment for eastbound and westbound, respectively.

Intersections	Westbound	Eastbound
MP 109	↓ ↓	↑ ↑
MP 70	↓ ↓	↑ ↑
MP 52	↓ ↓	↑ ↑
MP 32	↓ ↓	↑ ↑

Figure 6-3. Sensor locations along I-90

Three categories of travel time data collection technologies were deployed in this study. Details about these technologies are given in Appendix-III.

- Volume and speed estimation technologies
    - Inductive loop detectors (ILD)
        - EDI: Oracle 2
        - Reno A&E: 1100SS
    - Video detection processor unit (VDPU)
        - Traficon: VIP3D.2
    - Magnetic Signature Matching
        - Sensys: VSN540-F
- Vehicle re-identification technologies
    - Automated licence plate recognition (ANPR)
        - Pips Technology: P372 model
    - Bluetooth MAC address Matching
        - Trafficcast: BlueTOAD-BT-Cell-50W
        - BlipSystems: BlipTrack^{TM}-BT
        - BlipSystems: BlipTrack^{TM}-WiFi
    - Magnetic Signature Matching
        - Sensys: VSN540-F
- Probe vehicles technologies
        - 3rd Party INRIX

6.3.3 Sensor Availability on SR 522

The data availability by link for the East-bound and West-bound directions on SR 522 are shown in Figure 6-2. The arrows represent the direction of the traffic where there is available data. The list of technologies implemented at each intersection is summarised in Table 6-1 and Table 6-2.

6.3.4 Sensor Availability on I-90

The I-90 Snoqualmie Pass corridor is equipped with BlueTOAD Bluetooth sensors and makes use of the overlapping 3rd Party data feed from INRIX. I-90 segments are indicated in Figure 6-3. The list of technologies available on each intersection is summarised in Table 6-3 and
Table 6-4.

Table 6-1. List of technologies implemented on SR-522

Sensor	Manufacture	Model	Website
Loop	EDI	Oracle 2	http://www.editraffic.com/home.html
Loop	Reno A&E	1100-SS	http://www.renoae.com/traffic/
Video Detection Processor Unit (VDPU)	Traficon	VIP3D.2	http://www.kargor.com/traficon_master.html
Automated Licence Plate Reader (ANPR)	Pips Technology	P372 model	http://pipstechnology.com/home_us/
BlueTOAD	TrafficCast	BT-Cell-50W	http://trafficcast.com/
BlipTrack	Blip Systems	BlipTrack-BT	http://www.bliptrack.com
BlipTrack	Blip Systems	BlipTrack-WiFi	http://www.bliptrack.com
Magnetometer-Access point	Sensys	AP240-EC-Ver	http://www.sensysnetworks.com/
Magnetometer-Repeater	Sensys	RP240-B	http://www.sensysnetworks.com/
Magnetometer-Sensor	Sensys	VSN540-F	http://www.sensysnetworks.com/

Table 6-2. List of sensors mounted on SR-522 intersections

Technology	Intersection			
	NE 153rd St./SR 522	SR 104/SR522	68th Place NE/SR 522	83rd Place NE/SR 522
ILD	EDI-Oracle 2	EDI-Oracle 2	EDI-Oracle 2	EDI-Oracle 2
VDPU	-	Traficon- VIP3D.2	-	Traficon- VIP3D.2
ANPR	P372 model	P372 model	P372 model	P372 model
Bluetooth	BlueTOAD-BT-Cell-50W	BlueTOAD-BT-Cell-50W	BlueTOAD-BT-Cell-50W	BlueTOAD-BT-Cell-50W
	BlipTrack™-BT	BlipTrack™-BT	BlipTrack™-BT	BlipTrack™-BT
	BlipTrack™-WiFi	BlipTrack™-WiFi	BlipTrack™-WiFi	BlipTrack™-WiFi
Magnetometer	Access point AP240-EC-Ver	Access point AP240-EC-Ver	Access point AP240-EC-Ver	Access point AP240-EC-Ver
	Repeater- RP240-B	Repeater- RP240-B	Repeater- RP240-B	Repeater- RP240-B
	Sensor- VSN540-F	Sensor- VSN540-F	Sensor- VSN540-F	Sensor- VSN540-F

Note: Inrix data is not associated with individual intersections and is not listed here

Table 6-3. List of technologies implemented on I-90

Sensor	Manufacture	Model	Website
BlueTOAD	Trafficast	BT-Cell-50W	http://trafficcast.com/
APVD	Inrix	N/A	http://www.inrix.com/

Table 6-4. List of sensors mounted on I-90

Technology	Milepost			
	I-90 Milepost 32	I-90 Milepost 52	I-90 Milepost 70	I-90 Milepost 109
Bluetooth	BlueTOAD-BT-Cell-50W	BlueTOAD-BT-Cell-50W	BlueTOAD-BT-Cell-50W	BlueTOAD-BT-Cell-50W
APVD	Inrix	Inrix	Inrix	Inrix

APVD: Aggregated Probe Vehicle Data

6.3.5 Type of Data

Due to the differences between sensor availability and type of data collected by these sensors, the type of analyses conducted for eastbound and westbound varies. Sensor availability and types of data analysis for westbound and eastbound on SR 522 and I-90 are summarised in Table 6-5 and Table 6-6.

Table 6-5. Data availability and type of analysis on westbound and eastbound

Direction	Sensor	Sensor Availability	Data Collected	
			Travel Time	Sample Count
Eastbound	BlueTOAD	✓	✓	✓
	Sensys	x	x	x
	Inrix	✓	✓	x
	Blip-BT	✓	✓	✓
	Blip-WiFi	✓	✓	✓
	Blip-Combined	✓	✓	✓
	ANPR	x	x	x
Westbound	BlueTOAD	✓	✓	✓
	Sensys	✓	✓	✓
	Inrix	✓	✓	x
	Blip-BT	✓	✓	✓
	Blip-WiFi	✓	✓	✓
	Blip-Combined	✓	✓	✓
	ANPR	✓	✓	✓

Data available on I-90 is shown in Table 6-6. Due to the lack of ground truth data on this corridor travel time analysis are restricted to qualitative rather than quantitative analysis.

Table 6-6. Data availability and type of analysis on westbound and eastbound

Direction	Sensor	Sensor Availability	Data Collected	
			Travel Time	Sample Count
Eastbound	BlueTOAD	✓	✓	✓
	Inrix	✓	✓	x
Westbound	BlueTOAD	✓	✓	✓
	Inrix	✓	✓	x

6.3.6 Data Collection Period

Data collection on SR 522 started on December 2012 and continued until June 2013. Table 6-7 and Table 6-8 display the time intervals when data were collected for both westbound and eastbound, respectively. As can be seen, ANPR and Sensys data were only available on westbound, hence this direction will be used as the basis of travel time accuracy analysis. The gaps shown on the Table 6-7 and Table 6-8 represent time periods that a technology was not either installed or was not working.

In the time span between April 5th, 2013 through June 8th 2013 all systems collected data side-by-side. The most data overlap between various systems occurred during this time period which provided a sufficiently large dataset for analysis. Therefore, this time period allows comparing the accuracy of data collected by all different systems in terms of travel time and capture rate; (with the partial exception of BlueTOAD data which only reports match rates at 15 minute intervals). The 5 minute aggregated travel time and sample counts were used as the basis of analysis. Due to the difference of traffic pattern on weekends and working days, this study uses traffic data collected on weekdays for conducting the analyses.

Because of the differences between sensor availability and type of data collected by these sensors, the type of analyses conducted for eastbound and westbound directions are different. Sensor availability and types of data analysis for westbound and eastbound on SR 522 are summarised in Table 6-7 and Table 6-8, respectively. ANPR data are used as the ground truth both for travel time analysis and sample count comparison. Inrix data does not include sample counts, so that system is excluded from the sample count analysis.

When it comes to eastbound SR 522, there is no ANPR data that lines up with the other systems in the eastbound direction. This prevents analysis based on the ground truth. Also, there is no Sensys system on eastbound SR 522 to compare with the other sensors. Due to these limitations, travel time data obtained by BlueTOAD, Inrix, and BlipTrack are compared to each other. Westbound results are checked to see whether there is a similar pattern between data distributions on eastbound and westbound. Observation of such pattern could provide a better understanding of the sensors function.

The analysis of sensors placed on I-90 differs from the analysis of sensors installed on SR 522 in that there is not a system comparable to the ANPR system on SR 522 to use as a ground truth for travel time measurement. This restricts the analysis of I-90 data to be more qualitative than the SR 522 analysis. Specifically, the evaluation of I-90 data looks at data availability, daily pattern variation, and reaction to traffic events such as construction delays and mountain pass closures due to snow removal. Availability for the BlueTOAD and Inrix data is given in Table 6-9. Note that the BlueTOAD device at the summit (MP 52) experienced extended communications failures, interrupting data collection for segments between milepost 32 and milepost 70.

Table 6-7. Data availability on SR-522 Westbound

Segment	Sensor	Time						
		December	January	February	March	April	May	June
SR 104 → 153rd	ANPR							
	BlueTOAD							
	Inrix							
	Sensys							
	BlipTrack-BT							
	BlipTrack-WiFi							
	BlipTrack-Combined							
		December	January	February	March	April	May	June
68th → SR 104	ANPR							
	BlueTOAD							
	Inrix							
	Sensys							
	BlipTrack-BT							
	BlipTrack-WiFi							
	BlipTrack-Combined							
		December	January	February	March	April	May	June
83rd → 68th	ANPR							
	BlueTOAD							
	Inrix							
	Sensys							
	BlipTrack-BT							
	BlipTrack-WiFi							
	BlipTrack-Combined							

Table 6-8. Data availability on SR-522 Eastbound

Segment	Sensor	Time						
		December	January	February	March	April	May	June
153rd → SR 104	ANPR							
	BlueTOAD							
	Inrix							
	Sensys							
	BlipTrack-BT							
	BlipTrack-WiFi							
	BlipTrack-Combined							
		December	January	February	March	April	May	June
SR 104 → 68th	ANPR							
	BlueTOAD							
	Inrix							
	Sensys							
	BlipTrack-BT							
	BlipTrack-WiFi							
	BlipTrack-Combined							
		December	January	February	March	April	May	June
68th → 83rd	ANPR							
	BlueTOAD							
	Inrix							
	Sensys							
	BlipTrack-BT							
	BlipTrack-WiFi							
	BlipTrack-Combined							

Table 6-9. Data availability by month and system for I-90

Direction	Segment	Sensor	Time					
			January	February	March	April	May	June
Eastbound	MP 32 → MP 52	BlueTOAD						
		Inrix						
	MP 52 → MP 70	BlueTOAD						
		Inrix						
	MP 52 → MP 32	BlueTOAD						
		Inrix						
Westbound	MP 109 → MP 70	BlueTOAD						
		Inrix						
	MP 70 → MP 52	BlueTOAD						
		Inrix						
	MP 52 → MP 32	BlueTOAD						
		Inrix						

6.4 Evaluation Framework for Accuracy Analysis

Considering the extensive sensing capabilities installed along SR 522 and I-90, performing a systematic comparison of the available technologies is a matter of selecting the appropriate metrics, pulling the data from the various sources and then performing an error analysis. In this study, a framework has been designed and implemented to evaluate the accuracy and reliability of the various technologies.

6.4.1 Error and Reliability Matrix

In order to evaluate the accuracy and reliability of travel time estimates obtained by Bluetooth technology versus various ATIS technologies, two types of analysis are conducted.

- First, the distributions of the travel time data and sample rates are compared with the ground truth.
- Second, a number of accuracy measures are used to provide a quantitative evaluation of the error associated with each of the technologies.

In order to use a consistent data format, the comparisons are made based on 5 minutes aggregated travel time and capture rates. The two datasets that were not available on a five minute basis were BlueTOAD and Inrix. BlueTOAD capture rates were available at 15 minute intervals and divided by 3 to match up to the other systems as closely as possible. The Inrix data does not include a capture rate metric.

6.4.1.1 Data Distribution

Time plots are used to compare the distributions of the data around the ground truth. This provides an overview of the distributions of the data relative to the ground truth.

6.4.1.2 Travel Time Accuracy/Error

A number of accuracy metrics are used to represent the error. In these metrics, error is the difference between the observations and the ground truth travel time. These accuracy measures are:

1. Mean Absolute Deviation (MAD) (also known as the mean absolute error) – the average of errors.

$$\mathrm{MAD} = \frac{1}{\mathrm{N}}\sum_{\mathrm{i}=1}^{\mathrm{N}}\left|\hat{\mathrm{T}} - \mathrm{T_i}\right| \qquad \textbf{Equation 6-2}$$

Where:

$\boldsymbol{N}$: The number of observations

$\boldsymbol{T_i}$: The corresponding ground truth travel time, i

$\boldsymbol{\hat{T}}$: The ATIS estimated travel time

2. Mean Percent Error (MPE) (refer to Section 3.3.3)
3. Mean Absolute Percent Error (MAPE) (refer to Section 3.3.3)
4. Root Mean Squared Error (RMSE) (refer to Section 3.3.3)

There are reasons to use each error measurement methodology. The MAD is a good indication of how much error should be expected from an average reading, but does not indicate whether the results are consistently high or low. The MPE will indicate if there is systematic bias to the error, i.e. if readings are consistently high or low, but will allow positive and negative errors to cancel each other out. The MAPE is a combination of MAD and MPE, indicating average magnitude of error relative to the ground truth values. The RMSE gives a good indication of whether there are many small errors or a few larger errors. Hence, the adoption of various measures provides a better understanding of the errors associated with each method.

6.4.1.3 Data Analysis Resolutions

Since the reporting intervals of the data available vary among different technologies, analyses are conducted for different levels of resolutions. The levels of resolution considered for evaluation are: daily and monthly basis. It is important to consider the various temporal resolutions of data analysis while evaluating the various sensors. When looking at weekly data, the consistency of the travel times across multiple days provides a good measure of the highs and lows that should be expected for travel times between the two intersections. Monthly data can be used to analyse whether the travel times between the two intersections are consistent and cyclical. By analysing monthly data, it is also possible to indicate some days that recorded significantly longer travel times than others. This may be indicative of incidents blocking traffic. Further examinations would need to be undertaken to establish causal factors.

6.5 Data Analysis and Discussions for SR 522

Evaluations of various technologies are conducted in terms of sample count and accuracy of travel time estimation. The following sections present the results of data analysis based on visual and numerical methods.

6.5.1 Sample Count

Sample counts and the corresponding penetration rate are two important factors for evaluating various travel time technologies. These represent the proportion of the actual traffic flow being captured by the sensors. The results of the sample count analysis for westbound and eastbound are presented in the following sections.

6.5.1.1 Westbound Sample Count

The results of sample count on westbound for the period between April 5^{th}, 2013 through June 8^{th}, 2013 are summarised in Table 6-10. As mentioned earlier, the ANPR sample counts are used as the ground truth. Penetration rates are computed by dividing sample counts of various systems by the corresponding ANPR value.

$$Penetration\ rate_{Sensor\ (i)} = \frac{Sample\_Counts_{Sensor(i)}}{Sample\_Counts_{ANPR}} \qquad \textbf{Equation 6-3}$$

According to Table 6-10, on average, the penetration rate of Sensys is identical (103%) to the sample captured by ANPR. This is followed by Blip-Combined with more than 28% of the ANPR captures, Blip-WiFi with 17% and Blip-BT with 12% of ANPR capture rates. This also indicates that by combining Bluetooth and WiFi technologies, it is possible to capture twice as many samples compared to the use of a single technology. The Bluetooth capture rate is also sensors specific; as can be seen BlueTOAD capture rate is 6% compared to capture rate of Blip-BT.

Figure 6-4 shows the average penetration rate over the analysis period (April 5^{th}, 2013 through June 8^{th}, 2013) for various sensors on the westbound links. In order to give an overview of the sample counts variations over the weekdays, Figure 6-5 display the capture rates of the various systems on 83rd Pl. NE to 68th Ave. NE westbound links for a one week period May 1st, 2013 through May 8th, 2013. Results of the capture rate comparison for the other two segments are presented in Appendix III. Comparing the penetration rates of the various sensors on the three links shows that despite the differences in traffic flow on the various links, the capture rates are similar which indicates the reliability of sensor detection rates on different links.

Although Blip-BT, Blip-WiFi and Blip-Combined, and BlueTOAD have a significantly lower penetration rates compared to ANPR and Sensys, they still demonstrate responsiveness to the variations in traffic volumes during the day; in other words, the sampling appears to be uniform. BlueTOAD data in Figure 6-5 is blockier in profile due to being aggregated in 15-minute intervals instead of the 5-minute interval used by other sensor systems. In order to represent the BlueTOAD data on the same scales as the other systems, the BlueTOAD capture data was divided by 3, which may cause its capture rate to be underrepresented in low volume conditions due to rounding.

Table 6-10. Sample counts on westbound during April 5th through June 8th, 2013

83rd Pl. NE to 68th Ave. NE			
Sensor	**Sample Count**	**Capture Rate (%)**	**# Intervals**
BlueTOAD	25207	5	11659
Sensys	478421	99	11161
Inrix	Not Available	Not Applicable	13232
Blip-BT	51539	11	13248
Blip-WiFi	80285	17	13238
Blip-Combined	131823	27	13238
ANPR	483984	100	-
68th Ave. NE to SR 104			
Sensor	**Sample Count**	**Capture Rate (%)**	**# Intervals**
BlueTOAD	37980	7	12112
Sensys	639211	110	11162
Inrix	Not Available	Not Applicable	13232
Blip-BT	76493	13	13248
Blip-WiFi	108063	19	13247
Blip-Combined	184556	32	13247
ANPR	580379	100	-
SR 104 to NE 153rd St.			
Sensor	**Sample Counts**	**Capture Rate (%)**	**# Intervals**
BlueTOAD	31149	6	11933
Sensys	424688	82	11164
Inrix	Not Available	Not Applicable	13232
Blip-BT	65112	13	13248
Blip-WiFi	71211	14	13247
Blip-Combined	136323	26	13247
ANPR	517657	100	-

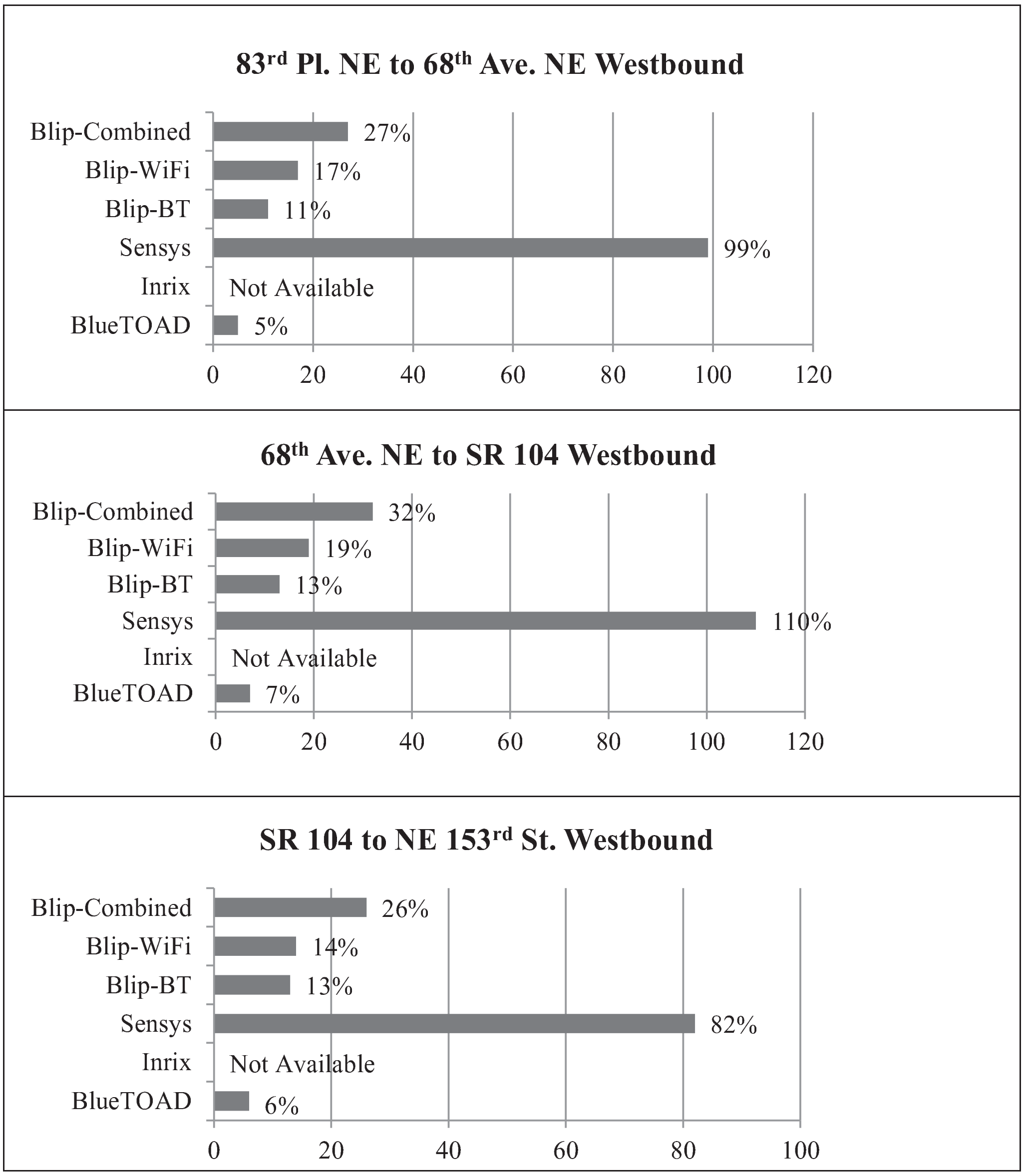

Figure 6-4. Capture rate comparison on westbound between April 5th, 2013 through June 8th 2013

Figure 6-5 shows the overlaid profiles of capture rate for various sensors on 83rd Pl. NE to 68th Ave. NE (WB) for May 1st, 2013 through May 8th, 2013. It clearly shows that Sensys and ANPR have higher capture rates, followed by Blip-Combined, Blip-WiFi and Blip-BT, and BlueTOAD. Figure 6-5 shows that regardless of the variations in capture rates for different systems; all of the systems were capable of registering the flow variation for peak and off-peak over the course of weekdays and weekends. Similar analysis for the sensors on 68th Ave. NE to SR 104 (WB) and sensors on SR 104 to NE 153rd St. (WB) are presented in Appendix III.

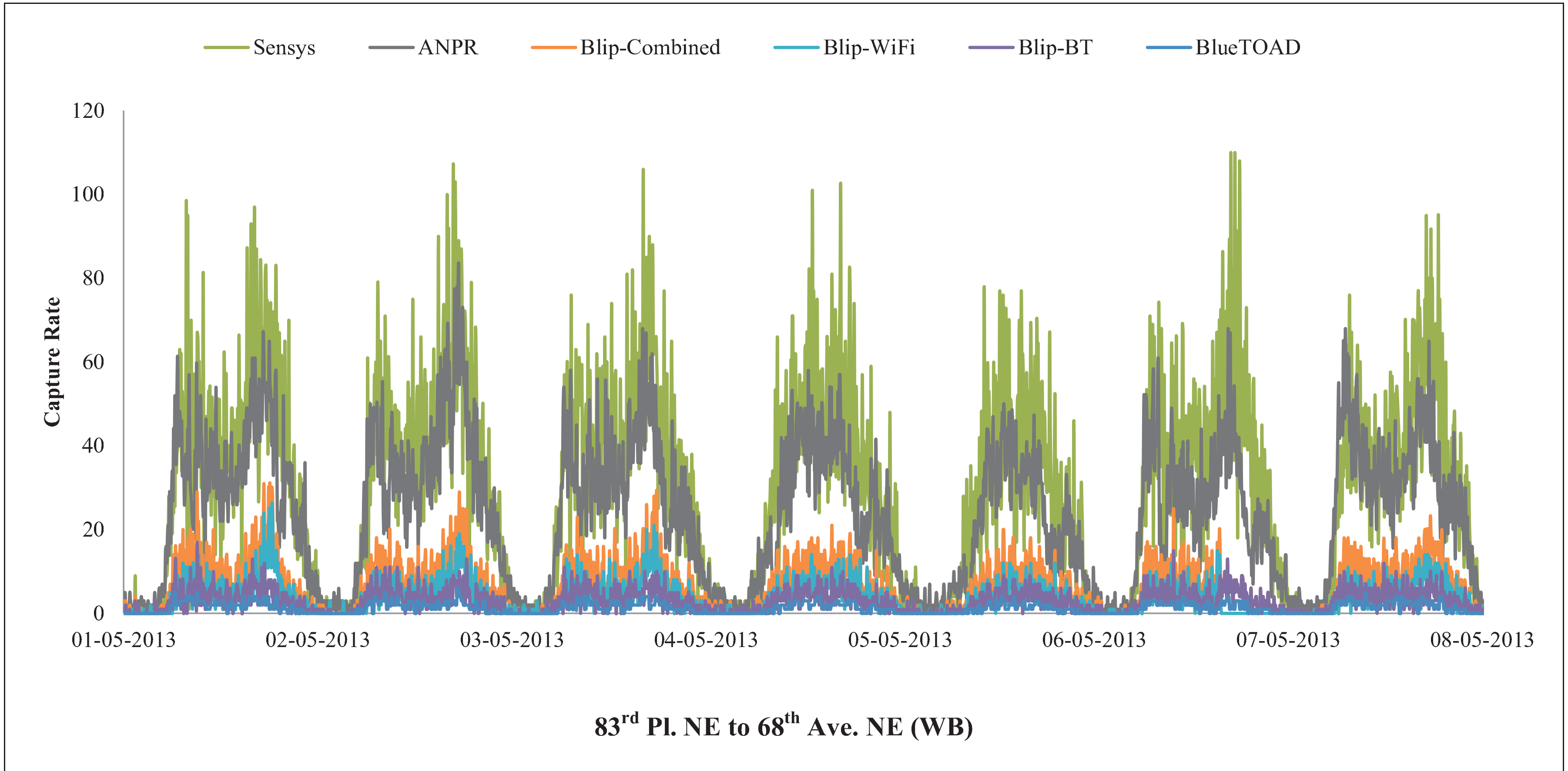

Figure 6-5. Comparing capture rate of different systems from 83rd Pl. NE to 68th Ave. NE (WB) for May 1st, 2013 through May 8th, 2013

When examining the various technologies, it is important to understand how well each technology performs in relative and absolute terms. While the ANPR system was chosen as a ground truth reference for travel time, the ANPR system was not designed as a volume measurement system. In the following figures volumes from each system that provides a volume measurement and the match rates for each system are shown. For comparison purposes, the advance loop detectors are shown as well as the Traficon system volumes at the 83rd Pl. NE and 68th Ave. NE intersections. Similar analysis for the sensors on 68th Ave. NE to SR 104 (WB) and sensors on SR 104 to NE 153rd St. (WB) are presented in Appendix III.

The placement of each system will have some implications to be taken into account when examining this data. Specifically, the advance loop detectors are upstream of the signal on the through movement lanes, while the ANPR, Sensys and Traficon systems are placed on the downstream side of the intersection. Traficon and Sensys counts generally agree, though they are not identical and Sensys does report marginally lower volumes.

The ANPR volumes follow the trends seen in the other three volume data sets, but are generally the lowest reported volumes. This is unsurprising since the ANPR system was not designed for volume data collection. A number of factors such as vehicle height, spacing, and licence plate cleanliness can affect the ANPR's ability to read a licence plate. Loop detectors, magnetometers and VIP units are not trying to read a small target, like a licence plate, and have generally more robust detection.

The placement of the advance loop detectors is likely to affect volume counts. The placement of the loop detectors means that only entering through vehicles are counted, left and right turning vehicles from the cross street are not counted. Additionally, the advance loop detectors may be subject to queuing and intersection signal timing impacts. With all of these factors, it is unsurprising that the advance detectors consistently report the second lowest volumes. The volume counts for other intersections are presented in Appendix III. The number of matches reported by each system for the westbound are presented in Figure 6-6 for 83rd Place NE to 68th Avenue NE. Similar analyses for the sensors on 68th Ave. NE to SR 104 (WB) and sensors on SR 104 to NE 153rd St. (WB) are presented in Appendix III.

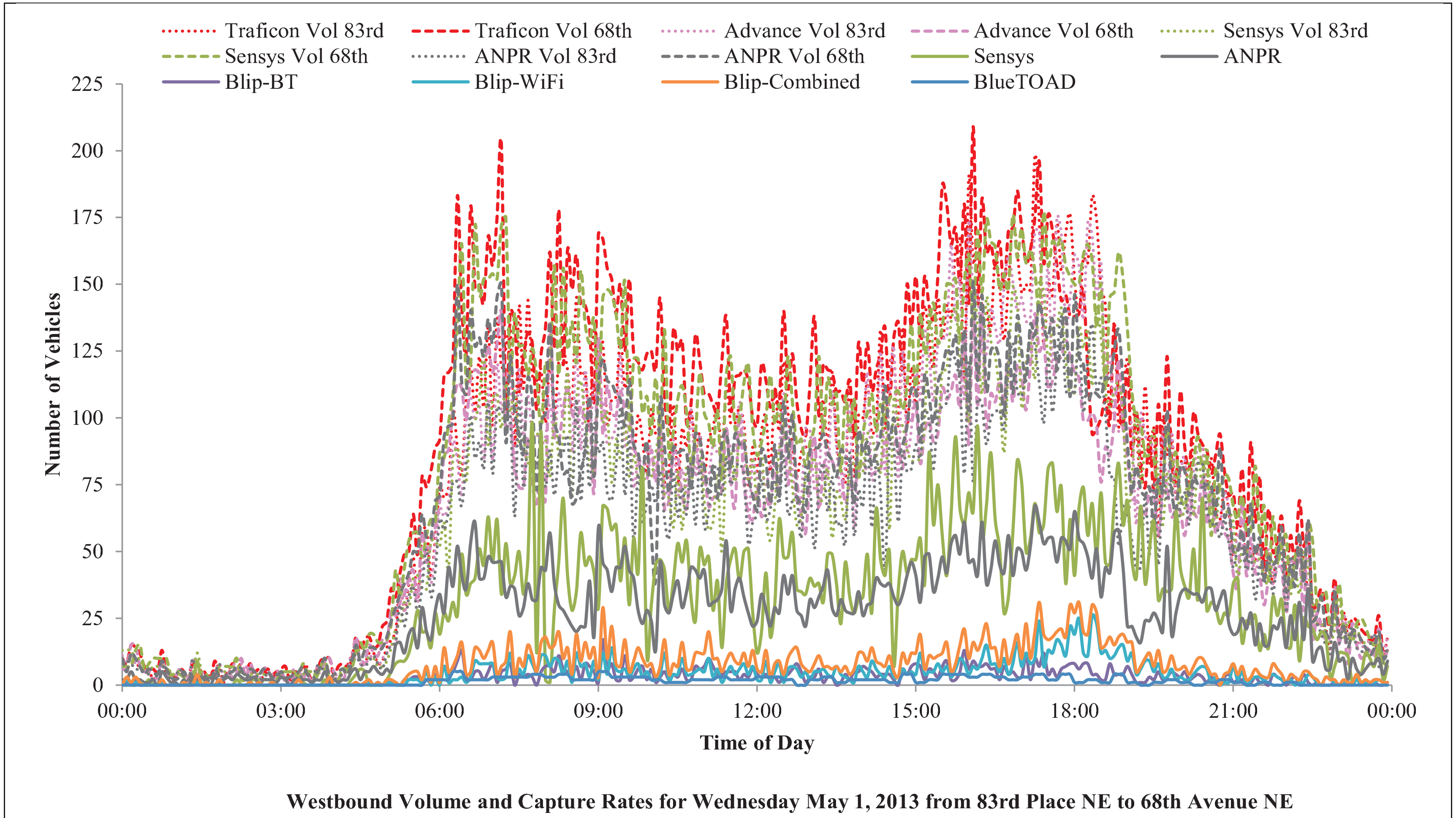

Figure 6-6. Westbound volume and capture rates for Wednesday May 1, 2013 from 83rd Place NE to 68th Avenue NE

6.5.1.2 Eastbound Sample Count

The results of sample count on eastbound for the period of April 5th, 2013 through June 8th, 2013 are summarised in Table 6-11. The noticeable point is that similar to westbound, the Blip-Combined capture rate is about two times higher than the capture rates of the Blip-BT and Blip-WiFi. Hence, integrating Bluetooth and WiFi makes it possible to double the detection rate. There is more matches on WiFi compared to Bluetooth. Results show that overall there is 20% more devices seen on WiFi compared to Bluetooth. The WiFi devices detected are primarily iPhones, Andorid and Windows Phone 8 (WP8) devices. These devices are not detected by the Bluetooth sensor, due to specific implementation of the Bluetooth software in these phones. So the WiFi detections could well complement the Bluetooth data. Figure 6-7 displays the capture rate of various systems on 68th Ave. NE to 83rd Pl. NE links for the period of one week (May 1st, 2013 through May 8th, 2013). Figure 6-7 demonstrates that regardless of the variations in capture rates for different systems; all systems were capable of detecting the cyclical pattern of traffic flow for peak and off-peak hours over the course of weekdays and weekends. Likewise, results of the capture rate for SR 104 to 68th Ave. NE and NE 153rd St. to SR 104 are shown in Appendix III. As seen for westbound, even though Blip-BT, Blip-WiFi and Blip-Combined have significantly lower capture rates but they are capable of representing the trends of traffic flow during the day. This could be seen by peaks during morning and afternoon on weekdays and likewise peaks on around noon on the weekends. However, due to lack of ground truth for this direction it was not possible to verify the travel time accuracy.

Table 6-11. Sample counts on eastbound during April 5th through June 8th, 2013

Sensor	**Sample Counts**		
	68th → 83rd	**SR 104 → 68th**	**153rd → SR 104**
BlueTOAD	18260	388239	36886
Sensys	Not Available	Not Available	Not Available
Inrix	Not Available	Not Available	Not Available
Blip-BT	52130	76701	68657
Blip-WiFi	62225	97644	62717
Blip-Combined	118324	174344	131373
ANPR	Not Available	Not Available	Not Available

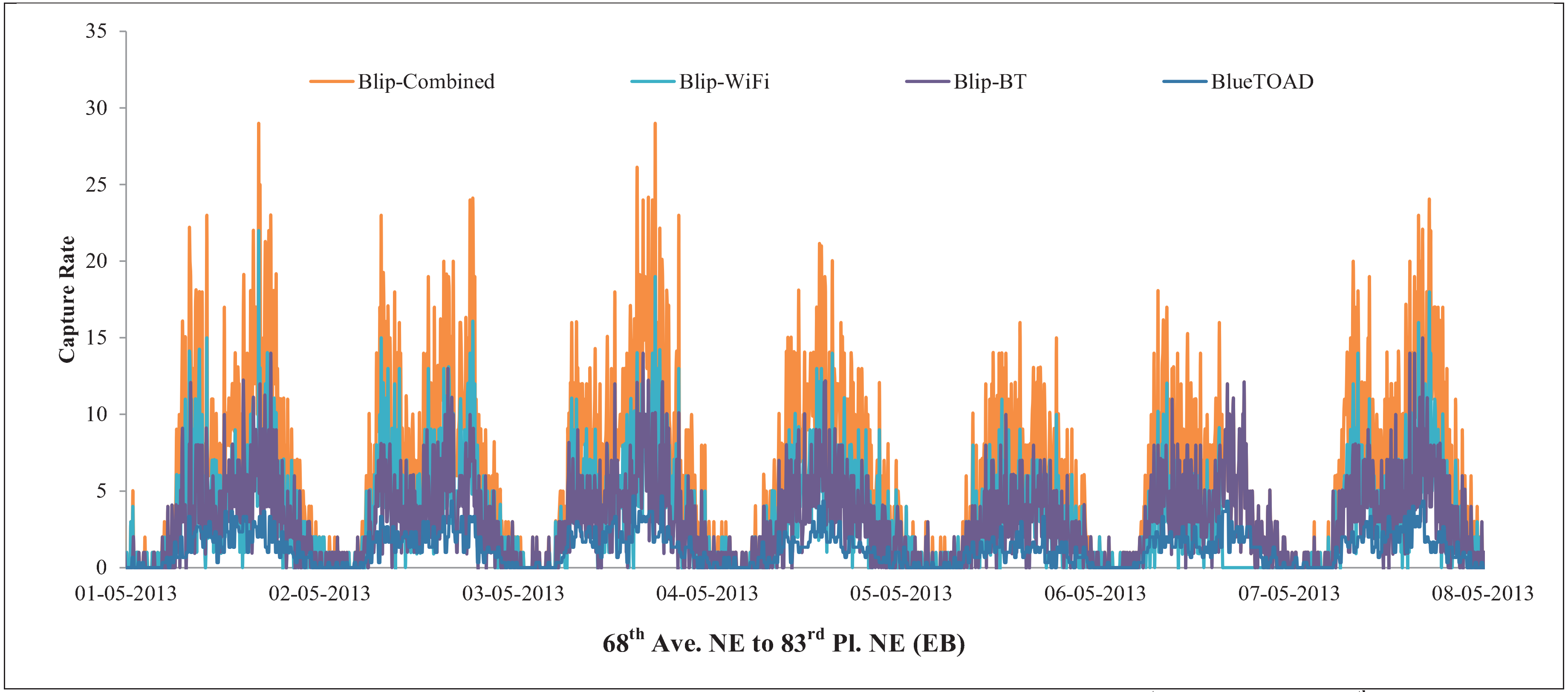

Figure 6-7. Comparing capture rate of different systems from 68th Ave. NE to 83rd Pl. NE (EB) for May 1st, 2013 through May 8th, 2013

6.5.2 Travel Time

The accuracy and reliability of the travel time estimations are critical parameters for evaluating various sensor technologies. Owing to the difference in data availability for westbound and eastbound directions, the results of the travel time analyses are presented separately by direction. On westbound, in order to provide a better foundation for comparing accuracy of different systems, analyses are conducted for different time resolutions. The accuracy analysis looks at the overall accuracy for April 5th, 2013 through June 8th, 2013, and also on a 24 hour daily resolution for all Wednesdays in this period (refer to Figure 6-10, Figure 6-11, and Figure 6-12). However, on eastbound due to the lack of ANPR data, analysis is limited to descriptive statistics.

6.5.2.1 Westbound Travel Time

Travel time plot for 83rd Pl. NE to 68th Ave. NE (WB) is shown in Figure 6-8 for the analysis period of May 1st, 2013 through May 8th, 2013. Travel time plots for segments 68th Ave. NE to SR 104 and SR 104 to NE 153rd St. are presented in Appendix III. The consistency of the travel times across the week provides a good measure of the highs and lows that should be expected for travel times on the three segments. The weekly data demonstrates that the travel times on all three corridors are consistent and cyclical. May 6th is a Saturday and May 7th is a Sunday. Saturday and Sunday have reduced peaks centred at midday. The regular workdays have earlier and longer peaks that have a minor peak in the morning and a major one in the evening for the 83rd Pl. NE to 68th Ave. NE segment and narrow major peaks in morning and wider evening peaks for the other two segments. These results are in accordance with expectations based on local traffic and commuter patterns.

Figure 6-9 shows the overlaid profiles of travel time for all the sensors on 83rd Pl. NE to 68th Ave. NE, 68th Ave. (WB) for Wednesday May 1st, 2013 in a zoomed view. It is clear that all the sensors are capable of representing the cyclical pattern of travel time over a day and for the morning and afternoon peaks. Over the peak and off-peak hours all sensors follow ANPR pattern and have a well overlap with the ground truth; however, Inrix tend to significantly overestimate the travel time during the off-peaks. A number of gaps or low travel time also has been reported for all methods over the mid night hours. Similarly, the overlaid profiles of travel time for the sensors on 68th Ave. NE to SR 104 and SR 104 to NE 153rd St. for Wednesday May 1st, 2013 are placed in Appendix III.

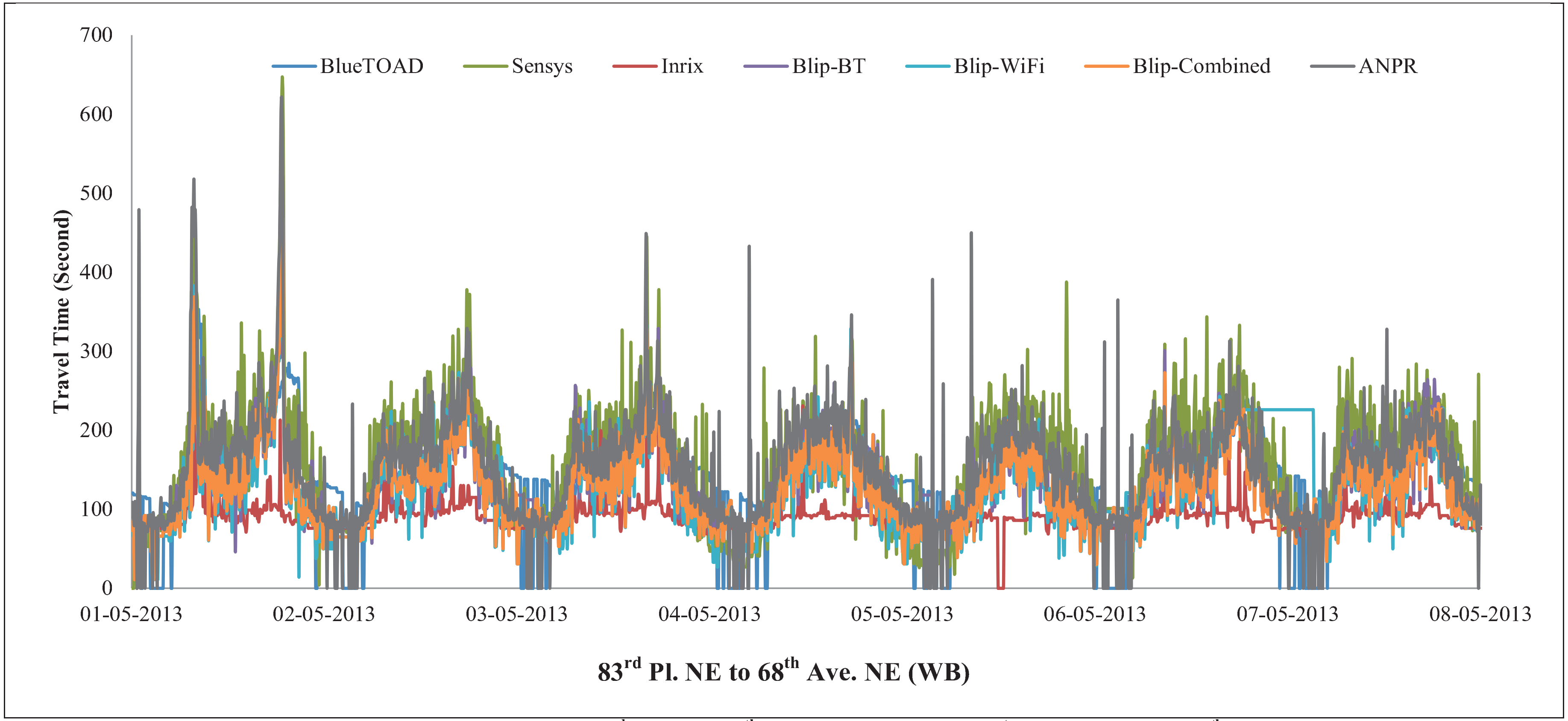

Figure 6-8. Travel time plot for 83rd Pl. NE to 68th Ave. NE (WB) for May 1st, 2013 through May 8th, 2013

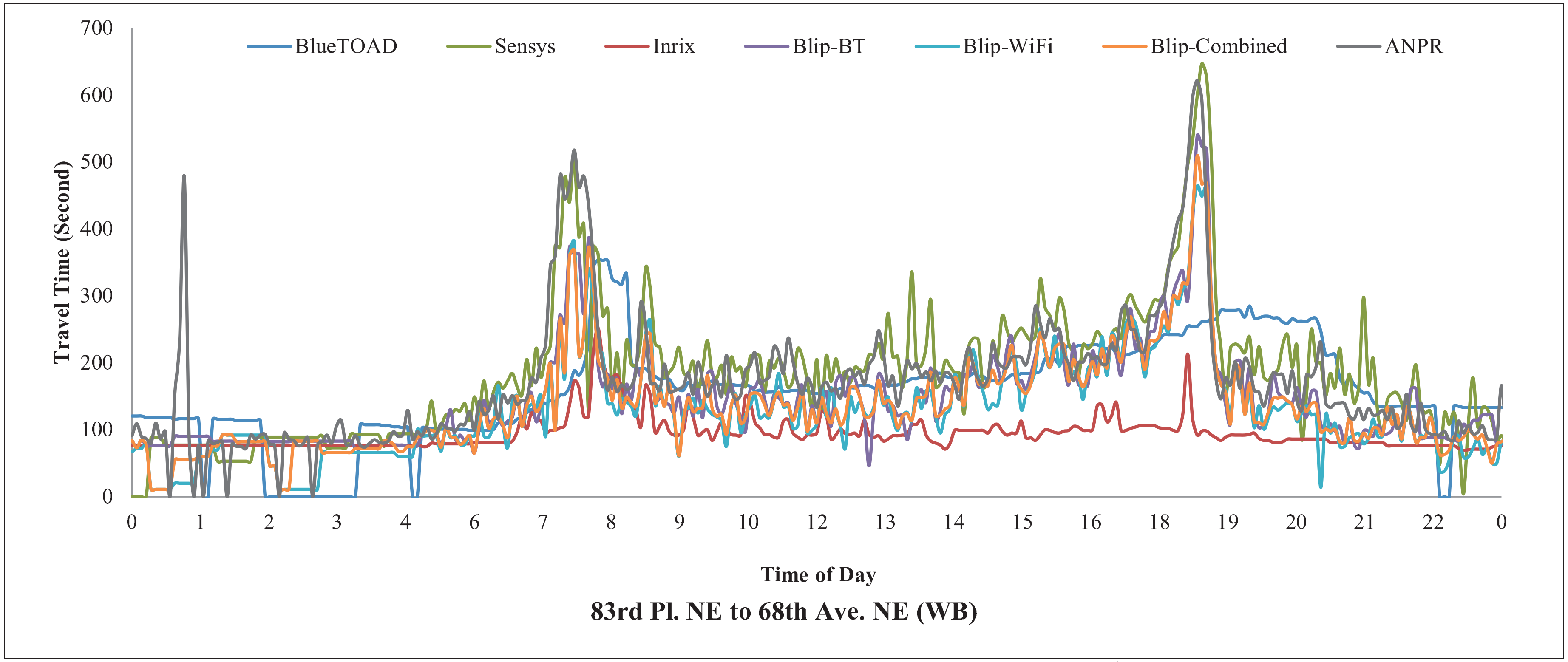

Figure 6-9. Travel time plot for 83rd Pl. NE to 68th Ave. NE (WB) on May 1st, 2013

6.5.2.2 Travel Time Accuracy Analysis on Westbound

In order to provide a daily overview of the accuracy of the travel time estimated by various technologies, the MAPE for all westbound segments are calculated for Wednesdays over the of two month period from April 5, 2013 to June 8, 2013. The results of the MAPE analysis are shown in Figure 6-10, Figure 6-11, and Figure 6-12. The patterns observed for the three segments are different; however, it can be seen that, in general, during the peak hours estimations tend to be more biased and the percentage of errors increase. For all three segments, during the peak hours Inrix tends to be more biased and less accurate than the Sensys and Blip-BT, Blip-WiFi and Blip-Combined. For the SR 104 to NE 153rd St. segment BlueTOAD also shows significant bias for the morning peak. BlueTOAD also show significant bias in the overnight hours for the 83rd Pl. NE to 68th Ave. NE segment. Although MAPE varies a lot between peak hours and off-peak hours for all systems, on average Blip-BT, Blip-WiFi, Blip-Combined and Sensys have around 20% error rate and are more reliable as they tend to keep the same level over the 24 hours.

Figure 6-10 presents the variation of MAPE over 24 hours for Wednesdays over the period of April 5th, 2013 through June 8th, 2013 at for 83rd Pl. NE to 68th Ave. NE (WB). It is clear that the accuracy of the various systems' estimated travel times varies between peak and off-peak hours. This is especially true of the morning peak from 8am to 9am. As shown, BlueTOAD has a lower MAPE over the course of the day followed by Blip-Combined, Blip-BT, Blip-WiFi, Sensys and Inrix. Compared to other systems, Inrix has significantly lower accuracy during the day and BlueTOAD shows significantly lower accuracy during the night.

Figure 6-11 presents the variation of MAPE over 24 hours for Wednesdays over the period of April 5th, 2013 through June 8th, 2013 at 68th Ave. NE to SR 104 (WB). The accuracy of the estimated travel times varies over the day, though not as significantly as on the 83rd Pl. NE to 68th Ave. NE segment. As shown Blip-BT, Blip-WiFi, and Blip-Combined estimate travel time with approximately 15% error over the course of the day. Although, accuracy of travel time estimated by BlueTOAD fluctuates between peak and off-peak hours, in off-peaks it can estimate travel time with less than 15% error which rises to 70% error during peak. In this segment, Sensys performance on this segment is acceptable overnight, with an error spike in the peak hour and just over the acceptable error threshold over the day. For this segment, Inrix has a modest accuracy, generally competitive with the other systems.

Figure 6-12 presents the variation of MAPE over 24 hours for Wednesdays over the period of April 5th, 2013 through June 8th, 2013 from SR 104 to NE 153rd St. (WB). It is clear that the accuracy of the estimated travel time by various systems varies between peak and off-peak hours. As shown Sensys and BlueTOAD have lower accuracy during the morning peak followed by Blip-Combined and Blip-BT with Blip-WiFi being the most accurate. During the morning peak there is a significant rise in the BlueTOAD and Sensys error rates which leveled out for the rest of the day. Inrix data for this segment was subject to significant error.

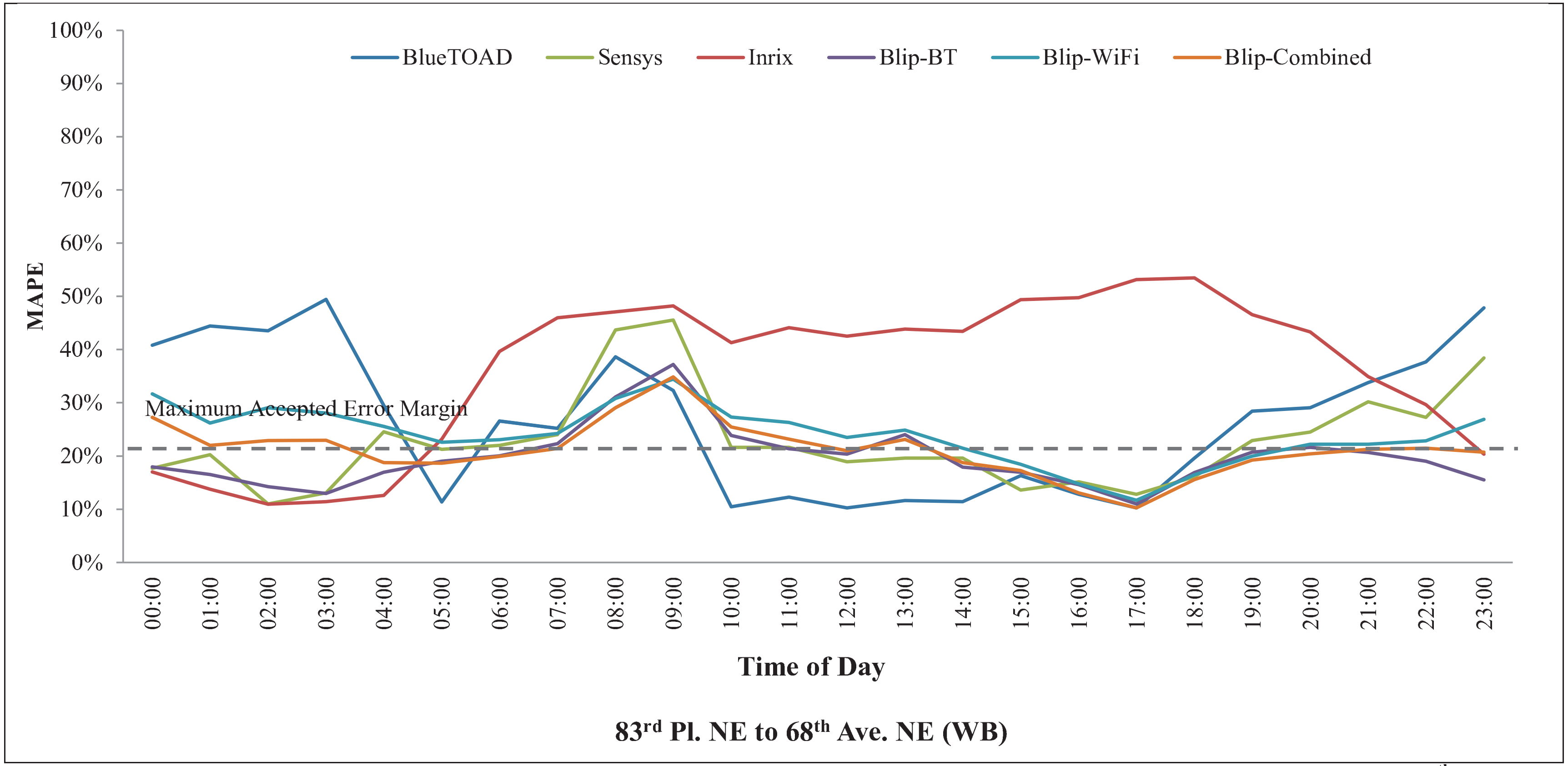

Figure 6-10. The MAPE variation for 83rd Pl. NE to 68th Ave. NE (WB) over 24 hours on Wednesdays over the period of April 5th, 2013 through June 8th, 2013

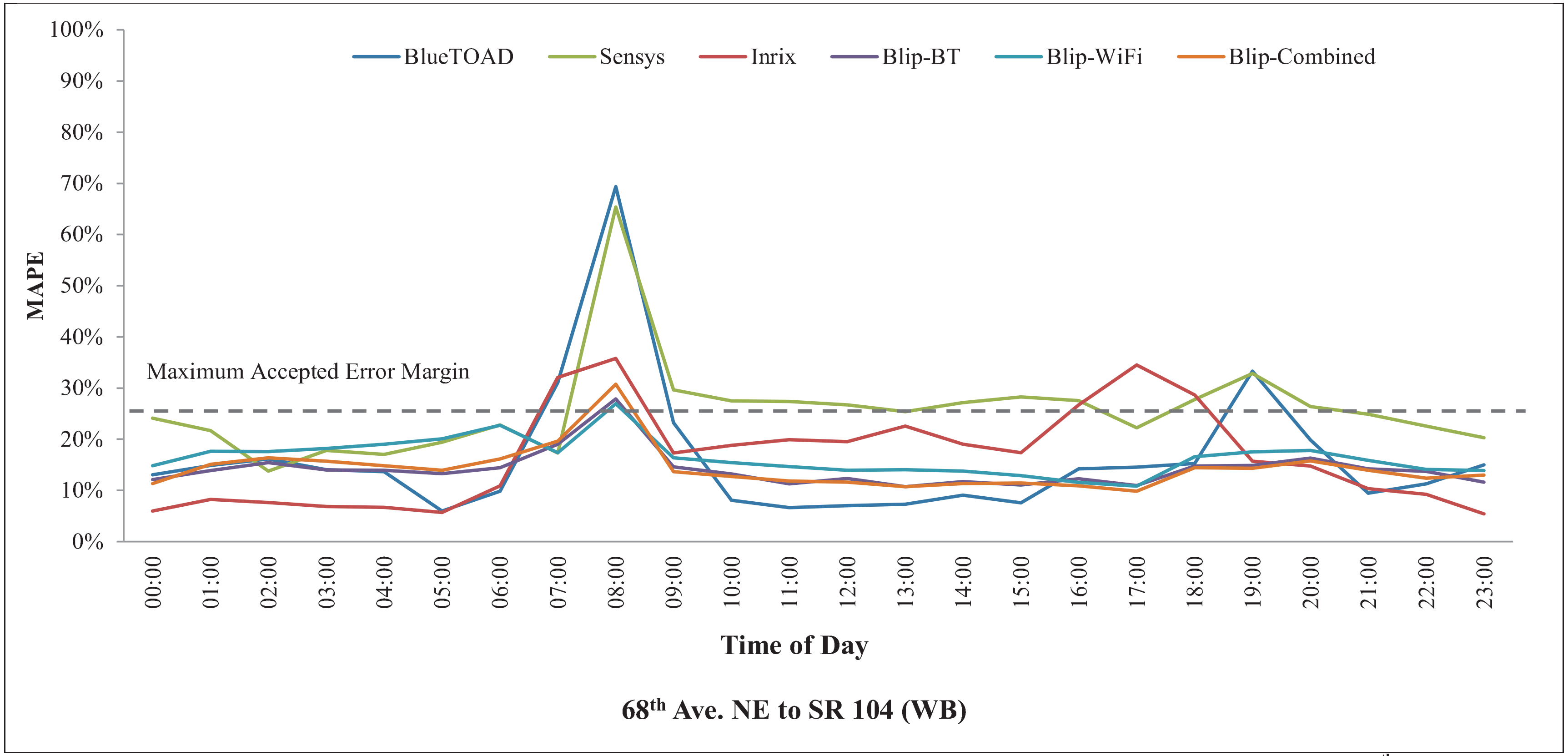

Figure 6-11. The MAPE variation from68th Ave. NE to SR 104 (WB) over 24 hours on Wednesdays over the period of April 5th, 2013 through June 8th, 2013

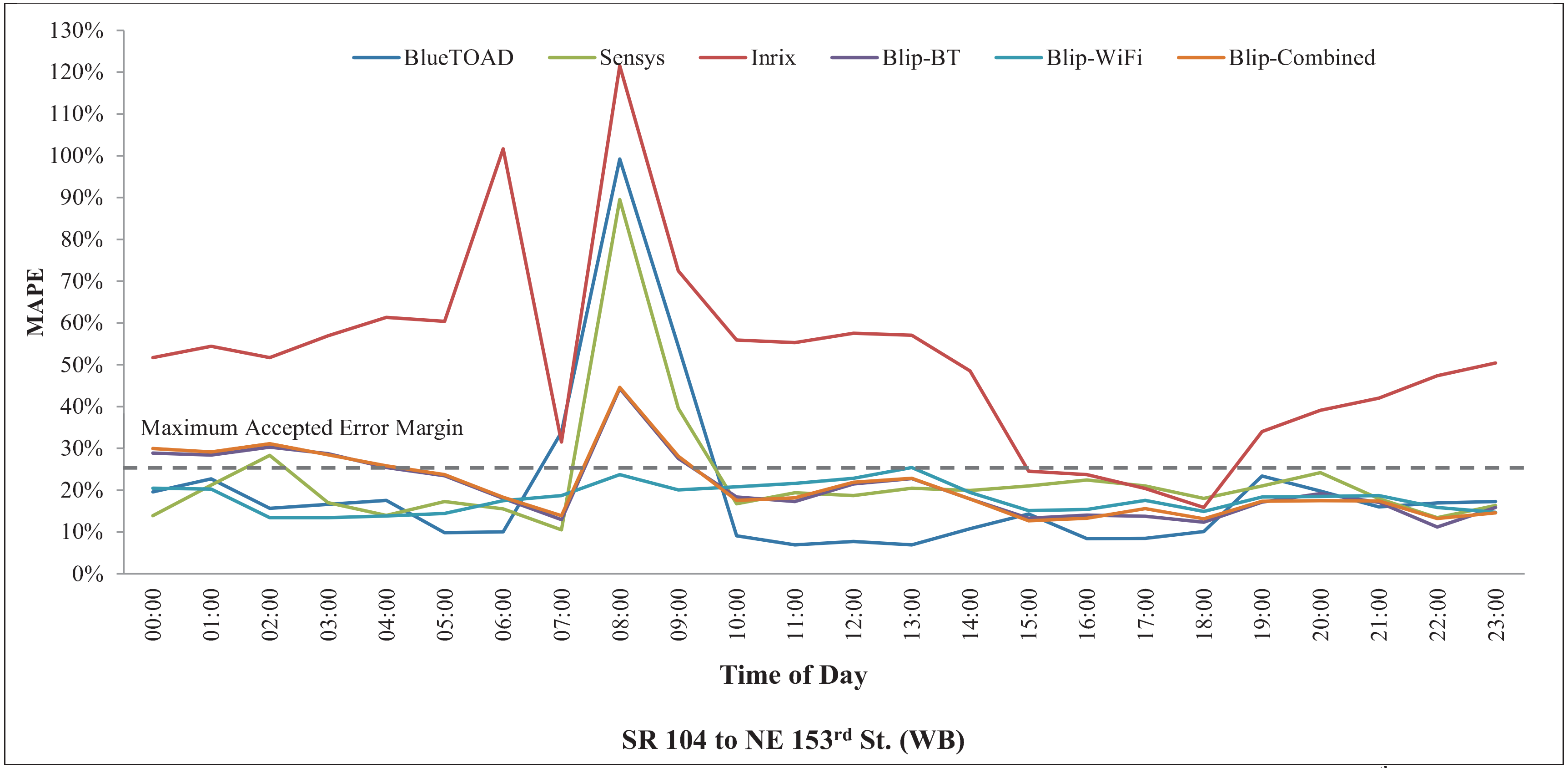

Figure 6-12. The MAPE variation from SR 104 to NE 153rd St. (WB) over 24 hours on Wednesdays over the period of April 5th, 2013 through June 8th, 2013

In order to further explore this pattern, data collected between 9am-10am (off-peak) on Wednesdays within two months (April 5th, 2013 through June 8th, 2013) are analysed. Table 6-13 presents descriptive statistics of the collected data. As seen in Table 6-13 the average ANPR travel time is closely estimated by all sensors. The Inrix data has the highest difference with ANPR.

To evaluate the accuracy of the sensors on an hourly basis, the MAPE for each sensor on each segment of the corridor is calculated for 9am-10am (off-peak) on Wednesdays during two months (April 5th, 2013 through June 8th, 2013), as seen in Table 6-12. As presented, in general the Blip-BT, Blip-WiFi, Blip-Combined, Sensys and BlueTOAD provide comparable results. On the opposite end of the spectrum, Inrix results are less representative. Since the accuracy varies between the three segments, it is wise to be cautious in drawing conclusions based on the limited number of segments analysed.

MAPE results for various sensors are compared for all three SR 522 segments in Table 6-12. As can be seen, all sensors are more accurate from 68th Ave. NE to SR 104 (WB). However, accuracy varies between the different segments and sensors, which might be attributed to the corridor length and the number of busy intersections as well as sensor ranges and operating principles.

Table 6-12. Results of the MAPE for hourly analysis over the period of April 5th through June 8th, 2013

Sensor	MAPE		
	83rd Pl. NE to 68th Ave. NE	**68th Ave. NE to SR 104**	**SR 104 to NE 153rd St.**
BlueTOAD	32.30%	23.20%	54.40%
Sensys	45.60%	29.60%	39.60%
Inrix	48.20%	17.30%	72.50%
Blip-BT	37.20%	14.60%	27.60%
Blip-WiFi	34.40%	16.40%	20.00%
Blip-Combined	34.90%	13.70%	28.10%

Note: The Maximum accepted level of accuracy is set as 25%. The MAPE is colored green below 15%, transitioning through yellow at 20% to red at or above 25%.

Table 6-12 summarises the MAPE results for all the sensors on SR 522 westbound segments for 9-10 am on Wednesdays over the period of April 5th, 2013 through June 8th, 2013. Confirming the results shown in Figure 6-10, Figure 6-11, and Figure 6-12, all the sensors tend to have a better performance on the 68th Ave. NE to SR 104 segment.

Table 6-13. Hourly descriptive statistics for westbound over the period of April 5th through June 8th, 2013

Segment	Sensor	Sample Count	Capture Rate (%)	Std. Dev.	Min	1st Qtr	Median	Mean	3rd Qtr	Max
83rd Pl. NE to 68th Ave. NE	BlueTOAD	309	7	14.4	144.9	163.0	168.5	170.2	173.9	243.4
	Sensys	4464	108	32.5	134.0	178.8	198.0	200.4	220.3	342.0
	Inrix	NA	-	19.3	67.0	94.0	101.0	103.8	110.3	169.0
	Blip-BT	551	13	27.1	70.0	130.8	144.0	147.6	163.3	224.0
	Blip-WiFi	725	18	29.7	60.0	126.0	142.0	145.2	161.0	262.0
	Blip-Combined	1276	31	26.9	61.0	128.5	143.0	145.5	162.5	243.0
	ANPR	4126	100	33.5	15.0	157.8	169.0	169.0	183.0	320.0

Segment	Sensor	Sample Count	Capture Rate	Std. Dev.	Min	1st Qtr	Median	Mean	3rd Qtr	Max
68th Ave. NE to SR 104	BlueTOAD	456	8	45.0	128.0	141.6	145.3	158.7	156.8	415.3
	Sensys	6459	112	35.3	120.0	160.0	181.0	187.0	211.3	283.0
	Inrix	NA	-	21.7	108.0	120.8	127.5	131.4	134.0	261.0
	Blip-BT	798	14	28.4	112.0	134.8	148.5	154.3	167.0	234.0
	Blip-WiFi	986	17	28.2	108.0	136.0	162.5	161.0	182.3	234.0
	Blip-Combined	1784	31	27.4	119.0	135.8	149.5	156.3	170.3	233.0
	ANPR	5784	100	25.0	103.0	128.0	143.0	149.3	168.3	217.0

Segment	Sensor	Sample Count	Capture Rate	Std. Dev.	Min	1st Qtr	Median	Mean	3rd Qtr	Max
SR 104 to NE 153rd St.	BlueTOAD	459	7	70.7	112.6	118.9	141.1	169.5	196.1	392.6
	Sensys	4939	80	60.9	88.0	119.0	129.5	146.1	147.0	399.0
	Inrix	NA	-	56.3	140.0	165.0	170.5	190.1	193.0	464.0
	Blip-BT	833	13	46.2	102.0	114.0	124.0	136.8	142.3	365.0
	Blip-WiFi	759	12	21.5	92.0	117.0	130.5	131.9	142.5	233.0
	Blip-Combined	1592	26	45.4	102.0	118.0	128.0	139.2	140.3	365.0
	ANPR	6175	100	15.9	67.0	106.0	112.5	114.1	119.0	189.0

In order to have a conclusive evaluation of the accuracy of all systems, accuracy measures for a period of two months (from April 5th, 2013 through June 8th, 2013) are calculated. This is intended to clarify the influence of traffic variation on accuracy of the estimated travel time. The results of the accuracy analysis are summarised in Table 6-14. For the hourly analysis, Sensys, Blip-BT, Blip-WiFi, Blip-Combined and BlueTOAD provide more accurate travel time estimates than Inrix. Second, sensors are generally less accurate on 83rd Pl. NE to 68th Ave. NE than other segments, though Inrix and BlueTOAD are least accurate on SR 104 to 68th Ave. NE.

Comparing the MPE values in Table 6-14 shows that the sensors tend to overestimate travel time on the 83rd Pl. NE to 68th Ave. NE and SR 104 to NE 153rd St. and underestimate travel time on the 68th Ave. NE to SR 104 (WB) segments. For 83rd Pl. NE to 68th Ave. NE, Blip-BT, Blip-WiFi and Blip-Combined underestimate the travel time. For the 68th Ave. NE to SR 104 segment all sensors are more accurate, except the Sensys sensors. On this segment all sensors report MAPE rates below the 25% error threshold. For the SR 104 to NE 153rd St. segment all sensors overestimate travel times relative to the ANPR system.

The MAPE and MAD also correlate to the results of the RMSE on all three corridors. The consistency of the three different accuracy measures on three corridors increases confidence in the evaluation results. It can be concluded that Blip-BT, Blip-Combined, Blip-WiFi and BlueTOAD achieve the most overall reliable travel times followed by Sensys and Inrix. The results of Table 6-14 are shown in Appendix III.

Table 6-14. Travel time accuracy analysis for westbound for the period of April 5th, 2013 through June 8th, 2013

83rd Pl. NE to 68th Ave. NE				
Sensor	**RMSE (Second)**	**MAD (Second)**	**MPE (%)**	**MAPE (%)**
BlueTOAD	141.81	33.99	5.51	20.76
Sensys	146.63	35.87	13.18	21.54
Inrix	149.24	65.21	-35.33	35.93
Blip-BT	134.25	33.46	-12.22	18.47
Blip-WiFi	136.19	38.63	-16.10	23.01
Blip-Combined	134.52	34.56	-15.18	19.68
68th Ave. NE to SR 104				
Sensor	**RMSE (Second)**	**MAD (Second)**	**MPE (%)**	**MAPE (%)**
BlueTOAD	38.94	23.10	3.94	13.33
Sensys	51.43	37.20	19.01	23.37
Inrix	45.32	29.63	-12.37	15.41
Blip-BT	36.17	23.03	2.31	13.36
Blip-WiFi	37.59	26.16	8.99	16.00
Blip-Combined	35.57	22.63	4.79	13.33
SR 104 to NE 153rd St.				
Sensor	**RMSE (Second)**	**MAD (Second)**	**MPE (%)**	**MAPE (%)**
BlueTOAD	40.33	22.63	7.88	15.85
Sensys	41.37	25.69	13.88	18.86
Inrix	69.33	57.24	46.11	47.84
Blip-BT	34.85	22.08	10.21	16.12
Blip-WiFi	35.44	24.01	11.53	17.38
Blip-Combined	34.83	22.29	11.26	16.35

Note: in the colour scheme minimum errors to the maximum errors are shown by the spectrum of green to red respectively. The Maximum accepted level of accuracy is set as 25%.
The percentage based values (MPE and MAPE) are colored green below 15%, transitioning through yellow at 20% to red at or above 25%.
The colourings for RMSE and MAD are green for the lowest values transitioning to red for the highest error values.

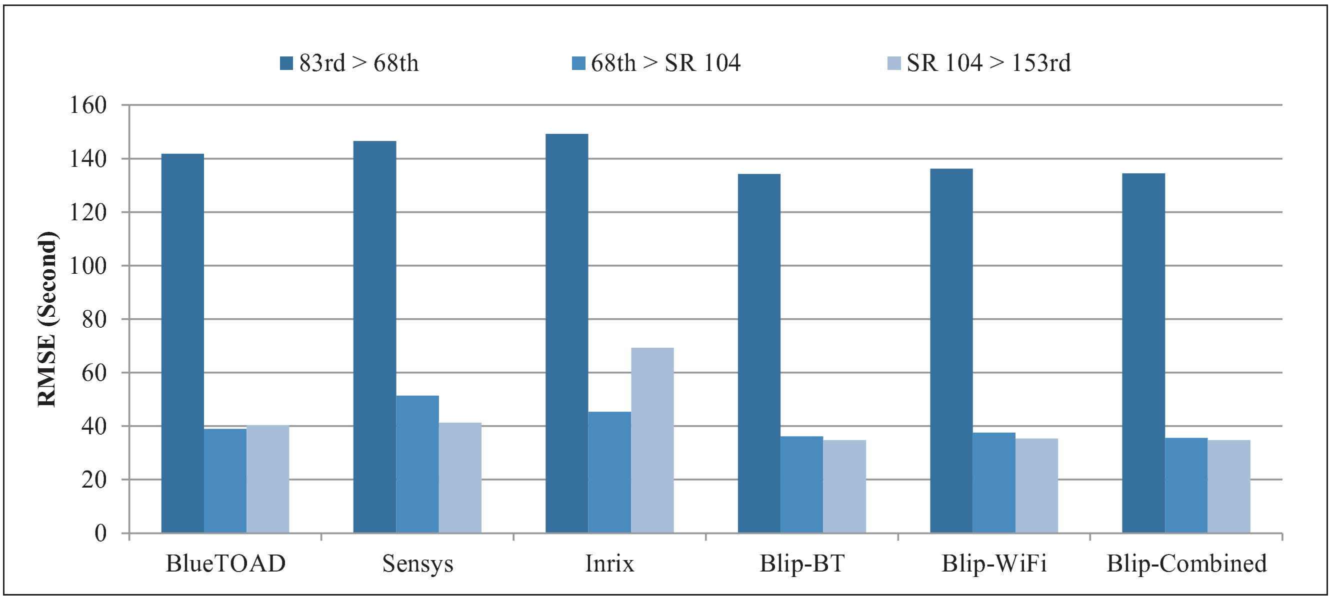

Figure 6-13. Comparing RMSE for various sensors on westbound segments

Figure 6-13 presents the results of RMSE for all the sensors across the three segments on SR 522. This clearly shows that the performance and accuracy of the estimated travel time by various sensors varies between segments. In this case, performance of all the sensors is lower for the 83rd Pl. NE to 68th Ave. NE segment compared to 68th Ave. NE to SR 104 (WB) and SR 104 to NE 153rd St. (WB) segments. This could be related to the length of the segment and the number of intersections between the detection points.

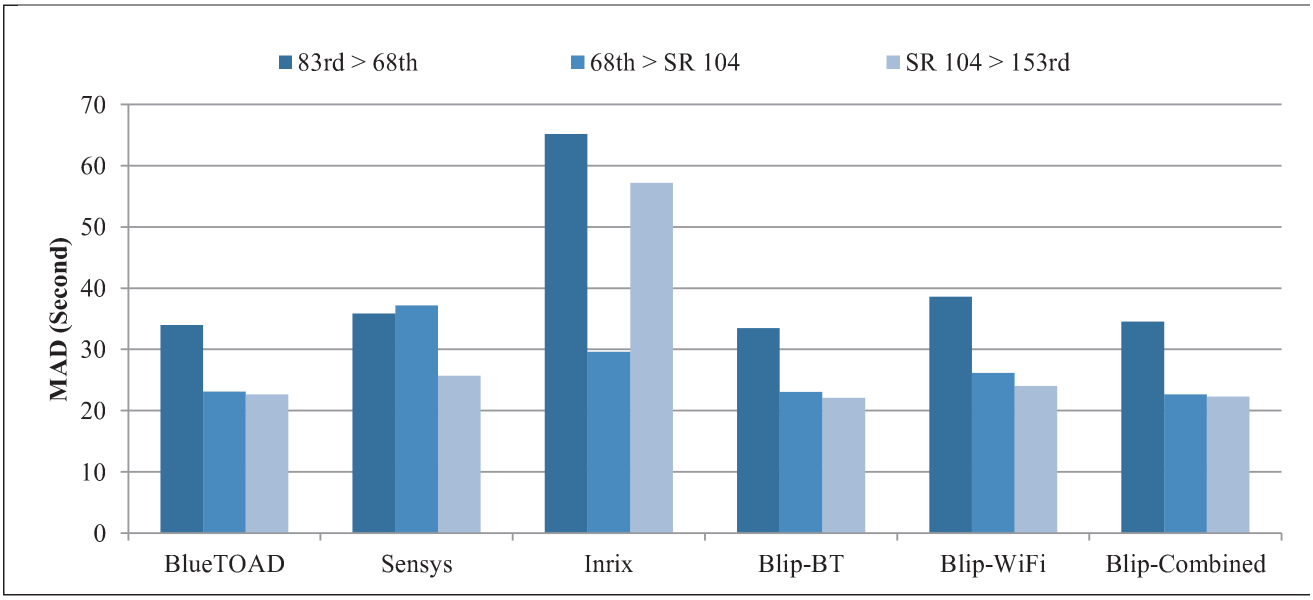

Figure 6-14. Comparing MAD for various sensors on westbound segments

Figure 6-14 shows the results of MAD for all the sensors across the three segments on SR 522 and confirms the results of Figure 6-14 with the MAD for the 83rd Pl. NE to 68th Ave. NE segment being on average higher than the other segments, though Inrix has significantly higher error on the 68th Ave. NE to SR 104 segment.

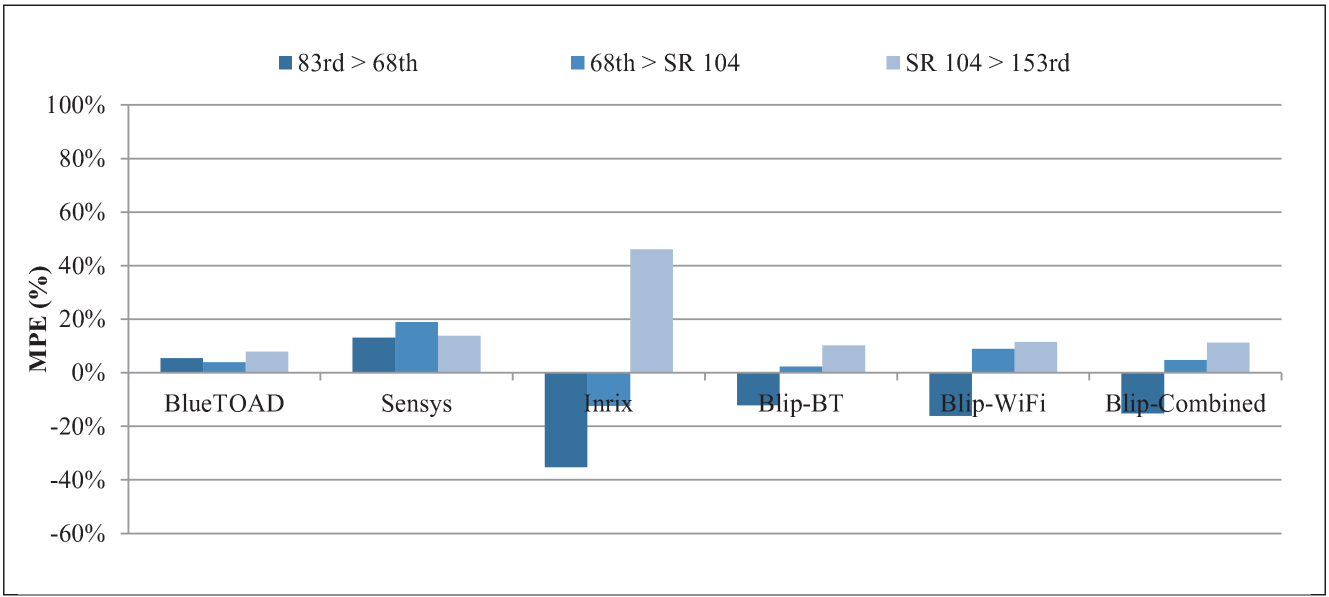

Figure 6-15. Comparing MPE for various sensors on westbound segments

Figure 6-15 shows the direction of MPE values for all the sensors on the three SR 522 segments. This reflects that Blip-Combined, Blip-BT, and Blip-WiFi tend to underestimate the travel time while Inrix, Sensys and BlueTOAD overestimate the travel time. This could also be related to the size of the detection zones and the off-set between various sensor locations.

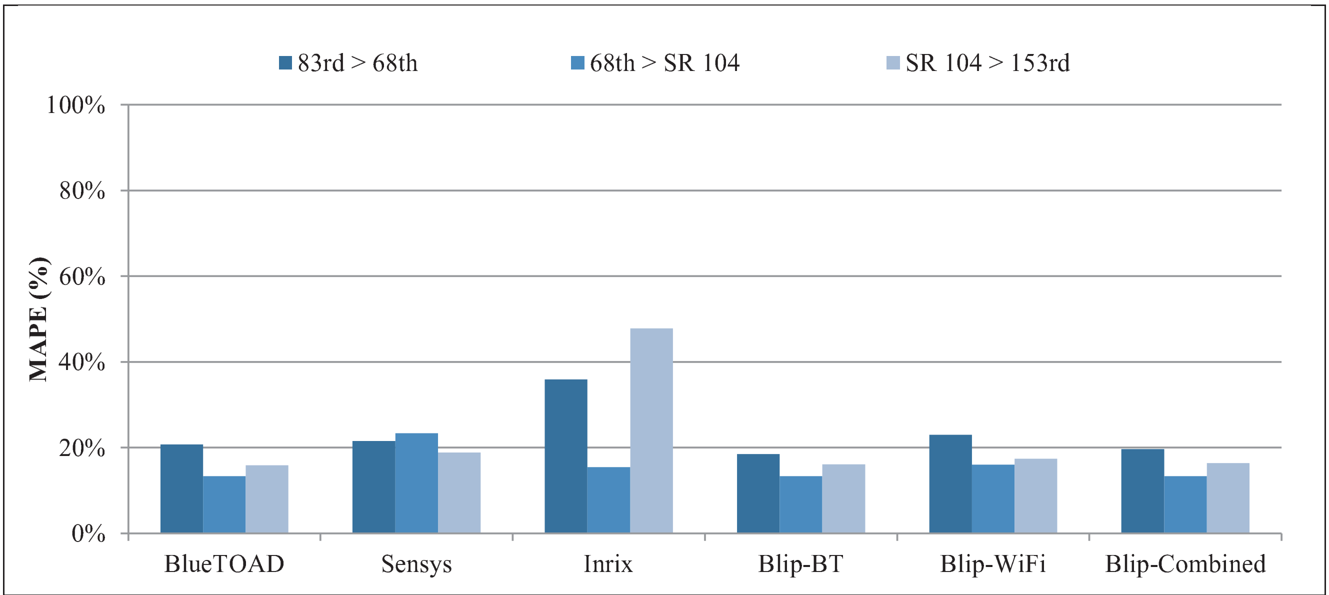

Figure 6-16.Comparing MAPE for various sensors on westbound segments

Figure 6-16 presents the MAPE results for the sensors on the three westbound SR 522 segments. As seen in Table 6-14, on average the sensors have a better performance and higher accuracy for the travel time estimations on 68th Ave. NE to SR 104 (WB) and SR 104 to NE 153rd St. (WB) segments than the 83rd Pl. NE to 68th Ave. NE segment. Blip-Combined, Blip-BT, BlueTOAD, Blip-WiFi have slightly higher accuracy in reporting travel time compared to Sensys and significantly more than Inrix.

6.5.2.3 Eastbound Travel Time

Travel time plot for 68th Ave. NE to 83rd Pl. NE is shown in Figure 6-17 for the analysis period of May 1st, 2013 through May 8th, 2013. Figure 6-17 shows that all the sensors are capable of detecting the cyclical pattern of travel time over weekdays and weekend and also for the morning and afternoon peaks. However, the Inrix reports a significantly lower and highly smoothed travel time on this segment compared to others. Overnight, BlueTOAD was observed to have a number of gaps in its data.

Travel time plots for segments NE 153rd St. to SR 104 and NE 153rd St. to SR 104 are presented in Appendix III. The weekly data demonstrates that the travel times on all three segments are consistent and cyclical. The difference between weekdays and weekends is distinguishable. These results are in accordance with expectations based on westbound performance.

For higher temporal resolution, travel time plots on 68th Ave. NE to 83rd Pl. NE (EB) for Wednesday May 1st, 2013 is shown in Figure 6-18. In this segment, Inrix reports a significantly lower and highly smoothed travel time compared to others. Considering the accuracy of the travel time reported by BlipTrack and BlueTOAD on westbound, it can be concluded that Inrix is reporting highly under estimated travel time on this segment.

Similarly, the overlaid profiles of travel time for the sensors on NE 153rd St. to SR 104 and NE 153rd St. to SR 104 for Wednesday May 1st, 2013 are placed in Appendix III. These show that BlueTOAD, and Blip-BT, Blip-WiFi and Blip-Combined were closely scattered. However, Inrix data does not overlap with others in all three segments. The daily data shows the difference in travel time during the peak and off-peak hours. This pattern is also consistent with the observations on weekly patterns.

The descriptive statistics for the two month period (April 5th, 2013 through June 8th, 2013) are summarised in Table 6-15. Due to the lack of ground truth on the eastbound segments it is not possible to evaluate the sensors' accuracy; however, it is clear the Inrix data indicates a significantly higher or lower and more highly smoothed travel time over the off-peak hours compared to the others. For the 68th Ave. NE to 83rd Pl. NE segment, the Inrix results are significantly lower and less responsive than the other systems. For SR 104 to 68th Ave. NE Inrix reports a lower travel time, but with less separation than the other two segments and more responsiveness to traffic conditions. For the NE 153rd St. to SR 104 segment Inrix data is generally higher and somewhat responsive to traffic conditions. Overnight, BlueTOAD was observed to have a number of gaps in its data. This is not necessarily a problem, as it is likely an effect of low traffic volumes, when travel time data is least likely to be needed, but the lack of data should be noted.

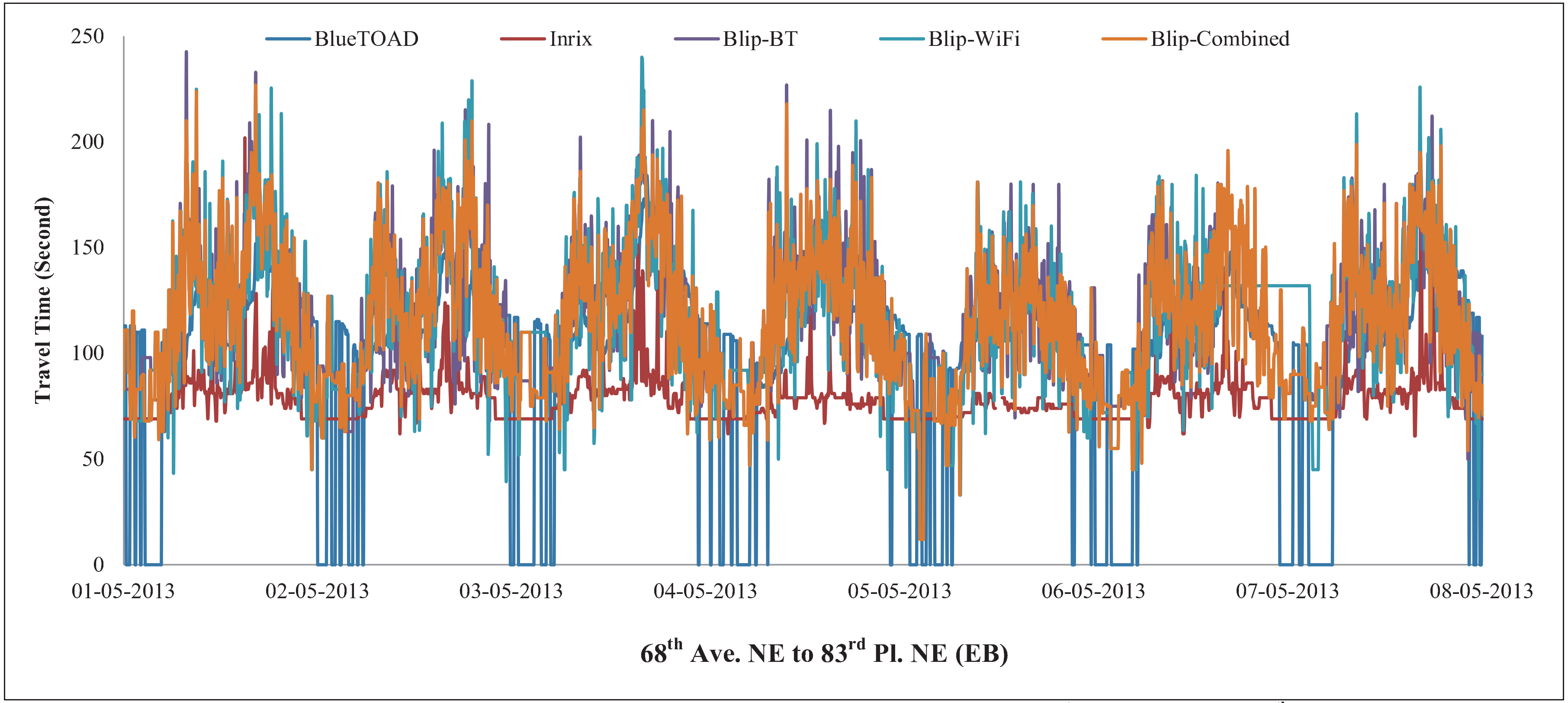

Figure 6-17. Travel time plot from 68th Ave. NE to 83rd Pl. NE (EB) for May 1st, 2013 through May 8th, 2013

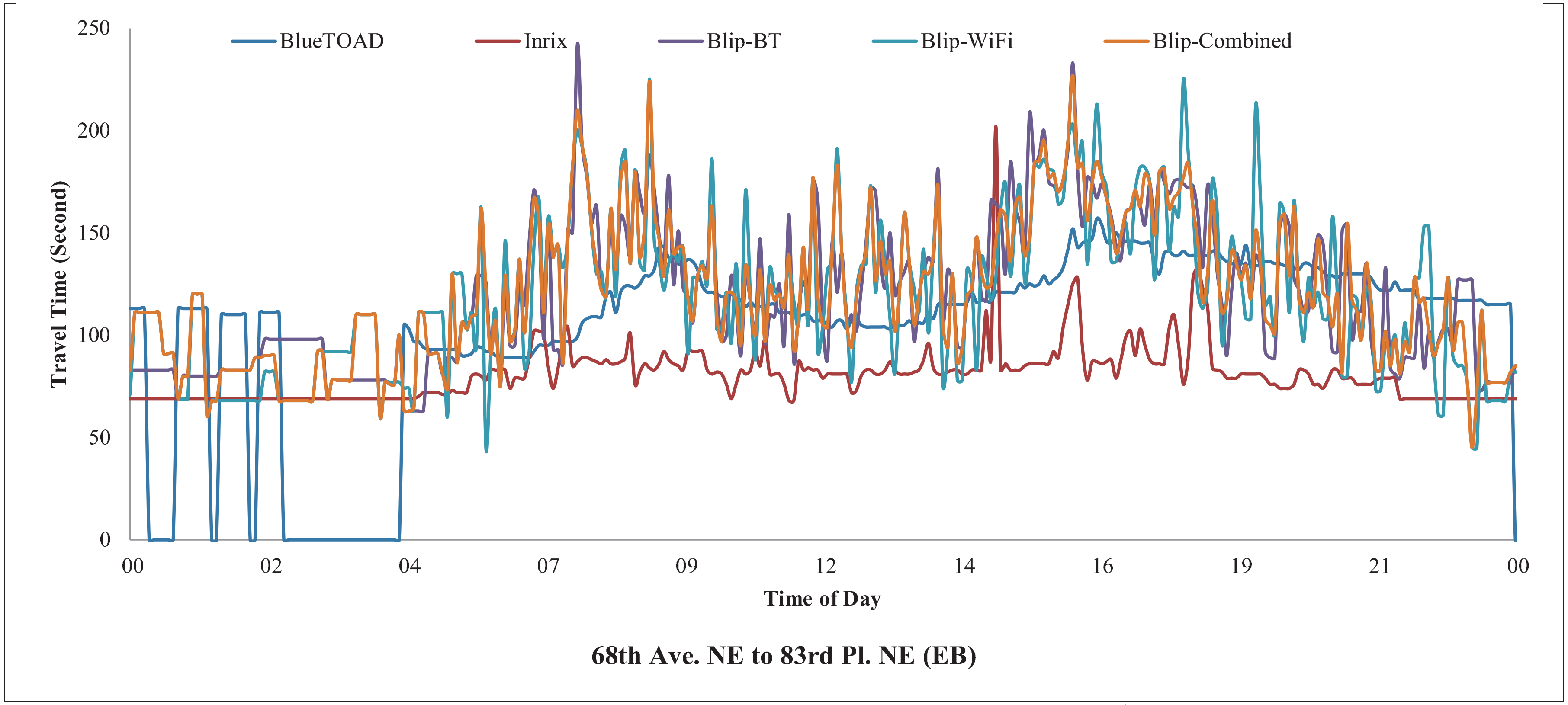

Figure 6-18. Travel time plot for 68th Ave. NE to 83rd Pl. NE (EB) on May 1st, 2013

Table 6-15. Hourly descriptive statistics for eastbound over the period of April 5th through June 8th, 2013

Segment	Sensor	Sample Count	Std. Dev.	Min	1st Qtr	Median	Mean	3rd Qtr	Max
68th Ave. NE to 83rd Pl.NE	BlueTOAD	192	4.4	122.4	126.0	128.3	129.2	132.1	141.4
	Sensys	NA	NA	NA	NA	NA	NA	NA	NA
	Inrix	NA	6.5	149.0	159.8	162.0	162.0	162.0	184.0
	Blip-BT	465	16.2	95.0	113.0	123.0	125.7	139.3	173.0
	Blip-WiFi	484	17.2	87.0	120.8	133.5	132.3	143.0	180.0
	Blip-Combined	1007	13.4	99.0	118.0	127.5	128.5	137.3	163.0
	ANPR	NA	NA	NA	NA	NA	NA	NA	NA
SR 104 to 68th Ave. NE	**Sensor**	**Sample Count**	**Std. Dev.**	**Min**	**1st Qtr**	**Median**	**Mean**	**3rd Qtr**	**Max**
	BlueTOAD	210	8.2	151.5	170.0	176.0	175.0	181.5	190.5
	Sensys	NA	NA	NA	NA	NA	NA	NA	NA
	Inrix	NA	13.4	114.0	127.8	134.0	135.7	138.0	192.0
	Blip-BT	534	26.7	111.0	131.8	149.5	153.5	167.5	271.0
	Blip-WiFi	775	28.5	106.0	139.8	159.5	160.6	179.0	259.0
	Blip-Combined	1309	23.3	111.0	136.8	153.0	155.0	169.3	226.0
	ANPR	NA	NA	NA	NA	NA	NA	NA	NA
NE 153rd St. to SR 104	**Sensor**	**Sample Count**	**Std. Dev.**	**Min**	**1st Qtr**	**Median**	**Mean**	**3rd Qtr**	**Max**
	BlueTOAD	216	11.4	97.6	113.1	117.5	120.7	129.2	152.5
	Sensys	NA	NA	NA	NA	NA	NA	NA	NA
	Inrix	NA	9.0	67.0	83.0	86.0	86.3	90.3	120.0
	Blip-BT	396	24.0	78.0	111.8	127.5	128.0	143.5	188.0
	Blip-WiFi	392	29.8	51.0	109.5	131.5	131.3	151.0	217.0
	Blip-Combined	788	23.1	76.0	113.8	127.5	127.4	139.3	224.0
	ANPR	NA	NA	NA	NA	NA	NA	NA	NA

6.6 Data Analysis and Discussions for I-90

The analysis of sensors placed on I-90 differs from the analysis of sensors installed on SR 522 in that there is not a system comparable to the ANPR system on SR 522 to use as a ground truth travel time measurement. This restricts the analysis of I-90 data to be more qualitative than the SR 522 analysis. Specifically, the evaluation of I-90 data looks at data availability, daily pattern variation, and reaction to traffic events such closures due to construction and snow removal.

In order to avoid repetition in this section, the time plots of daily travel times for the I-90 links from May 1st, 2013 through May 8th, 2013 are presented in Appendix III.

The importance of analyses in I-90 is related to the lane closures and accuracy of the sensors in reflecting that abnormal situation. Note that I-90 from milepost 56 to 61 has been closed occasionally for rock blasting related to construction. These closures are typically about an hour in length and close both directions. The evening of May 2nd, 2013 includes one such closure which shows as a travel time peak in Figure 6-19. This event is shown more closely in Figure 6-19, and a similar closure on May 15th, 2013 is shown in Figure 6-20.

Figure 6-19 and Figure 6-20 show how the Inrix and BlueTOAD data react to the absence of traffic. The BlueTOAD system continues to report the last travel time for approximately a half hour until ceasing to report travel times pending new vehicle identification. The Inrix data has a more variable response. The Inrix travel time data is the sum of data from many smaller segments. This factor is of limited impact on the SR-522 corridor due to smaller segment size and fewer segments involved. For I-90, the longer distance between sensor placements means that instead of one to three Inrix segments, ten to twenty may be involved. The difference in Inrix response between Figure 6-19 and Figure 6-20 is that is that a number of segments reverted to average travel time on May 15th and on May 2nd they reported null values instead. In both cases the travel times are not representative of the closure.

However, other data produced by the systems are useful in identifying the closures. Inrix reports a confidence level for its segment readings that can be used to judge the reliability of the data. For both closures, the Inrix data reported significant decreases in average confidence and complete absence of confidence for specific segments. The BlueTOAD data includes a useful data point, the last reported matching vehicle. When the closure occurred, no more vehicles were being detected to update the travel time information. After a half hour with no new samples the BlueTOAD data ceased reporting a travel time.

It is important to note that calculating the travel time by averaging Inrix segment data is very limited in the case of closures. This is because it is nearly impossible to accurately judge the delay from being backed up and held at the closure site without some kind of arrival information. This is a non-issue for BlueTOAD data, which presents a reasonable travel time, once traffic flow has resumed, to judge by the travel times of approximately an hour reported after reopening the road.

Figure 6-19 shows a detailed view of the data for May 2nd, 2013 on I-90. The vertical blue dotted lines indicate the start and end of the closure. The blue triangles show the times of the last and first detected vehicles by BlueTOAD and the red dashed line indicates Inrix's average confidence value for the data. In this case the Inrix travel time responds immediately, but actually indicates a faster travel time than during free flow. The BlueTOAD data shows a travel time for the segment for 30 minutes before ceasing to report data until detecting the next vehicle. Of note is that the BlueTOAD data reflects a reasonable travel time upon resumption of traffic flow and Inrix's travel time quickly returns to normal.

Figure 6-20 shows a similar event on May 15th, 2013. The vertical blue dotted lines indicate the start and end of the closure. The blue triangles show the times of the last and first detected vehicles by BlueTOAD and the red dashed line indicates Inrix's average confidence value for the data. This time the Inrix data does not respond to the closure, but the confidence level drops dramatically during the interval. Note that the confidence level shown in this figure is an average across multiple segments. Individual segments have zero or near zero confidence during the closure.

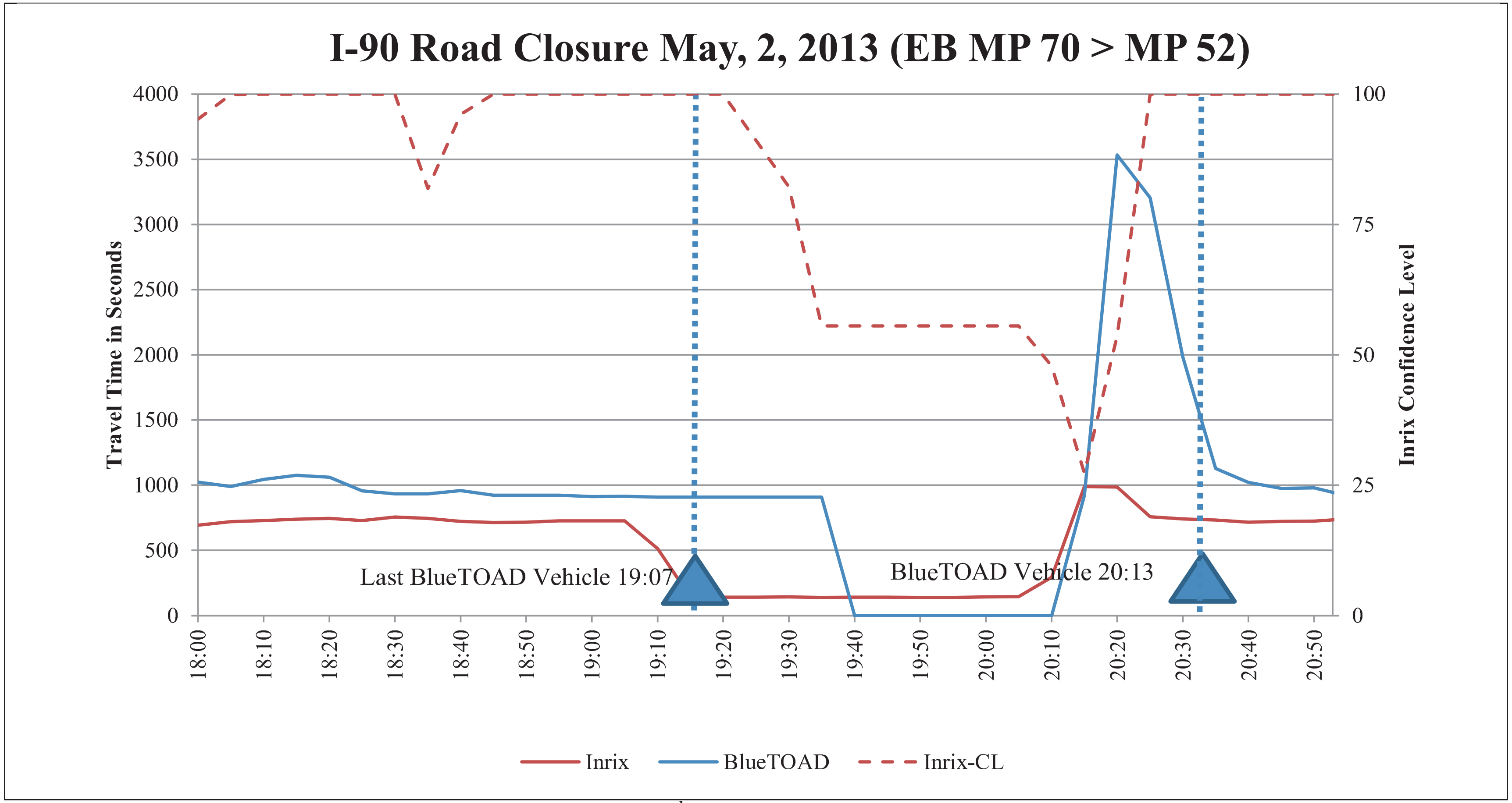

Figure 6-19. May 2nd closure of I-90 and sensor response

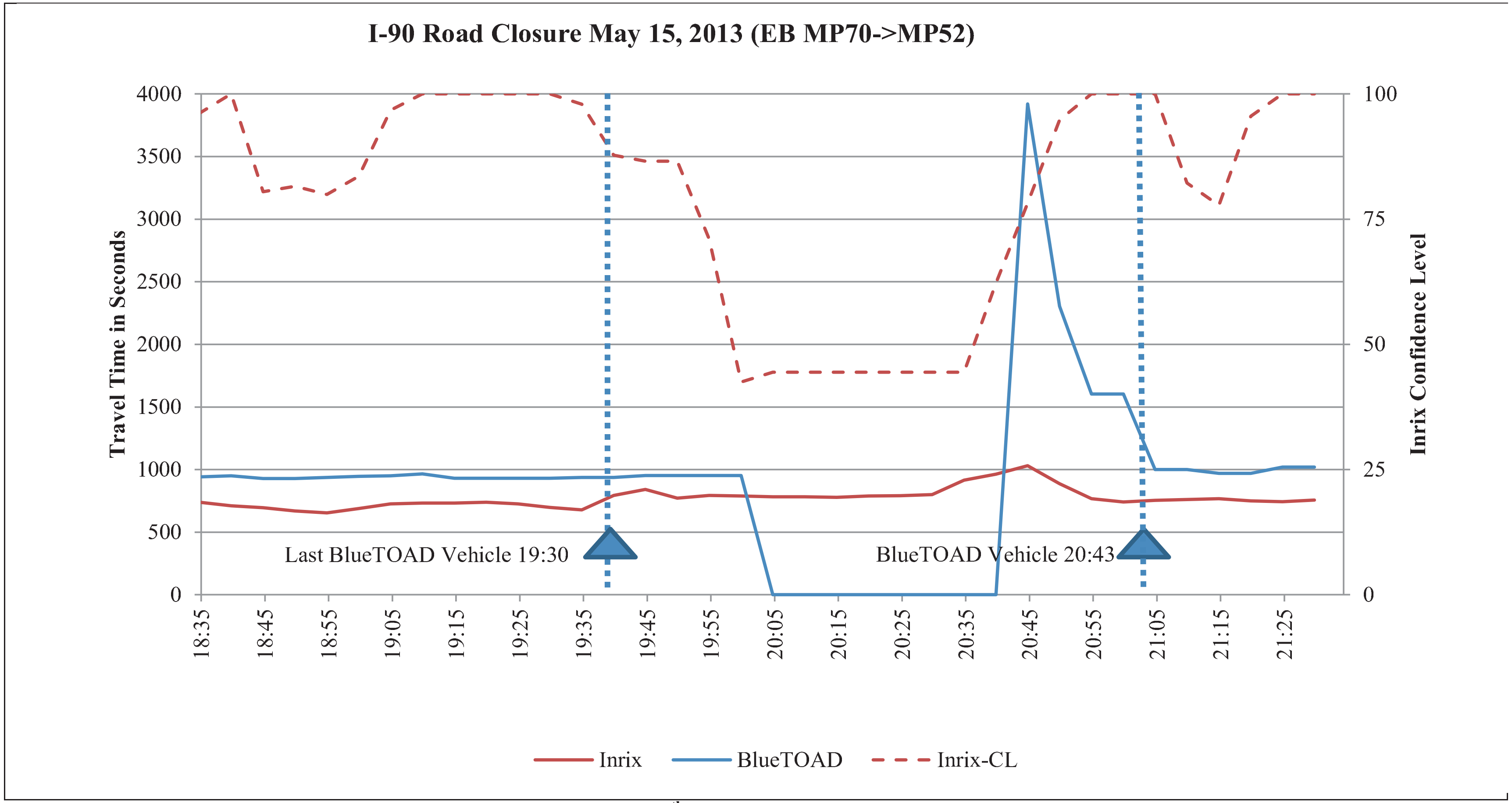

Figure 6-20. May 15th closure of I-90 and sensor responses

6.7 Data Manipulation and Sensor Evaluation Observations

One of the major tasks of this project was collecting and manipulating the data from each of the vendors. Each vendor uses different data formats, algorithms and frequency, technologies making the task of collecting and organising the data one that bears closer inspection. Collecting and organising data from an individual vendor is not an overly daunting task. Coordinating data from four vendors and the WSDOT with seven distinct systems each generating multiple datasets is a significant resource investment.

The major points of note in the data collection for this project are ease of data collection, completeness of data, ease of mapping to existing data structures and consistency of availability. Each vendor has a different means of distributing data, typically web based, though the WSDOT ANPR and loop data and Inrix data came through email and network connections. The Sensys, BlueTOAD and BlipTrack data all came through websites of differing utility.

Over the course of the project several changes were made to the vendor websites. Specific issues encountered during the project were limitations in length of time, number of sensors and speed of download. Initially, the Sensys website was a major limitation with small data download limits requiring significant manual effort to collect all of the project data. The BlueTOAD and BlipTrack websites were not as labour intensive but still required significant effort to collect and collate all of the desired data.

Mapping the data collected to existing data structures; in this case, the data and sensor placement of the ANPR system on SR 522 and the milepost/exit pattern for I-90 was trivial in some cases and more difficult in others. For SR 522 WB, the sensor sites were chosen to match existing westbound ANPR locations, making the matchup between each set of data easy. Eastbound SR 522 has a different ANPR setup in that there is no ANPR at the SR-104 intersection for eastbound traffic. The nearest ANPR for eastbound traffic is located 0.2 miles west at the Beach Drive NE intersection. This makes a direct mapping of sensors to eastbound ANPR data impossible. Incidentally, the ANPR data for eastbound experienced a data collection failure during the analysis period, precluding an analysis in any case.

Inrix data has been the major source of issues mapping data to existing data structures. Inrix data is keyed to a different base mapping system than the other systems and the ANPR data. Inrix data uses TMC codes to identify roadway segments in a system developed for GPS systems instead of the route and milepost or arbitrary sensor number/placement data systems used by the other systems. Where Inrix TMC segments do not exactly map to existing segments; its travel time will be over or underestimated compared to the other systems as seen in the SR 522 analysis in particular. Another consequence of this difference in mapping is that an analysis segment composed of more than one Inrix TMC segments will need to reconcile potentially very different travel times on an individual TMC segment and normal travel times on others. Specifically, this occurs when delay or stoppage is incurred. For example at an intersection or blockage on a freeway, an individual TMC segment may report a high travel time (even exceeding the 5 minute reporting interval) while the surrounding TMC segments report normal travel times. The sum of travel time across TMC segments used in this research fails when significant stoppage or delay occurs, because the sum of travel time across the relevant TMC segments will include free flowing segments beyond the blockage as seen in the I-90 data analysis.

An additional point of interest that falls under data mapping is the inclusion of different data collected by each system and different smoothing algorithms. Each system includes time and travel time information in its basic data formats. BlueTOAD data includes its match rates in a separate file system at 15 minute time intervals instead of the 5 minute intervals used for the other data. Inrix data does not include a capture rate as such, but does have a confidence value as shown in the I-90 analysis. The remaining systems report their matches and travel times in the same files and data structures. The Sensys system has the most additional data associated with it. Specifically Sensys includes travel time measurements at 10% intervals, measured speeds and upstream and downstream volumes. For this research the 90% travel time was chosen to represent the Sensys travel time, as that was the value used by Sensys to represent travel times in their presentation to the lab. This is a conservative measure that can underestimate the accuracy of the Sensys system. It should be noted that even with this potential handicap, the Sensys system proved to have acceptable levels of accuracy in several cases.

Data availability is a multifaceted problem. First, the data must be collected by the system in question. This includes all of the communications and storage endemic to collecting the data. The second aspect is that the data must be retrievable by the system. Finally, there are temporal availability considerations. These include considerations of delay between collection and accessibility of the data and how long the data is available after collection. In this project, immediate temporal availability has not been of primary concern, however it should be noted that the data delivery methods for data from the WSDOT and Inrix included delays between collection and availability.

6.8 Conclusion

The daily analysis revealed that the systems experienced error spikes during the morning peak period on all segments. With the exception of the Inrix data, all systems generally reported satisfactory results, with the Bluetooth and WiFi based systems staying below the 25% error threshold except during overnight hours and some spikes in the peak periods. It should be noted that the Sensys travel time used was the 90th percentile travel time, where the other systems reported mean or median values, yet still the Sensys system posted acceptable accuracy in most cases. The Sensys travel time error may be reduced by selecting another one of the ten provided travel time values.

The systems did have some notable accuracy limitations. Specifically, the BlueTOAD system can be less reliable overnight. The Inrix system was generally the least responsive to traffic changes and tended to have systematically high or low travel times, probably the results of conservative free flow travel time estimation.

The I-90 and eastbound SR 522 analysis of travel time focused on more qualitative aspects of system performance. The eastbound SR 522 results met expectations based on the westbound analysis, with most patterns repeating, including the systematic over or underestimation of travel time by Inrix. For I-90, the research team was looking for reasonable travel times and daily traffic patterns as well as response to known road closure events. The I-90 analysis noted that both systems were able to respond to daily patterns; however, Inrix and BlueTOAD reported significantly different results on some segments. When the road closure time periods were examined, both systems had their flaws. The BlueTOAD system continued to report a travel time for 30 minutes after the road closure and the Inrix data either failed to react significantly to the closure or reported impossible travel times. Both systems include specific data that can be used to identify when such event occur.

The second important factor to consider in the sensor analysis is the sample size used to calculate the travel time. If the sample size is too small, the travel time may not be representative. Sample size is affected by several factors, including traffic volume and mobile device penetration rates (for Bluetooth and WiFi sensors). For westbound SR 522 the ALPR and Sensys systems have comparable absolute detection rates (i.e. compared to ILD) with between 25% and 50% of traffic being detected, depending on time of day and location, refer to Figure 6-6. The Bluetooth and

WiFi systems detect significantly fewer vehicles. Compared to ANPR and Sensys, BlueTOAD captured about 6% of the volume captured by the ANPR system for an absolute capture rate near 2% of total traffic. The BlipTrack system captured roughly double the number of Bluetooth readings and two and a half times as many on WiFi. The BlipTrack sensor also reports combined totals for its Bluetooth and WiFi sensors, which pushes the combine BlipTrack system to approximately 25% of the ANPR capture rate. Because of the nature of the Inrix data, there is no capture rate to analyse.

The collection of sensors assembled for this study was comprehensive. By setting up so many sensors on the same corridor and having reliable ground truth data in the form of an established ANPR system, the WSDOT has made it possible to perform an in-depth analysis of the different systems. This work shows that sensors of different types and complexities can accomplish the goal of measuring travel time.

Ultimately, each system in the analysis has different strengths and weaknesses that should be considered in addition to their accuracy and sample rates. Some systems can provide additional data; others trade accuracy and coverage for cost or portability. Ultimately, engineers will need to weigh their requirements for accuracy and sample rates against the other engineering constraints imposed on their system. For example, the BlueTOAD units installed on SR 522 and I-90 are solar powered and use cellular data networks, reducing infrastructure and deployment costs. The BlipTrack units have higher sampling rates and marginal accuracy superiority in exchange for power requirements. The Inrix data does not require any roadside infrastructure and has wide availability but at a cost. ANPR units have high accuracy and a comparatively high installation cost. The Sensys have perhaps the most complicated set of trade-offs. Sensys can be used as replacements for loop detectors in intersection operations, making the marginal costs of adding Sensys re-identification lower at some intersections than others.

CHAPTER 7

CONCLUSIONS AND FUTURE RESEARCH

7 Conclusions and Future Research

This chapter summarises the findings of this research and discusses future research avenues based on these findings.

7.1 Revisiting the Objectives

The aim of this research was to develop a framework for improving the accuracy and reliability of travel time estimated using Bluetooth technology. The main objectives of this research, as set out in Chapter 1, were as follows:

- Evaluate the reliability of Bluetooth technology and estimate the location ambiguity associated with Bluetooth detections,
- Identify the influence of aggregation method and sample size on accuracy of estimated travel time,
- Develop methods for travel time estimation to minimise the impact of location ambiguity, without compromising on reliability,
- Develop new methods for mode-specific travel time estimation, utilising CoD information,
- Compare the accuracy of travel time estimated by Bluetooth technology versus other sensor technologies, to provide a holistic overview of the accuracy and reliability of Bluetooth Technology compared to other technologies in the market.

For the first objective, a controlled field experiment was carried out, as described in Section 2.6. The aim was to evaluate the influence of Bluetooth sensors' detection zone size and the Bluetooth device discovery procedure on the number of detection events triggered for a single passing Bluetooth-enabled device and the location ambiguity associated with detections. The results of this study revealed that the detection reliability of Bluetooth is about 84%. However, the detection rate could be lower on some occasions. Comparing the capture rate of different antennae also highlighted the importance of antenna configuration, the location of the installed sensor and the mount design. Analysing the geo-referenced detection events revealed that although the expected detection range of Bluetooth sensors was 70-200 metres on each side of the sensor, more than 80% of the detections were within 100 metres of the actual sensor location.

For the second objective, two sources of FCD were used as the ground truth to quantify and evaluate the accuracy of travel time profiles estimated using Bluetooth technology. Three aggregation techniques including arithmetic mean, geometric mean and harmonic mean were used to construct the travel time profile using Bluetooth data. Comparing the three aggregation methods showed that harmonic mean and geometric mean could significantly reduce the impact of outliers, especially in intervals with low sample sizes. This study also focused on quantifying the impact of sample size on the accuracy of travel time estimates. A series of sensitivity analyses were conducted to determine the range of optimum sample size for travel time profile construction using Bluetooth datasets. The results of this study suggested 5 observations of travel time by MAC address matching as the minimum sample size. Moreover, including intervals with sample size in the range of 5-15 travel time records per 15 minutes would lead to an improvement in the accuracy of the estimated travel time profile.

For the third objective, based on the information obtained about the reliability and accuracy of multiple Bluetooth detection events in Chapter 2, new travel time estimation methods were developed. Eight alternative travel time estimation methods were developed for two different sensor designs; sensors with single antenna or multiple antennae. Comparing the results of all the methods using the RMSE metric showed that two of the methods, *Combined* and *Peak-Peak,* yielded the most accurate travel time estimates.

In single antenna design, the higher accuracy of *Peak-Peak* method in comparison to the commonly used *Enter-Enter* and *Leave-Leave* methods implied that higher RSSI leads to a lower location ambiguity for the detection event. Thus, the value of the RSSI could be used as an indicator for selecting the detection event closest to the sensor and minimising the effect of location ambiguity. Therefore, it is concluded that *Peak-Peak* method is simple and more accurate than the *Enter-Enter* and *Leave-Leave*, which makes it a suitable alternative in the case of sensors with a single antenna.

For multiple antenna design, a sensor with three antennae consisting of one short range antenna and two long-range antennae were used. The short-range antenna had the smallest detection zone and accordingly, the least location ambiguity. However, the smaller the size of the detection zone, the lower the detection rate, which can reduce the accuracy of estimates when short-term travel time variability is high. Therefore, there has to be a trade-off between an acceptable level of location ambiguity and penetration rate for designing the configuration and coverage of the antennae. Hence, the *Combined* method was developed to investigate how a combination of detection events obtained by different antennae can be used to improve the accuracy of travel time estimates. The accuracy of *Combined* method revealed the fact that the new method that combines detection events recorded by various antennae could yield better results.

For the fourth objective, a new method for mode-specific travel time estimation was developed. This method aimed to distinguish between Bluetooth devices carried by different modes and provide a mode-specific travel time estimate. This method was developed based on CoD information, RSSI, travel time, sensor location and traffic condition i.e. peak and off-peak. Accuracy of the mode-specific travel time estimation method was evaluated against the ground truth obtained by a video based survey. Moreover, the accuracy of the mode-specific travel time estimation method was also compared with ANPR, a commercially deployed Bluetooth-based method (BlipTrack), and clustering method. The results showed that the proposed method is able to estimate travel time with almost the same accuracy as ANPR. This indeed proved the capability of Bluetooth technology to be used as an alternative method for arterial road travel time estimation. This highlighted the importance of using CoD as well as RSSI as secondary information to improve the travel time obtained by simple MAC address matching.

For the fifth objective, a side-by-side evaluation of Bluetooth technology from two different vendors (BlipTrack and BlueToad) versus ANPR, Magnetometers, and floating vehicle data from Inrix was conducted. In order to evaluate the efficiency of various technologies, two important factors were considered. The first was the accuracy of the reported travel time. The second was the sample size used to calculate the travel time. Analyses were conducted for two test sites: SR 522 and I-90 in Washington State, United States. With the exception of the Inrix data, all systems generally reported satisfactory results. The Bluetooth and WiFi based systems provided an accurate estimate below the 25% error threshold except during overnight hours and a few instances during peak periods. The Bluetooth and WiFi systems detected significantly fewer vehicles compared to ANPR and magnetometer. BlueTOAD Bluetooth sensors captured about 6% of the volume captured by the ANPR system for an absolute capture rate near 2% of total traffic. The BlipTrack Bluetooth system captured roughly double the number of Bluetooth readings and two and a half times as many on WiFi. The BlipTrack sensor also reported combined totals for its Bluetooth and WiFi sensors, with the combined BlipTrack system providing approximately 25% of the ANPR capture rate. Inrix data does not include sample counts, so that system is excluded from sample count analysis.Ultimately, each system in the analysis had different strengths and weaknesses that should be considered in addition to their accuracy and sample rates. Some systems can provide additional data; others trade accuracy and coverage for cost or portability. Ultimately, engineers will need to weigh their requirements for accuracy and sample rates against the engineering constraints imposed on their system.

7.2 Contributions

This PhD research has made contributions to knowledge about Bluetooth device discovery procedure and its impact on detection reliability and location ambiguity. This research also made contributions to knowledge by developing new travel time estimation methods by including the RSSI and CoD information to reduce location ambiguity, improve accuracy and provide mode-specific travel time estimates on arterial roads with mixed traffic. Additionally, a comprehensive comparative study of Bluetooth technology with other traffic sensor technologies for travel time estimation was conducted, which will hopefully provide useful insights to researchers and practitioners alike.

7.3 Future Research

A number of research avenues have been opened up based on this PhD thesis, as summarised below:

1) This research developed an automated screening algorithm which incorporates three different filtering layers. Due to limited time, the author could not evaluate the impact of third layer which incorporates the information of layout of the Bluetooth sensors on the network. This layer aimed to use the sequence of the detection recorded for a unique MAC address at different sensors over a predetermined time window for re-checking the mode of detected device. Further research could evaluate the efficiency of using third layer on accuracy of estimated travel time. Furthermore, the accuracy of the algorithm was tested against ground truth on a single link for a short time period. Further research could focus on evaluating the algorithm for a longer period and over a wider network. It could also be tested during abnormal traffic conditions such as incidents. The algorithm associated an equal weight to the input parameters (e.g. CoD information, travel time etc.). Further research could investigate the impact of assigning different weights for the parameters, on the accuracy of algorithm.
2) According to the result of this research, a combination of Bluetooth and WiFi technologies can increase the sampling rate by 25% and also such combined data can result in more accurate travel time estimation. Since, the focus of this research mainly was on exploring the detection procedure of Bluetooth technology and its impact on the reliability and location ambiguity of the detections, the detection procedure of WiFi technology was not explored. Therefore, further research could focus on exploring the detection procedure of WiFi so that the combination could result in a more accurate travel time estimate.
3) This research focused on evaluating the capability of Bluetooth technology for providing accurate travel time estimation, but it did not investigate short-term travel time prediction. Further research could explore the feasibility of using Bluetooth-based travel time estimates as an input to short-term travel time prediction models.
4) Bluetooth technology is capable of tracking vehicles throughout their trips within urban networks and across highway stretches. This information can be used for analysing Origin-Destination (O-D) pattern by aggregation and clustering of the individual trips. Therefore, further research could develop a framework for using the MAC address data collected by Bluetooth sensors as a basis for O-D estimation.

References

1. Ahmed, H., El-Darieby, M., Abdulhai, B. & Morgan, Y. (2008) Bluetooth- and Wi-Fi-Based Mesh Network Platform for Traffic Monitoring. *Transportation Research Board 87th Annual Meeting*, *13-17 January 2008, Washington DC, United States.*

2. Barceló, J., Montero, L., Marquès, L., & Carmona, C. (2010). Travel Time Forecasting and Dynamic Origin-Destination Estimation for Freeways Based on Bluetooth Traffic Monitoring. *Transportation Research Record: Journal of the Transportation Research Board*, 2175(1), pp.19-27.

3. Brennan Jr, T.M., Ernst, J.M., Day, C.M., Bullock, D.M., Krogmeier, J.V. & Martchouk, M. (2010). Influence of Vertical Sensor Placement on Data Collection Efficiency from Bluetooth MAC Address Collection Devices. *Journal of Transportation Engineering*, 136(12), pp.1104-1109.

4. Blip Systems Company (n.d.) *BlipTrack collecting real-time travel information.* [Online] Available from: http://media.brintex.com/Occurrence/27/Brochure/1279/brochure.pdf [Accessed 15th November 2013].

5. Blip Systems Company (n.d.) *BlipTrack Wi-Fi Traffic Sensor*. [Online] Available from: http://www.blipsystems.com/traffic/products/bliptrack-wi-fi-traffic-sensor/ [Accessed 15th November 2013].

6. Bullock, D., Haseman, R., Wasson, J. & Spitler, R. (2010) Anonymous Bluetooth Probes for Measuring Airport Security Screening Passage Time: The Indianapolis Pilot Deployment. *Transportation Research Board 89th Annual Meeting. CD-ROM. Transportation Research Board, Washington D.C.*

7. Chakraborty, G., Naik, K., Chakraborty, D., Shiratori, N. & Wei, D. (2010). Analysis of the Bluetooth device discovery protocol. *Wireless Networks*, 16(2), pp.421-436.

8. Eberle Design Inc (n.d.) *Oracle Enhanced Series*. [Online] Available from: http://www.editraffic.com/wp-content/uploads/Oracle_2EC_4EC_Catalog_Sheet.pdf [Accessed 15th November 2013].

9. Farokhi, S.K., Hamedi, M. & Haghani, A. (2010) Evaluating Moving Average Techniques in Short-Term Travel Time Prediction Using an AVI Data Set. *Transportation Research Board 89th Annual Meeting, 10 -14 January 2010, Washington D.C.*

10. Franssens, A. (2010) *Impact Of Multiple Inquires on the Bluetooth Discovery Process: and Its Application to Localization*. Master Thesis, EEMCS: Electrical Engineering, Mathematics and Computer Science, University of Twente, the Netherlands.

11. Golmie, N., Rebala, O. & Chevrollier, N. (2003). Bluetooth Adaptive Frequency Hopping and Scheduling. *Military Communications Conference, 2003. MILCOM '03, 2003 IEEE, 13-16 October 2003.* 2, pp. 1138-1142.

12. Gramaglia, M., Bernardos, C.J. & Calderon, M. (2013) Virtual Induction Loops Based on Cooperative Vehicular Communications. *Sensors,* 13, pp.1467–1476.

13. Haghani, A., Hamedi M., Sadabadi, K.F., Yound Young, S. & Tarnoff, P.J. (2010) Data Collection of Freeway Travel Time Ground Truth with Bluetooth Sensors. *Transportation Research Record: Journal of the Transportation Research Board*, 2160(1), pp.60-68

14. Hamedi, M., Haghani, A., & Sadabadi, F. (2009) Using Bluetooth Technology for Validating Vehicle Probe Data. *16th ITS World Congress and Exhibition on Intelligent Transport Systems and Services.21-25 September 2009, Stockholm, Sweden.*

15. Han, B., Hui, P., Kumar, V.A., Marathe, M.V., Shao, J. & Srinivasan, A. (2012). Mobile Data Offloading Through Opportunistic Communications and Social Participation. *Mobile Computing, IEEE Transactions on*, 11(5), pp.821-834.

16. Haseman, R.J., Wasson, J. & Bullock, D. (2010) Work Zone Travel Time Delay and Evaluation Metrics Using Bluetooth Probe Tracking. *In Transportation Research Board 89th Annual Meeting*. CD-ROM. Transportation Research Board, Washington D.C.

17. Hewlett-Packard Company (2002) *Wi-Fi and Bluetooth Interference Issues*. [Online] Available from: http://www.hp.com/rnd/library/pdf/WiFi_Bluetooth_coexistance.pdf [Accessed 5th July 2013].

18. Holm, J., Foller, J. & Overgaard Hansen, Ch. (2009). GPS Data as Source for a National Travel Time Database. *16th ITS World Congress and Exhibition on Intelligent Transport Systems and Services, 21-25 Sep 2009, Stockholm, Sweden*.

19. Holm, J., Foller, J. & Overgaard Hansen, Ch. (2011). Probe Speeds for National Traffic Information. *18th World Congress on Intelligent Transportation Systems, 16-20 October 2011, Orlando, United States.*

20. Huang, A.S., & Rudolph, L. (2007) *Bluetooth Essentials for Programmers.* Cambridge University Press, New York, NY.

21. Innamaa, S. (2009) *Short-Term Prediction of Traffic Flow Status for Online Driver Information*. VTT Publications 708. VTT Technical Research Centre of Finland, Finland.

22. INRIX (n.d.) Available from: http://www.inrix.com/. [Accessed 15th November 2013].

23. Jiang, J.R., Lin, B.R., & Tseng, Y.C. (2004). Analysis of Bluetooth Device Discovery and Some Speedup Mechanisms. *Journal of the Institute of Electrical Engineering*, 11(4), pp.301-310.

24. Johnson Consulting (2004) *How Does Bluetooth Work?* [Online] Available from: http://www.swedetrack.com/images/bluet13.htm [Accessed 5th July 2013].

25. Jung, S., Larkin, J., Shah, V., Toppen, A., Vasudevan, M. & Wunderlich, K. (2003). *On-Time Reliability Impacts of ATIS, Volume III: Implications for ATIS Investment Strategies*. Prepared for Federal Highway Administration. 900610-D1.

26. Kavaler, R., Kwong, K., Raman, A., & Varaiya, P. (2010) Arterial Performance Measurement with Wireless Magnetic Sensors. *In Proceedings 89th Annual Meeting Transportation Research Board, 10-14 January 2010, Washington, the United States.*

27. KMJ Consulting (2010) *Bluetooth Travel Time Technology Evaluation Using the BlueTOAD™*. E01271 PennDOT District 6-0 ITS & Support Open End Contract – Work Order #1, Submitted To: Pennsylvania Department of Transportation.

28. Lahrmann, H., Skoven Pedersen, K., & Christensen, L. T. (2010). Bluetooth detektorer som ny cost-effektiv sensor i vejtrafikken. *In Selected Proceedings from the Annual Transpor Conference at Aalborg University*.

29. Lahrmann H, Agerholm N, Tradisauskas N, Berthelsen K. K., Harms L. (2012) Pay as You Speed, ISA With Incentives for Not Speeding: Results and Interpretation of Speed Data. Accident Analysis & Prevention, 48, pp.17-28.

30. Lee, U., Jung, S., Cho, D. K., Chang, A., Choi, J., & Gerla, M. (2010). P2P Content Distribution to Mobile Bluetooth Users. *Vehicular Technology, IEEE Transactions on*, 59(1), pp.356-367.

31. Chen L.J & Hung H.H. (2011) A Two-State Markov-based Wireless Error Model for Bluetooth Networks. *Wireless Personal Communications Journal*, 58(4), pp.657-668.

32. Lighthill M.J, Whitham G.B (1955) *On Kinematic Waves. II. A Theory of Traffic Flow on Long Crowded Roads*. Royal Society of London. Series A, Mathematical and Physical Sciences, 229, pp. 317-345

33. Ma, X., Wu, Y.J. & Wang, Y. (2011) DRIVE Net: E-Science of Transportation Platform for Data Sharing, Visualization, Modeling, and Analysis. *Transportation Research Record: Journal of the Transportation Research Board*, 2215, pp.37-49.

34. Malinowski, Y., Wu, Y.J, Wang, Y. & Lee, U. (2010) Field Experiments on Bluetooth-based Travel Time Data Collection. *Transportation Research Board 89th Annual Meeting*. CD-ROM. Transportation Research Board (No. 10-3134), Washington D.C.

35. Malinovskiy, Y., Lee, U.K., Wu Y.J. & Wang, Y. (2011) Investigation of Bluetooth-Based Travel Time Estimation Error on a Short Corridor. *Transportation Research Board 90th Annual Meeting*. CD-ROM. Transportation Research Board, Washington D.C.

36. Mathe, T.V. (2013) *Travel Time Data Collection*. [Online] Available from: http://www.civil.iitb.ac.in/~vmtom/1111_nptel/527_AutoGPS/plain/plain.html [Accessed: November 14th 2013].

37. Mizuta, K. (2007) Automated License Plate Readers Applied to Real-Time Arterial Performance: A Feasibility Study. Department of Civil & Environmental Engineering: University of Washington.

38. Monsere, C., Breakstone, A., Bertini R.L., Deeter, D. & McGill, G. (2006) Validating Dynamic Message Sign Freeway Travel Times Using Ground Truth Geospatial Data. *Transportation Research Record: Journal of the Transportation Research Board*, 1959, pp.19–27.

39. Namaki Araghi, B., Tørholm, L.C., Krishnan, R. & Lahrmann, H. (2012) Application of Bluetooth Technology for Mode-Specific Travel Time Estimation on Arterial Roads: Potentials and Challenges". *In Proceedings Trafikdage Conference at Aalborg University, 27-28 August, Aalborg, Denmark.*

40. Namaki Araghi, B. (2010). *Using the K-NN Method for Incident Duration Prediction Based on TPEG Data*. MSc Thesis, Centre for Transport Studies, Imperial College London, UK.

41. Paniati, F.J. (2004) *Information and Action: Dynamic Message Sign (DMS) Recommended Practice and Guidance. Federal Highway Administration*. [Online] Available from: http://mutcd.fhwa.dot.gov/res-memorandum_dms.htm [Accessed 10th October 2010].

42. Quixote Transportation Technologies, Inc. (n.d.) *Automated License Plate Recognition (ALPR) Systems*. Available from: http://www.ae-traffic.com/NuMetrics/AE_Traffic_ALPR.pdf [Accessed 15th November 2013].

43. Pokrajac, D., Borcean, C., Johnson, A., Hobbs, A., Agodio, L., Nieves, S., Balbes, M., McCauley, L., Tice, J., Dare, N., McKie, J., Lombardo, B., Self, B.J. & Austin, J. (2009) Evaluation of Automated License Plate Reader Accuracy. *9th International Conference on Telecommunication in Modern Satellite, Cable, and Broadcasting Services, 7-9 Oct 2009, Nis, Serbia*.

44. Quayle, S.M., Koonce, P., DePencier, D., & Bullock, D.M. (2010). Arterial Performance Measures with Media Access Control Readers. *Transportation Research Record: Journal of the Transportation Research Board*, 2192(1), pp.185-193.

45. Puckett, D.D. & Vickich, M.J. (2010) *Bluetooth®-Based Travel Time/Speed Measuring Systems Development*. University Transportation Center for Mobility™, Texas Transportation Institute, No. UTCM 09-00-17.

46. Rakha, H., & Van Aerde, M. (1995) Accuracy of Vehicle Probe Estimates of Link-Travel Time and Instantaneous Speed. *In Proceedings of the Annual Meeting of ITS America, 15-17 March 1995, Washington DC, United States*.

47. RENO A&E (n.d.) *Model C-1000 Series*. Available from: http://www.signalcontrol.com/products/reno/RenoAE_C_Series_Rack_Mount_LCD_Det.pdf [Accessed 15th November 2013].

48. Saunier, N. & Morency, C. (2011) Comparing Data from Mobile and Static Traffic Sensors for Travel Time Assessment. *Transportation and Development Institute Congress 2011: Integrated Transportation and Development for a Better Tomorrow. 13-16 March 2011, Chicago, Illinois, United States.* Transportation Operations and Safety Section, pp. 1178-1187

49. Sensys Networks (n.d.) *VSN240 Wireless Flush-Mount Sensor*. [Online] Available from: http://www.sensysnetworks.com/downloads/data-sheets/Datasheet-VSN240-Sensor.pdf [Accessed 15th November 2013].

50. Sreedevi, I. (2005) *ITS Decision Services and Technologies Loop Detectors*. [Online] Available from: http://www.calccit.org/itsdecision/serv and tech/Traffic Surveillance/road-based/in- road/loop summary.html [Accessed 15th November 2013].

51. Tarnoff, P.J., Bullock, D.M., Young, S.E., Wasson, J., Ganig, N. & Sturdevant, J.R. (2009) Continuing Evolution Of Travel Time Data Information Collection And Pro oylcessing. *In Transportation Research Board 88th Annual Meeting, Paper ID: 09-2030.*

52. Toppen, A. & Wunderlich, K. (2003) *Travel Time Data Collection for Measurement of Advanced Traveler Information Systems Accuracy*. Federal Highway Administration, Project No. 0900610-D1. 20 p.

53. Tayal, M.A. & Raghuwanshi, M.M. (2010) Review on Various Clustering Methods for the Image Data. *Journal of Emerging Trends in Computing and Information Sciences*, 2, pp.34-38.

54. Theodoridis, S. & Koutroumbas, K. (1999) *Pattern recognition*. Academic Press, New York.

55. TraffiCast (n.d.) *Bluetooth™ Detection for Travel Times & Road Speeds*. [Online] Available from: http://trafficcast.com/products/view/blue-toad/ [Accessed 15th November 2013]

56. Traficon (n.d.) *VIP3D.1 & VIP3D.2 Vehicle Presence & Data Detector*. The Original 170, NEMA TS-1 & TS-2 Plug-In Module, 2nd Generation. [Online] Available from: http://www.kargor.com/CL_VIP3D_USAsize_Sep08_email.pdf [Accessed 15th November 2013].

57. Tsubota, T., Bhaskar, A., Chung, E. & Billot, R. (2011) Arterial Traffic Congestion Analysis Using Bluetooth Duration Data. In Tisato, Peter, Oxlad, Lindsay, & Taylor, Michael (Eds.) *Australasian Transport Research Forum 2011*, *28-30 September 2011, Adelaide Hilton Hotel, Adelaid, SA.*

58. Turner, S.M., Eisele, W.L., Benz, R.J. & Holdene, D.J. (1998) *Travel Time Data Collection Handbook*. Federal Highway Administration, U.S. Department of Transportation and Texas Transportation Institute, Texas A&M University System, CD-ROM (FHWA-PL-98-035).

59. Washington State Office of Financial Management (2009) *Rank of Cities and Towns by April 1, 2009 Population Size*. [Online] Available from: http://www.ofm.wa.gov/pop/april1/rank2009.pdf. [Accessed 10th October 2010].

60. Wasson, J.S., Sturdevant, J.R. & Bullock, D.M. (2008) Real-Time Travel Time Estimates Using Media Access Control Address Matching. *ITE Journal*, 78(6), pp.20-23.

61. Wasson, J., Haseman, R., Bullock, D.M. (2010). Real-Time Measurement of Work Zone Travel Time Delay and Evaluation Metrics Using Bluetooth Probe Tracking. *In Proceedings 89th Annual Meeting Transportation Research Board, Washington.*

62. Wu, X., & Shi, J. (2007) Anti-Interference Performance Analysis In Bluetooth Frequency Hopping System. *Anti-counterfeiting, Security, Identification, 2007 IEEE International Workshop on, 16-18 April 2007*.

63. Xu, R. & Wunsch, D. II (2005) Survey of clustering algorithms. *IEEE Transactions on Neural Networks*, 16(3), pp.645–678.

64. Zhang, T., Ramakrishnan, R. & Livny, M. (1996) BIRCH: an Efficient Data Clustering Method for Very Large Databases. *Proceedings of the ACM SIGMOD Conference on Management of Data. Montreal, Canada*.

Appendix I

I.1 Components of Bluetooth Sensor

The Bluetooth sensors manufactured by various vendors differ in terms of design; however, the main components of the sensors are similar. The major elements of a Bluetooth sensor includes procession unit, a communication unit, GPS antenna, internal clock, power supply, cover and mounting brackets and Bluetooth radio antenna. Details of sensors components are placed in Appendix I. Figure I-1 shows the main components of Bluetooth sensors for Blip systems.

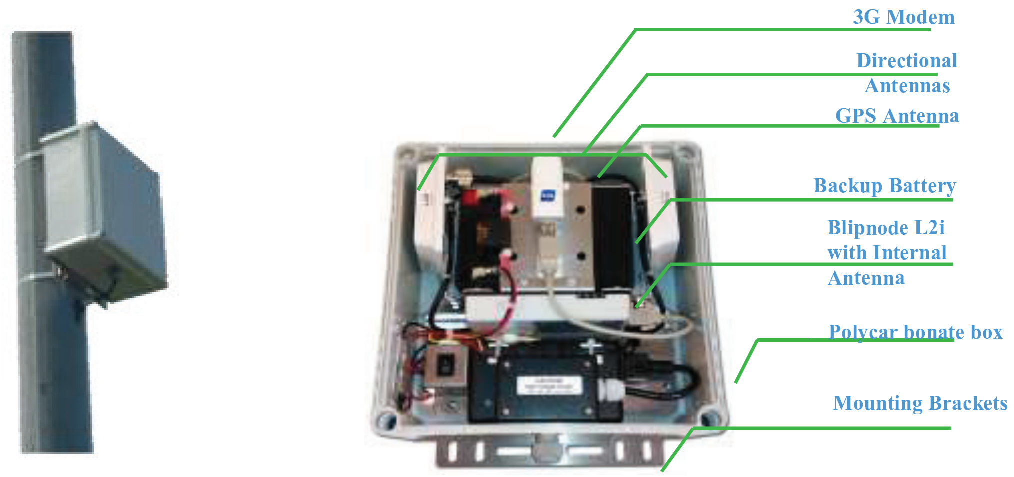

Figure I-1. BlipTrack sensor design and components

Processing Unit

The processing unit is the core part of the sensor which records the MAC addresses and timestamp the detections.

Communication Unit

The Bluetooth sensors are typically capable of Ethernet or cellular communication. The communication unit is usually a built-in 3G modem for communicating the data to the backend servers.

GPS Antenna

The use of GPS antenna is optional. The GPS sensor is used for auto positioning of the Bluetooth sensors.

Internal Clock

Internal clock is used for time stamping the MAC addresses and synchronising various Bluetooth sensors installed across the road network.

Power Supply

The Bluetooth sensors can get powered through electrical main supply, solar power or built in backup battery.

Cover and Mounting Brackets:
The sensor components are enclosed in a weatherproof enclosure. Usually there are some mounting brackets are used to fix the installation to a pole or other suitable structures.

Bluetooth Radio Antenna
The antenna is a device for transmitting and/or receiving signals – so called the eyes and ears of the communication system (RFI, 2011). Two main characteristics of antenna can be recognised as type and power of antenna. In the following sections a brief description of these aspects are provided:

- *Antenna Power*

The efficiency of an antenna is defined as the power delivered to the antenna and the power radiated or dissipated within the antenna. A high efficiency antenna has most of the power present at the antenna's input radiated away. A low efficiency antenna has most of the power absorbed as losses within the antenna, or reflected away due to impedance mismatch. In this context, the losses associated within an antenna are typically associated to the conduction losses (due to finite conductivity of the antenna) and dielectric losses (due to conduction within a dielectric which may be present within an antenna) (Antenna Theory, 2011). The antenna efficiency (or radiation efficiency) can be written as the ratio of the radiated power to the input power of the antenna:

$$\varepsilon_R = \frac{P_{Radiated}}{P_{Input}} \qquad \textbf{Equation I-1}$$

Efficiency is ultimately a ratio, giving a number between 0 and 1. Efficiency is very often quoted in terms of a percentage; for example, an efficiency of 0.5 is the same as 50%. Antenna efficiency is also frequently quoted in decibels (dB); an efficiency of 0.1 is 10% or (-10 dB), and an efficiency of 0.5 or 50% is -3 dB. Mobile phone antennas, or WiFi antennas in consumer electronics products, typically have efficiencies from 20%-70% (-7 to -1.5 dB). The losses are often due to the electronics and materials that surround the antennae; these tend to absorb some of the radiated power (converting the energy to heat), which lowers the efficiency of the antenna (Antenna Theory, 2011).
The term Antenna Gain describes how much power is transmitted in the direction of peak radiation to that of an isotropic source. Antenna Gain is sometimes discussed as a function of angle, but when a single number is quoted the gain is the 'peak gain' over all directions (Antenna Theory, 2011). Antenna Gain (G) can be related to directivity (D) by:

$$G = \varepsilon_R D \qquad \textbf{Equation I-2}$$

Mobile antennas should radiate in a symmetrical pattern 360° around the antenna. As gain is increased, the radiation gets compressed into a thinner pattern and reaches out further to the sides. The more gain an antenna has the thinner the pattern becomes and the further the signal can travel or reach. This has been shown in Figure I-2, for an antenna mounted on a roof car (RFI, 2011).

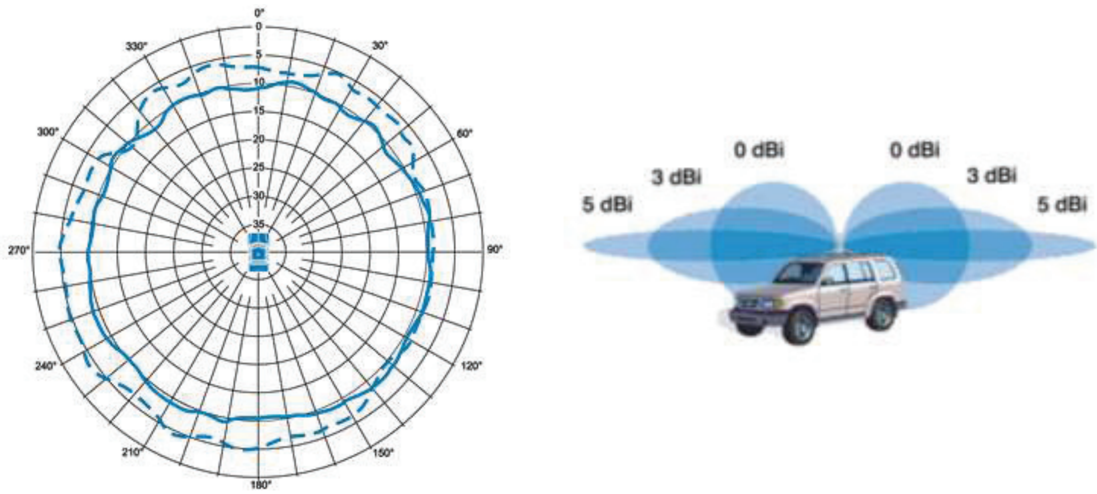

Figure I-2. Antenna gain and radiation pattern (Source: RFI, 2011)

- *Antenna Type*

Bluetooth antenna could be external or internal. Regardless of the antenna design and configuration, in current design of the Bluetooth sensors by various manufacturers, two main types of antenna including directional and omnidirectional or the combination of both (i.e. directional and omnidirectional) have been used. The difference between directional and omnidirectional and their coverage area have been discussed in relevant literature. In the following sections it is tried to simply explain the basic concepts and the coverage area of the directional vs. omnidirectional antenna.

a. Directional Antenna

Directional antennas as the name implies refers to signal coverage in a specified direction (Simple WiFi, 2011). The 2D and 3D radiation patterns of a directional antenna are shown in Figure I-3 and Figure I-4 respectively.

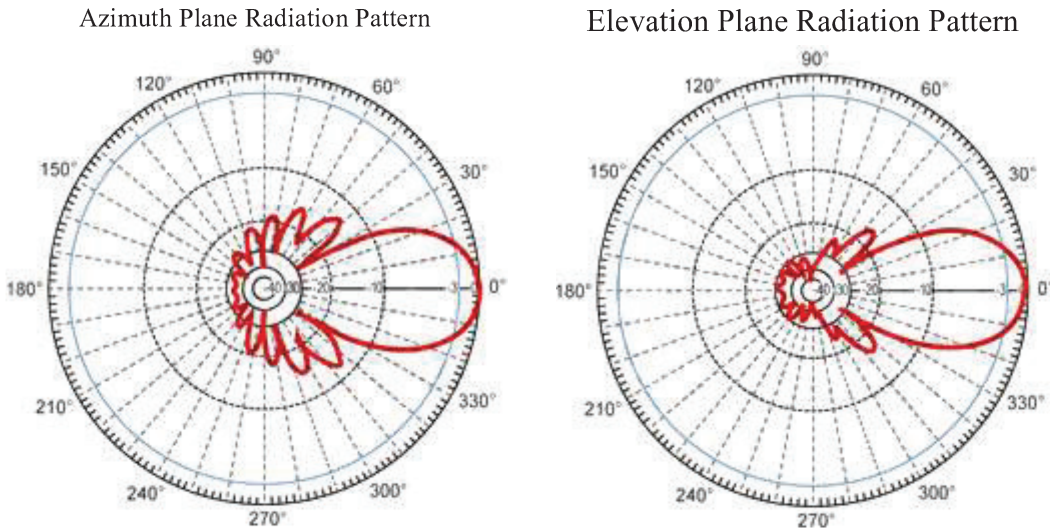

Figure I-3. The directional antenna radiation pattern (Source: CA WORLD WIFI, INC 2013)

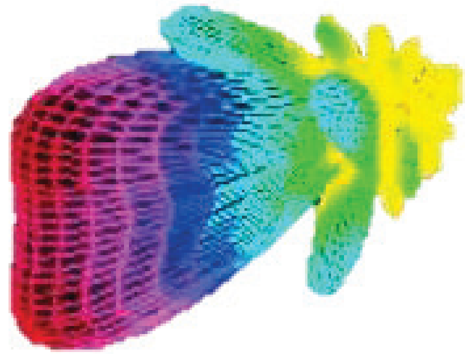

Figure I-4. The mesh presents a 3D view of the directional antennas radiation pattern (source: Marlon K. Schafer, 2001)

b. Omnidirectional Antenna

An omnidirectional antenna is one which radiates power uniformly in all directions in one plane (Simple WiFi, 2011). The omnidirectional antenna radiates or receives equally well in all directions. It is also called "non-directional" as it does not favour any particular direction. The 2D and 3D radiation patterns of a directional antenna are shown in Figure I-5and Figure I-6, respectively.

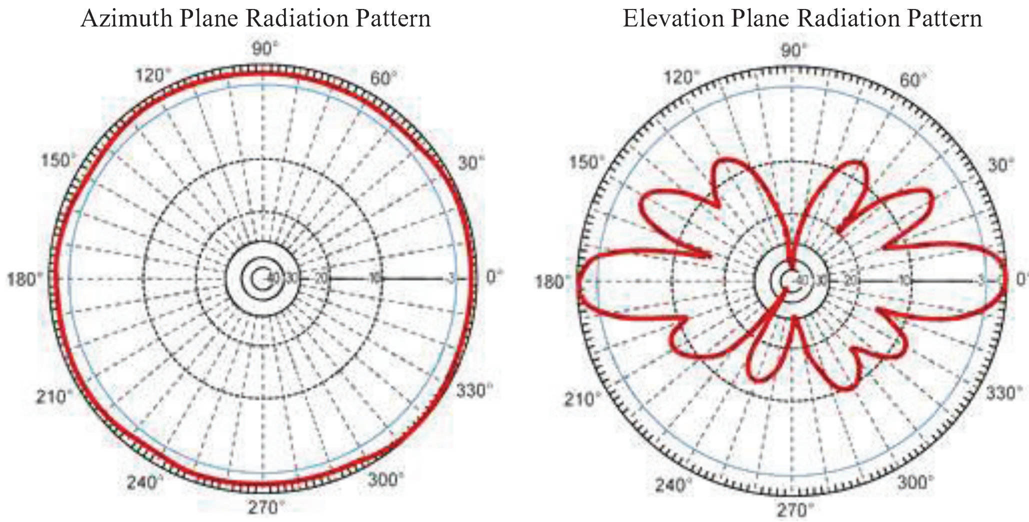

Figure I-5. The omnidirectional antenna radiation pattern (Source: CA WORLD WIFI, INC 2013)

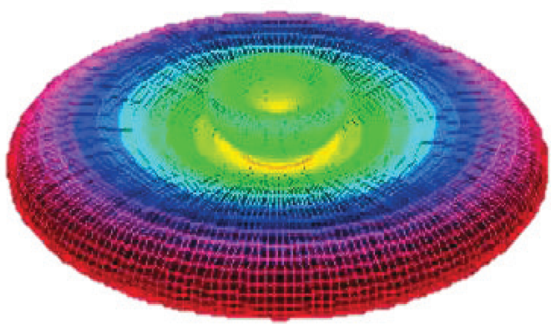

Figure I-6. The mesh presents a 3D view of the omnidirectional antennas radiation pattern (source: Marlon K. Schafer, 2001)

I.2 Technical Deployment, Installation and Maintenance

Detection rate of Bluetooth sensors is highly dependent to the shape and size of its detection zone and the time span the device is within the detection zone. This outlines the importance of the location of the installed sensor, the height and the mount design. These factors affect Bluetooth device detection rate and hence travel time accuracy. These engineering aspects should be given due consideration in order to achieve reliable travel time estimates using Bluetooth sensors. This section focuses on sensor placement, installation and maintenance of Bluetooth sensors.

Sensor Placement Practices

In general, Bluetooth sensor placement, as with many other technologies in transportation systems mainly depends on the access to power. In many cases, this factor plays a significant role on the sensor placement design, as usually there are limited locations in the road network which could provide access to power. However, it should be noted that this problem is less significant if the Bluetooth sensor is powered by solar panels or other types of batteries. Essentially two different locations can be considered for sensor placement; at intersections and at mid-link locations. There are advantages and disadvantages associated with each:

- *At Intersections*

Existence of power sources such as traffic signals and street lights and communication infrastructures would significantly facilitate the installation and reduce the associated costs. However, due to the traffic interactions and various turning movements at the intersection, the quality of data might reduce. The intersection placement usually provide a node-to-node travel time information, however, it cannot specify the turning movements. It is also necessary to consider the impact of free movement (i.e. open right turn), as this could affect the accuracy of travel time. This has been shown in Figure I-7. Intersection placement of sensors and interacting movements. This Figure shows how various movements interact with each other in the Bluetooth sensor detection zone (i.e. shown by dashed circle) at the intersection. Compare to the through traffic, the open right turns is not influenced by delay associated to the cycle length. However, at the intersection placement, these movements are not distinguishable and could influence the accuracy of travel time. This placement layout has been used in the city of Aalborg for collecting network wide real time travel time and traffic information, see Figure I-8. Intersection Sensor Placement, Aalborg City, DenmarkFigure I-8.

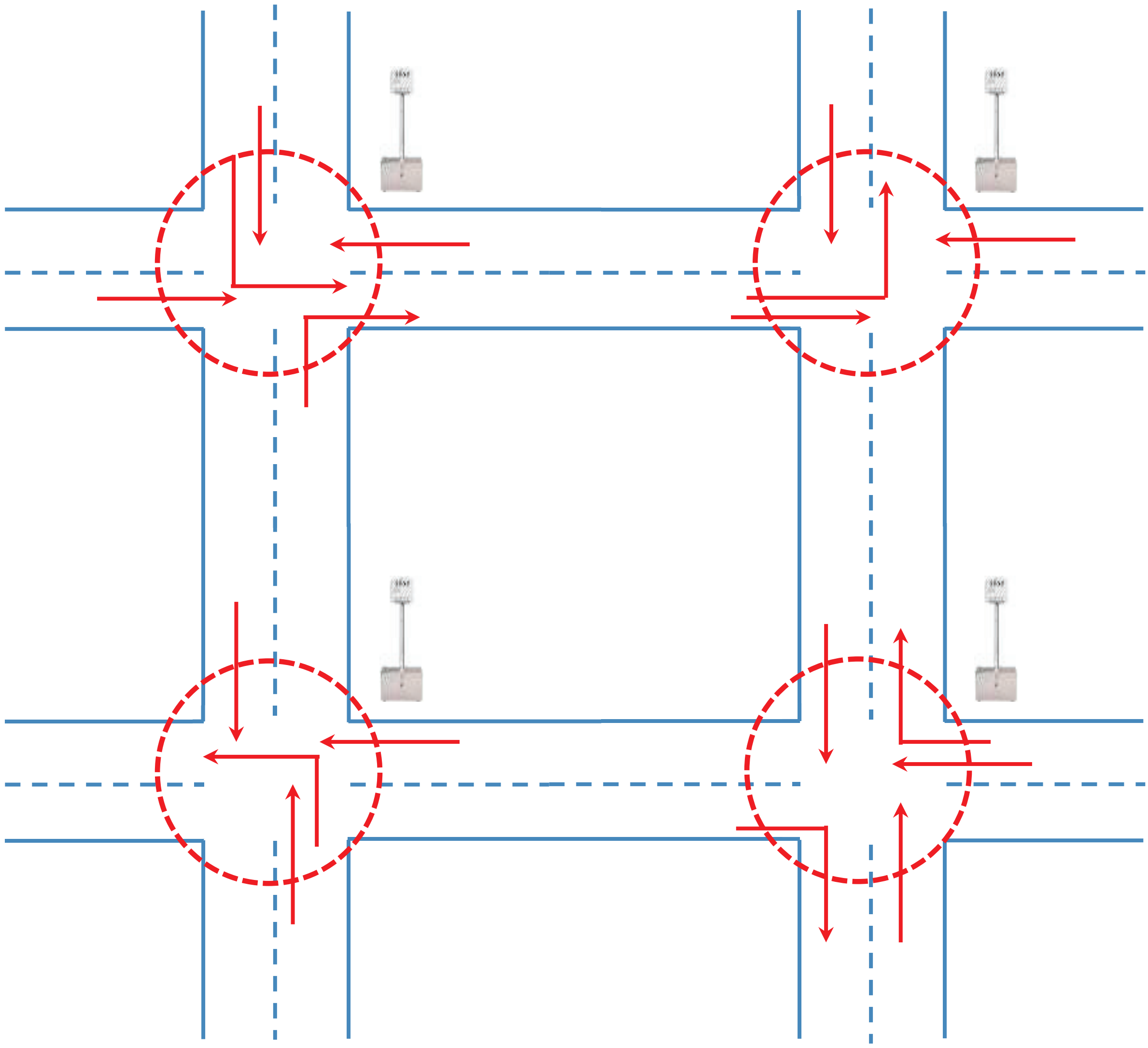

Figure I-7. Intersection placement of sensors and interacting movements

Figure I-7 represents the interacting movements at the intersections. These movements are presented by red arrows. In city of Aalborg due to the predetermined conditions for installing the Bluetooth sensors along with the ANPR systems, intersection placement has been used. Figure I-8 represents the location of Bluetooth sensors installed in Aalborg area. Bluetooth sensors are presented by numbers 1 or 2.

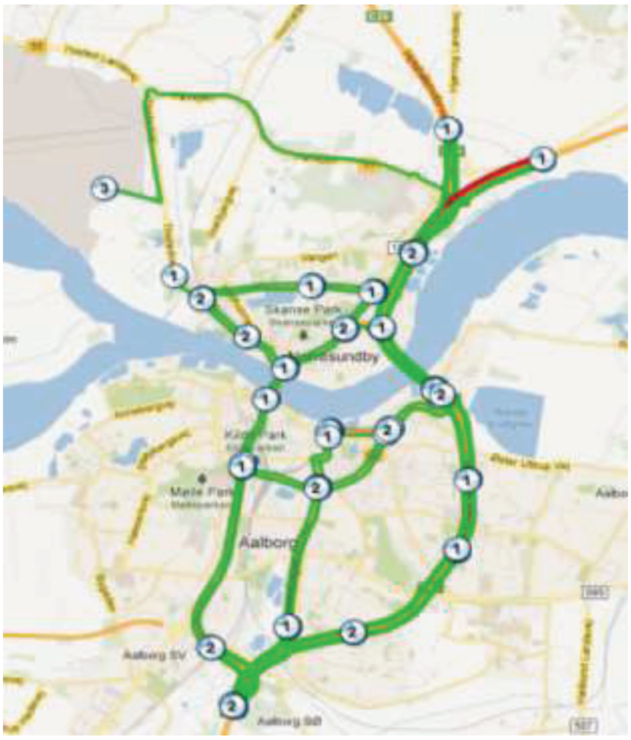

Figure I-8. Intersection sensor placement, Aalborg city, Denmark

At Mid-Link Locations

Limited access to the power sources and communication infrastructure might increase the costs of implementation. However, equipping the sensors with solar power and cellular communications can reduce the costs. Since there are fewer interactions between vehicles with each other and also there are fewer control infrastructures (i.e. Traffic lights) the quality of the data could be higher. Moreover, mid-link placement would provide more information about turning movements. This has been shown in Figure I-9. Compared to intersection placement at mid-link placement, turning movements are not interacting with through traffic. This could reduce the impact of interacting traffic and cycle length on the accuracy of travel time. This placement layout has been used in the city of Århus for collecting network wide real time travel time and traffic information, see Figure I-10.

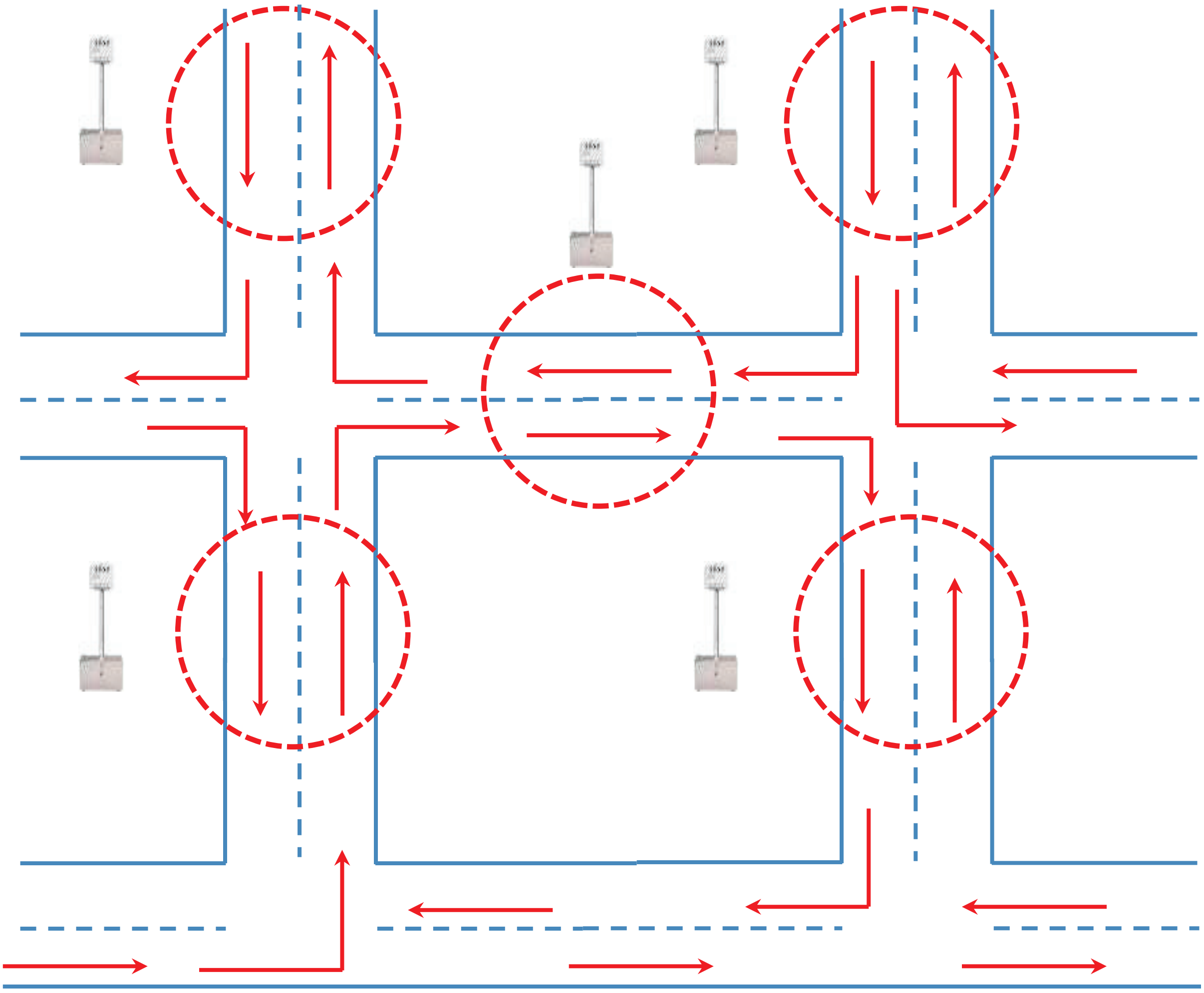

Figure I-9. Mid-link sensor placement

Figure I-9 represents how by mid-link installation it is possible to reduce the interacting movements. Moreover, it provides the information of right turning and left turning movements. These movements are presented by red arrows. In city of Århus mid-link placement has been used. Figure I-8 represents the location of Bluetooth sensors installed in Århus area. Bluetooth sensors are presented by numbers 1 or 2.

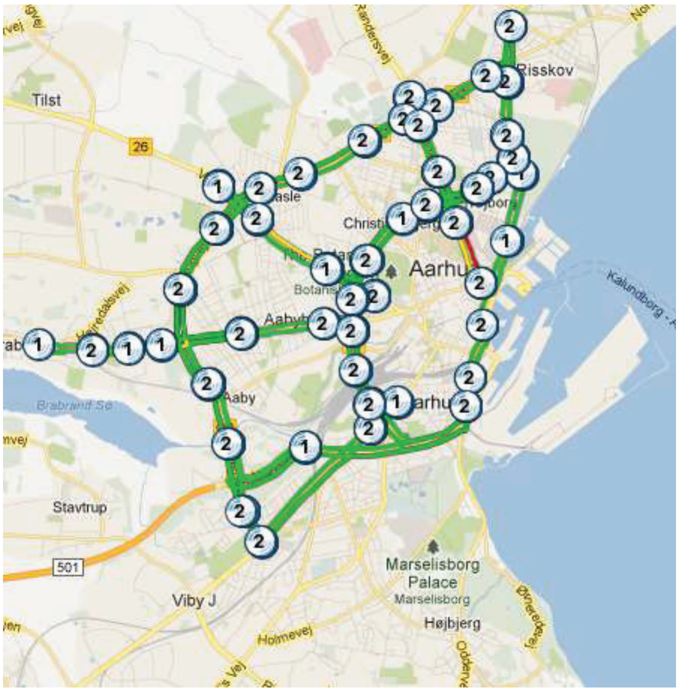

Figure I-10. Mid-Link sensor placement, Aarhus city, Denmark.

Accuracy of travel time for intersection and mid-link (i.e. mid-link) sensor locations were tested by Day et al. (2012). It is concluded that midblock detector locations are preferable as they will more accurately capture increases in travel time due to queuing at intersections. However, since power and communication facilities are not usually available at midblock establishing permanent midblock locations is challenging. Therefore, intersection locations may be used when a midblock sensor is infeasible. It is also recognised that intersection-located sensors will capture delay accumulated at any intersections in between the endpoints of the route, but will not capture delay occurring at the endpoints. At intersection placement there is higher uncertainty regarding travel time for through vehicles compared to mid-link placement.

Sensor Installation Height

The installation height of Bluetooth transceiver (or the vertical position of antenna) is another influencing factor on the Bluetooth MAC address detection rate, which needs to be considered in the mount design. The influence of height of the transceiver on the detection rate could be associated to:

1. Reducing the potential of blockage of Bluetooth transceiver by passing vehicles
2. Increasing the size of detection zone

Figure I-11 represents how the overheight vehicles could block the Bluetooth transceiver. Increasing the height of Bluetooth sensor, could potentially reduce the impact of blocking the signal by overheight vehicle.

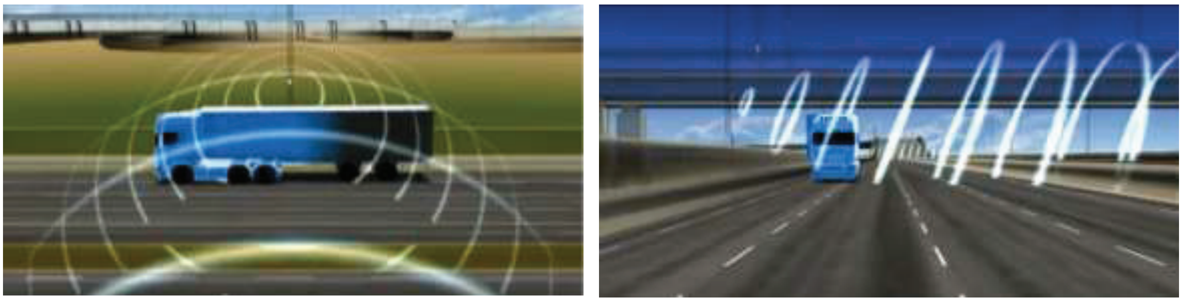

Figure I-11. The vertical position of Bluetooth transceiver and blockage by overheight vehicles

FigureI-12 shows the influence of the height of transceiver on increasing the size of detection zone considering the same angle.

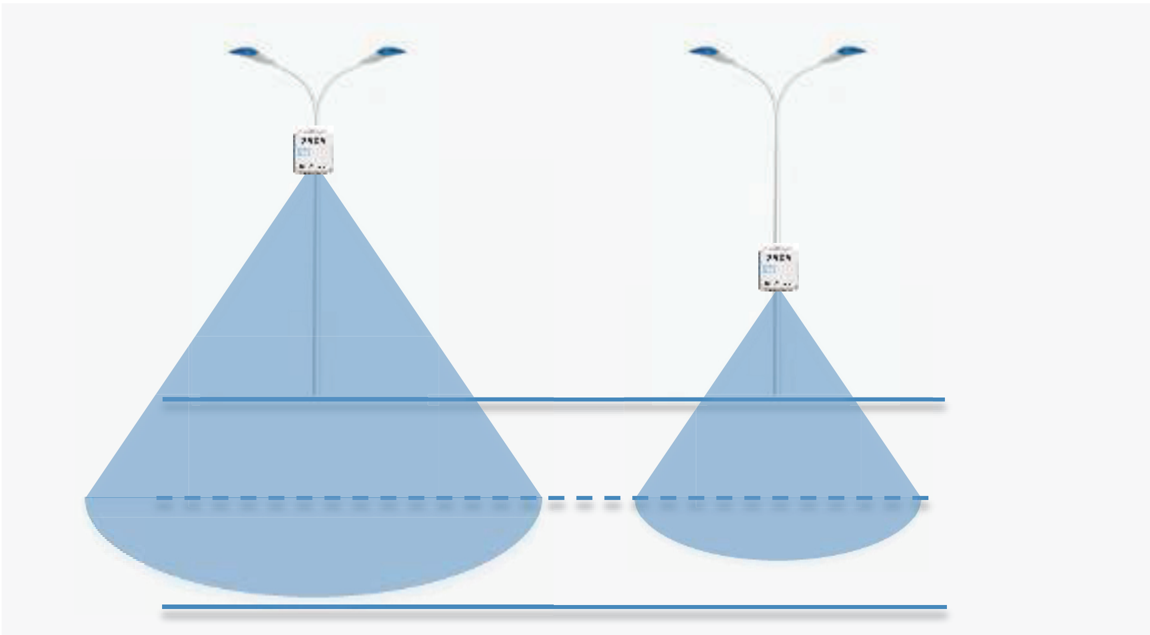

FigureI-12. The vertical position of the Bluetooth transceiver and size of detection zone

The impact of the height of antenna on detection rate has also been investigated by Day et al. (2012). Temporary sensors with different transceiver antenna heights (0 ft, 2.5 ft, 5 ft, 7.5 ft, and 10 ft) were tested in the field to determine which height would produce the largest sample size. The sensors were stationed at various positions along the southbound direction on I-65 in the U.S. along a segment with no intermediate entrances or exits. The results of the study are shown in Figure I-13. This Figure shows the total number of detected vehicle IDs (MAC addresses) for each antenna height, broken down by whether these vehicles were known to be traveling northbound or southbound (by matching the vehicle ID at another sensor), or whether the direction was unknown (i.e., no match as found). Notably, the sensor that lacked an antenna (i.e., the ‘‘0 ft’’ antenna) produced the least counts. The study concluded that a height of 7.5 ft (2.30 meters) was best for roadside location because it detected a high number of vehicle IDs, and the far side lanes were not substantially underrepresented in the data.

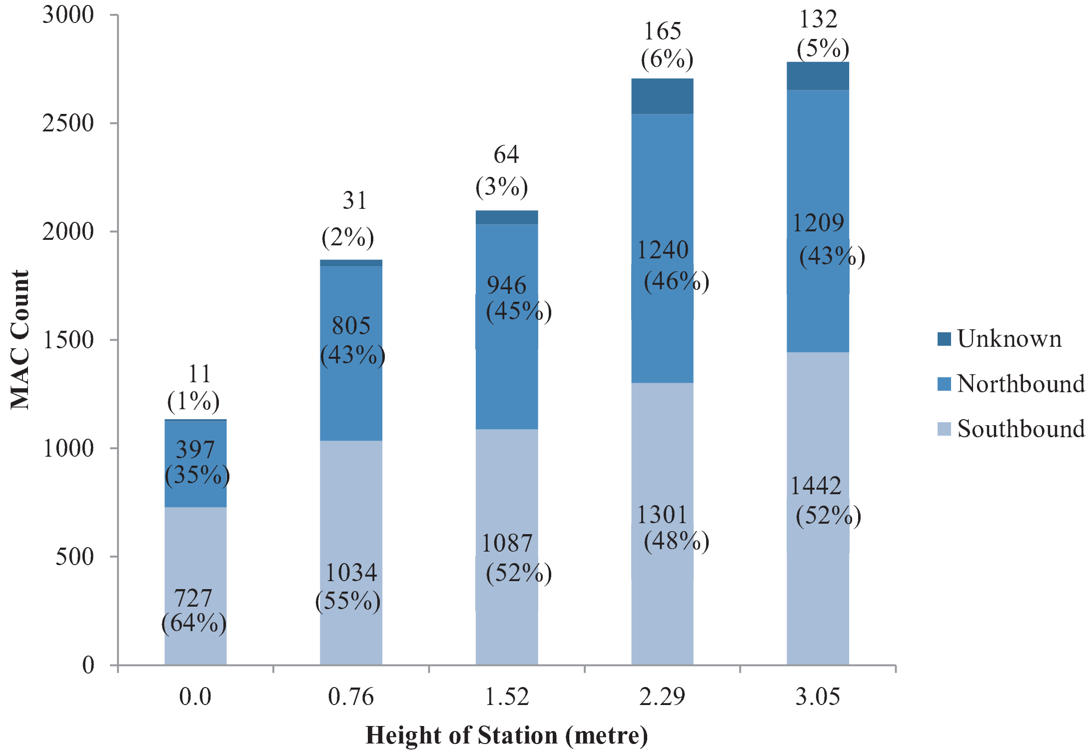

Figure I-13. Traceable MAC address counts by antenna height and direction (Brenen et al., 2010)

In summary, for the arterial roads the mid-link placement is preferable. In situations where the mid-link placement is not feasible, an intersection placement can be used for permanent stations. As can be seen in Figure I-13, for vertical position of the Bluetooth transceiver the antenna height of 2.30-2.50 is highly recommended as it maximises the sample rate.

Appendix II

II.1 Profile Construction

Arithmetic Mean

The 15-minute and 30-minute Bluetooth based travel time profiles are obtained by aggregating the Bluetooth based estimated travel time using the arithmetic mean (i.e. average) over the specified time interval.

$$AriMin\text{–}BT_{(I)} = \frac{1}{n}\sum_{i=0}^{n} Min\text{–}BT_i \qquad \textbf{Equation II-1}$$

$$AriMax\text{–}BT_{(I)} = \frac{1}{n}\sum_{i=0}^{n} Max\text{–}BT_i \qquad \textbf{Equation II-2}$$

$$AriAvg\text{–}BT_{(I)} = \frac{1}{n}\sum_{i=0}^{n} Avg\text{–}BT_i \qquad \textbf{Equation II-3}$$

$$AriMed\text{–}BT_{(I)} = \frac{1}{n}\sum_{i=0}^{n} Med\text{–}BT_i \qquad \textbf{Equation II-4}$$

Where:
$AriMin\text{–}BT_{(I)}$: Arithmetic mean of $Min\text{–}BT$ (refer to equation 1) for the Ith interval
$AriAvg\text{–}BT_{(I)}$: Arithmetic mean of $Max\text{–}BT$ (refer to equation 2) for the Ith interval
$AriAvg\text{–}BT_{(I)}$: Arithmetic mean of $Avg\text{–}BT$ (refer to equation 3) for the Ith interval
$AriMed\text{–}BT_{(I)}$: Arithmetic mean of $Med\text{–}BT$ (refer to equation 4) for the Ith interval
n*:* number of observations in Ith interval

Geometric Mean

The 15-minute and 30-minute Bluetooth based travel time profiles are obtained by aggregating the Bluetooth based estimated travel time using the geometric mean over the specified time interval.

$$GeoMin\text{–}BT_{(I)} = \sqrt[n]{Min\text{–}BT_1 * Min\text{–}BT_2 \dots Min\text{–}BT_n} \qquad \textbf{Equation II-5}$$

$$GeoMax\text{–}BT_{(I)} = \sqrt[n]{Max\text{–}BT_1 * Max\text{–}BT_2 \dots Max\text{–}BT_n} \qquad \textbf{Equation II-6}$$

$$GeoAvg\text{–}BT_{(I)} = \sqrt[n]{Avg\text{–}BT_1 * Avg\text{–}BT_2 \dots Avg\text{–}BT_n} \qquad \textbf{Equation II-7}$$

$$GeoMed\text{–}BT_{(I)} = \sqrt[n]{Med\text{–}BT_1 * Med\text{–}BT_2 \dots Med\text{–}BT_n} \qquad \textbf{Equation II-8}$$

Where:
$GeoMin\text{–}BT_{(I)}$: Geometric mean of $Min\text{–}BT$ (refer to equation 1) for the Ith interval
$GeoAvg\text{–}BT_{(I)}$: Geometric mean of $Max\text{–}BT$ (refer to equation 2) for the Ith interval

$GeoAvg\text{–}BT_{(I)}$: Geometric mean of $Avg\text{–}BT$ (refer to equation 3) for the Ith interval
$GeoMed\text{–}BT_{(I)}$: Geometric mean of $Med\text{–}BT$ (refer to equation 4) for the Ith interval
n: number of observations in Ith interval

Harmonic Mean

The 15-minute and 30-minute Bluetooth based travel time profiles are obtained by aggregating the Bluetooth based estimated travel time using the harmonic mean over the specified time interval.

$$HarMin\text{–}BT_{(I)} = \left(\frac{1}{n} \cdot \sum_{i=0}^{n} Min\text{–}BT_i^{\,-1}\right)^{-1}$$ **Equation II-9**

$$HarMax\text{–}BT_{(I)} = \left(\frac{1}{n} \cdot \sum_{i=0}^{n} Max\text{–}BT_i^{\,-1}\right)^{-1}$$ **Equation II-10**

$$HarAvg\text{–}BT_{(I)} = \left(\frac{1}{n} \cdot \sum_{i=0}^{n} Avg\text{–}BT_i^{\,-1}\right)^{-1}$$ **Equation II-11**

$$HarMed\text{–}BT_{(I)} = \left(\frac{1}{n} \cdot \sum_{i=0}^{n} Med\text{–}BT_i^{\,-1}\right)^{-1}$$ **Equation II-12**

Where:
$HarMin\text{–}BT_{(I)}$: Harmonic mean of $Min\text{–}BT$ (refer to equation 1) for the Ith interval
$HarAvg\text{–}BT_{(I)}$: Harmonic mean of $Max\text{–}BT$ (refer to equation 2) for the Ith interval
$HarAvg\text{–}BT_{(I)}$: Harmonic mean of $Avg\text{–}BT$ (refer to equation 3) for the Ith interval
$HarMed\text{–}BT_{(I)}$: Harmonic mean of $Med\text{–}BT$ (refer to equation 4) for the Ith interval
n: number of observations in Ith interval

II.2 Accuracy Analysis

Time Plot of GPS-V1 vs. Bluetooth Travel Time Estimates for App.1 and App.2 for North-South Direction are presented bellow.

a: Comparison of Min-BT, Max-BT, Avg-BT and Med-BT for three aggregation technique

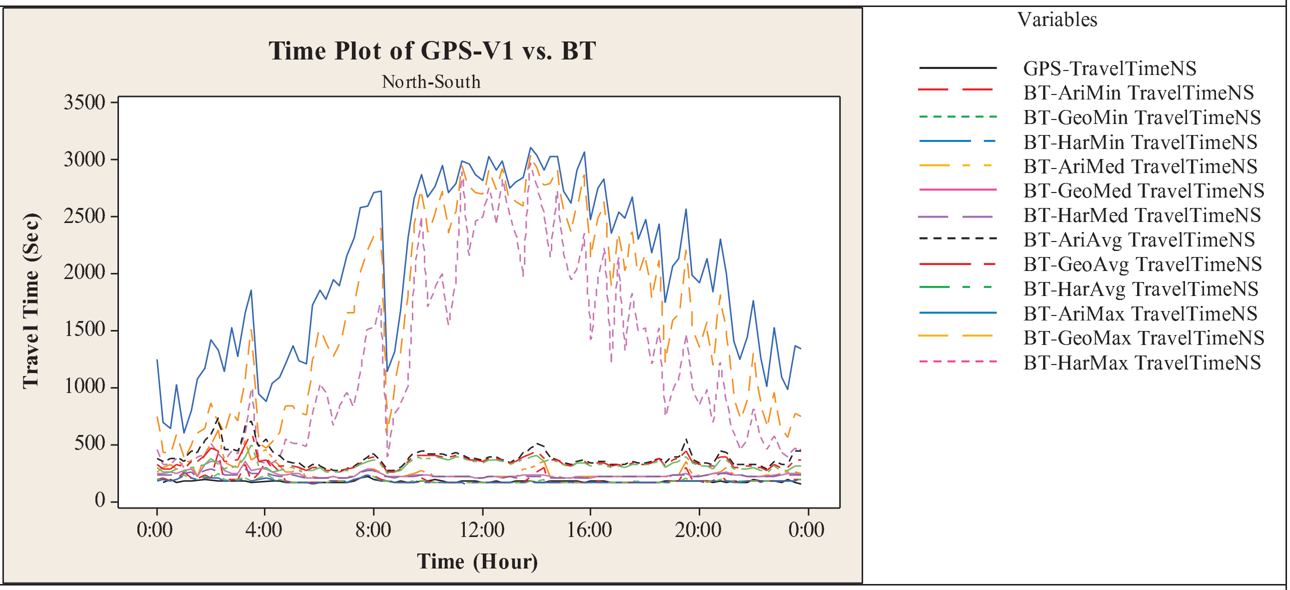

b: Comparison of Min-BT, and Med-BT for three aggregation technique

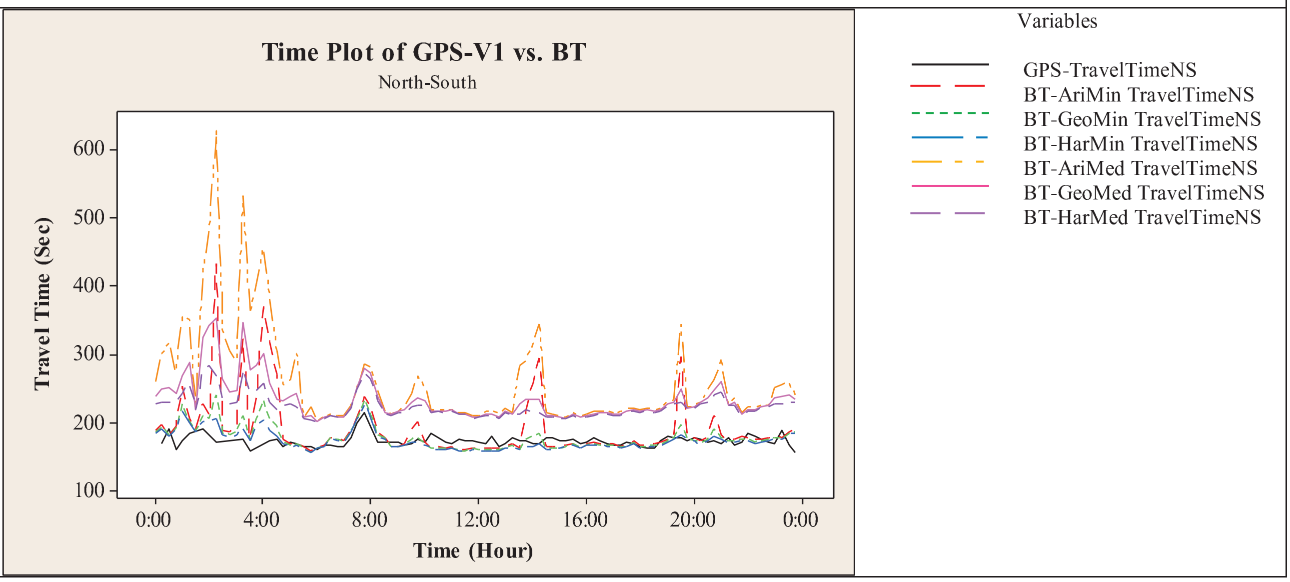

Figure II-1. Time plot of GPS-V1 vs. BT travel time estimates for App.1 for North-South direction

a: Comparison of Min-BT, Max-BT, Avg-BT and Med-BT for three aggregation technique

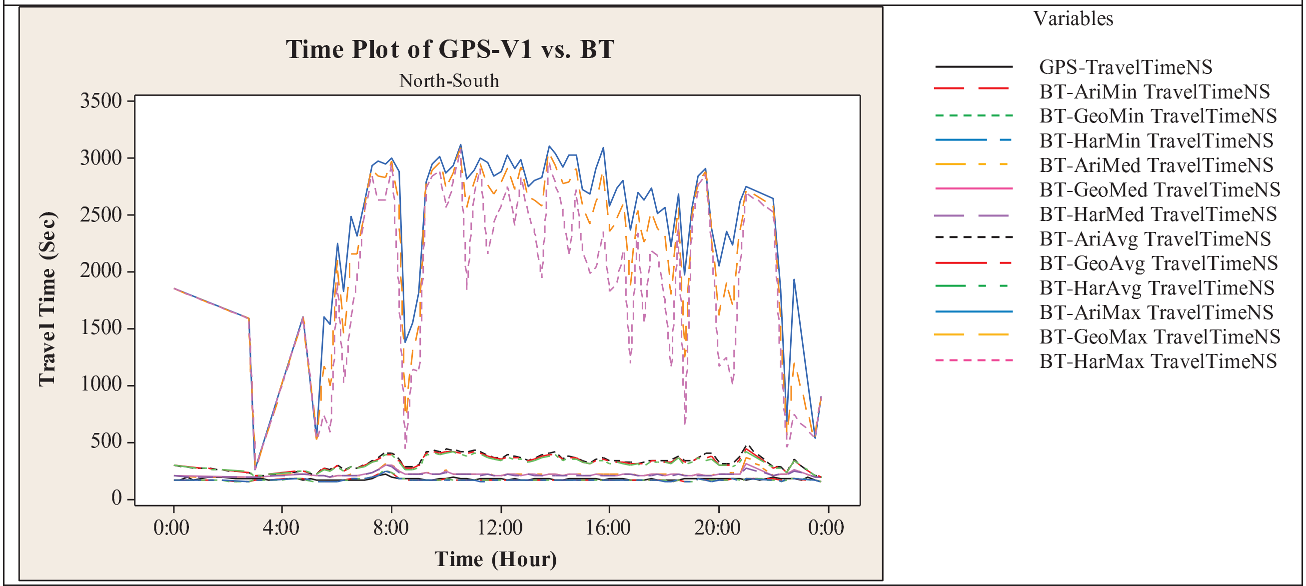

b: Comparison of Min-BT, and Med-BT for three aggregation technique

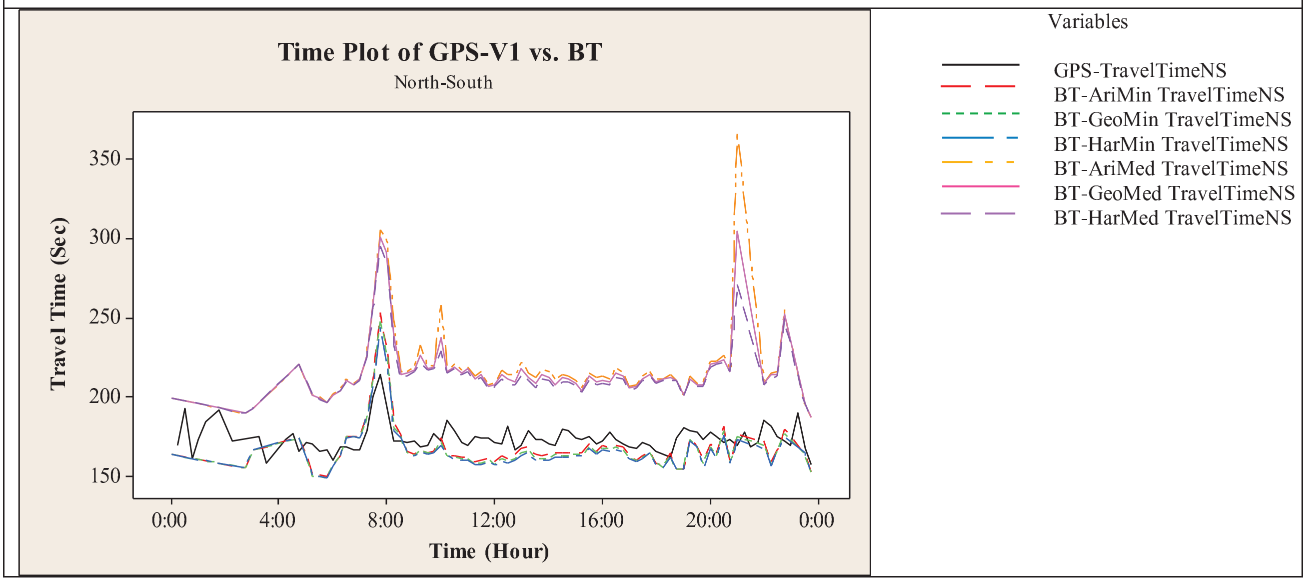

Figure II-2. Time plot of GPS-V1 vs. BT travel time estimates for App.2 for North-South direction

a: Comparison of Min-BT, Max-BT, Avg-BT and Med-BT for three aggregation technique

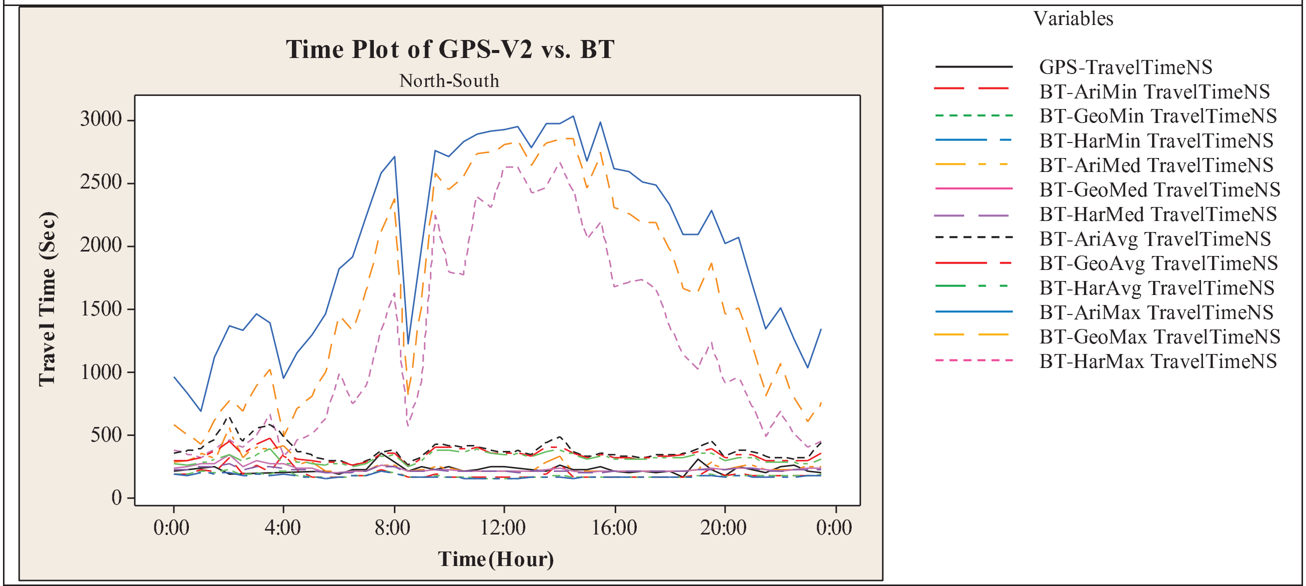

b: Comparison of Min-BT, and Med-BT for three aggregation technique

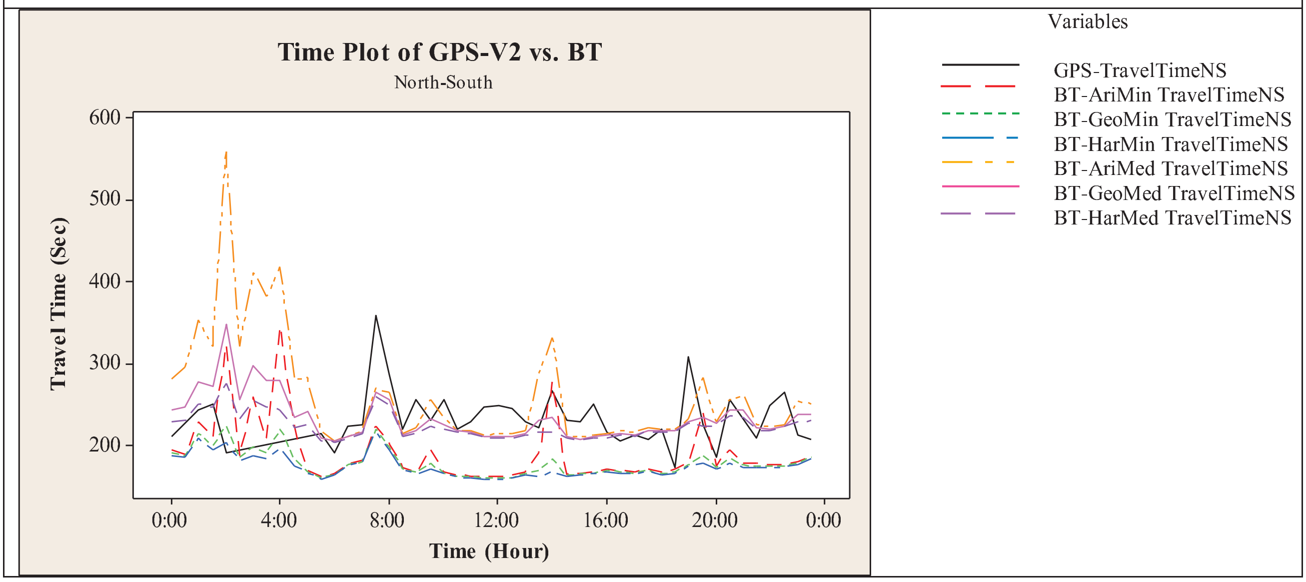

Figure II-3. Time plot of GPS-V2 vs. BT travel time estimates for App.1 for North-South direction

a: Comparison of Min-BT, Max-BT, Avg-BT and Med-BT for three aggregation technique

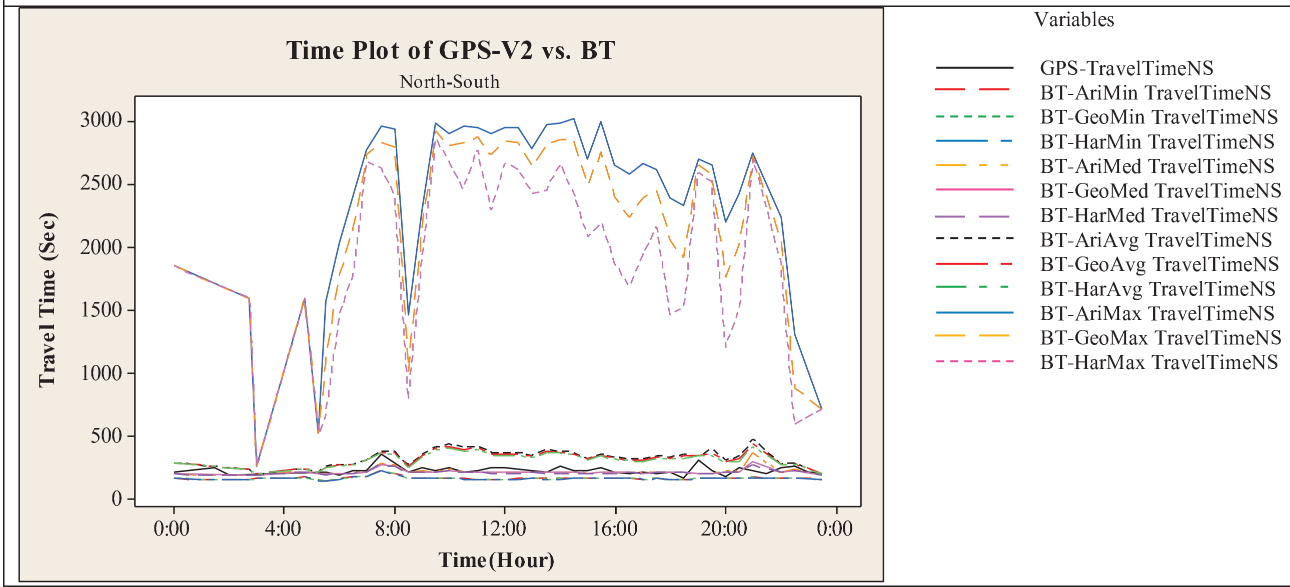

b: Comparison of Min-BT, and Med-BT for three aggregation technique

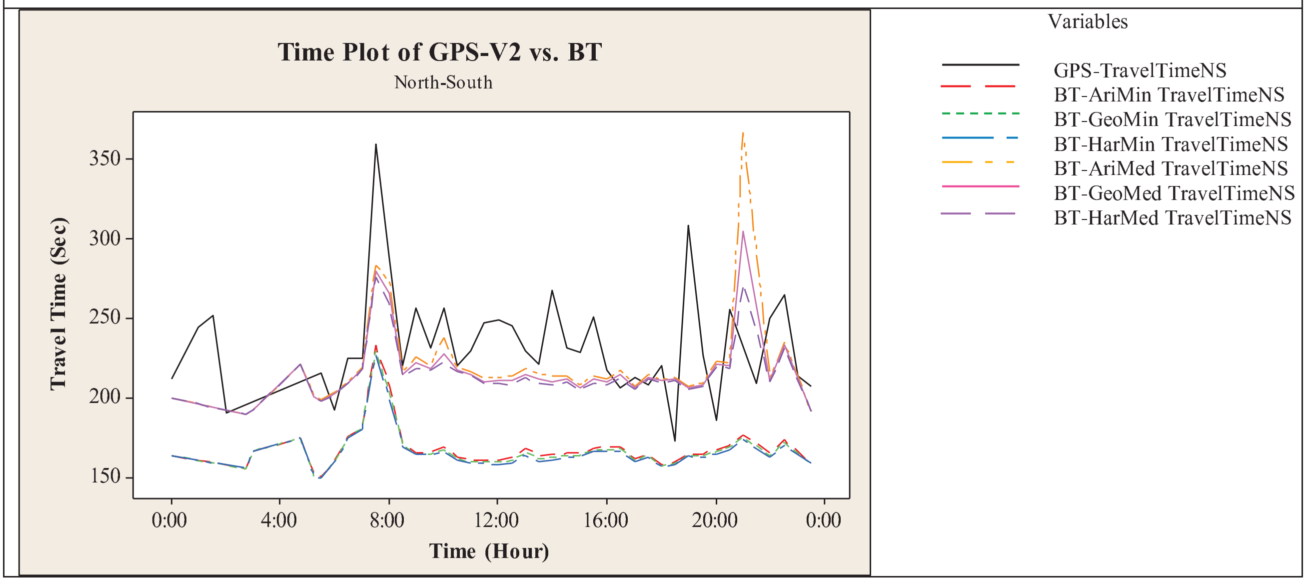

Figure II-4. Time plot of GPS-V2 vs. BT travel time estimates for App.2 for North-South direction

II.3 Sample Size Sensitivity Analyses

Results of the sample size sensitivity analyses for North-South direction are presented bellow.

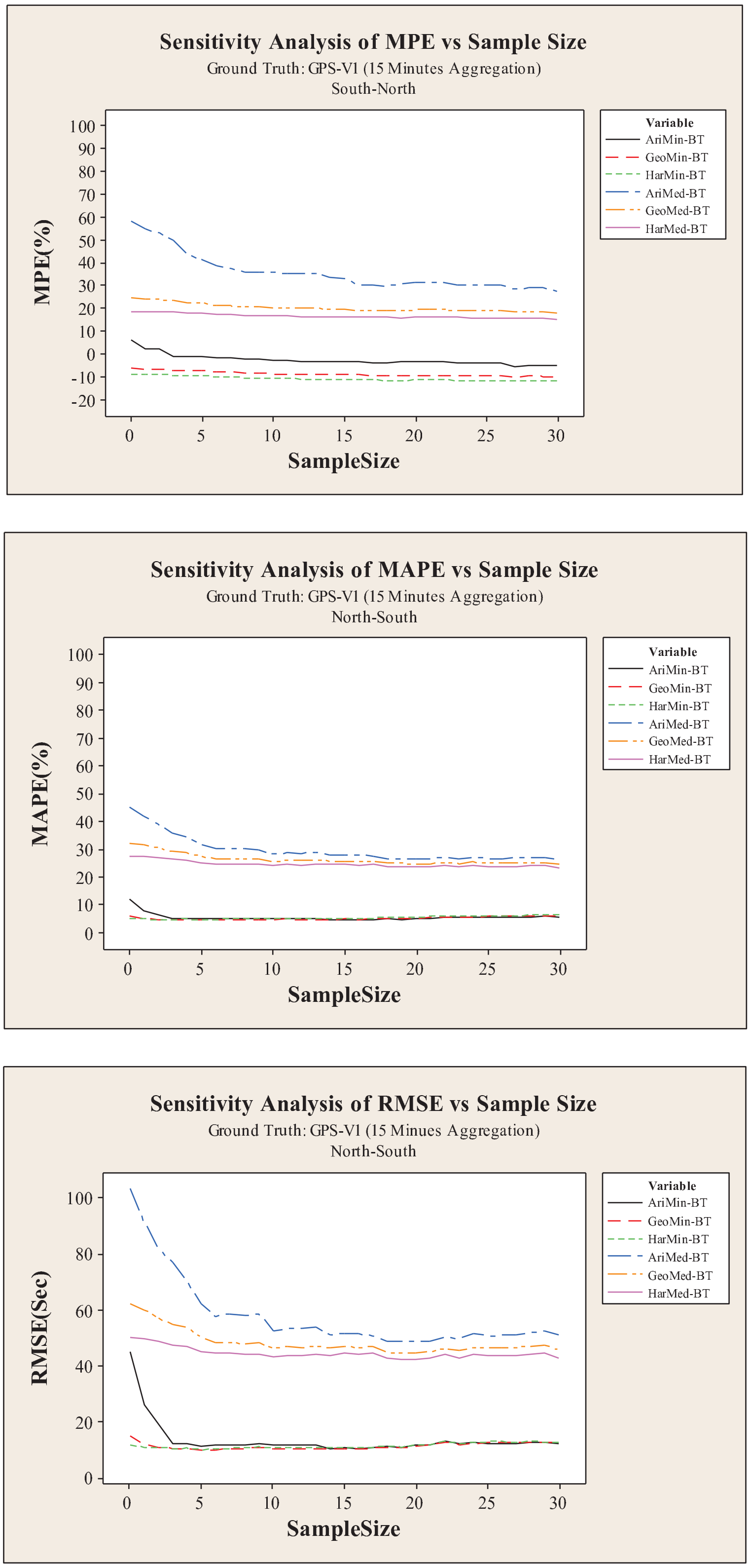

Figure II-5. Sensitivity analysis of MPE, MAPE, and RMSE vs. sample size for GPS-V1 for North- South direction

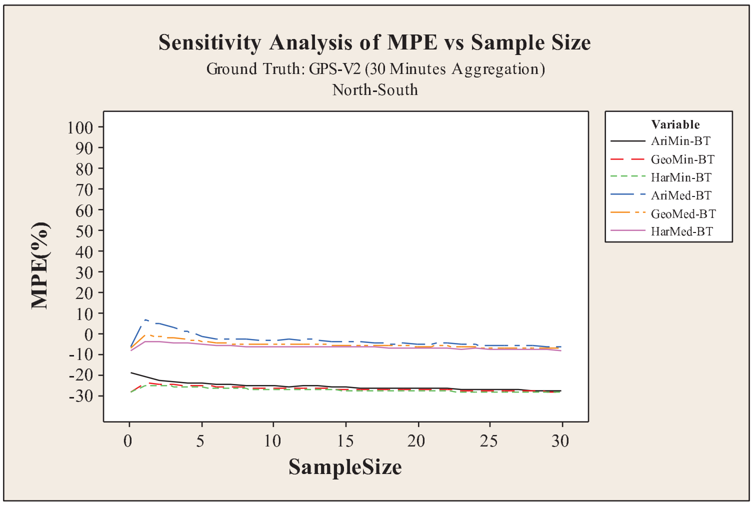

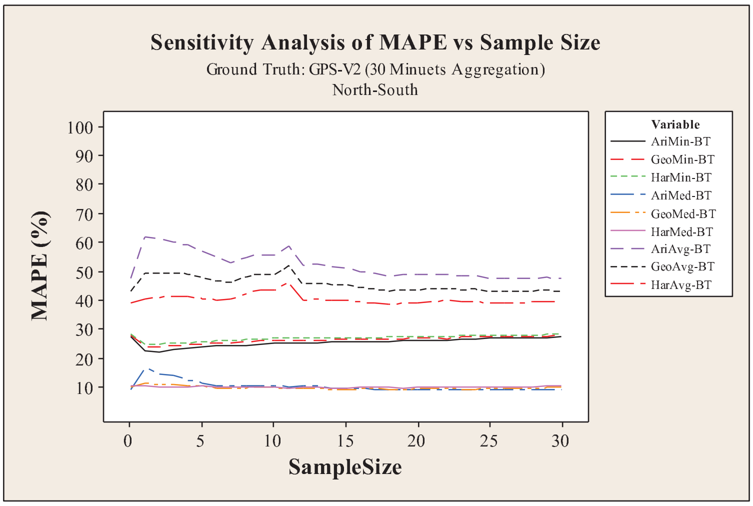

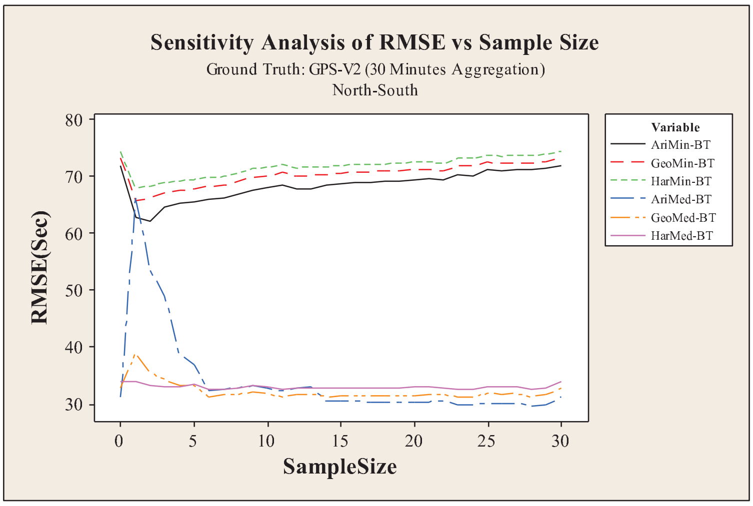

Figure II-6. Sensitivity analysis of MPE, MAPE, and RMSE vs. sample size for GPS-V2 for North- South direction

APPENDIX III

III.1 Volume and Speed Estimation Technologies

There are multiple techniques that make use of point sensor data to create travel time estimates. In this study area, two types of inductive loop detectors are used (providing advance loop volumes). Additionally, a VDPU system from Traficon (i.e. Traficon- VIP3D.2) is used which emulates traditional double or single loop detectors. Their locations are shown in Figure III-1.

Inductive Loop Detectors

The operating principles and design factors for the two types of inductive loop detectors namely EDI Oracle 2 and Reno A&E: 1100SS used in this study are explained in next sections.

- *EDI Oracle 2 Series Inductive Loop Detectors*

The EDI Oracle2 is an inductive loop detector from Eberle Design Inc (EDI). The ORACLE 2E (2EC) Enhanced Loop Monitor™ series is a full featured two channel inductive loop vehicle detector. The ORACLE "ENHANCED" detectors not only indicate vehicle presence, but also incorporate a complete built-in loop analyzer for optimum detector set-up and loop diagnostic purposes. Each channel incorporates a loop inductance meter which assists in determining optimum sensitivity setting by displaying the magnitude of change in inductance caused by traffic moving over the roadway loop (Eberle Design, Inc. Product Overview, 2013).

Figure III-1. EDI Oracle 2E series inductive loop detector

The system architecture used to collect and convey ILD data to the WSDOT is shown in Figure III-2. Loop detector cards such as the EDI Oracle 2E are connected to loop coils embedded in the roadway. These detector cards then process the inductance readings read form the loop coils to determine whether a vehicle is present or not. The signal control cabinet's controller polls the loop detector cards to determine whether a given loop is currently occupied many times each second. At regular intervals, 20 seconds for the WSDOT, the controller reports the number of vehicles detected and the number of scanning intervals during which the ILD was occupied. This information is then carried along the corridor's communications backbone to the WSDOT network where data can be processed, aggregated and stored in a database. Note that this loop detector architecture that applies to ILDs in general.

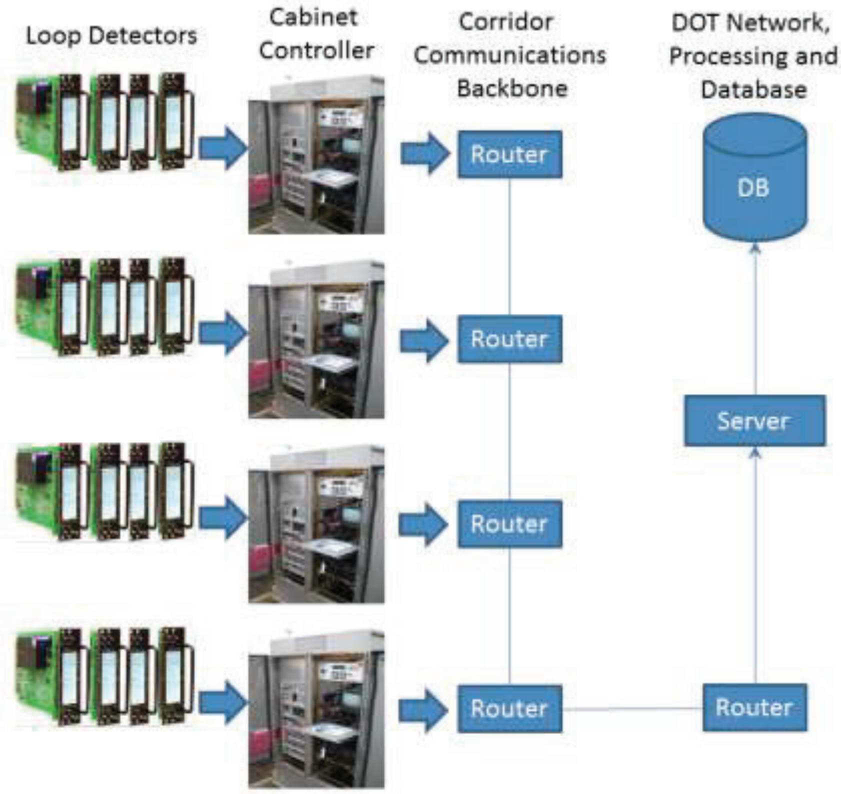

Figure III-2. Loop detector system architecture

- *Reno A&E 1100 Series Inductive Loop Detectors*

The C-1100-ss is an ILD from standard model C by Reno A&E. The Reno A&E model C-1100 series is a scanning detector. The C-1100 series is a two channel, loop detector with individual channel detect and loop fail indications provided via two high intensity red light-emitting-diode (LED)s and an easy to read Liquid-crystal display (LCD) screen. The C-1100-ss offers advanced features providing built-in diagnostic capabilities all of which are viewable by means of the LCD screen. These include: 1.) real-time loop frequency, 2.) loop inductance and -ΔL/L% (*L* = Inductance, henrys), 3.) a bar-graph indication of relative inductance change (which assist in proper selection of sensitivity level), 4.) a record of accumulated loop failures, and 5.) a timer countdown of programmed timing functions. See Figure III-2 for system architecture (RENO A&E Product Overview, 2013).

Figure III-3. Reno A&E Model C-1100 series inductive loop detectors

Video Detection Processor Unit

The video detection technique involves setting up a series of virtual detection loops in each approach lane at a specified distance from the stop line. These virtual loops provide the same speed, volume and density information as in pavement loops. VIP3D can emulate traditional double or single loop detectors. A VDPU unit from Traficon is implemented in this study. Its operating principle and design factors are briefly explained in the following section.

- *Traficon Video Detection*

The key factor in a Traficon detection system is the Video Image Processor (VIP). In addition to the traffic data, it provides pulses similar to those provided by inductive loops. The VIP 3D.2 provides 4 data detection zones per camera and collects count, speed, classification, occupancy, density, headway and gap time. It also provides double and single loop data simulation. Queue length measurements and directional counts on the intersection can also be conducted (Traficon Product Overview, 2013). The system architecture for VDPUs is very similar to the system architecture for ILDs shown in Figure III-2. The architecture differs from the ILD one only in the use of cameras in place of loop coils as shown in Figure III-5.

Cabinet

VIP 3D2 unit

Figure III-4. Traficon VIP3D.2 sensor

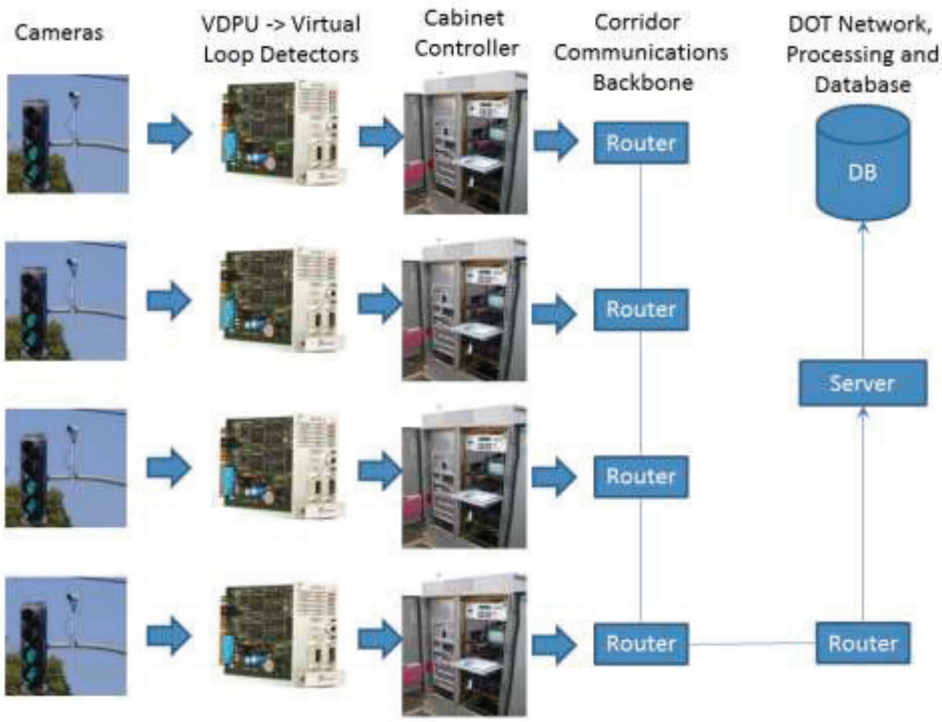

Figure III-5. VDPU system architecture

III.2 Vehicle Re-Identification Technologies

A wide range of vehicle re-identification technologies are now in use. In this study, six different vehicle re-identification technologies are used, which can be classified into three categories: automated license plate recognition, Bluetooth / WiFi MAC address matching and magnetic signature matching. Their operating principles and design factors are discussed in the following sections.

Automated License Plate Reader

One traditional method of vehicle re-identification is license plate matching. License plate matching techniques consist of collecting vehicle license plate characters (i.e. unique ID or signature) and arrival times at various checkpoints. The license plate characters are then matched between consecutive checkpoints and travel times computed from the difference between arrival times (Travel Time Data Collection Handbook, 1998). In this study, the ANPR system manufactured by Pips Technology is used.

- *Pips Technology ANPR Sensor*

The P372 Spike (a trademark of PIPS Technology, A Federal Signal Company and Motorola, Inc.) is a compact, rugged, fully integrated license plate reading camera incorporating the camera, illuminator and the ANPR processor within a single sealed enclosure. The unit is comprised of a monochrome CCD camera with a built-in infra-red (IR) LED illuminator. The Spike will output ANPR data comprised of a vehicle license plate reading, time, date, location (sensor ID), plate patch image or full IR image, overview image (if camera fitted), and read confidence. There is an option for wireless LAN connectivity, which may save on installation and cabling costs. Setup and monitoring of the unit is by web-browser interface from a PC or PDA (Pips Technology Product Overview, 2013).

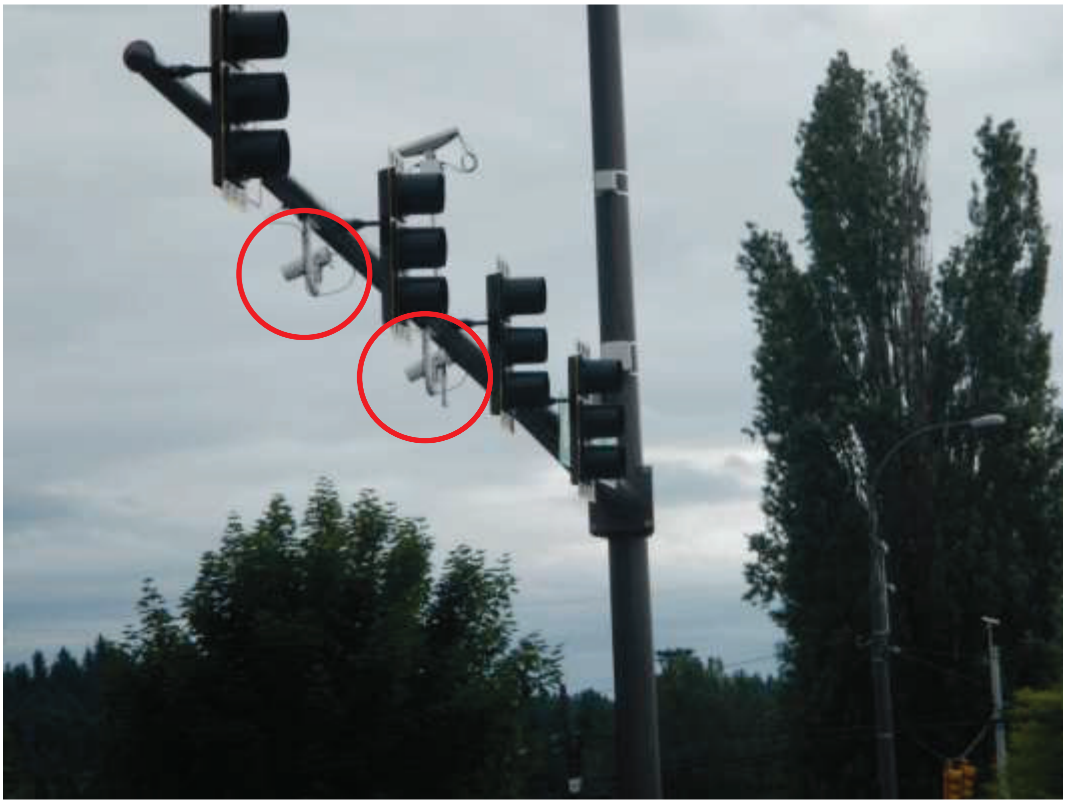

Figure III-6. Pips P327 Spike ANPR sensor

MAC Address Matching Technology

Bluetooth-based travel time measurement is one of the emerging methods of vehicle re-identification. This method involves identifying and matching the unique Media Access Control or Media Access Control (MAC) address of Bluetooth-enabled devices carried by motorists as they pass a detector location. As with ANPRs, the difference in time between the two observations yields the travel time. This approach relies on having a device with an active Bluetooth or Wi-Fi adapter in the sensor's detection range. In this Bluetooth technology from two different manufacturers are evaluated.

- *BlueTOAD Bluetooth Sensors*

BlueTOAD (a trademark of TrafficCast) is a Bluetooth MAC address detection system developed by TrafficCast International (TCI). The BlueTOAD device consists of the MAC address reader, a power source, and a communication source. The BlueTOAD devices are capable of Ethernet or cellular communication. The options for power are hard wire or solar power. The BlueTOAD cellular solar power option requires a service provider in order to communicate with the TCI servers. The Ethernet option allows for a direct connection to a hard wired network. The hard wire option can be connected to any power source capable of supporting 110V of AC power (TrafficCast Product Overview, 2013). The BlueTOAD cellular Solar Power 50W is used in this research, shown in Figure III-7.

The device reads the MAC address broadcast from any active Bluetooth device and sends the time of the read and MAC information to the TrafficCast central processing server to calculate travel times. TrafficCast then filters the data to remove outliers and provides the information to clients via a web interface. The TrafficCast secure cyber-center processes the data collected by BlueTOAD devices. Data can be viewed in real-time or analyzed historically through a BlueTOAD web interface, which provides travel times, road speeds, and MAC address detection counts.

Figure III-7. BlueTOAD sensor design and components

- *BlipTrack Bluetooth Sensors*

BlipTrack (a trademark of Blip Systems) is a Bluetooth sensor developed by Blip Systems. The BlipTrack Traffic sensor has 3 Bluetooth antennae including 2 directional antennae and 1 omnidirectional. The size of the detection zone varies from 70-200m on either side of the sensor along the road. When using 3 Bluetooth radios, BlipTrack has a 3 times greater chance of detecting a Bluetooth device and also covers an area more than 3 times as large as a single radio solution. BlipTrack also has built-in 3G and LAN connectivity for easy upload and a GPS sensor for auto positioning. The BlipTrack Bluetooth Traffic sensor uses 220V power with a battery backup (Blip Systems A/S Product Overview, 2013). The sensor configuration and components are shown in Figure III-8.

BlipTrack works by detecting Bluetooth devices in proximity to a BlipTrack Access Point. The sensors relay each detection event to a central server using their 3G connection. Each detection event is comprised of the MAC address of the detected device and the detection timestamp. Blip Systems then filters the data to remove outliers and provides the information to clients via a web interface. BlipTrack has a graphical interface with Google Maps integration, widgets and a wide range of real-time and historical analytical tools, which provides travel times, road speeds, and MAC address detection counts.

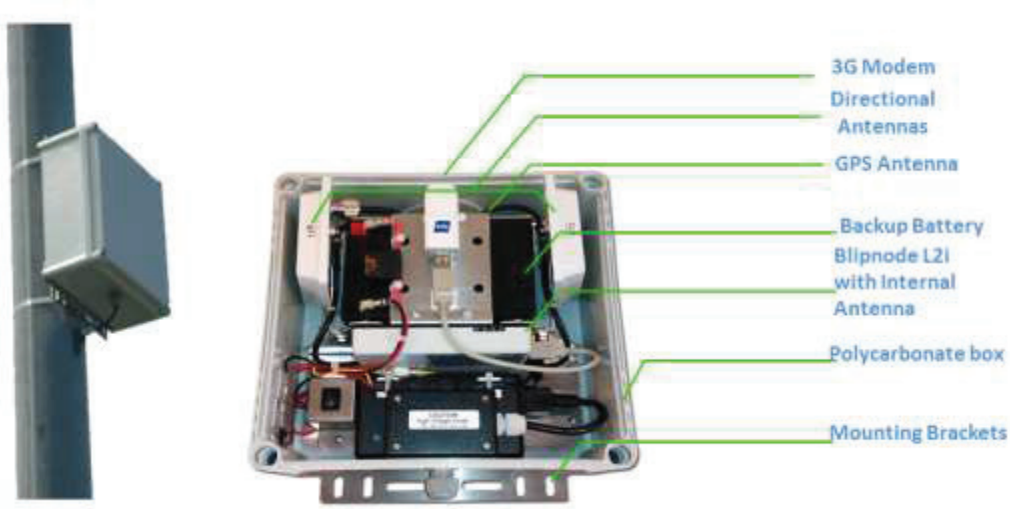

Figure III-8. BlipTrack sensor design and components

The new model of BlipTrack sensor incorporates a WiFi processor into the design. In this design an external WiFi unit can be connected to the Bluetooth unit. The joint WiFi/Bluetooth unit has the capability of detecting the MAC addresses transmitted by both WiFi and Bluetooth-enabled devices (Blip Systems A/S Product Overview, 2013). The architecture of BlipTrack solution is shown in Figure III-10.

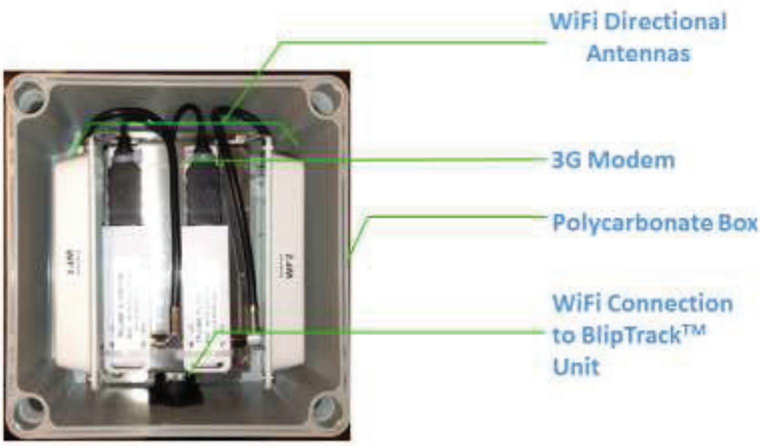

Figure III-9. BlipTrack WiFi sensor design and components

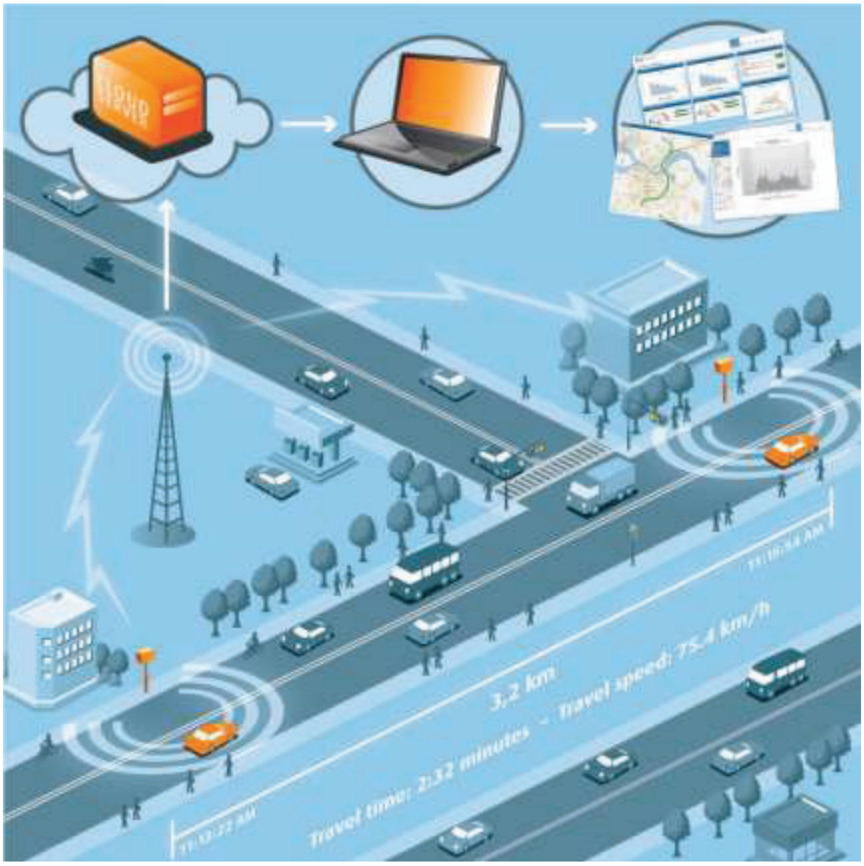

Figure III-10. Architecture of BlipTrack solution

Magnetic Signature Matching
This method relies on matching vehicle signatures from wireless sensors. The sensors provide a noisy magnetic signature of a vehicle and the precise time when it crosses the sensors. A match (re-identification) of signatures at two locations gives the corresponding travel time of the vehicle.

- *Sensys Wireless Vehicle Detection System*

The Sensys (a trademark of Sensys Networks, Inc.) wireless vehicle detection system uses pavement-mounted magnetic sensors to detect the presence and movement of vehicles. The magneto-resistive sensors are wireless, transmitting their detection data in real-time via low-power radio technology to a nearby Sensys access point that then relays the data to one or more local or remote traffic management controllers and systems.
The Sensys VSN240-F is an in-pavement wireless vehicle sensor designed for permanent deployment in all traffic conditions from freeways to intersections to parking lots to gates. The VSN240-F detects vehicular traffic and reports it back to an AP240 access point. Each sensor node contains a 3 axis magnetometer, microprocessor, memory, low power radio and batteries within a watertight case. After a vehicle passes over the sensor array, each sensor transmits its unique magnetic signature information to a wireless access point located within 150 feet of the array. If the sensor array is located outside this range, a battery operated repeater can retransmit the information up to 1,000 feet away. The access point collects the data from each sensor or repeater and retransmits the information to a data archiving server. Once the information is collected by the data archive server, it is used by the re-identification engine for travel time analysis. A Sensys access point (AP240-EC) is an intelligent device operating under the Linux operating system that maintains two-way wireless links to an installation's sensors and repeaters, establishes overall time synchronization, transmits

configuration commands and message acknowledgements, and receives and processes data from the sensors. The Sensys access point then uses either wired or wireless network connections (or both) to relay the sensor detection data to a roadside traffic controller or remote server, traffic management system, or other vehicle detection application. A Sensys repeater (RP240-B) extends the range and coverage of an installation's access point. The three devices may be seen Figure III-11 (Sensys Networks Product Overview, 2013).

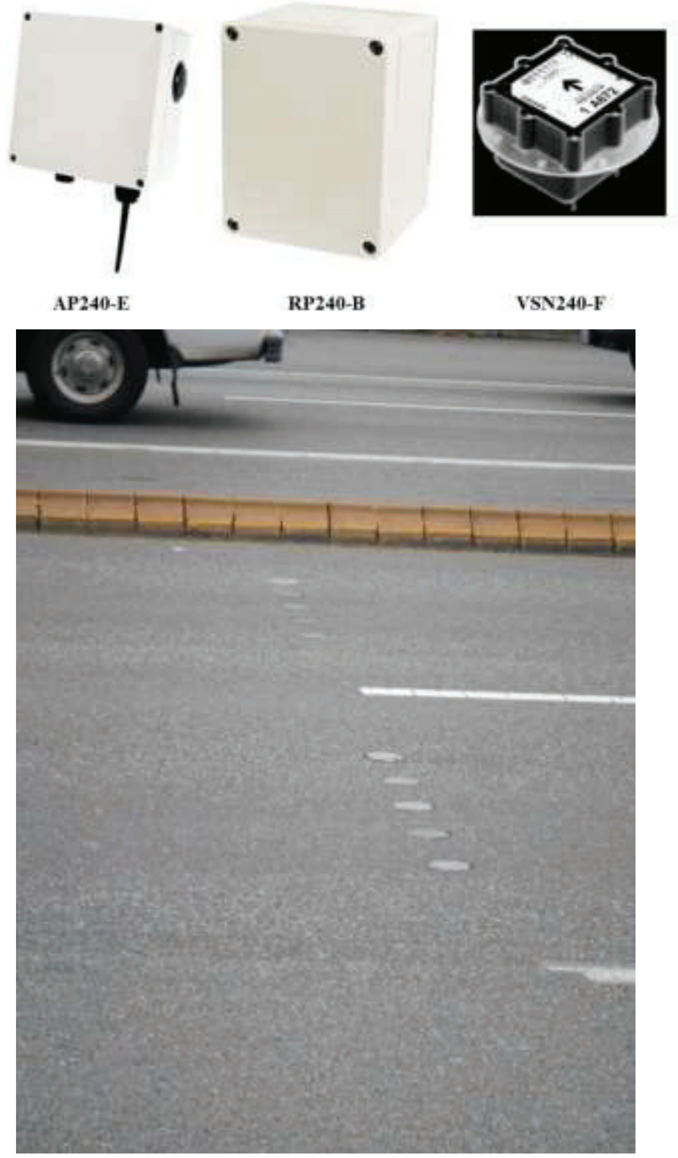

Figure III-11. Sensys wireless vehicle detection system

IV.1 3rd Party Inrix Data

INRIX aggregates traffic-related information from millions of GPS-enabled vehicles and mobile devices, traditional road sensors and hundreds of other sources. The result is a real-time, historical and predictive traffic services on freeways, highways, and secondary roadways, including arterials and side streets (Inrix, 2013).

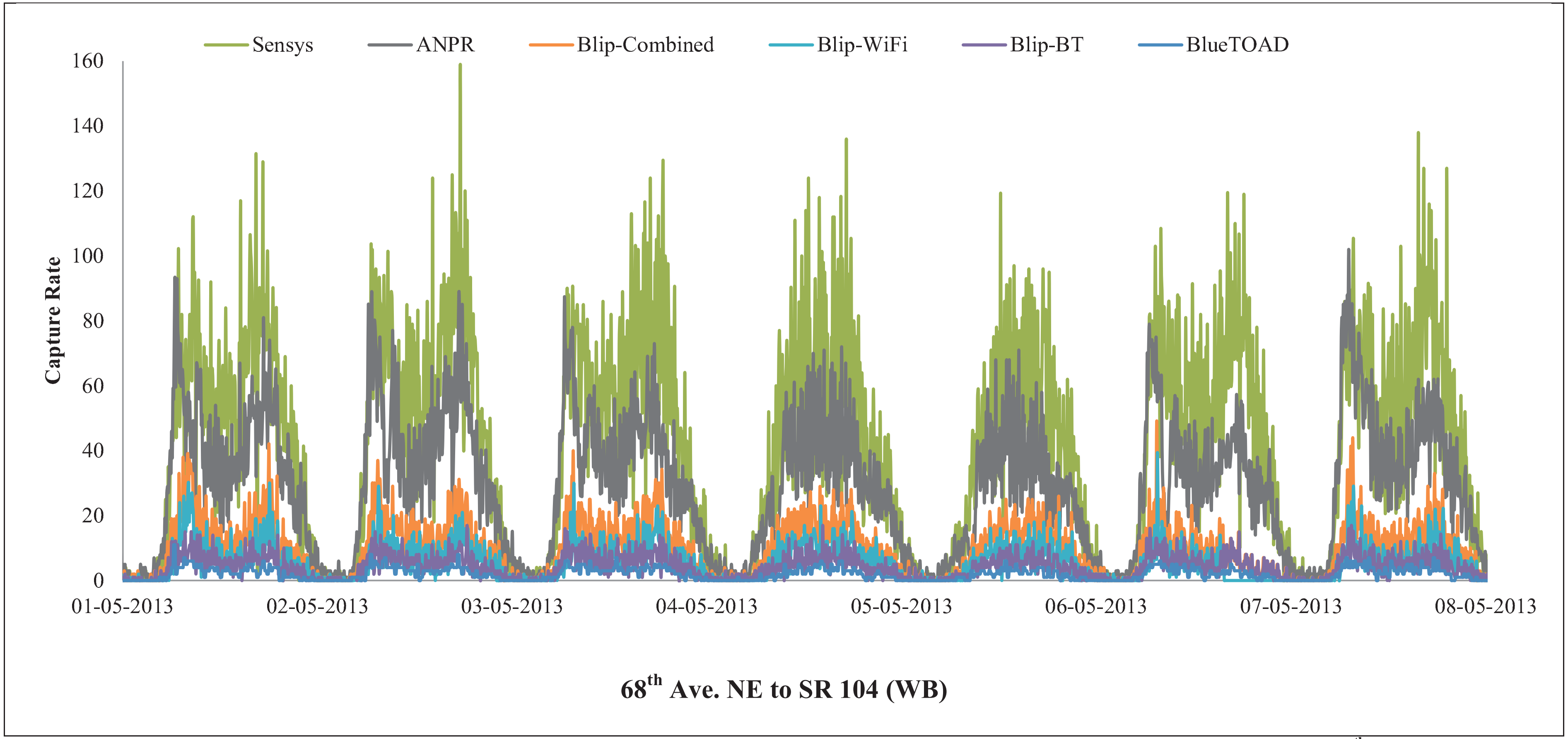

Figure III-12. Comparing capture rate of different systems from 68th Ave. NE to SR 104 (WB) for May 1st, 2013 through May 8th, 2013

Figure III-12 shows the overlaid profiles of capture rate for various sensors on 68th Ave. NE to SR 104 (WB) for May 1st, 2013 through May 8th, 2013. It clearly shows that Sensys and ANPR have the higher capture rate which followed by Blip-Combined, Blip-WiFi and Blip-BT, and BlueTOAD. Figure III-12 shows that all of the systems were capable of registering the flow variation for peak and off-peak over the course of weekdays and weekends.

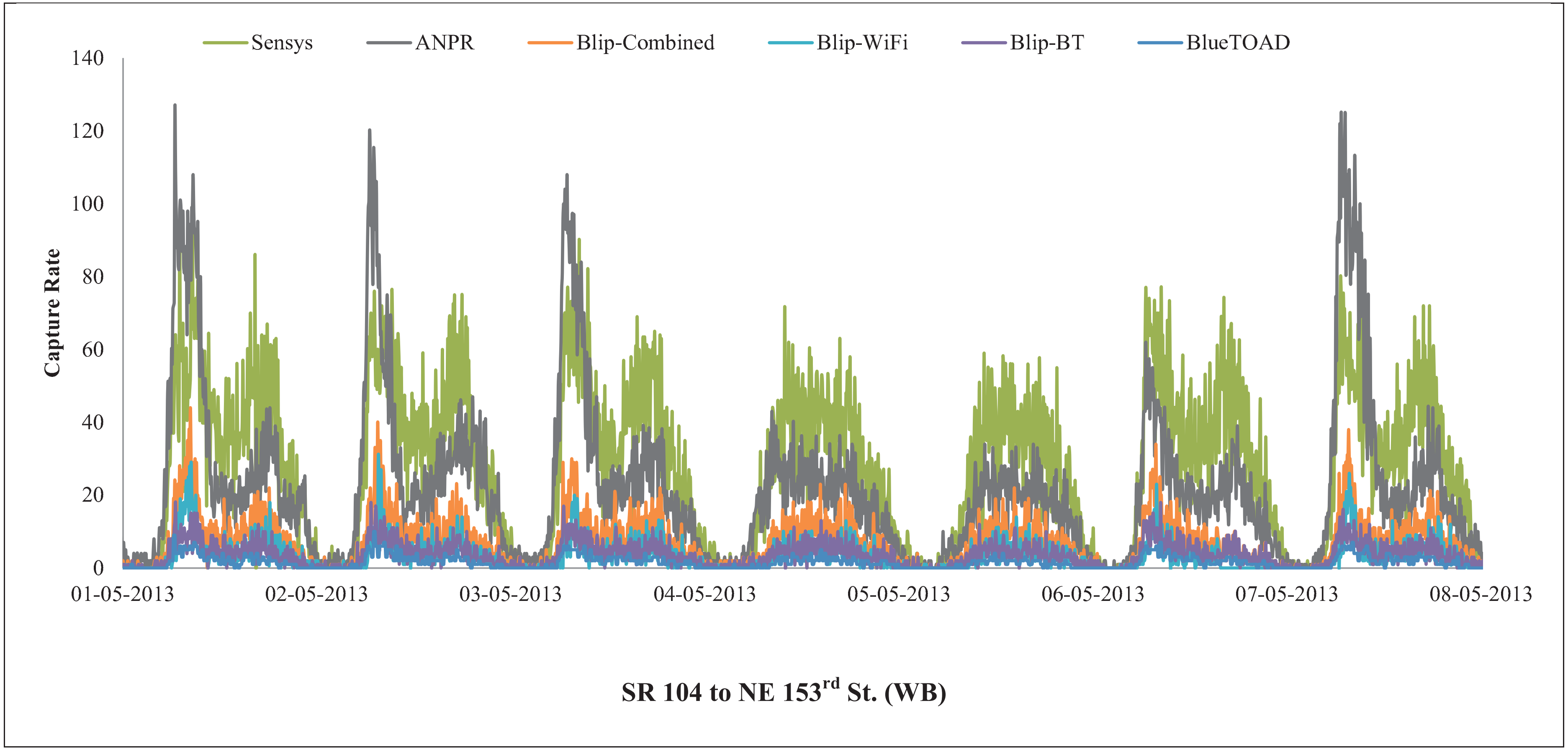

Figure III-13. Comparing capture rate of different systems from SR 104 to NE 153rd St. (WB) for May 1st, 2013 through May 8th, 2013

Figure III-13 shows the overlaid profiles of capture rate for various sensors from SR 104 to NE 153rd St. (WB) for May 1st, 2013 through May 8th, 2013. It clearly shows that Sensys and ANPR have the higher capture rate which followed by Blip-Combined, Blip-WiFi and Blip-BT, and BlueTOAD. Figure III-13 shows that all of the systems were capable of registering the flow variation for peak and off-peak over the course of weekdays and weekends.

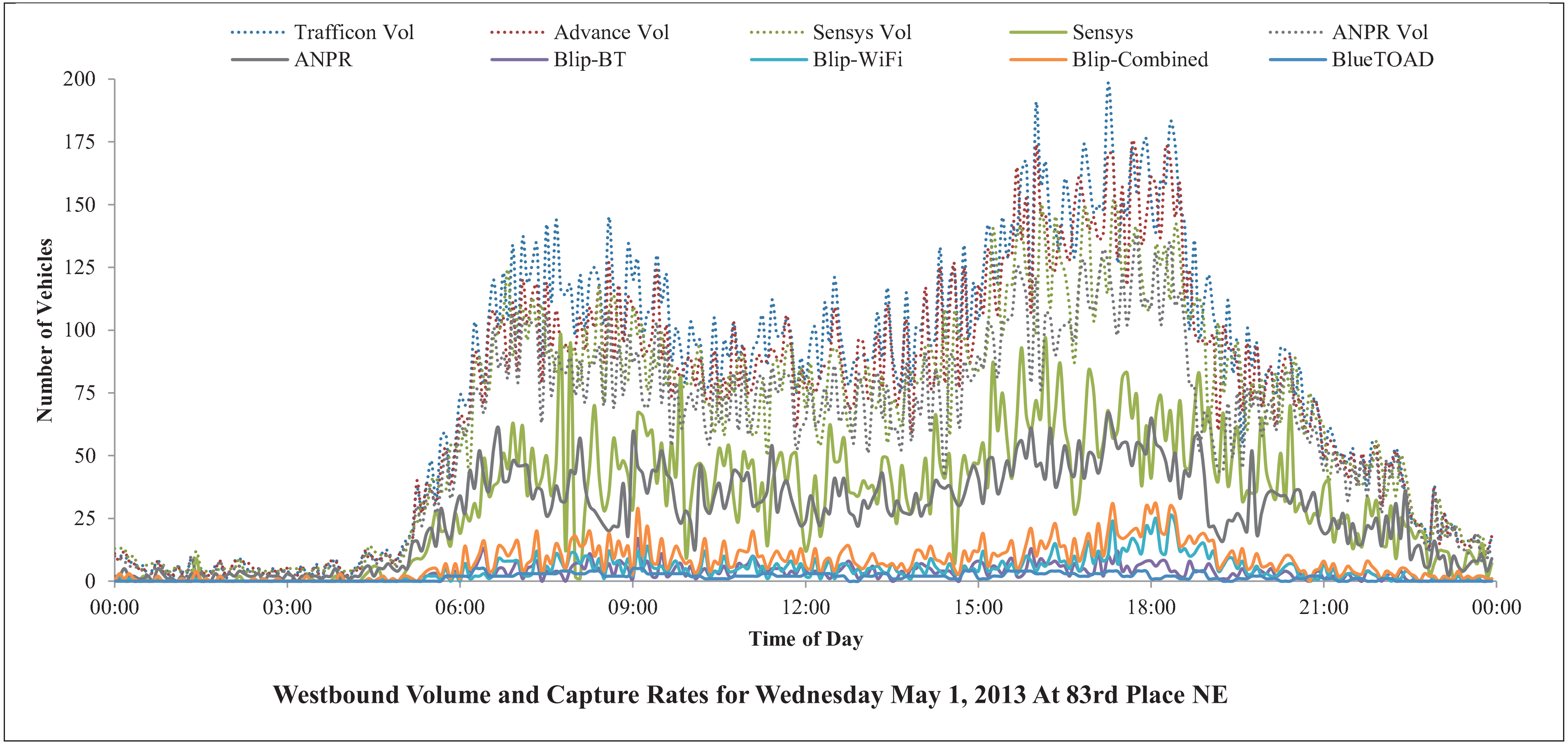

Figure III-14. Comparing number of detected vehicles by different systems versus loop detectors traffic volume on SR 522_ 83 PINE (WB) on 01-05-2013

Figure III-14 shows the number of vehicles detected and capture rates for Wednesday May 1, 2013 at 83rd PINE. The number of detected and matched vehicles for all systems are compared with the Traficon loop and advanced loop detectors to evaluate the actual number of detected vehicles versus the matched one for all techniques.

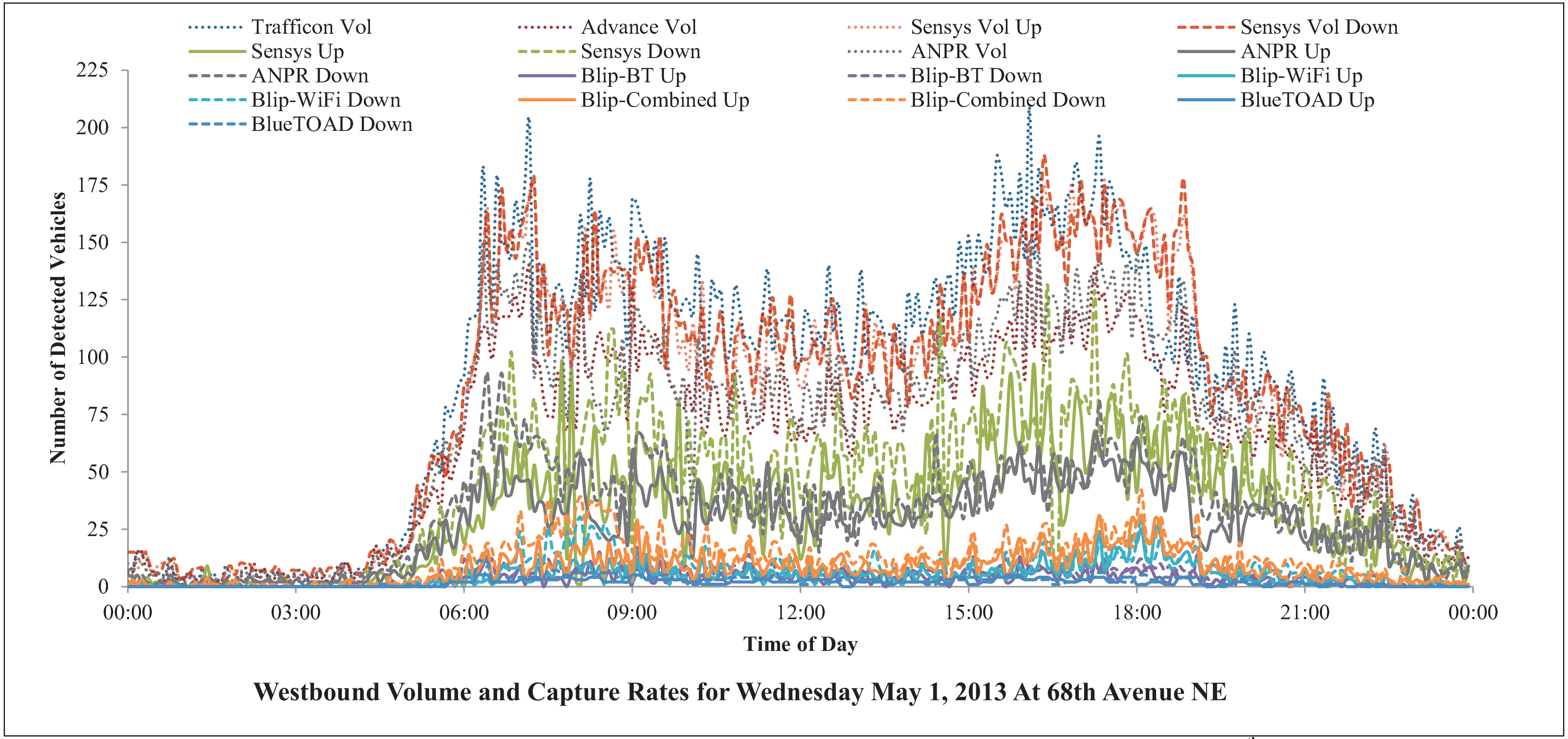

Figure III-15. Comparing number of detected vehicles by different systems versus loop detectors traffic volume on SR 522_68th Ave (WB) on 01-05-2013

Figure III-15 shows the number of vehicles detected and capture rates for Wednesday May 1st, 2013 at 68th Avenue NE. The number of detected at upstream and downstream of the segment and matched vehicles for all systems are compared with the Traficon loop and advanced loop detectors to evaluate the actual number of detected vehicles versus the matched one for all techniques. Up and Down refer to whether the sensor is counting upstream or downstream respectively.

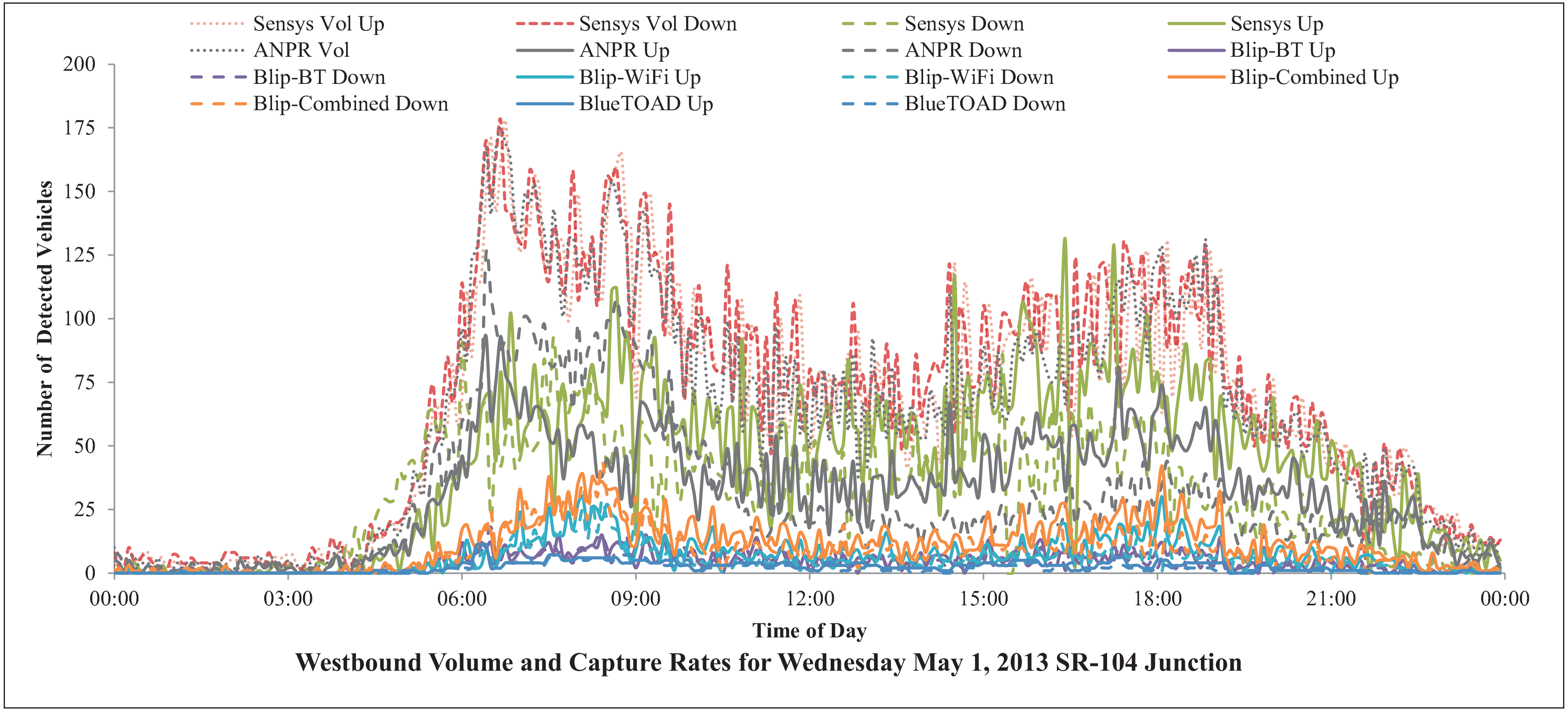

Figure III-16. Comparing number of detected vehicles by different systems versus loop detectors traffic volume on SR 522_SR 104 (WB) on 01-05-2013

Figure III-16 shows the number of vehicles detected and capture rates for Wednesday May 1st , 2013 at SR-104 Junction. The number of detected at upstream and downstream of the segment and matched vehicles for all systems are compared with the Traficon loop and advanced loop detectors to evaluate the actual number of detected vehicles versus the matched one for all techniques.

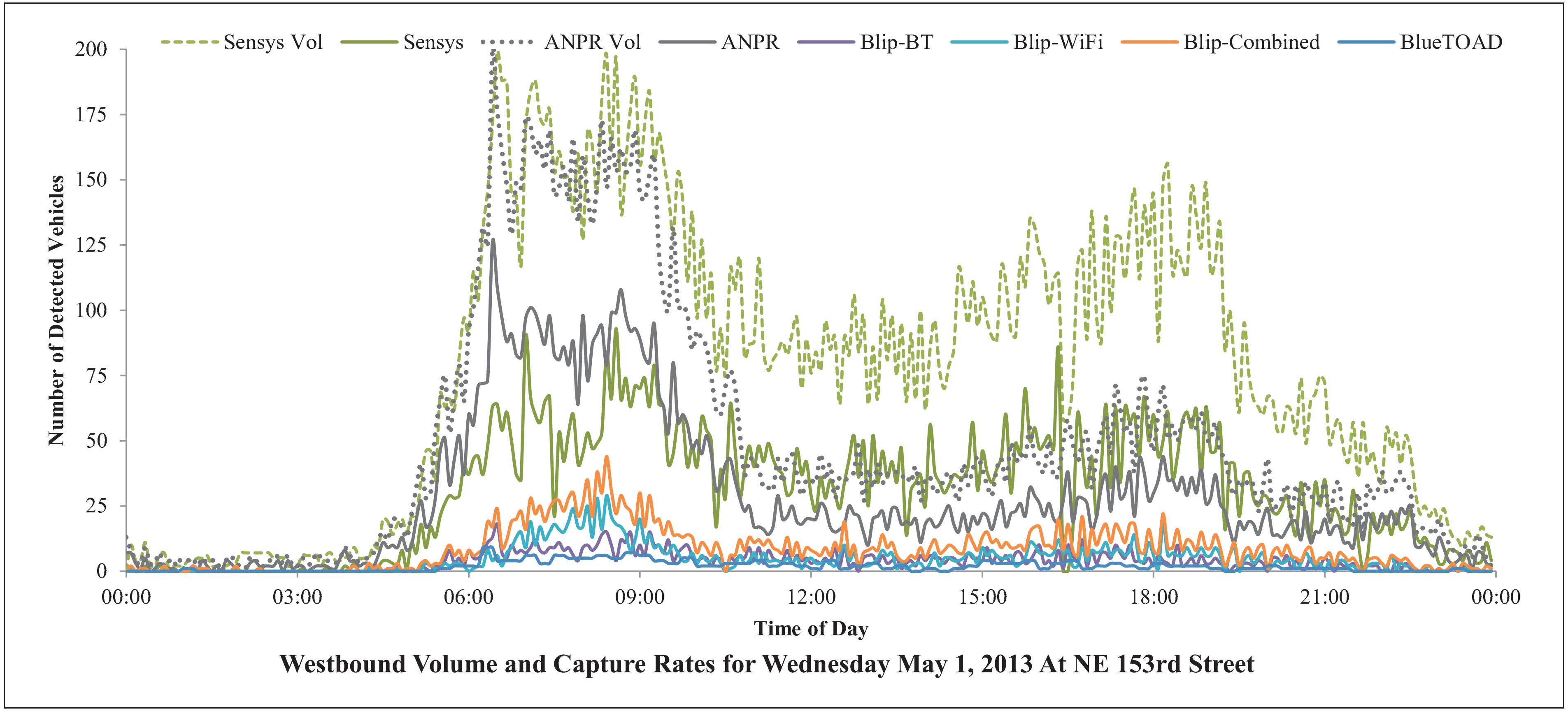

Figure III-17. Comparing number of detected vehicles by different systems versus loop detectors traffic volume on SR 522_NE 153rd (WB) on 01-05-2013

Figure III-17 shows the number of vehicles detected and capture rates for Wednesday May 1st, 2013 at NE 153rd Street. The number of detected at upstream and downstream of the segment and matched vehicles for all systems are compared with the Traficon loop and advanced loop detectors to evaluate the actual number of detected vehicles versus the matched one for all techniques.

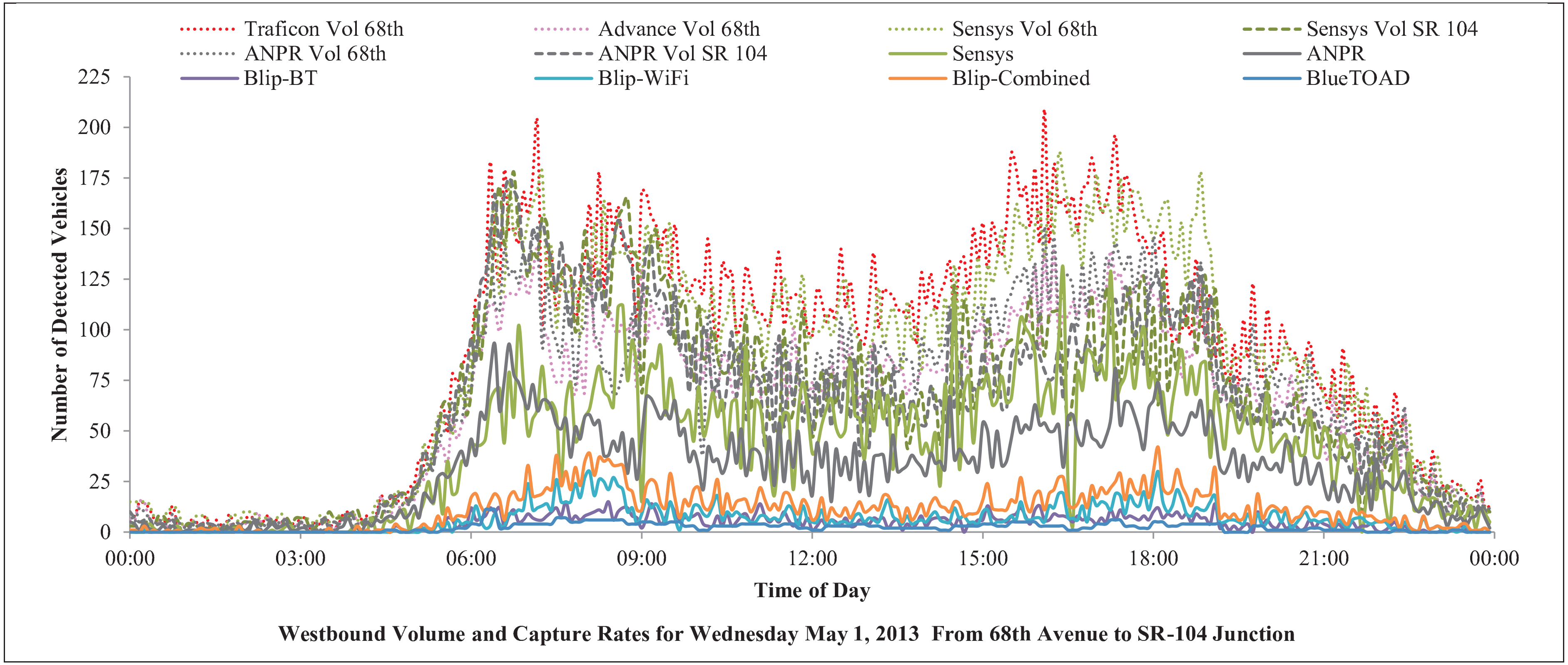

Figure III-18. Westbound Volume and Capture Rates for Wednesday May 1, 2013 From 68th Avenue to SR-104 Junction

In Figure III-18 the number of matches reported by each system are represented by solid lines. Dotted lines are used to represent the volumes reported at the upstream intersection and dashed lines are used to represent the volume at the downstream intersection. Sensys volumes and match rate are shown in green. ANPR volumes and match rate are shown in dark gray. The BlueTOAD match rate is shown in dark blue. The Blip Bluetooth, WiFi and Combined match rates are shown in purple, light blue and orange, respectively. The 68th Avenue NE intersection includes Traficon and advance loop detectors for volume counts, shown in by red and magenta dashed lines, respectively. It should be noted that the Sensys and ANPR systems report significantly higher match rates than the other systems. The ANPR system appears to be more effective during the morning peak. Also of interest is that the two Bluetooth systems perform comparably with regards to match rates. The additional matches reported by Blip-Combined are a result of the added WiFi sensors. The WiFi sensors also appear to have stronger morning and evening peaks than Bluetooth.

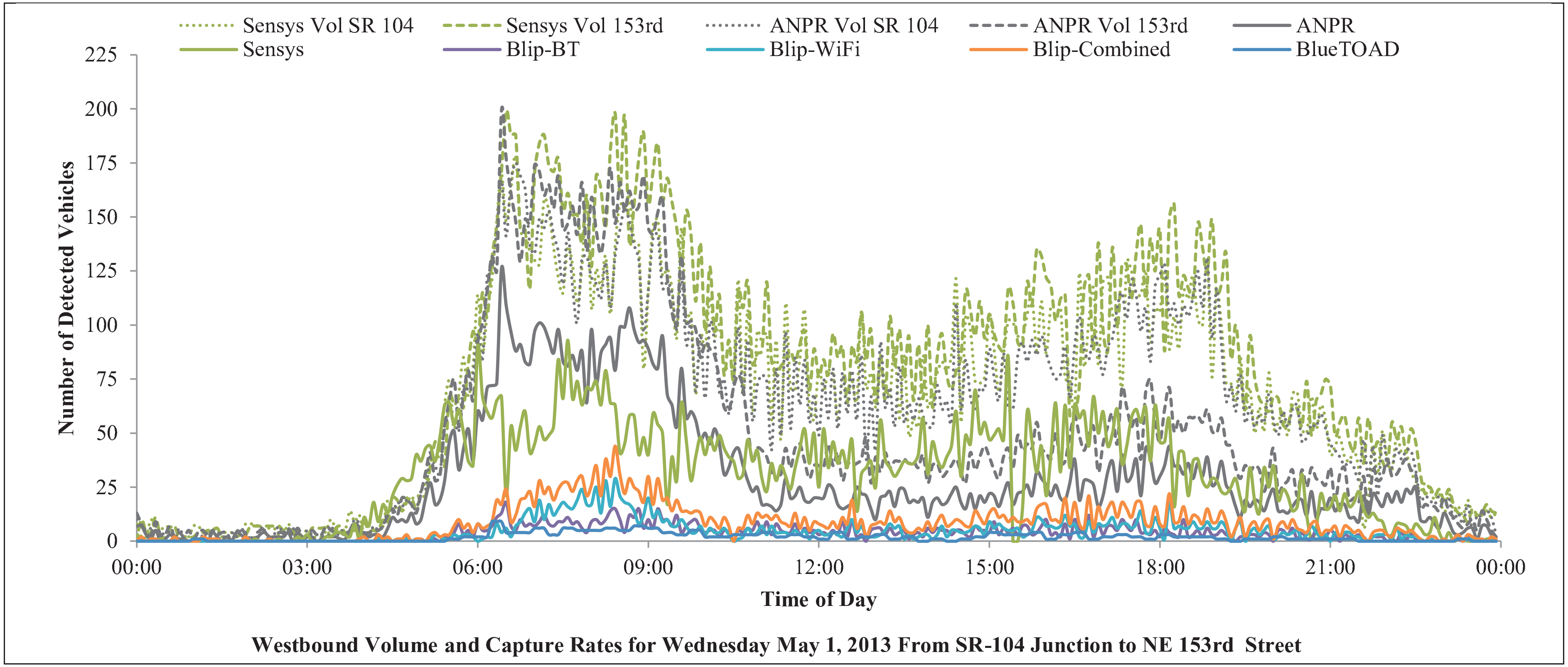

Figure III-19. Westbound Volume and Capture Rates for Wednesday May 1, 2013 From SR-104 Junction to NE 153rd Street

In Figure III-19 the number of matches reported by each system are represented by solid lines. Dotted lines are used to represent the volumes reported at the upstream intersection and dashed lines are used to represent the volume at the downstream intersection. Readers should note that the Sensys and ANPR systems report significantly higher match rates than the other systems. Also of interest is that the two Bluetooth systems perform comparably with regards to match rates. The additional matches reported by Blip-Combined are a result of the added WiFi sensors. The WiFi sensors also appear to have stronger morning and evening peaks than Bluetooth.

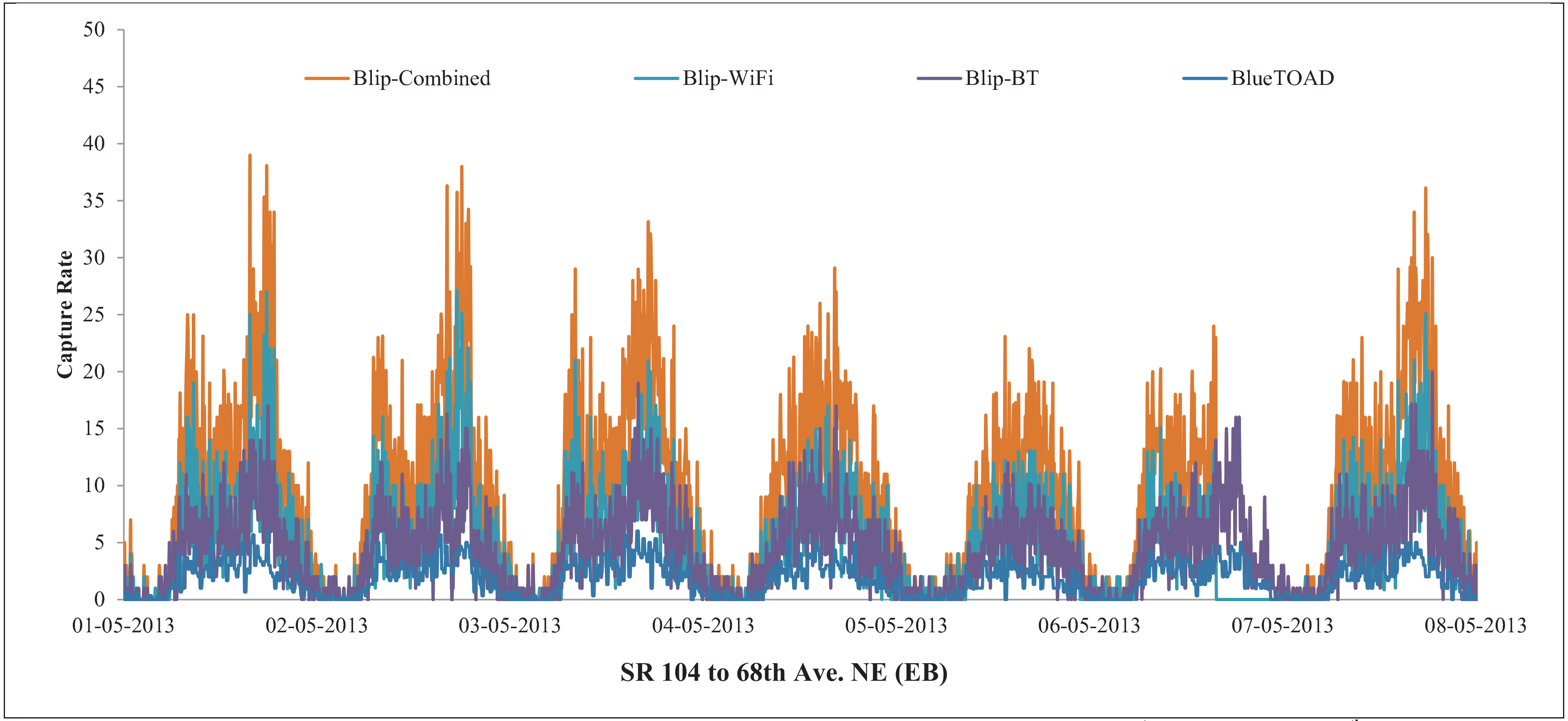

Figure III-20. Comparing capture rate of different systems from SR 104 to 68th Ave. NE (EB) for May 1st, 2013 through May 8th, 2013

Figure III-20 shows capture rate for Blip-Combined, Blip-WiFi, Blip-BT, and BlueTOAD on SR 104 to 68th Ave. NE (EB) segment for May 1st, 2013 through May 8th, 2013. Figure III-20 shows that regardless of the variations in capture rates for different systems; all systems were capable of detecting the cyclical pattern of traffic flow for peak and off-peak hours over the course of weekdays and weekends.

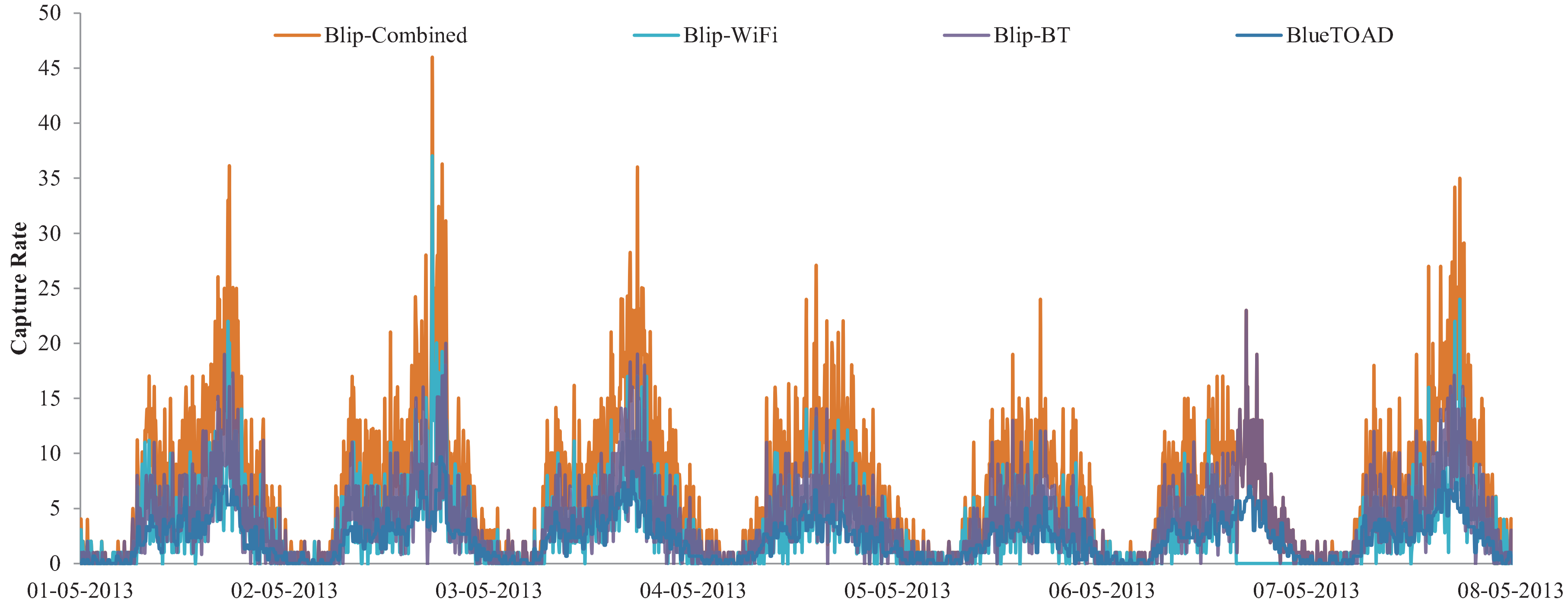

NE 153rd St. to SR 104 (EB)

Figure III-21. Comparing capture rate of different systems from NE 153rd St. to SR 104 (EB) for May 1st, 2013 through May 8th, 2013

Figure III-21 shows capture rate for Blip-Combined, Blip-WiFi, Blip-BT, and BlueTOAD on NE 153rd St. to SR 104 (EB) segment for May 1st, 2013 through May 8th, 2013. Figure III-21 indicates that regardless of the variations in capture rates for different systems; all systems were capable of detecting the cyclical pattern of traffic flow for peak and off-peak hours over the course of weekdays and weekends.

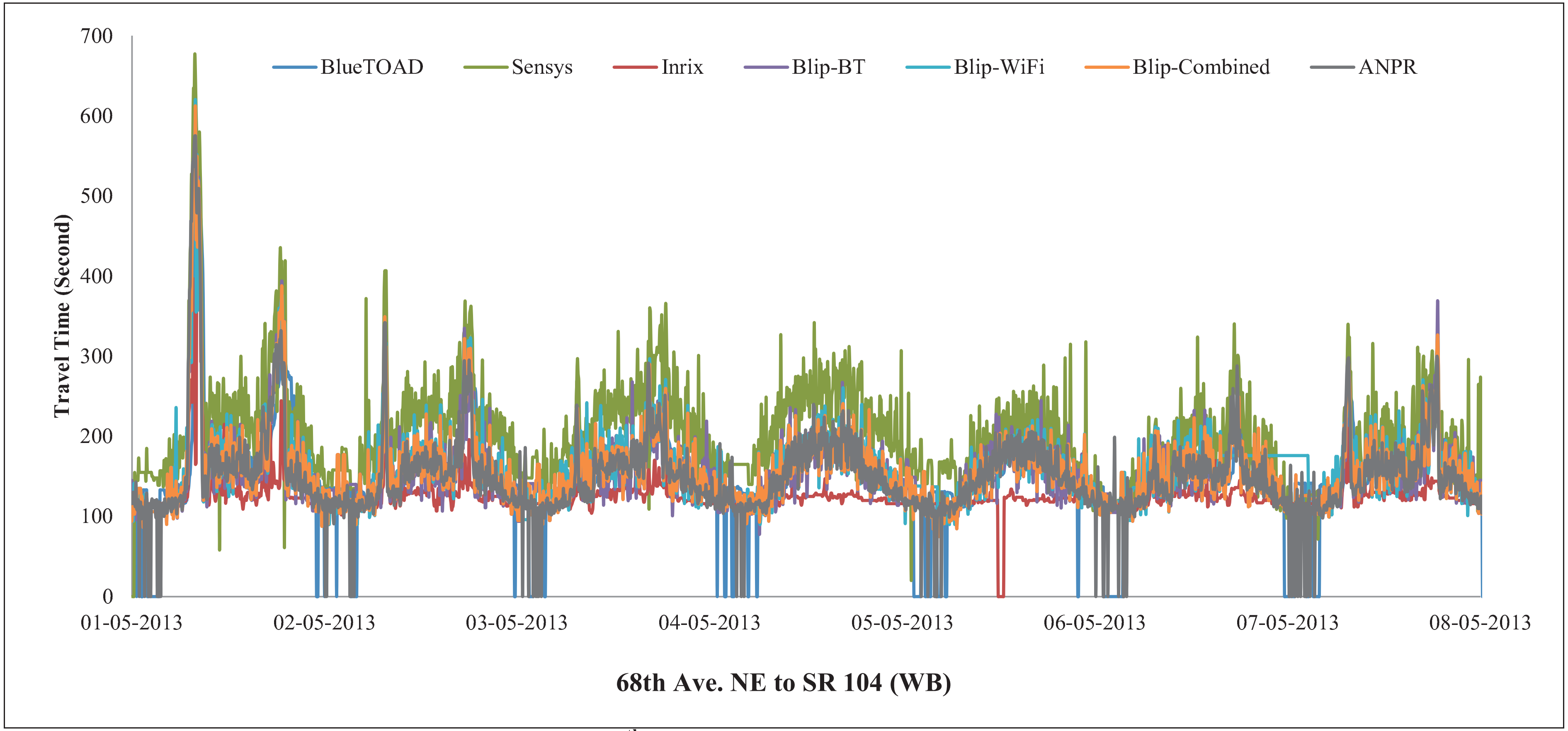

Figure III-22. Travel time plot for 68th Ave. NE to SR 104 (WB) for May 1st, 2013 through May 8th, 2013

Figure III-22 shows the overlaid profiles of travel time for all the sensors from 68th Ave. NE to SR 104 (WB) over the course of a week from May 1st, 2013 through May 8th, 2013. It is clear that all the sensors are capable of responding to the cyclical pattern of travel time over weekdays and weekends and also for the morning and afternoon peaks. Over the peak and off-peak hours all sensors follow the ANPR pattern and therefore have a strong overlap with the ground truth. However, Inrix data tend to significantly underestimate the travel times. A number of gaps or low travel times were reported for all methods (except Inrix) over the mid night hours.

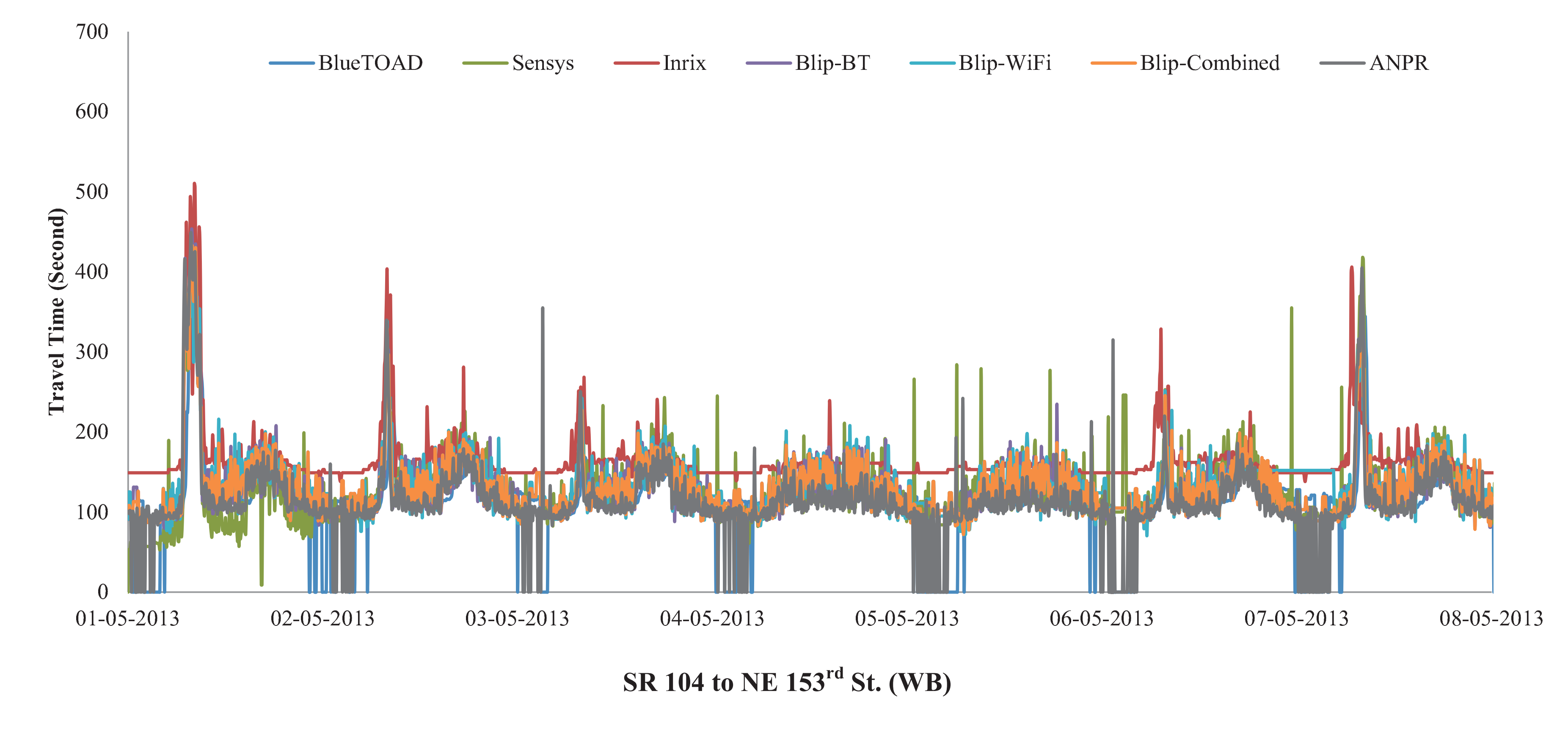

Figure III-23. Travel time plot from SR 104 to NE 153rd St. (WB) for May 1st, 2013 through May 8th, 2013

Figure III-23 shows the overlaid profiles of travel time for all the sensors from SR 104 to NE 153rd St. (WB) over the course of a week from May 1st, 2013 through May 8th, 2013. It is clear that all the sensors are capable of responding to the cyclical pattern of travel time over weekdays and weekend and also for the morning and afternoon peaks. Over the peak and off-peak hours all sensors follow the ANPR pattern and have a strong overlap with the ground truth. However, Inrix data tend to significantly overestimate the travel time during off-peak intervals. A number of gaps or low travel times have also been reported for all methods (except Inrix) over the mid night hours.

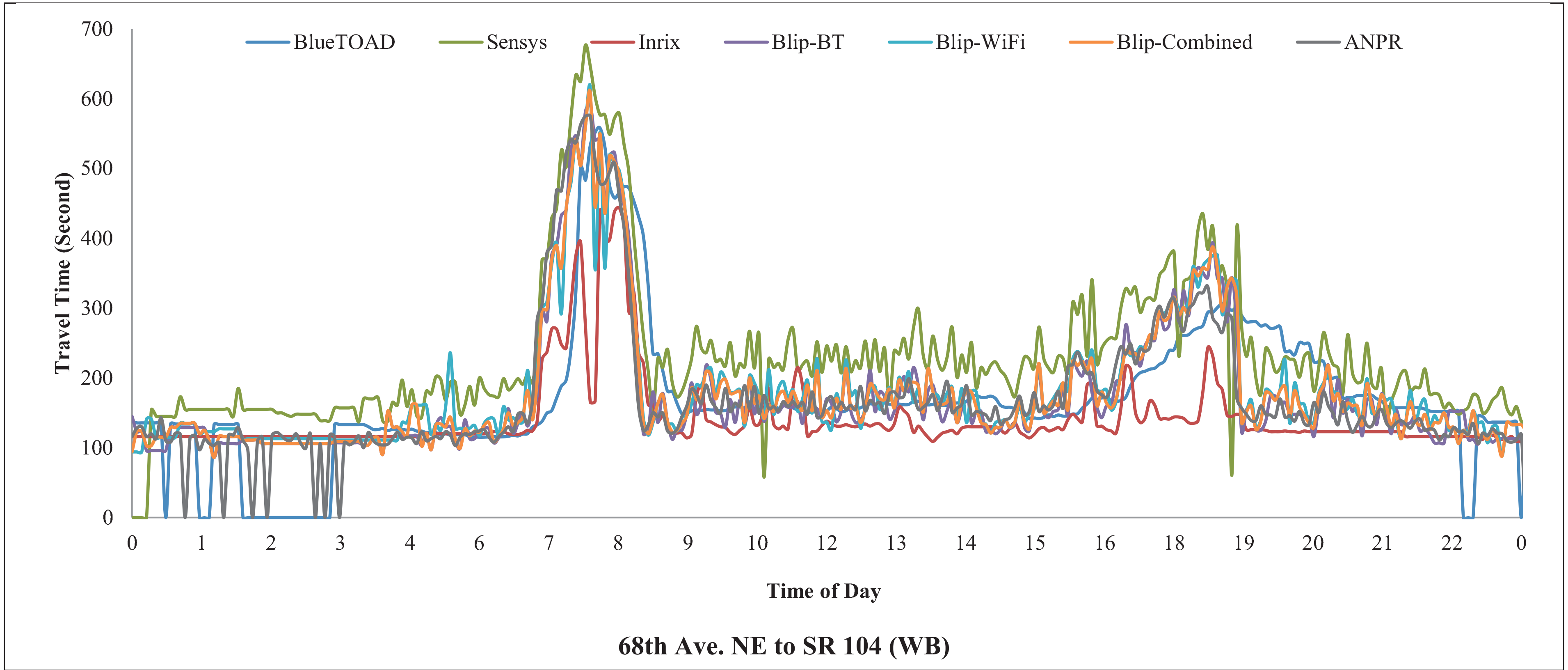

Figure III-24. Travel time plot for 68th Ave. NE to SR 104 (WB) on May 1st, 2013

Figure III-24 shows the overlaid profiles of travel time for all the sensors on 68th Ave. NE to SR 104 (WB) for Wednesday May 1st, 2013 in a zoomed view. It is clear that all the sensors are capable of representing the cyclical pattern of travel time over a day and for the morning and afternoon peaks. Over the peak and off-peak hours all sensors follow ANPR pattern and have a well overlap with the ground truth; however, Inrix tend to significantly overestimate the travel time during the off-peaks. A number of gaps or low travel time also has been reported for all methods over the mid night hours.

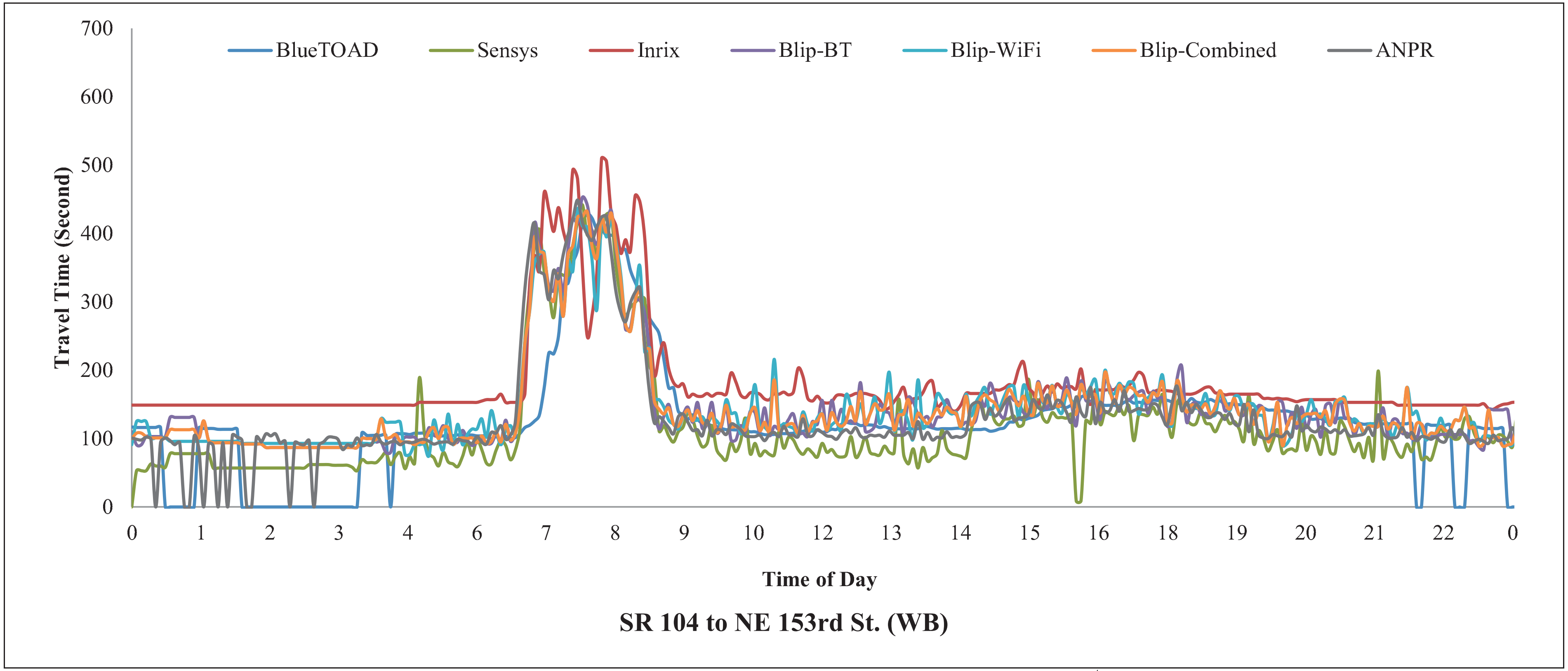

Figure I-25. Travel time plot for SR 104 to NE 153rd St. (WB) on May 1st, 2013

Figure III-25 shows the overlaid profiles of travel time for all the sensors on SR 104 to NE 153rd St. (WB) for Wednesday May 1st, 2013 in a zoomed view. It is clear that all the sensors are capable of representing the cyclical pattern of travel time over a day and for the morning and afternoon peaks. Over the peak and off-peak hours all sensors follow ANPR pattern and have a well overlap with the ground truth; however, Inrix tend to significantly overestimate the travel time during the off-peaks. A number of gaps or low travel time also has been reported for all methods over the mid night hours.

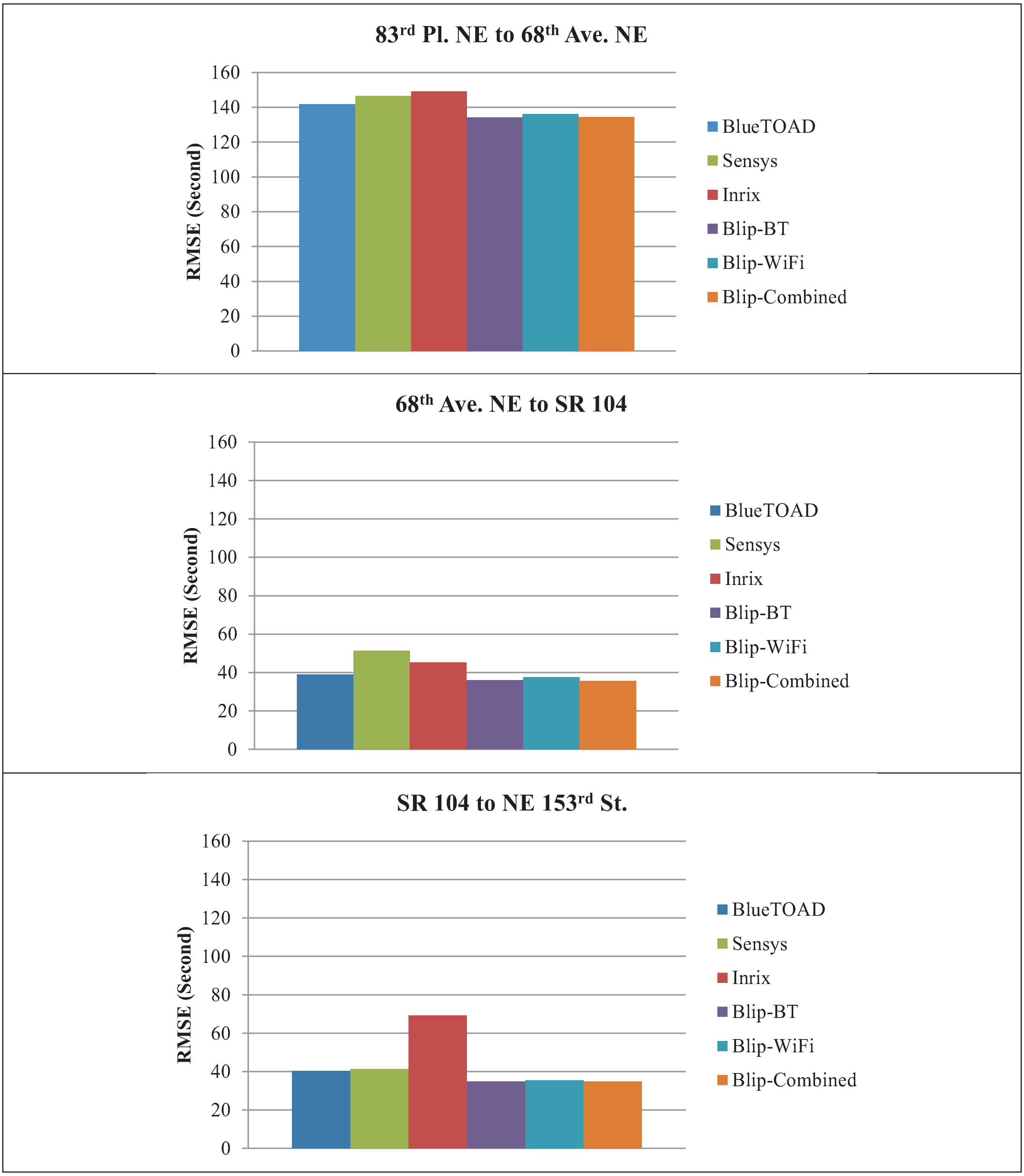

Figure III-26. Comparing RMSE on SR-522 westbound corridor over the period of April 5th, 2013 through June 8th, 2013

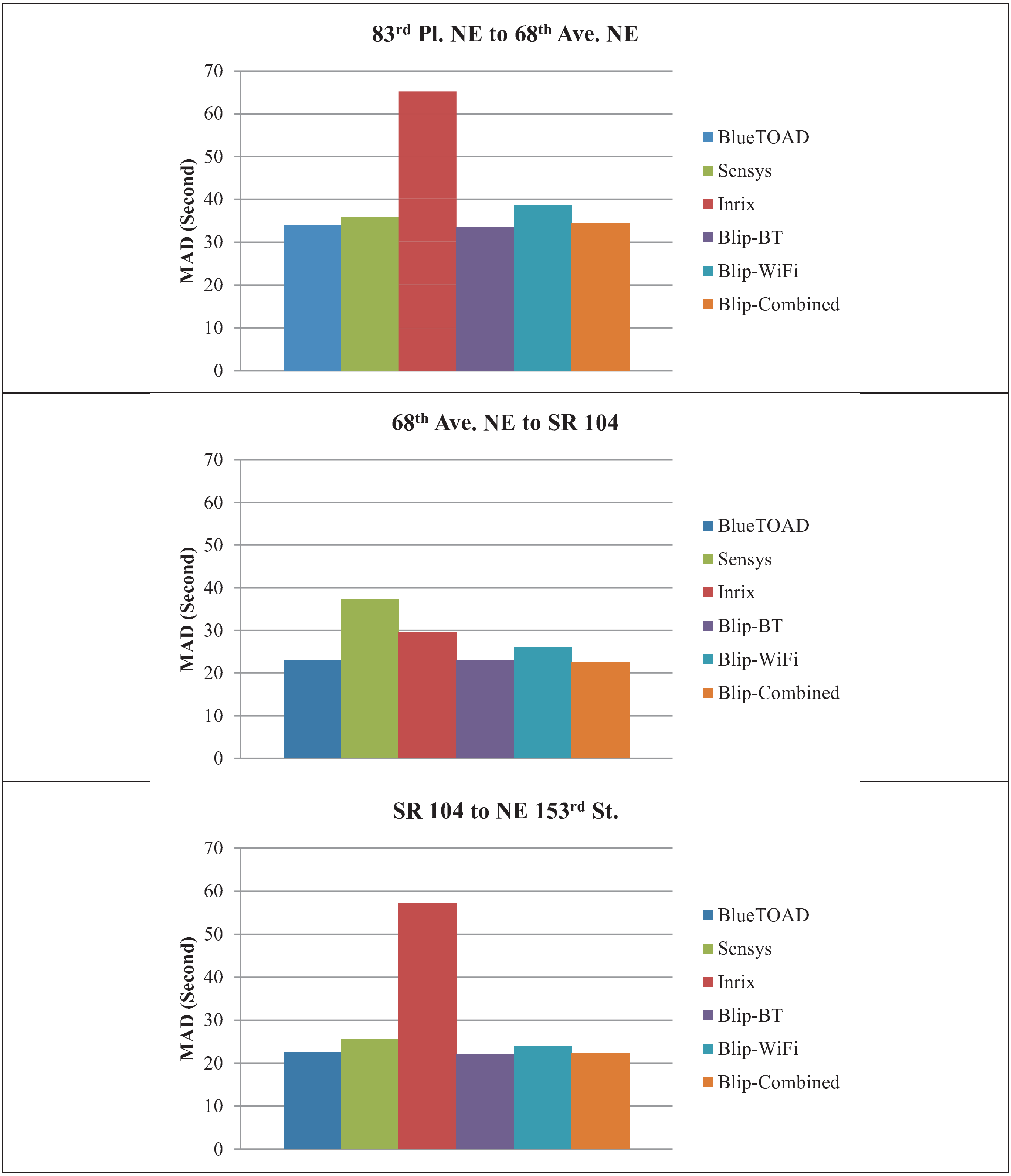

Figure III-27. Comparing MAD on SR-522 westbound corridor over the period of April 5th, 2013 through June 8th, 2013

Figure III-28. Comparing MPE on SR-522 westbound corridor over the period of April 5th, 2013 through June 8th, 2013

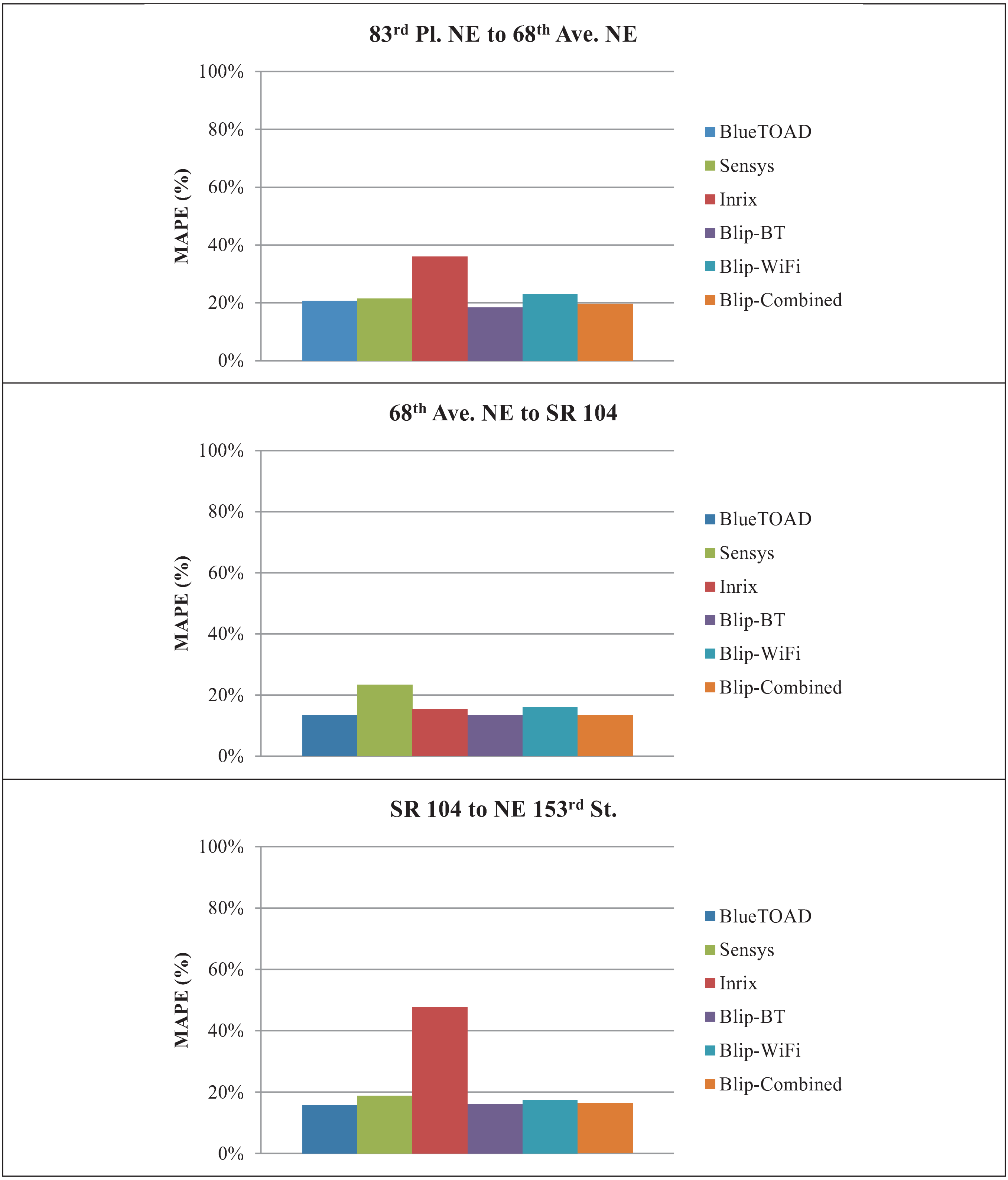

Figure III-29. Comparing MAPE on SR-522 westbound corridor over the period of April 5th, 2013 through June 8th, 2013

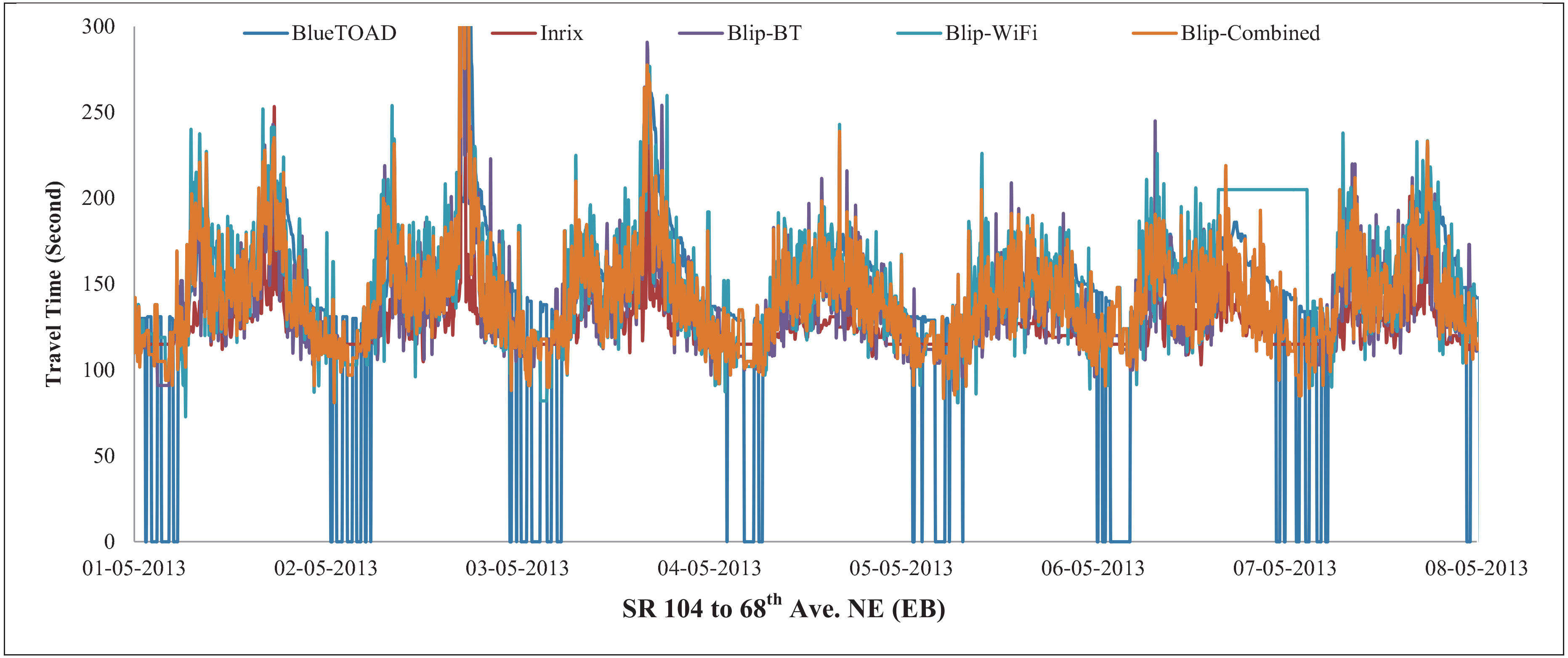

Figure III-30. Travel time plot from NE 153rd St. to SR 104 (EB) for May 1st, 2013 through May 8th, 2013

Figure III-30 shows the overlaid profiles of travel time for all the sensors on SR 104 to 68th Ave. NE (EB) over the course of a week from May 1st, 2013 through May 8th, 2013. It is clear that all the sensors are capable of detecting the cyclical pattern of travel time over weekdays and weekend and also for the morning and afternoon peaks. Overnight, BlueTOAD was again observed to have a number of gaps in its data. The evening of May 2nd, an incident caused a significant spike in travel times registered by all sensors.

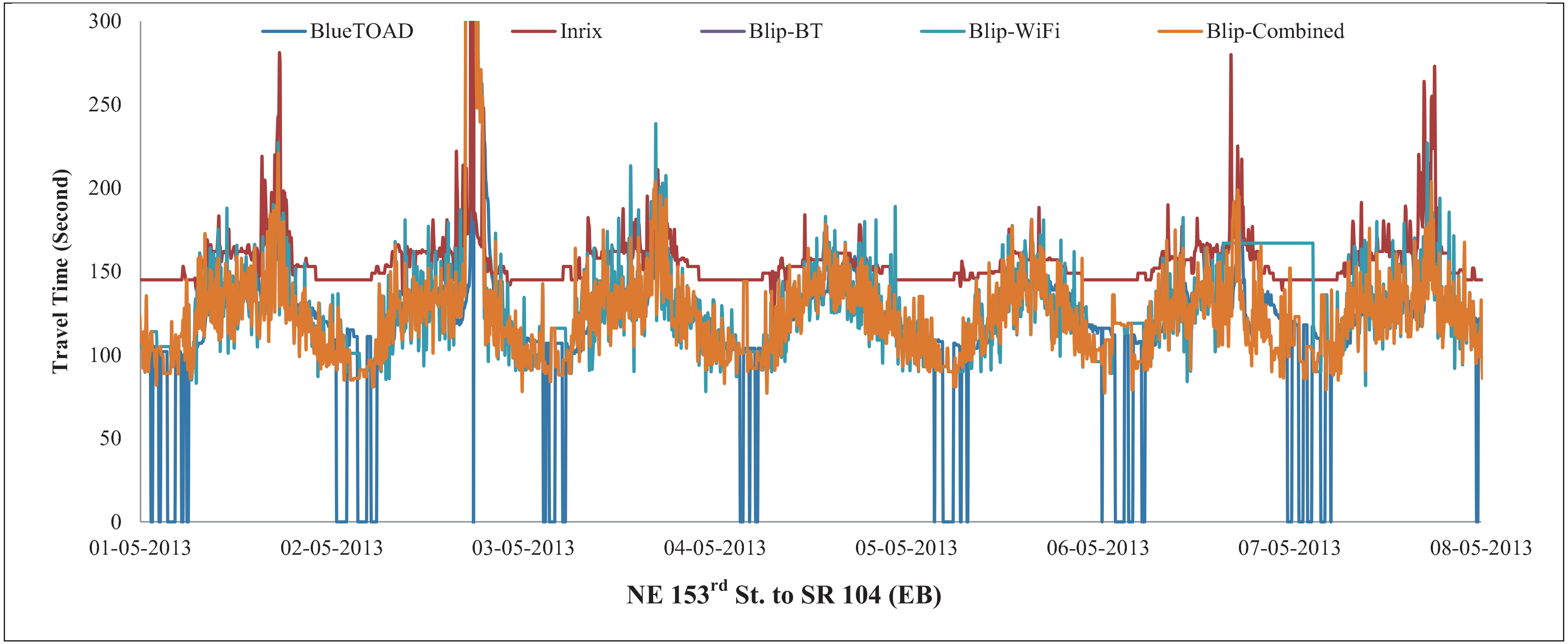

Figure III-31. Travel time plot from NE 153rd St. to SR 104 (EB) for May 1st, 2013 through May 8th, 2013

Figure III-31 shows the overlaid profiles of travel time for all the sensors from NE 153rd St. to SR 104 (EB) over the course of a week from May 1st, 2013 through May 8th, 2013. It is clear that all the sensors are capable of detecting the cyclical pattern of travel time over weekdays and weekend and also for the morning and afternoon peaks. Inrix reports a significantly higher and highly smoothed travel time over the off-peak hours on this segment compared to others. Overnight, BlueTOAD was observed to have a number of gaps in its data. The evening of May 2nd, an incident caused a significant spike in travel times registered by all sensors.

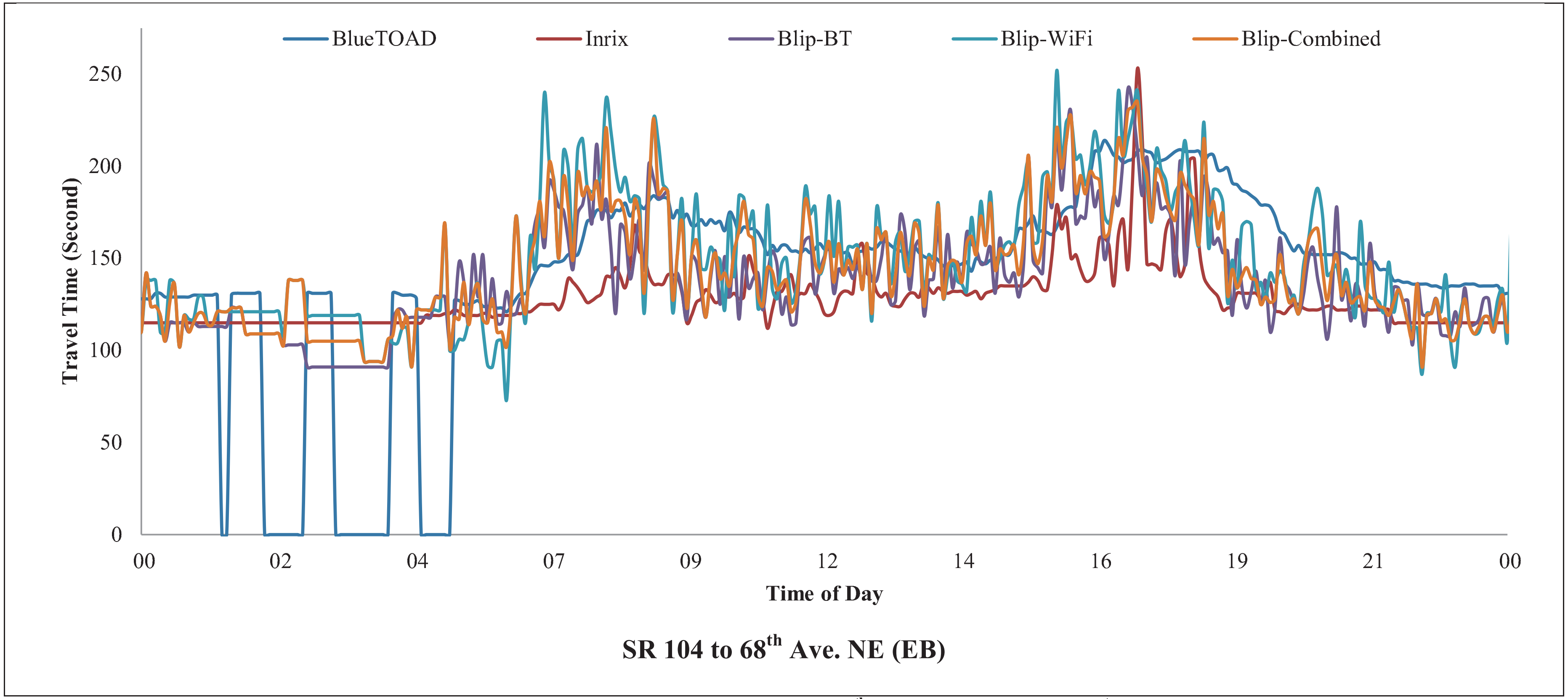

Figure III-32. Travel time plot for SR 104 to 68th Ave. NE (EB) on May 1st, 2013

Figure III-32 shows the overlaid profiles of travel time for all the sensors from SR 104 to 68th Ave. NE (EB) for Wednesday May 1st, 2013. It is clear that all the sensors are capable of reacting to the cyclical pattern of travel time over a day and for the morning and afternoon peaks. For this segment Inrix reports a lower and slightly more smoothed travel time on this segment compared to others. A large number of gaps in the early morning can be observed for BlueTOAD.

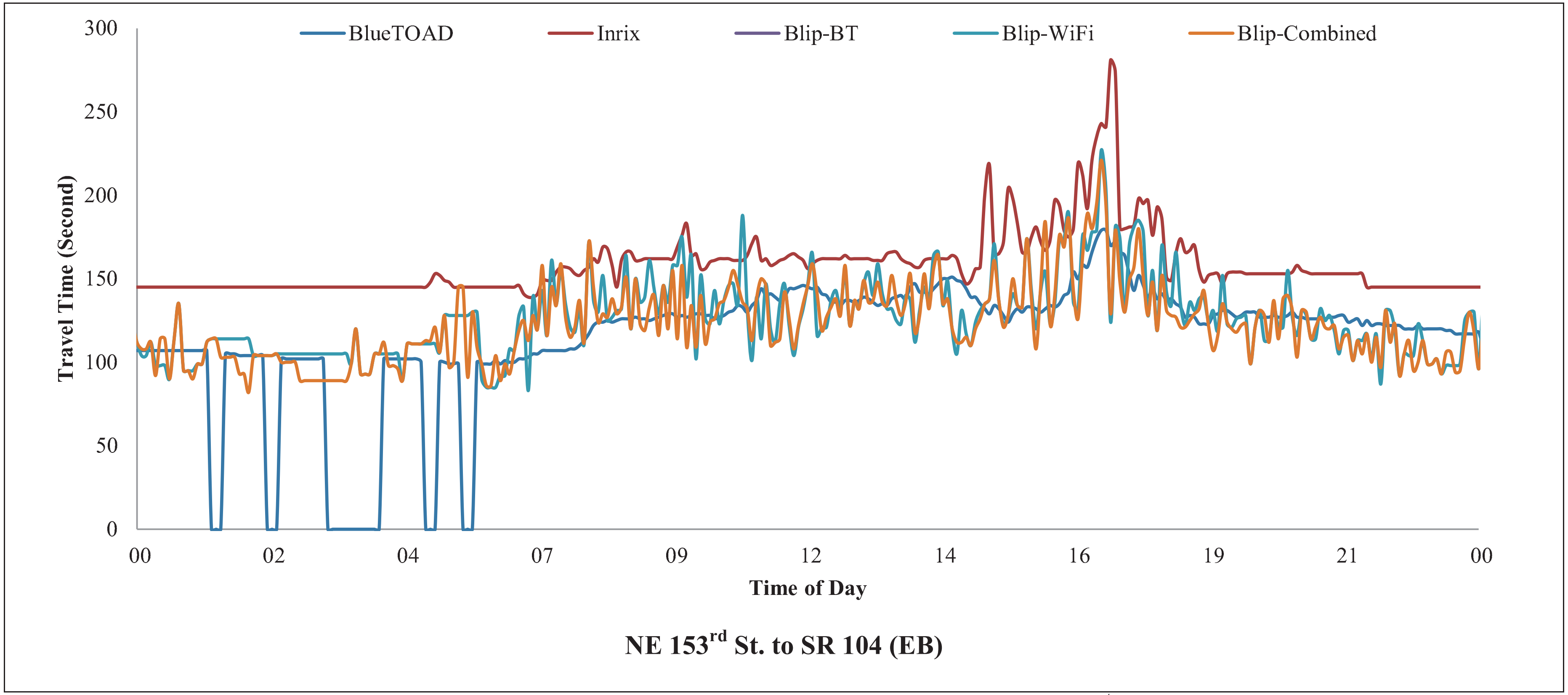

Figure III-33. Travel time plot for NE 153rd St. to SR 104 (EB) on May 1st, 2013

Figure III-33 shows the overlaid profiles of travel time for all the sensors from NE 153rd St. to SR 104 (EB) for Wednesday May 1st, 2013. Inrix reports a significantly higher and highly smoothed travel time over the off-peak hours on this segment compared to others. A large number of gaps in the early morning can be observed for BlueTOAD.

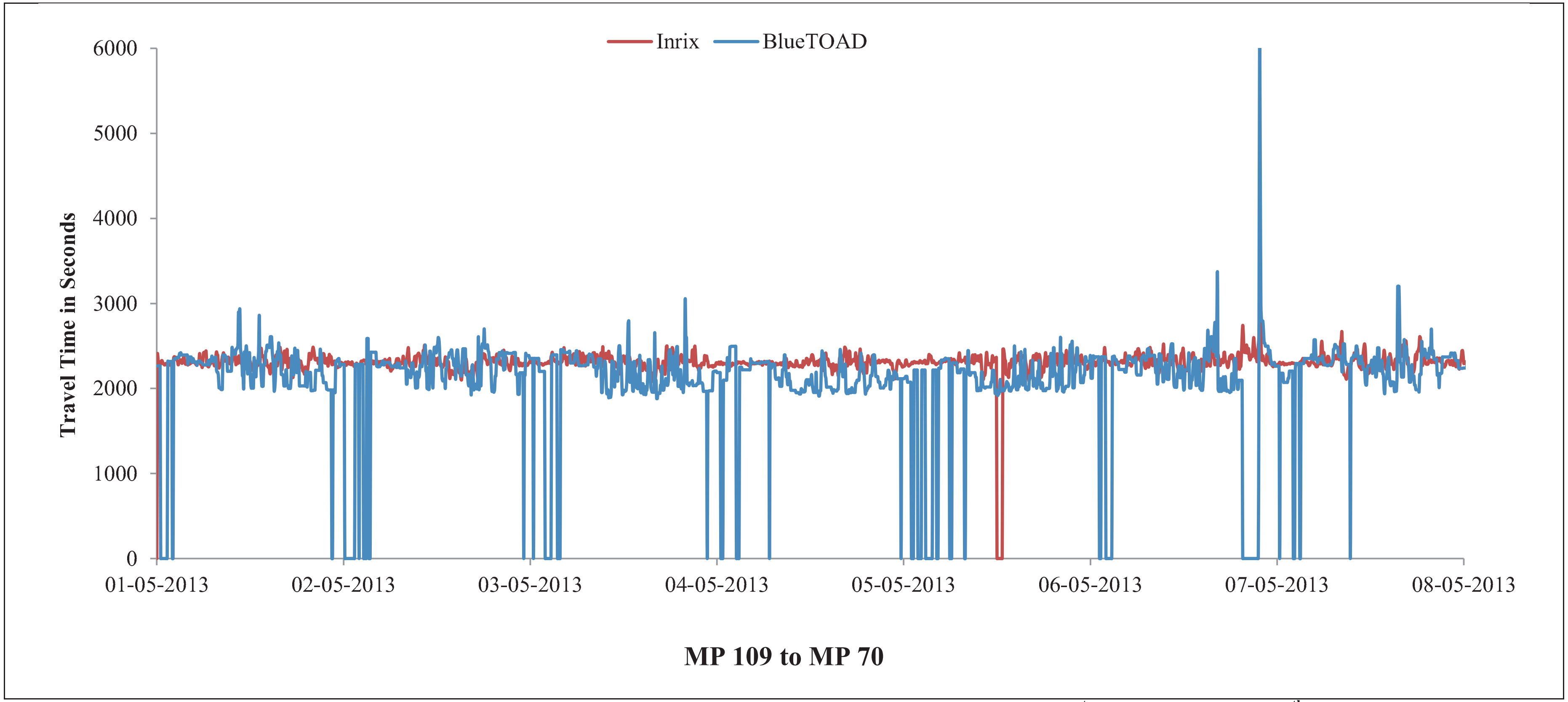

Figure III-34. Travel times on I-90 from Ellensburg (MP 109) to Easton (MP 70) for May 1st, 2013 through May 8th, 2013

Figure III-34 shows a comparison of the travel time generated by BlueTOAD and Inrix from milepost 109 to Milepost 70 on I-90. This segment has relatively lighter traffic and therefore shows little day to day variation. Of note is a possible blocking incident on May 7.

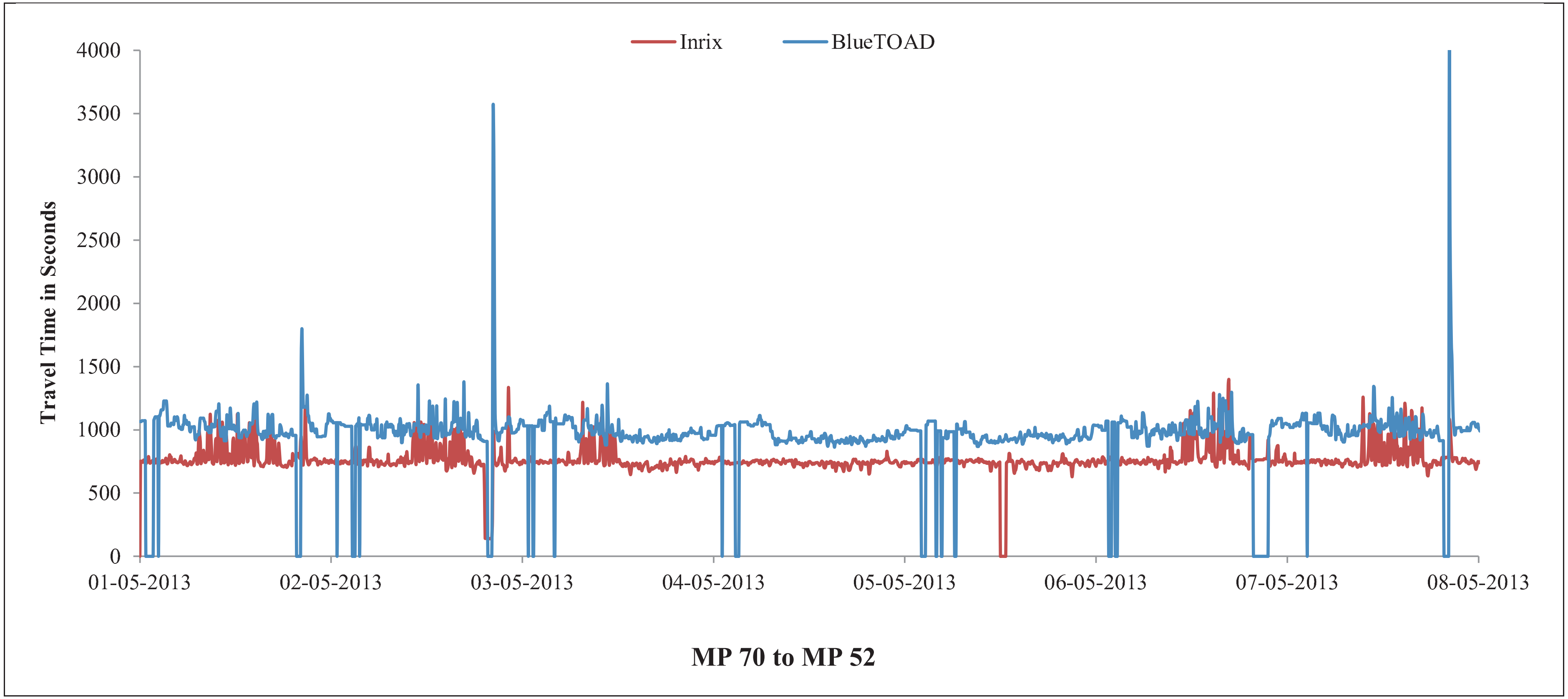

Figure III-35. Travel times on I-90 from Easton (MP 70) to the Snoqualmie Pass (MP 52) for May 1st, 2013 through May 8th, 2013

Figure III-35 shows the BlueTOAD and Inrix travel time data from milepost 70 to milepost 52. It is noteworthy that this segment has a hint of cyclic daily pattern for the weekdays (May 1-3 and 6-8). The large spike on May 2 is due to closure for blasting. The spike on May 8 is another possible incident. It is noteworthy that the Inrix and BlueTOAD data show similar activity during peak periods, but have significantly different travel times. The Inrix data is suggestive of one or more missing segments, given that at 60 mph, the 18 mile trip should take 18 minutes or 1080 seconds.

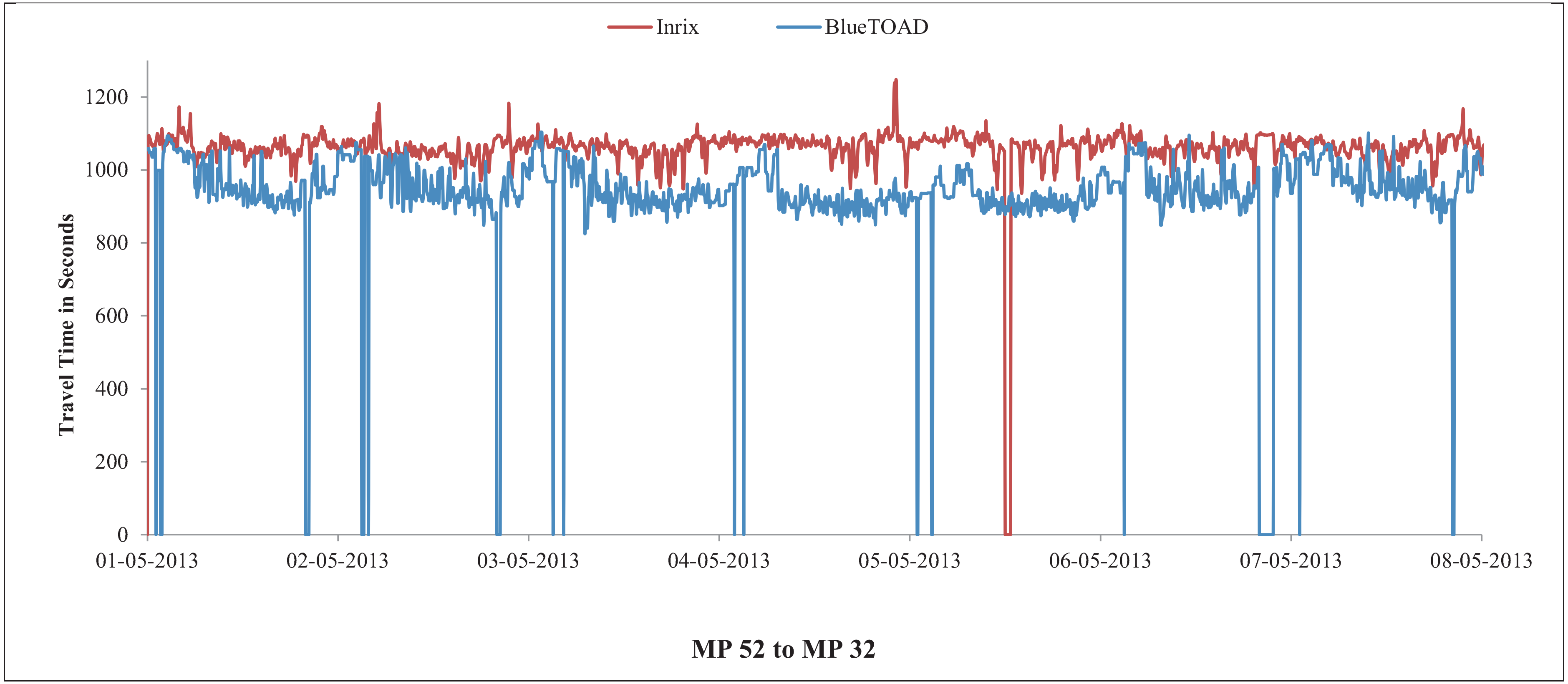

Figure III-36. Travel times on I-90 from the summit (MP 52) to North Bend (MP 32) for May 1st, 2013 through May 8th, 2013

Figure III-36 shows the travel time data for Inrix and BlueTOAD from milepost 52 to milepost 32. This time it appears that BlueTOAD is underestimating the travel time. The 20 mile segment should take 1200 seconds at 60 mph. Considering that this segment is downhill from the Snoqualmie Pass summit it is reasonable to assume that speeds may be higher than expected by the speed limit. However, the BlueTOAD travel time corresponds to a speed near 75 mph (which is quite possible on this section of I-90).